A New Equation of State for Carbon Dioxide Covering the Fluid Region from the Triple-Point Temperature to 1100 K at Pressures up to 800 MPa

R. Span and W. Wagner

Lehrstuhl für Thermodynamik, Ruhr-Universität Bochum, D-44780 Bochum, Germany

Received 25 May 1994

This work reviews the available data on thermodynamic properties of carbon dioxide and presents a new equation of state in the form of a fundamental equation explicit in the Helmholtz free energy. The function for the residual part of the Helmholtz free energy was fitted to selected data of the following properties: (a) thermal properties of the single-phase region ($p\rho T$) and (b) of the liquid-vapor saturation curve (p_s, ρ', ρ'') including the Maxwell criterion, (c) speed of sound w and (d) specific isobaric heat capacity c_p of the single phase region and of the saturation curve, (e) specific isochoric heat capacity c_v, (f) specific enthalpy h, (g) specific internal energy u, and (h) Joule–Thomson coefficient μ. By applying modern strategies for the optimization of the mathematical form of the equation of state and for the simultaneous nonlinear fit to the data of all these properties, the resulting formulation is able to represent even the most accurate data to within their experimental uncertainty. In the technically most important region up to pressures of 30 MPa and up to temperatures of 523 K, the estimated uncertainty of the equation ranges from ±0.03% to ±0.05% in the density, ±0.03% to ±1% in the speed of sound, and ±0.15% to ±1.5% in the isobaric heat capacity. Special interest has been focused on the description of the critical region and the extrapolation behavior of the formulation. Without a complex coupling to a scaled equation of state, the new formulation yields a reasonable description even of the caloric properties in the immediate vicinity of the critical point. At least for the basic properties such as pressure, fugacity, and enthalpy, the equation can be extrapolated up to the limits of the chemical stability of carbon dioxide. Independent equations for the vapor pressure and for the pressure on the sublimation and melting curve, for the saturated liquid and vapor densities, and for the isobaric ideal gas heat capacity are also included. Property tables calculated from the equation of state are given in the appendix. © *1996 American Institute of Physics and American Chemical Society.*

Key words: carbon dioxide; correlation; critical region; data evaluation; equation of state; extrapolation; fundamental equation; melting line; property tables; sublimation line; thermal and caloric properties; and vapor-liquid coexistence curve.

Contents

Nomenclature 1513
Physical Constants for Carbon Dioxide 1513
1. Introduction 1514
1.1 Background 1514
1.2 Prior Correlations of Carbon Dioxide Properties and Demands on the New Correlation 1514
1.3 Organization of the Article 1516
2. Basic Elements of the Development of Equations of State in Form of a Fundamental Equation 1516
2.1 Helmholtz Function 1516
2.2 Helmholtz Energy of the Ideal Gas 1516
2.3 Residual Part of the Helmholtz Energy 1517
2.3.1 Fitting an Empirical Equation for ϕ^r to Data 1517
2.3.2 Optimizing the Mathematical Form 1518
2.3.3 The Procedure of Weighting 1518
3. Phase Equilibria of Carbon Dioxide 1519
3.1 Triple Point 1519
3.2 Critical Point 1519
3.3 Melting Pressure 1520
3.4 Sublimation Pressure 1521
3.5 Vapor Pressure 1521
3.6 Saturated Liquid Density 1524
3.7 Saturated Vapor Density 1525
3.8 Caloric Data on the Liquid–Vapor Phase Boundary 1526
4. Experimental Basis of the New Equation of State 1526
4.1 Thermal Properties 1527
4.2 Specific Isobaric Heat Capacity 1528
4.2.1 Experimental Results for the Specific Isobaric Heat Capacity 1528
4.2.2 Results for the Specific Isobaric Heat

Capacity in the Ideal-Gas State..... 1529
4.3 Specific Isochoric Heat Capacity..... 1530
4.4 Speed of Sound..... 1532
4.5 Enthalpy..... 1532
4.6 Internal Energy..... 1532
4.7 Joule–Thomson Coefficient..... 1532
4.8 Virial Coefficients..... 1533
4.9 Liquid–Vapor Equilibrium..... 1533
4.10 Adjustment of Data..... 1534
4.10.1 Adjustment of Data Sets Describing the Critical Region..... 1534
4.10.2 Adjustment of $p\rho T$ Data..... 1534
4.10.3 Correction of Isobaric Heat Capacities..... 1535
5. Description of Thermodynamic Properties in the Critical Region..... 1535
5.1 Limitations of Analytical Equations of State. 1536
5.2 Use of Nonanalytic Terms as an Integral Component in an Empirical Wide-Range Equation of State..... 1537
6. New Equation of State..... 1541
6.1 Ideal-Gas Part of the Helmholtz Energy..... 1541
6.2 Residual Part of the Helmholtz Energy..... 1543
7. Comparisons of the New Equation of State with Experimental Data and Other Equations of State. 1546
7.1 Liquid–Vapor Boundary..... 1546
7.1.1 Thermal Properties on the Coexistence Curve..... 1546
7.1.2 Caloric Properties on the Coexistence Curve..... 1547
7.2 Single-Phase Region..... 1547
7.2.1 Thermal Properties in the Single-Phase Region..... 1547
7.2.2 Caloric Properties in the Single-Phase Region..... 1553
7.3 Extrapolation Behavior of the New Fundamental Equation..... 1556
7.3.1 Extrapolation Beyond the Range of Primary Data..... 1557
7.3.2 Representation of "Ideal Curves"..... 1557
8. Uncertainty of the New Fundamental Equation... 1559
9. Conclusions..... 1559
10. Appendix: Thermodynamic Properties of Carbon Dioxide..... 1559
11. Acknowledgments..... 1593
12. References..... 1593

List of Tables

1. Available wide-range equations of state for carbon dioxide 1515
2. Selected scaled equations of state for carbon dioxide 1515
3. Relations of thermodynamic properties to the dimensionless Helmholtz function ϕ consisting of ϕ^0 and ϕ^r; see Eq. (2.1)..... 1517
4. Selected data for the triple point of carbon dioxide..... 1520
5. Selected data for the critical point of carbon dioxide 1520
6. Summary of the data sets for the sublimation pressure of carbon dioxide 1521
7. Summary of the data sets for the vapor pressure of carbon dioxide 1522
8. Summary of the data sets for the saturated liquid density of carbon dioxide 1523
9. Summary of the data sets for the saturated vapor density of carbon dioxide 1524
10. Summary of the data sets for caloric properties on the liquid-vapor phase boundary of carbon dioxide 1526
11. Summary of the data sets available for the $p\rho T$ relation of carbon dioxide 1527
12. Summary of selected $p\rho T$ data for carbon dioxide; detailed information is given on the uncertainty values estimated by the authors and those estimated by ourselves and used in the weighting procedure..... 1529
13. Summary of the data sets available for the specific isobaric heat capacity of carbon dioxide.. 1530
14. Summary of selected data for the specific isobaric heat capacity of carbon dioxide; detailed information is given on the uncertainty values estimated by the authors and those estimated by ourselves and used in the weighting procedure... 1530
15. Data sets for the isobaric heat capacity in the ideal-gas state of carbon dioxide calculated by theoretical approaches..... 1530
16. Summary of the data sets available for the specific isochoric heat capacity of carbon dioxide..... 1531
17. Summary of selected data for the specific isochoric heat capacity of carbon dioxide; detailed information is given on the uncertainty values estimated by the authors and those estimated by ourselves and used in the weighting procedure... 1531
18. Summary of the data sets available for the speed of sound of carbon dioxide..... 1531
19. Summary of selected data for the speed of sound of carbon dioxide; detailed information is given on the uncertainty values estimated by the authors and those estimated by ourselves and used in the weighting procedure..... 1532
20. Summary of the data sets available for enthalpy differences of carbon dioxide..... 1532
21. Summary of the data sets available for differences of the internal energy of carbon dioxide..... 1532
22. Summary of the data sets available for the Joule–Thomson coefficient of carbon dioxide..... 1533
23. Summary of data available for the second and third virial coefficient of carbon dioxide. For reasons explained in the text, no data were assigned to Group 1..... 1533

24. Summary of selected data describing the liquid-vapor phase equilibrium of carbon dioxide; detailed information is given on the uncertainty values estimated by the authors and those estimated by ourselves and used in the weighting procedure. 1534
25. Temperature dependent corrections of isobaric heat capacity data. 1535
26. Examples for power laws describing thermodynamic properties along certain paths throughout the critical region. 1535
27. Coefficients of the correlation equations, Eq. (6.2) and Eq. (6.3), for c_p^o and ϕ^o, respectively... 1540
28. The ideal-gas part of the dimensionless Helmholtz energy ϕ^o and its derivatives. 1541
29. Summary of the data used for the linear optimization procedure and for the nonlinear fit. . 1541
30. Parameters of the nonanalytic terms in the bank of terms. 1543
31. Coefficients and exponents of Eq. (6.5). 1544
32. The residual part of the dimensionless Helmholtz energy ϕ^r and its derivatives. 1545
33. The definition of the zeroth- and first-order ideal curves of the compression factor Z. 1557
34. Thermodynamic properties of saturated carbon dioxide. 1560
35. Thermodynamic properties of carbon dioxide. . . . 1562

List of Figures

1. Relative deviations of experimental melting pressure data from values calculated from the melting pressure equation, Eq. (3.10). In this figure, both the corrected and the uncorrected data are plotted (see Sec. 3.3). 1521
2. Absolute deviations $\Delta p_{sub}=(p_{sub,exp}-p_{sub,calc})$ of selected experimental sublimation pressure data from values calculated from the sublimation pressure equation, Eq. (3.12). In this figure, both the corrected and the uncorrected data of Bilkadi *et al.*[74] are plotted (see Sec. 3.4). 1522
3. Relative deviations of selected experimental vapor pressure data from values calculated from the vapor pressure equation, Eq. (3.13). Vapor pressures calculated from the corresponding equation of Angus *et al.*[3] are plotted for comparison. 1523
4. Relative deviations $100\Delta\rho'=100(\rho'_{exp}-\rho'_{calc})/\rho'_{exp}$ of selected experimental saturated liquid density data from values calculated from Eq. (3.14). Saturated liquid densities calculated from the corresponding equation of Angus *et al.*[3] are plotted for comparison. 1524
5. Relative deviations of selected experimental saturated vapor density data from values calculated from Eq. (3.15). Saturated vapor densities calculated from the corresponding equation of Angus *et al.*[3] are plotted for comparison. 1525
6. Relative deviations $100\Delta\rho=100(\rho_{exp}-\rho_{calc})/\rho_{exp}$ of experimental $p\rho T$ data from values calculated from Eq. (6.1). This figure illustrates the reason for adjusting the data of Kirillin *et al.*[140] and Michels *et al.*[123] (see Sec. 4.10.2). 1534
7. Relative deviations $100\Delta c_p=100(c_{p,exp}-c_{p,calc})/c_{p,exp}$ of experimental c_p data from specific isobaric heat capacities calculated from Eq. (6.1). This figure illustrates the reason for correcting the data of Ernst *et al.*[179] and Bender *et al.*[177] (see Sec. 4.10.3). 1534
8. Relative deviations $100\Delta p=100(p_{exp}-p_{calc})/p_{exp}$ of experimental $p\rho T$ data on the critical isotherm from values calculated from Eq. (6.1). Values calculated from the crossover equation of Chen *et al.*[27] and from refitted equations using the CH_4- and O_2-form (see Sec. 5.1) are plotted for comparison. 1536
9. Representation of representative isochoric heat capacity data in the critical region. The plotted curves correspond to values calculated from the crossover equation of Chen *et al.*[27] and from refitted equations using the CH_4- and O_2-form (see Sec. 5.1). 1536
10. While preliminary equations of state showed a discontinuous plot of the third density derivative of the reduced Helmholtz energy, the new equation of state, Eq. (6.1), yields continuous plots for the third derivatives. 1538
11. Representation of representative isochoric heat capacity data in the critical region. The plotted curves correspond to values calculated from Eq. (6.1), the crossover equation of Chen *et al.*,[27] and a refitted equation using the CH_4-form (see Sec. 5.1). 1538
12. Representation of the speed of sound on isotherms in the critical region. The plotted curves correspond to values calculated from Eq. (6.1), the crossover equation of Chen *et al.*,[27] and a refitted equation using the CH_4-form (see Sec. 5.1). 1538
13. Representation of the isochoric heat capacity on isotherms in the critical region. The plotted curves correspond to values calculated from Eq. (6.1), the crossover equation of Chen *et al.*,[27] and a refitted equation using the CH_4-form (see Sec. 5.1). 1539
14. Representation of experimental isochoric heat capacity data in the single phase ($T>T_c$) and two phase ($T<T_c$) region in a double logarithmic diagram. The plotted curves correspond to data on the critical isochore calculated from Eq. (6.1), the crossover equation of Chen *et al.*,[27] and a refitted equation using the O_2-form (see Sec. 5.1). 1539

15. For temperatures between T_c and T_c+1 K Eq. (6.1) results in an oscillating plot for the isobaric heat capacity around the critical density.. 1539
16. Relative deviations of c_p^o data from values calculated from Eq. (6.2). The upper diagram shows data calculated from statistical thermodynamics (see Table 15) and the lower diagram shows data extrapolated from experimental results (see Table 13). Values of c_p^o calculated from the corresponding equations of Angus *et al.*[3] and Ely *et al.*[15] are plotted for comparison.. 1540
17. Distribution of the experimental data used for the establishment of the residual part of the new fundamental equation, Eq. (6.5), in a pT diagram.. 1542
18. Relative deviations $100\Delta y=100(y_{exp}-y_{calc})/y_{exp}$ $(y=p_s,\rho',\rho'')$ of the experimental saturation data of Duschek *et al.*[58] from values calculated from Eq. (6.1). Values calculated from the auxiliary equations presented in Sec. 3, the equation of state of Ely *et al.*[15] and the auxiliary equations of Angus *et al.*[3] are plotted for comparison.. 1546
19. Relative deviations $100\Delta y=100(y_{exp}-y_{calc})/y_{exp}$ $(y=p_s,\ \rho',\ \rho'')$ of the near critical experimental saturation data of Duschek *et al.*[58] from values calculated from Eq. (6.1). Values calculated from the auxiliary equations presented in Sec. 3 and from the crossover equation of Chen *et al.*[27] are plotted for comparison.. 1546
20. Relative deviations $100\Delta y=100(y_{exp}-y_{calc})/y_{exp}$ $(y=w'',w',c_p')$ of experimental caloric data at saturation from values calculated from Eq. (6.1). Data calculated from the wide-range equations of Ely *et al.*[15] and Angus *et al.*[3] are plotted for comparison.. 1547
21. Relative density deviations of very accurate $p\rho T$ data at subcritical temperatures from values calculated from Eq. (6.1). Values calculated from the wide-range equations of Ely *et al.*[15] and Angus *et al.*[3] are plotted for comparison.. 1548
22. Relative pressure deviations of very accurate $p\rho T$ data in the extended critical region from values calculated from Eq. (6.1). Values calculated from the wide-range equations of Ely *et al.*[15] and Pitzer and Schreiber[16] and from the crossover equation of Chen *et al.*[27] are plotted for comparison.. 1549
23. Relative density deviations of very accurate $p\rho T$ data at supercritical temperatures from values calculated from Eq. (6.1). Values calculated from the wide-range equations of Ely *et al.*[15] and Angus *et al.*[3] are plotted for comparison.. 1550
24. Relative density deviations of selected $p\rho T$ data from values calculated from Eq. (6.1). Values calculated from the wide-range equations of Ely *et al.*[15] and Angus *et al.*[3] are plotted for comparison.. 1551
25. Relative density deviations of selected $p\rho T$ data at high temperatures from values calculated from Eq. (6.1). Values calculated from the wide-range equations of Ely *et al.*[15] and Angus *et al.*[3] are plotted for comparison.. 1552
26. Relative density deviations of selected $p\rho T$ data at high pressures from values calculated from Eq. (6.1). Values calculated from the wide-range equations of Ely *et al.*[15] and Angus *et al.*[3] are plotted for comparison; in this pressure range, these two equations of state are at least partly extrapolated (see Table 1).. 1552
27. Relative deviations of selected isobaric heat capacity data from values calculated from Eq. (6.1). Values calculated from the wide-range equations of Ely *et al.*[15] and Angus *et al.*[3] are plotted for comparison.. 1553
28. Representation of the isobaric heat capacity on isobars in the gas region and in states on the sublimation curve (saturated vapor). Values calculated from the wide-range equations of Ely *et al.*[15] and Angus *et al.*[3] are plotted for comparison.. 1553
29. Relative deviations of isobaric heat capacity data at high temperatures from values calculated from Eq. (6.1). Values calculated from the wide-range equations of Ely *et al.*[15] and Angus *et al.*[3] are plotted for comparison.. 1554
30. Relative deviations of selected isochoric heat capacity data from values calculated from Eq. (6.1). Values calculated from the wide-range equations of Ely *et al.*[15] and Angus *et al.*[3] are plotted for comparison.. 1554
31. Representation of the isochoric heat capacity on high-density isochores. For each of the isochores the plotted pressure range starts at the corresponding vapor pressure. Values calculated from the wide-range equations of Ely *et al.*[15] and Angus *et al.*[3] are plotted for comparison.. 1554
32. Relative deviations of speed of sound data at supercritical temperatures from values calculated from Eq. (6.1). Values calculated from the wide-range equations of Ely *et al.*[15] and of Pitzer and Schreiber,[16] and, in the range of its validity, from the crossover equation of Chen *et al.*[27] are plotted for comparison.. 1555
33. Relative deviations of speed of sound data at high pressures from values calculated from Eq. (6.1). Values calculated from the wide-range equations of Ely *et al.*[15] and Angus *et al.*[3] are plotted for comparison; in this pressure range, these two equations of state are at least partly

extrapolated (see Table 1).. 1555
34. Relative deviations of experimentally determined Joule–Thomson coefficients from values calculated from Eq. (6.1). Values calculated from the wide-range equations of Ely *et al.*[15] and Angus *et al.*[3] are plotted for comparison. The data of Vukalovich *et al.*[206] were not used when establishing Eq. (6.1).. 1556
35. Representation of experimentally determined fugacities on isotherms at very high temperatures and pressures. Values calculated from the wide-range equations of Ely *et al.*[15] and Angus *et al.*[3] are plotted for comparison.. 1556
36. Representation of experimental data describing the Hugoniot curve of carbon dioxide. Hugoniot curves calculated from the wide-range equations of Ely *et al.*[15] and Angus *et al.*[3] are plotted for comparison.. 1557
37. The so-called ideal curves calculated from Eq. (6.1) and plotted in a ρ/ρ_c, $\log(T/T_c)$ diagram. The Joule–Thomson inversion curve and the Joule inversion curve exceed the temperature range in which Eq. (6.1) is fitted to experimental data.. 1557
38. Tolerance diagram for densities calculated from Eq. (6.1). In region B the uncertainty in pressure is given.. 1558
39. Tolerance diagram for speed of sound data calculated from Eq. (6.1). In the immediate vicinity of the critical point (region G) it is difficult to estimate an uncertainty in w because of the growing influence of uncertainties in temperature and pressure measurement.. 1558
40. Tolerance diagram for isobaric heat capacities calculated from Eq. (6.1). In the immediate vicinity of the critical point (region G) it is difficult to estimate an uncertainty in c_p because of the growing influence of uncertainties in temperature and pressure measurement.. 1558

Nomenclature

Symbol	Description
A,B,C,D,a,b,d,n,t	Adjustable parameters
A	Specific Helmholtz energy
B	Second virial coefficient
C	Third virial coefficient
c_p	Specific isobaric heat capacity
c_v	Specific isochoric heat capacity
c_σ	Specific heat capacity along the saturated liquid line
g	Specific Gibbs energy
h	Specific enthalpy
i,j,k,l,m	Serial numbers
I,J	Maximum number of the serial numbers i,j
M	Number of data, molar mass
p	Pressure
R	Gas constant
s	Specific entropy
T	Thermodynamic temperature, ITS-90
u	Specific internal energy
v	Specific volume
w	Speed of sound
x,y	Independent variables
z	Any thermodynamic property
Z	Compression factor
Greek	
$\alpha,\beta,\gamma,\Delta,\theta$	Adjustable parameters
$\alpha,\beta,\gamma,\delta$	Critical exponents
Δ	Difference in any quantity
Δ,θ,ψ	Functions
δ	Reduced density ($\delta=\rho/\rho_c$)
∂	Partial differential
φ	Fugacity
ϕ	Dimensionless Helmholtz energy [$\phi=A/(RT)$]
μ	Joule–Thomson coefficient
ρ	Mass density
σ	Variance
τ	Inverse reduced temperature ($\tau=T_c/T$)
χ^2	Weighted sum of squares
Superscripts	
o	Ideal gas property
r	Residual
$'$	Saturated liquid state
$''$	Saturated vapor state
$-$	Denotes a vector
Subscripts	
c	At the critical point
calc	Calculated
corr	Corrected
exp	Experimental
i,j,k,l,m	Indices
m	Denotes the melting pressure
s	Denotes the vapor pressure
sub	Denotes the sublimation pressure
t	At the triple point
wt	Weighting
σ	Along the saturated liquid curve
0	In the reference state
0H	In the initial state of Hugoniot curve measurements
90	Temperatures according to the ITS-90
68	Temperatures according to the IPTS-68
48	Temperatures according to the IPTS-48

Physical Constants for Carbon Dioxide

M Molar mass: $M=(44.009\,8\pm0.001\,6)$ g/mol; see Ref. 1

R_m Molar gas constant: $R_m=(8.314\,510\pm0.000\,210^a)$ J/(mol K); see Ref. 2
R Specific gas constant: $R=R_m/M=(0.188\,924\,1\pm0.000\,011\,6)$ kJ/(kg K)
T_c Critical temperature: $T_c=(304.128\,2\pm0.015)$K; see Sec. 3.2
p_c Critical pressure: $p_c=(7.377\,3\pm0.003\,0)$MPa; see Sec. 3.2
ρ_c Critical density: $\rho_c=(467.6\pm0.6)$ kg/m^3; see Sec. 3.2
T_t Triple-point temperature: $T_t=(216.592\pm0.002)$ K; see Sec. 3.1
p_t Triple-point pressure: $p_t=(0.517\,95\pm0.000\,10)$ MPa; see Sec. 3.1
T_0 Reference temperature: $T_0=298.15$ K
p_0 Reference pressure: $p_0=0.101\,325$ MPa
h_0^o Reference enthalpy in the ideal gas state at T_0: $h_0^o=0$ kJ/kg
s_0^o Reference entropy in the ideal gas state at T_0, p_0: $s_0^o=0$ kJ/(kg K)

1. Introduction

1.1 Background

Over the past fifteen years great interest in the properties of carbon dioxide has developed. This interest has evolved from both industrial and scientific applications. From an engineering angle, carbon dioxide has proved to be the most commonly used solvent for supercritical fluid extraction and to be an excellent tool for enhanced oil recovery. Carbon dioxide processing and pipelining technologies have become of considerable commercial importance. Furthermore, the discussion on the greenhouse effect has focused technical interest on carbon dioxide as the most significant combustion product which effects the atmosphere.

From a thermodynamic point of view, carbon dioxide usually serves as the best known reference for a molecule with a strong quadrupole moment and as a testing fluid for calibration purposes. However, in sciences related to thermodynamics, interest is mainly based on the widespread occurrence of carbon dioxide. Geophysical calculations of chemical equilibria, under outer mantle conditions for example, require reliable thermodynamic data of carbon dioxide at very high pressures and temperatures.

Besides this, investigations of thermodynamic properties of carbon dioxide have always been influenced by the location of the critical region. On the one hand, the critical temperature of approximately 304 K allows many technical processes, for example pipelining processes, to be carried out within the critical or at least in the extended critical region. Therefore, from a technical point of view a sufficiently accurate calculation of thermodynamic properties is more difficult for carbon dioxide than for other substances. On the other hand, the data situation in the critical region is exceptionally good, which makes carbon dioxide a reference substance for theoretical approaches dealing with the critical region of pure fluids. Almost every physical model for the description of the critical region has been tested for carbon dioxide.

In 1965, an international research project on the thermodynamic properties of carbon dioxide was established at the instigation of the International Union of Pure and Applied Chemistry (IUPAC). In 1976, Angus *et al.*[3] published a monograph which reviewed the experimental data available up to 1973 and presented extensive tables of the thermal and caloric properties derived from the selected equation of state. Nevertheless, knowledge of the thermodynamic properties of carbon dioxide remained unsatisfactory. Thus, since 1973 numerous experiments including state-of-the-art experiments with significantly improved accuracy have been performed in order to improve the quality of the entire data set; a third of the data sets available today belongs to this group.

In addition to the increased amount of experimental data, correlation techniques have significantly improved during the last decade. Sophisticated "multi-property" fitting procedures[4,5] and a new strategy for optimizing the structure of empirical correlation equations[6] have resulted in a new basis for the development of an empirical equation of state.

1.2 Prior Correlations of Carbon Dioxide Properties and Demands on the New Correlation

Since 1960 numerous correlation equations for the thermodynamic properties of carbon dioxide have been developed, but only a few of them describe the properties within a sufficiently large range including the gas, liquid, and supercritical states. Table 1 summarizes the equations of state for carbon dioxide which have been developed since 1970. After examining the wide-range equations of state available in 1973, Angus *et al.*[3] discussed three equations in the IUPAC monograph, namely the equations of Bender,[7] Altunin and Gadetskii,[8] and Stein,[9] which form the beginning of Table 1. Finally, Angus *et al.* decided to use the equation of Altunin and Gadetskii[8] as a basis for the IUPAC monograph. At that time, none of the existing wide-range equations of state offered a reasonable description of the critical region. Thus, Angus *et al.*[3] combined the wide-range equation with a scaled equation of state developed by Schofield[19] and a switching function developed by Chapela and Rowlinson.[20] Although it was known that the evaluation of the combined correlation equations causes numerical problems and yields incorrect results for derived properties in the switching region, the equation was generally accepted as a reference for carbon dioxide. In 1988, Pitzer and Schreiber[16] took up the IUPAC compilation again and showed that very similar results can be achieved with less numerical expense if special terms for the description of the critical region are added to the equation of Altunin and Gadetskii.[8]

The only correlations which really improve the results of Angus *et al.*[3] are the equations developed at the National Institute of Standards and Technology by Ely[14] and Ely

[a]Reference 2 gives a standard deviation of ±0.000 070 J/(mol K).

TABLE 1. Available wide-range equations of state for carbon dioxide

Authors	Year	Temperature range (K)	Pressure range (MPa)	Structure of the equation	Number of coeff. in residual part	Data used in the correlation
Bender[7]	1970	216–1 076	0–50	Extended BWR[a]	20	$p\rho T, p_S \rho' \rho''$
Altunin and Gadetskii[8]	1971	215–1 300	0–300	Polynomial	50	$p\rho T, c_p$
Stein[9]	1972	...[b]	...[b]	Polynomial	44	$p\rho T, p_S \rho' \rho''$
Starling *et al.*[10]	1972	243–413	0–48	Extended BWR[a]	11	$p\rho T, h, p_S$
Meyer–Pittroff[11]	1973	200–1 273	0–60	Polynomial	84	$p\rho T, p_S \rho' \rho'', c_v, h$
Angus *et al.*[3] (IUPAC)	1976	220–1 100	0–100	Combined	50+5+4	$p\rho T, c_p$
Huang *et al.*[12]	1985	216–423	0–310	Extended BWR[a,c]	27	$p\rho T, p_S \rho' \rho''$
Ely[14]	1986	216–1 023	0–300	Schmidt and Wagner[4]	32	$p\rho T, p_S \rho' \rho'', c_v, c_\sigma$
Ely *et al.*[15]	1987	216–1 023	0–300	Schmidt and Wagner[4]	32	$p\rho T, p_S \rho' \rho'', c_v, c_\sigma$
Pitzer and Schreiber[16]	1988	230–1 030	0–100	Extended polynomial	53	$p\rho T, p_S \rho' \rho'', c_v$[d]
Ely *et al.*[17]	1989	216–1 023	0–316	Jacobsen and Stewart[18]	32	$p\rho T, p_S \rho' \rho'', c_v, c_\sigma$
Pitzer and Sterner[18a]	1994	220–2 000	0–10 000	Fractional form	28	$p\rho T, p_S \rho' \rho'', B, f$[e]

[a]Benedict–Webb–Rubin.
[b]No information published.
[c]Terms developed by Ewers and Wagner[13] for the description of the critical region were also used.
[d]Besides some experimental data, mainly data from the IUPAC tables[3] were used as input data.
[e]Besides some experimental data, mainly data calculated from the equation of Ely *et al.*[17] were used as input data.

et al.[15,17] These equations take into account almost all of the published experimental results. However, some of the most important state-of-the-art experiments on carbon dioxide were not yet available at that time. A detailed comparison[21] shows that the equation given in Refs. 14 and 15 using the form developed by Schmidt and Wagner[4] is superior to the equation given in Ref. 17 which uses the form developed by Jacobsen and Stewart.[18]

Tests of these correlations have yielded that all of the existing equations of state, independent of their different quality, show the following limitations:

- State-of-the-art data for the $p\rho T$ relation are not represented to within their experimental uncertainty.
- State-of-the-art data describing the liquid-vapor phase equilibrium are not represented to within their experimental uncertainty.
- Within the critical region, the calculation of caloric properties yields unreasonable results.
- Unreasonable behavior can be observed in regions with a poor data situation.
- Extrapolation to temperatures and pressures outside the range of validity yields unreasonable results.
- The temperature values used do not correspond to the current International Temperature Scale of 1990 (ITS-90).

The equation of Pitzer and Sterner[18a] can mainly be considered to be an example for an empirical equation of state with reasonable extrapolation behavior; the authors do not claim that this equation improves the description of thermodynamic properties in the region where accurate data exist.

The problems related to the description of properties within the critical region can essentially be solved by using scaled equations of state; Table 2 shows selected correlations with such scaling approaches for the description of the critical region of carbon dioxide. However, the relatively small range of validity and the mathematically complex structure of these equations limit their use.

An exception with regard to the range of validity is the empirical equation of Erickson *et al.*[26] This equation uses an improved form of the transformation procedure, originally developed by Fox,[29] to achieve a reasonable but not an as-

TABLE 2. Selected scaled equations of state for carbon dioxide

Authors	Year	Temperature[a] range (K)	Density[b] range (kg/m^3)	Scaling technique used	Number of fitted coefficients
Schofield[19]	1969	...[c]	...[c]	Simple scaling	5
Vicenti-Missoni *et al.*[22]	1969	301–313	327–608	Simple scaling	6
Murphy *et al.*[23]	1973	304–314	336–598	Simple scaling	5
Albright *et al.*[24]	1987	301–323	290–595	Revised and extended	13
Albright *et al.*[25]	1987	298–322	245–600	Crossover	12
Erickson *et al.*[26]	1987	...[d]	...[d]	Transformation	32+7
Chen *et al.*[27]	1990	291–373	193–712	Crossover	19
Kiselev *et al.*[28]	1991	298–395	280–655	Crossover	12

[a]Range of validity for $\rho = \rho_c$.
[b]Range of validity for $T = T_c$.
[c]No information published.
[d]Scaled wide-range equation, valid for pressures up to 300 MPa at temperatures from 212 K to 1000 K.

ymptotically correct description of the caloric properties in the critical region. Like other parametric approaches, this equation still requires complicated iteration procedures, but it is valid in a range which is sufficiently wide for engineering applications. Tests carried out by Erickson *et al.*[26] showed that outside the critical region the transformed equation based on the form developed by Jacobsen and Stewart[18] is inferior to Ely's equation.[14,15]

The purpose of this article is to present a new equation of state for carbon dioxide explicit in the Helmholtz energy, which is designed to overcome the disadvantages of the existing correlations. The consistent use of sophisticated fitting[30] and optimization[6] procedures allows the representation of even the most accurate data within their experimental uncertainty. Extensive investigations of the data set prevent the equation from unreasonable behavior within the fitting region, and new procedures are introduced to guarantee a reasonable extrapolation behavior of the new equation. The representation of caloric properties in the critical region has been improved by an empirical approach which yields reasonable results even in the immediate vicinity of the critical point.

All the correlation equations given in this article correspond to the ITS-90 temperature scale.

1.3 Organization of the Article

In Sec. 2 we give a brief review of the application of empirical equations of state explicit in the Helmholtz energy as a function of density and temperature; this combination of variables is one form of a fundamental equation. The techniques used for the development of the new equation (multi-property fitting, optimization procedure) are described briefly. Section 3 deals with the liquid-vapor, solid-vapor, and solid-liquid phase equilibria of carbon dioxide. The available data are discussed. In addition to the equation of state, short supplementary equations have been developed for the temperature dependence of the melting pressure p_m, the sublimation pressure p_{sub}, the vapor pressure p_s, the saturated liquid density ρ', and the saturated vapor density ρ''. The experimental information available for the single phase region of carbon dioxide is discussed in Sec. 4. In Sec. 5 a detailed description of the new approach for representing the critical region is given. Possibilities and limitations of the use of nonanalytic terms in empirical wide-range equations of state are outlined. The new correlation equations for both the ideal and the residual part of the Helmholtz free energy are presented in Sec. 6. The final data set and the bank of terms used for the development of the new equation are given. Comparisons of properties calculated from the new equation of state for carbon dioxide with selected experimental data and those values calculated from prior correlations are presented in Sec. 7. A discussion of the extrapolation behavior of the new fundamental equation is included in this section. Finally, the uncertainties of the new formulation are estimated and tables of the thermodynamic properties of carbon dioxide are listed in the Appendix.

2. Basic Elements of the Development of Equations of State in Form of a Fundamental Equation

The new equation of state, developed for the representation of the thermodynamic properties of carbon dioxide, is an empirical representation of the fundamental equation explicit in the Helmholtz energy. Since the application of optimization procedures and the technique of multi-property fitting were extensively discussed by Setzmann and Wagner[6,30] and Saul and Wagner,[5] this section is restricted to some basic facts giving a rough understanding of the procedures used for the development of the new equation. However, those facts which have not previously been published are outlined in more detail.

2.1 Helmholtz Function

The fundamental equation given in this article is expressed in form of the Helmholtz energy A with the two independent variables density ρ and temperature T. The dimensionless Helmholtz energy $\phi = A/(RT)$ is commonly split into a part depending on the ideal-gas behavior ϕ^o and a part which takes into account the residual fluid behavior ϕ^r, namely

$$\phi(\delta,\tau) = \phi^o(\delta,\tau) + \phi^r(\delta,\tau), \tag{2.1}$$

where $\delta = \rho/\rho_c$ is the reduced density and $\tau = T_c/T$ is the inverse reduced temperature. Both the density ρ and the temperature T are reduced with their critical values, ρ_c and T_c, respectively.

Since the Helmholtz energy as a function of density and temperature is one form of a fundamental equation, all the thermodynamic properties of a pure substance can be obtained by combining derivatives of Eq. (2.1). Table 3 gives the relations between Eq. (2.1) and the properties considered in this article. The vapor pressure and the densities of saturated liquid and saturated vapor can be determined from an equation explicit in ϕ by simultaneous solution of the equations

$$\frac{p_s}{RT\rho'} = 1 + \delta' \phi^r_\delta(\delta',\tau), \tag{2.2a}$$

$$\frac{p_s}{RT\rho''} = 1 + \delta'' \phi^r_\delta(\delta'',\tau), \tag{2.2b}$$

$$\frac{p_s}{RT}\left(\frac{1}{\rho''} - \frac{1}{\rho'}\right) - \ln\left(\frac{\rho'}{\rho''}\right) = \phi^r(\delta',\tau) - \phi^r(\delta'',\tau), \tag{2.2c}$$

which correspond to the equality of pressure, temperature, and specific Gibbs energy (Maxwell criterion) in the coexisting phases.

2.2 Helmholtz Energy of the Ideal Gas

The Helmholtz energy of the ideal gas is given by

$$A^o(\rho,T) = h^o(T) - RT - Ts^o(\rho,T). \tag{2.3}$$

TABLE 3. Relations of thermodynamic properties to the dimensionless Helmholtz function ϕ consisting of ϕ^0 and ϕ^r; see Eq. (2.1)

Property and common thermodynamic definition	Relation to the reduced Helmholtz energy ϕ and its derivatives[a]
Pressure: $p(T,\rho)=-(\partial A/\partial v)_T$	$\frac{p(\delta,\tau)}{\rho RT}=1+\delta\phi^r_\delta$
Entropy: $s(T,\rho)=-(\partial A/\partial T)_v$	$\frac{s(\delta,\tau)}{R}=\tau(\phi^o_\tau+\phi^r_\tau)-\phi^o-\phi^r$
Internal energy: $u(T,\rho)=A-T(\partial A/\partial T)_v$	$\frac{u(\delta,\tau)}{RT}=\tau(\phi^o_\tau+\phi^r_\tau)$
Isochoric heat capacity: $c_v(T,\rho)=(\partial u/\partial T)_v$	$\frac{c_v(\delta,\tau)}{R}=-\tau^2(\phi^o_{\tau\tau}+\phi^r_{\tau\tau})$
Enthalpy: $h(T,p)=A-T(\partial A/\partial T)_v-v(\partial A/\partial v)_T$	$\frac{h(\delta,\tau)}{RT}=1+\tau(\phi^o_\tau+\phi^r_\tau)+\delta\phi^r_\delta$
Isobaric heat capacity: $c_p(T,p)=(\partial h/\partial T)_p$	$\frac{c_p(\delta,\tau)}{R}=-\tau^2(\phi^o_{\tau\tau}+\phi^r_{\tau\tau})+\frac{(1+\delta\phi^r_\delta-\delta\tau\phi^r_{\delta\tau})^2}{1+2\delta\phi^r_\delta+\delta^2\phi^r_{\delta\delta}}$
Saturated liquid heat capacity: $c_\sigma(T)=(\partial h/\partial T)_p+T(\partial p/\partial T)_v\cdot(\mathrm{d}p_S/\mathrm{d}T)/(\partial p/\partial v)_{T\|_{v=v'}}$	$\frac{c_\sigma(\tau)}{R}=-\tau^2(\phi^o_{\tau\tau}+\phi^r_{\tau\tau})+\frac{1+\delta\phi^r_\delta-\delta\tau\phi^r_{\delta\tau}}{1+2\delta\phi^r_\delta+\delta^2\phi^r_{\delta\delta}}\cdot\left[(1+\delta\phi^r_\delta-\delta\tau\phi^r_{\delta\tau})-\frac{\rho_c}{R\delta}\frac{\mathrm{d}p_s}{\mathrm{d}T}\right]$
Speed of sound: $w(T,p)=\sqrt{(\partial p/\partial\rho)_s}$	$\frac{w^2(\delta,\tau)}{RT}=1+2\delta\phi^r_\delta+\delta^2\phi^r_{\delta\delta}-\frac{(1+\delta\phi^r_\delta-\delta\tau\phi^r_{\delta\tau})^2}{\tau^2(\phi^o_{\tau\tau}+\phi^r_{\tau\tau})}$
Joule–Thomson coefficient: $\mu(T,p)=(\partial T/\partial p)_h$	$\mu R\rho=\frac{-(\delta\phi^r_\delta+\delta^2\phi^r_{\delta\delta}+\delta\tau\phi^r_{\delta\tau})}{(1+\delta\phi^r_\delta-\delta\tau\phi^r_{\delta\tau})^2-\tau^2(\phi^o_{\tau\tau}+\phi^r_{\tau\tau})(1+2\delta\phi^r_\delta+\delta^2\phi^r_{\delta\delta})}$
Fugacity: $\ln(\varphi(T,p))=\int_0^p\left[\frac{v(T,p)}{RT}-\frac{1}{p}\right]\mathrm{d}p_T$	$\ln\varphi(\delta,\tau)=\phi^r+\delta\phi^r_\delta-\ln(1+\delta\phi^r_\delta)$
Second virial coefficient: $B(T)=\lim_{\rho\to0}(\partial(p/(\rho RT))/\partial\rho)_T$	$B(\tau)\rho_c=\lim_{\delta\to0}\phi^r_\delta(\delta,\tau)$
Third virial coefficient: $C(T)=\frac{1}{2}\lim_{\rho\to0}\{\partial^2[p/(\rho RT)]/\partial\rho^2\}_T$	$C(\tau)\rho_c^2=\lim_{\delta\to0}\phi^r_{\delta\delta}(\delta,\tau)$

[a] $\phi_\delta=\left[\frac{\partial\phi}{\partial\delta}\right]_\tau$, $\delta_{\delta\delta}=\left[\frac{\partial^2\phi}{\partial\delta^2}\right]_\tau$, $\phi_\tau=\left[\frac{\partial\phi}{\partial\tau}\right]_\delta$, $\phi_{\tau\tau}=\left[\frac{\partial^2\phi}{\partial\tau^2}\right]_\delta$, and $\phi_{\delta\tau}=\left[\frac{\partial^2\phi}{\partial\delta\,\partial\tau}\right]$.

The enthalpy h^o of the ideal gas is a function of temperature only, and the entropy s^o of the ideal gas depends on temperature and density. Both properties can be derived from an equation for the ideal-gas heat capacity c_p^o. When c_p^o is inserted into the expression for $h^o(T)$ and $s^o(\rho,T)$ in Eq. (2.3) one obtains

$$A^o=\int_{T_0}^T c_p^o\mathrm{d}T+h_0^o-RT-T\int_{T_0}^T\frac{c_p^o-R}{T}\,\mathrm{d}T-RT[\ln(\rho/\rho_0)]-Ts_0^o, \tag{2.4}$$

where $\rho_0=p_0/(RT_0)$ is the density, h_0^o the enthalpy, and s_0^o the entropy of the ideal gas in a reference state. The final equation for $\phi^o=A^o/(RT)$ is given in Sec. 6.1.

2.3 Residual Part of the Helmholtz Energy

In contrast to the Helmholtz energy of the ideal gas, no theoretical approach is known which yields a sufficiently accurate equation for the residual part of the Helmholtz energy and which is valid in the whole fluid region of a pure substance. Thus, the equation for the residual part has to be determined in an empirical way by optimizing its functional form and fitting its coefficients to experimental results.[b] Since the Helmholtz energy is not accessible to direct measurements, a procedure has been developed which allows the establishment of an empirical equation for the residual part of the Helmholtz energy by using data of different properties.

2.3.1 Fitting an Empirical Equation for ϕ^r to Data

An empirical equation for the residual part of the Helmholtz energy can be written as $\phi^r(\delta,\tau,\bar{n})$, where $\bar{n}$ represents the vector of coefficients to be fitted. Ahrendts and Baehr[31] showed that the determination of an optimum set of coefficients results in the minimization of a sum of squares, defined as the sum of partial sums of squares belonging to the different properties included into the fit:

[b]Throughout this article the word "data" is used to characterize such experimental results.

$$\chi^2=\sum_{j=1}^{J}\chi_j^2=\sum_{j=1}^{J}\sum_{m=1}^{M_j}\left[\frac{[z_{\rm exp}-z_{\rm calc}(x_{\rm exp},y_{\rm exp},\bar{n})]^2}{\sigma_{\rm tot}^2}\right]_{j,m}, \quad (2.5)$$

where J is the number of properties involved in the fit, M_j the number of data points used for the jth property, $z_{\rm exp}$ the value measured for any property $z(x,y)$, and $z_{\rm calc}$ the value calculated for $x_{\rm exp}$, $y_{\rm exp}$ from the correlation equation with the parameter vector $\bar{n}$. The universal variable x usually corresponds to T, but y can correspond to ρ [e.g., $p(T,\rho)$] or to p [e.g., $w(T,p)$] and can even vanish [e.g., $p_s(T)$]. The variance $\sigma_{\rm tot}^2$ is explained in Sec. 2.3.3.

The determination of $\bar{n}$ by minimizing χ^2 results in a linear system of normal equations if z depends on T and ρ and if the relations between z and ϕ^r and the derivatives of ϕ^r are linear (see Table 3). If these conditions are not fulfilled, the data have to be linearized by suitable procedures[32,5] or nonlinear algorithms[33] have to be used. A detailed description of the iterative fitting process resulting from the use of data with nonlinear relation to ϕ^r is given by Setzmann and Wagner.[30] In this article, the linear data of the $p\rho T$ relation, of the internal energy u, of the isochoric heat capacity c_v, of the third virial coefficient C, and linearized data of the enthalpy h, of the isobaric heat capacity c_p of the homogeneous region and the saturated liquid, of the speed of sound w of the homogeneous region, the saturated liquid, and the saturated vapor, and of the Maxwell criterion were used in linear fitting algorithms. Within the nonlinear fitting process, data of all these properties and of the Joule–Thomson coefficient μ, which cannot be linearized in a reasonable way, were used directly which means without any linearization.

2.3.2 Optimizing the Mathematical Form

The fitting procedure described above supposes that the mathematical form of a correlation equation is already known and only the coefficients $\bar{n}$ have to be determined. Since a universal form for an equation describing the residual part of the Helmholtz energy is not known, this requirement is not satisfied. Thus, a suitable mathematical structure has first to be established. With the exception of the equation of state developed by Ely and co-workers,[14,15] the form of the equations existing for carbon dioxide has been determined in a subjective way, based on the experience of the equation maker by trial and error. To improve this procedure, Wagner and co-workers developed different optimization strategies[34,13,6] by introducing objective criteria for the selection of a mathematical structure. The mathematical structure applied by Ely and co-workers was developed by Schmidt and Wagner[4] for oxygen by the use of the "evolutionary optimization method," EOM.[13]

In this work, the optimization method developed by Setzmann and Wagner[6] was used for the determination of a suitable mathematical structure. Minor improvements were introduced, concerning the stochastic part of the optimization procedure. More important, however, are the changes made in the Setzmann–Wagner procedure with regard to the handling of different functional forms from the "bank of terms."

A sophisticated correlation equation for the residual part of the Helmholtz energy consists of an extensive sum of terms. Hence, the mathematical form of a single term can be associated with different functional groups ranging from simple polynomials of the reduced density δ and the inverse reduced temperature τ to complicated exponential expressions (see the bank of terms given in Sec. 6.2). In the known optimization procedures, only the total number of terms of the optimized equation is limited to a preselected value. During this work, additional limitations with respect to the number of terms belonging to special functional groups have turned out to be useful. The actual revision of the optimization procedure allows the definition of such limits to special term forms. The new equation for carbon dioxide has been developed with a limit to four nonanalytic terms to avoid unreasonable behavior in the critical region (cf. Sec. 5.2) and eight polynomial terms to improve the extrapolation behavior (cf. Sec. 7.3 and Span and Wagner[35]).

As pointed out by Setzmann and Wagner,[6,30] the optimization procedure only works with linear or linearized data. This restriction leads to the previously described[30] cyclic process, consisting of linearizing the data, optimizing the mathematical structure of the correlation equation, and nonlinear fitting of the coefficients; these steps are typical for the development of such fundamental equations of state.

2.3.3 The Procedure of Weighting

When data sets of different properties are used for the development of a correlation equation, it is necessary that the residual $(z_{\rm exp}-z_{\rm calc})$ in Eq. (2.5) is reduced with a suitable measure for the uncertainty of the data point. According to the Gaussian error propagation formula, the uncertainty of a measured data point is given by

$$\sigma_{\rm exp}^2=\left(\left[\frac{\partial\Delta z}{\partial x}\right]_{y,z}^2\sigma_x^2+\left[\frac{\partial\Delta z}{\partial y}\right]_{x,z}^2\sigma_y^2+\left[\frac{\partial\Delta z}{\partial z}\right]_{x,y}^2\sigma_z^2\right), \quad (2.6)$$

where σ_x, σ_y, and σ_z are the uncertainties with respect to the uncorrelated single variables x, y, and z; the partial derivatives of z can be calculated from a preliminary equation of state.

In order to have an additional influence on the data set, a weighting factor $f_{\rm wt}$ is introduced. The total variance $\sigma_{\rm tot}$ of a data point used in Eq. (2.5) is defined as

$$\sigma_{\rm tot}^2-\sigma_{\rm exp}^2/f_{\rm wt}^2. \quad (2.7)$$

In this way, weighting factors $f_{\rm wt}>1$ enlarge the influence of a data point with respect to the sum of squares and weighting factors $f_{\rm wt}<1$ reduce it. Usually $f_{\rm wt}$ is equal to one and $\sigma_{\rm tot}^2$ is equal to $\sigma_{\rm exp}^2$; in some cases, however, different weighting factors are used to compensate for effects caused by the structure of the data set. These effects may be divided into the following groups:

- In a special region there are only a few ($f_{\rm wt}>1$) or exceptionally many ($f_{\rm wt}<1$) data points.
- An extensive data set with large experimental uncertainties can be transformed into a smaller, but more consistent data

set by suitable data selection ($f_{wt}>1$).

- After correcting systematic deviations, a data set yields results much better than expected from its original experimental uncertainty ($f_{wt}>1$).
- In a special region, enlarged, but difficult assignable uncertainties of the selected data are expected ($f_{wt}<1$).

To achieve as much transparency with regard to the data set as possible, the tables presenting the selected data (see Sec. 4) contain additional information on the uncertainties used in the weighting procedure as well as on the mean value of the weighting factor. Weighting factors deviating significantly from $f_{wt}=1$ are discussed.

3. Phase Equilibria of Carbon Dioxide

An accurate description of phase equilibria by auxiliary equations is an important precondition for the development of a wide-range equation of state and is also helpful for users who are only interested in phase equilibria. Therefore, all available experimental information on the triple point, the critical point, the melting pressure, the sublimation pressure, the vapor pressure, the densities of saturated liquid and vapor, and on caloric properties on the liquid-vapor phase boundary have been reviewed. With the exception of the caloric properties, simple correlation equations have been developed for the temperature dependency of these quantities.

To condense the description of the data situation, the characteristic information on the single data sets is summarized in tables for the corresponding property. The data sets have been divided into three groups. The assignment considers the critically assessed uncertainty of the data, size of the data set, and covered temperature range. In addition, attention is paid to the data situation for the respective property. Group 1 contains the data sets used for the development of the corresponding correlation equation. Group 2 contains data sets suitable for comparisons. Compared with group 1 data, these data decline at least under one of the three aspects mentioned above. Group 3 contains very small data sets and data sets with rather high uncertainty. Consideration of these data is not reasonable on the level of accuracy aspired to here. Nevertheless this means no devaluation of these data sets — the whole ranking is influenced more by the quality in relation to the best available reference data than by an absolute level of uncertainty; for other purposes even group 3 data sets may be very useful.

Since the new correlation equations and all temperature values in this article correspond to the ITS-90 temperature scale,[36] the temperature values of the available data, based on older temperature scales, were converted to ITS-90. The conversion from the IPTS-68 temperature scale to ITS-90 temperatures was carried out based on the internationally agreed procedure of Preston-Thomas *et al.*,[37] explained by Rusby.[38] The number of digits of the converted values was increased by one digit in order to guarantee numerically consistent reconversion, but not more than four digits to the right of the decimal point were used. Data corresponding to the IPTS-48 temperature scale were converted to IPTS-68 according to the procedure given by Bedford and Kirby.[39] For temperatures between 90 K and 900 K, the temperature scales ITS-27 and IPTS-48 do not deviate from each other and data older than 1927 were not used.

The algorithm used for the conversion from IPTS-68 to the ITS-90 temperature scale[38] causes an additional uncertainty of ± 1.5 mK for temperatures below 273.15 K and ± 1 mK for temperatures above 273.15 K. This additional uncertainty is *not* considered in the uncertainties given in the tables of this section, since these uncertainties were mainly used for consistency tests between data of different authors. In this case, the uncertainty in the absolute temperature, which is influenced by the uncertainty of the conversion, is less important. The comparison between two very similar temperature values is not influenced by the uncertainty of the conversion if both temperatures are converted with the same procedure.

3.1 Triple Point

During the last 90 years, the triple-point temperature of carbon dioxide has been determined by numerous authors but the data situation for the triple-point pressure is rather poor. Fortunately, the few measurements available are very consistent with each other. Table 4 shows selected data of the triple point of carbon dioxide. After a comprehensive review of the existing data, we have chosen the following:

$$T_t=(216.592\pm 0.003)\text{K}, \tag{3.1}$$

$$p_t=(0.51795\pm 0.00010)\text{MPa}. \tag{3.2}$$

Data of the density of the saturated liquid and the saturated vapor at the triple point are not available, but the evaluation of the corresponding correlation equations given in Secs. 3.6 and 3.7 yields

$$\rho_t'=(1178.53\pm 0.18)\text{kg/m}^3, \tag{3.3}$$

$$\rho_t''=(13.7614\pm 0.0034)\text{kg/m}^3. \tag{3.4}$$

3.2 Critical Point

Altogether, data of the critical point of carbon dioxide are given in 75 papers. Table 5 shows selected values of the critical temperature, the critical pressure, and the critical density. The values found for the critical density agree well within the expected uncertainties, but the values for the critical temperature show significant differences, far beyond the uncertainties given by some of the authors. Essentially, the differences in the critical pressures can be explained by the variation of the vapor pressure with the assumed critical temperature.

In the course of this work, no new attempt has been made to determine the critical parameters of carbon dioxide, but the evaluation of Duschek *et al.*[58] was tested under different aspects. No reason for altering the data became obvious. Thus, we have used

TABLE 4. Selected data for the triple point of carbon dioxide

Source	Year	T (K)[a]	ΔT (K)[b]	p (MPa)	Δp (MPa)
Meyers and Van Dusen[40]	1933	216.588 5	±0.005	0.517 99	±0.000 06
Ambrose[41]	1957	216.588 5	±0.002		
Lovejoy[42]	1963	216.591 5	±0.001		
Haro *et al.*[43]	1979	216.594 5	±0.002		
Staveley *et al.*[44]	1981	216.591		0.517 96	
Blanes-Rex *et al.*[45]	1982	216.594 5	±0.001		
Pavese and Ferri[46]	1982	216.591 5	±0.002		
Bedford *et al.*[47]	1984	216.590 5	±0.001		
Bonnier *et al.*[48]	1984	216.591 7	±0.000 2		
Duschek[49]	1989	216.591 5	±0.003	0.517 95	±0.000 1

[a]All temperatures were converted to ITS-90. Up to an uncertainty of 0.1 mK an additional digit is added to guarantee consistent reconversion to IPTS-68 temperatures.
[b]The uncertainty of the conversion from IPTS-68 to ITS-90 is not considered here.

$$T_c=(304.1282\pm 0.015)\text{K}, \tag{3.5}$$

$$p_c=(7.3773\pm 0.0030)\text{MPa}, \tag{3.6}$$

$$\rho_c=(467.6\pm 0.6)\text{kg/m}^3. \tag{3.7}$$

(The additional digit in T_c is given to guarantee numerical consistency in any reconversion to the IPTS-68 temperature scale.)

3.3 Melting Pressure

There are only two available sets of measurements describing the melting pressure of carbon dioxide. In 1942 Michels *et al.*[60] measured 25 melting pressures at temperatures between 217 K and 266 K, corresponding to pressures between 0.9 MPa and 284 MPa. In 1960, Clusius *et al.*[61] published 21 data, covering the range from 217 K to 222 K, corresponding to 0.5 MPa to 24 MPa.

Unfortunately, these data sets are inconsistent with each other and with recent data of the triple point pressure. In both experiments, the thermometers were calibrated at the triple-point of carbon dioxide. Since the values of the triple-point temperature assumed by Michels *et al.*[60] and Clusius *et al.*[61] deviate from the recent value [cf. Eq. (3.1)], all their temperature values were corrected according to

$$T_{90}=T_{Cl,90}-0.05\text{ K}, \tag{3.8}$$

$$T_{90}=T_{\text{Mi},90}-0.04\text{ K} \tag{3.9}$$

after their conversion to ITS-90 temperatures.

The corrected data are consistent within the expected uncertainties and were used to establish a simple correlation equation for the melting pressure:

$$\frac{p_m}{p_t}=1+a_1\left(\frac{T}{T_t}-1\right)+a_2\left(\frac{T}{T_t}-1\right)^2, \tag{3.10}$$

with T_t=216.592 K, p_t=0.51795 MPa, a_1=1955.5390, and a_2=2055.4593. The equation is constrained to the triple-point pressure by its functional form. The representation of both the corrected and uncorrected data is shown in Fig. 1. The uncertainty of Eq. (3.10) is estimated to be $\Delta p_m/p_m \leq \pm 1.5\%$ for $T_t \leq T \leq 225$ K and $\Delta p_m/p_m \leq \pm 0.5\%$ for

TABLE 5. Selected data for the critical point of carbon dioxide

Source	Year	T_c (K)[a,b]	p_c (MPa)	ρ_c (kg/m^3)
Levelt Sengers and Chen[50]	1972	304.182		
Moldover[51]	1974	304.1192±0.004	7.3753	467.8±2.2
Angus *et al.*[3]	1976	304.202±0.05	7.3858±0.005	468±5
Lipa *et al.*[52]	1977	303.9170±0.005		
Moldover *et al.*[53]	1979	304.122	7.375	467
Baade[54]	1983	304.122	7.375	467
Edwards[55]	1984	304.0984±0.0001		
Sengers and Levelt Sengers[56]	1986	304.122	7.372	468
Albright *et al.*[24]	1987	304.0992	7.3719	467.67
Ely *et al.*[21]	1987	304.1192	7.37479	466.5
Chen *et al.*[57]	1990	304.0992	7.3916	467.69
Chen *et al.*[27]	1990	304.1192	7.3753	467.83
Duschek *et al.*[58]	1990	304.1282±0.015	7.3773±0.003	467.6±0.6
Abdulagatov *et al.*[59]	1991	304.1272±0.010		467.5

[a]All temperatures were converted to ITS-90. Up to four digits beyond the decimal point an additional digit is added to guarantee consistent reconversion to IPTS-68 temperatures.
[b]The uncertainty of the conversion from IPTS-68 to ITS-90 is not considered here.

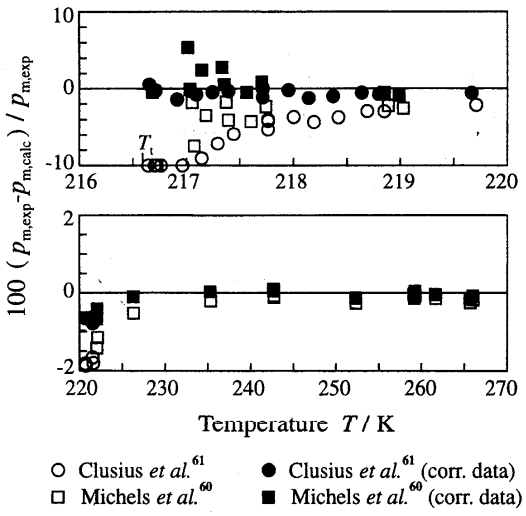

FIG. 1. Relative deviations of experimental melting pressure data from values calculated from the melting pressure equation, Eq. (3.10). In this figure, both the corrected and the uncorrected data are plotted (see Sec. 3.3).

225 K$<T\leqslant$270 K. The simple form of the equation should ensure reasonable extrapolation to higher temperatures.

3.4 Sublimation Pressure

Due to the widespread use of solid carbon dioxide, the data situation for the sublimation pressure is exceptionally good. The available data sets for the sublimation pressure of carbon dioxide are given in Table 6. The data are classified according to the procedure described above. The data set of Bilkadi *et al.*[74] had to be corrected due to a difference between the recent triple-point temperature and the one used by Bilkadi *et al.* for calibration purposes. The corrected temperature is given by

$$T_{90}=T_{\mathrm{Bi},90}-0.049\ \mathrm{K}. \tag{3.11}$$

The sublimation pressure can be described by the correlation equation

$$\ln\left(\frac{p_{\mathrm{sub}}}{p_{\mathrm{t}}}\right)=\frac{T_{\mathrm{t}}}{T}\cdot\left\{a_1\left(1-\frac{T}{T_{\mathrm{t}}}\right)+a_2\left(1-\frac{T}{T_{\mathrm{t}}}\right)^{1.9}+a_3\left(1-\frac{T}{T_{\mathrm{t}}}\right)^{2.9}\right\}, \tag{3.12}$$

with T_{t}=216.592 K, p_{t}=0.51795 MPa, $a_1=-14.740846$, $a_2=2.4327015$, and $a_3=-5.3061778$. The equation is constrained to the triple-point pressure by its functional form. Figure 2 compares group 1 and group 2 data with values calculated from Eq. (3.12). The uncertainty of the new equation is estimated to be $\Delta p_{\mathrm{sub}}\leqslant\pm250$ Pa for 185 K$\leqslant T\leqslant T_{\mathrm{t}}$, $\Delta p_{\mathrm{sub}}\leqslant\pm100$ Pa for 170 K$\leqslant T\leqslant$185 K, and $\Delta p_{\mathrm{sub}}\leqslant\pm50$ Pa for $T\leqslant$170 K. Bedford *et al.*[47] concluded that the most recent value for the sublimation temperature at normal pressure (p_0=0.101325 MPa) is T=194.6857 K$\pm$0.0030 K; iteration with Eq. (3.12) yields T=194.6855 K.

Equation (3.12) was fitted to data at temperatures above 154 K. The low temperature data of Bryson *et al.*[75] are not represented to within the uncertainty given by the authors, but the deviations do not exceed 0.01 Pa for $T>$85 K and 0.0001 Pa for $T\leqslant$85 K, respectively.

3.5 Vapor Pressure

Information on the vapor pressure of carbon dioxide is given by 36 data sets; the corresponding information is summarized in Table 7 (repeatedly published data sets were only listed once). The very accurate data set of Duschek *et al.*[58] describes the vapor pressure from the triple-point temperature up to the critical temperature. Only this data set was selected to develop the new vapor pressure equation. For the data converted to the ITS-90 temperature scale, the optimi-

TABLE 6. Summary of the data sets for the sublimation pressure of carbon dioxide

Source	Year	No. of data	Temp. range, T (K)	ΔT (mK)	Δp_{sub}	Group
Bois and Wills[62]	1899	8	149–196			3
Kuenen and Robson[63]	1902	6	195–215	±32		3
Onnes and Weber[64]	1913	9	90–106			3
Siemens[65]	1913	29	118–195	±20		3
Weber and Onnes[66]	1913	15	104–138			3
Henning[67]	1914	18	192–195		±100 Pa	3
Heuse and Otto[68]	1931	19	193–195	±2		3
Heuse and Otto[69]	1932	7	195	±1		3
Meyers and Van Dusen[40]	1933	28	195–217		±0.02%	3
Giauque and Egan[70]	1936	12	154–196	±1	±3 Pa	2
Tickner and Lossing[71]	1951	13	106–154	±300		3
Ambrose[72]	1955	16	179–198	±1	±4 Pa	1
Hiza[73]	1970	1	216	±10		3
Bilkadi *et al.*[74]	1974	132	154–217	±20		1
Bryson *et al.*[75]	1974	62	70–103			2
Bedford *et al.*[47]	1984	1	195	±3		1
Fernandez-Fassnacht and del Rio[76]	1984	21	194–243	±1	±100 Pa	1

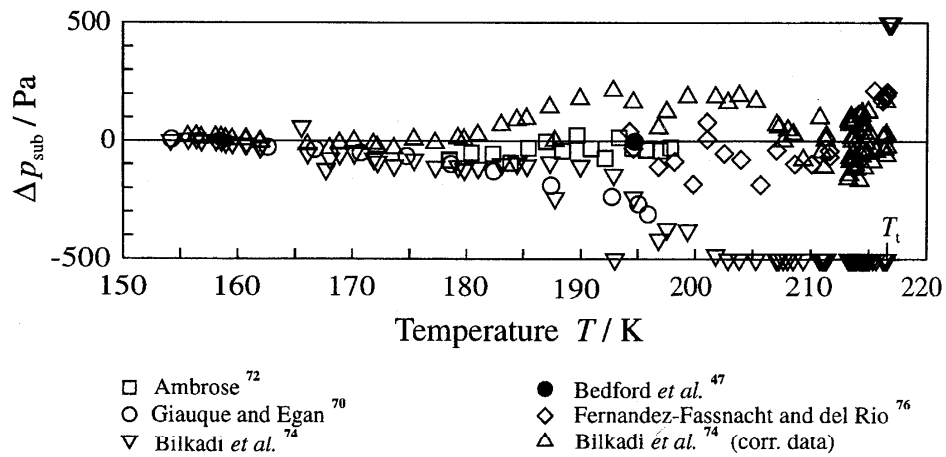

FIG. 2. Absolute deviations $\Delta p_{sub} = (p_{sub,exp} - p_{sub,calc})$ of selected experimental sublimation pressure data from values calculated from the sublimation pressure equation (3.12). In this figure, both the corrected and the uncorrected data of Bilkadi *et al.*[74] are plotted (see Sec. 3.4).

TABLE 7. Summary of the data sets for the vapor pressure of carbon dioxide

Source	Year	No. of data	Temp. range, T (K)	ΔT (mK)	Δp_s	Group
Kuenen and Robson[63]	1902	13	217–273	±32		3
Keesom[77]	1903	4	298–304	±20	±1000 Pa	3
Jenkin and Pye[78]	1914	23	222–296	±10	±0.2%	3
Bridgeman[79]	1927	30	273		±140 Pa	3
Meyers and Van Dusen[40]	1933	67	217–304		±0.01%	2
Michels *et al.*[80]	1936	9	276–304	≤±10	≤ ± 100Pa	3
Roebuck *et al.*[81]	1942	10	223–304			3
Michels *et al.*[82]	1950	19	217–276			2
Reamer *et al.*[83]	1951	2	279, 294	±14	±0.1%	3
Bierlein and Webster[84]	1953	9	274–304	±20	±0.01%	2
Cook[85]	1953	9	293–304	±10		3
Cook[86]	1953	6	293–303	±10	±1000 Pa	3
Schmidt and Thomas[87]	1954	6	274–304		±0.05%	3
Wentorf[88]	1956	8	304	±1	±132 Pa	3
Kletskii[89]	1964	2	260, 266			3
Greig and Dadson[90]	1966	1	273		±0.003 4%	3
Edwards and Johnson[91]	1968	28	273			3
Vukalovich *et al.*[92]	1968	4	301–304			3
Kirillin *et al.*[93]	1969	3	283–303			3
Kholodov *et al.*[94]	1972	5	243–283			3
Levelt Sengers and Chen[50]	1972	37	267–304	±2	±500 Pa	2
Fredenslund and Mollerup[95]	1974	5	223–293	±20	±2000 Pa	3
Gugoni *et al.*[96]	1974	3	241–269			3
Besserer and Robinson[97]	1975	1	274	±60	±24000 Pa	3
Davalos *et al.*[98]	1976	3	230–270	±10	±3000 Pa	3
Stead and Williams[99]	1980	9	220–300	±10	≤±0.1%	3
Kwang-Bae *et al.*[100]	1982	5	263–298	±30	±3500 Pa	3
Al-Sahhaf *et al.*[101]	1983	4	219–270		±0.14%	3
Baade[54]	1983	227	220–304	±3	±80 Pa	2
Fernandez-Fassnacht and del Rio[76]	1984	21	217–243	±1	±100 Pa	2
Kratz[102]	1984	7	289–294	±3	±0.005%	2
Holste *et al.*[103]	1987	12	250–303	±10		2
Brown *et al.*[104]	1988	4	220–270	±20	±0.1%	3
Duschek *et al.*[58]	1990	109	217–304	±3	≤±0.005%	1
Shah *et al.*[105]	1991	2	276+293	±20	±0.5%	3
Yurttas *et al.*[105a]	1994	9	230–280	±3	±0.01%	2

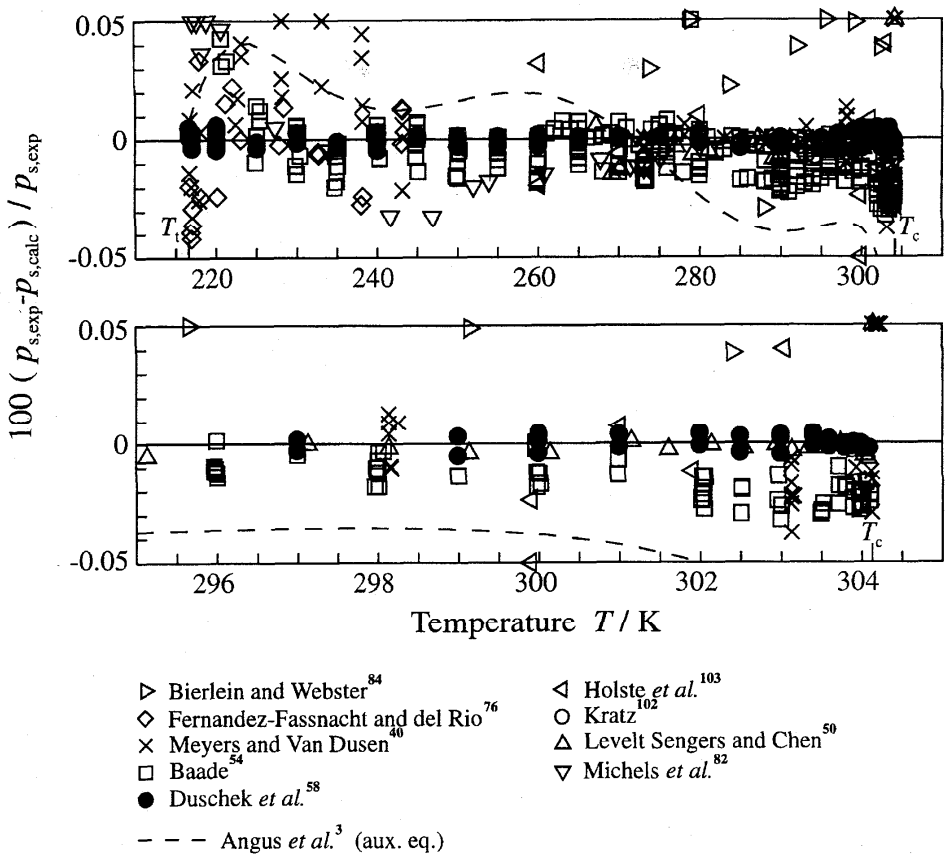

FIG. 3. Relative deviations of selected experimental vapor pressure data from values calculated from the vapor pressure equation, Eq. (3.13). Vapor pressures calculated from the corresponding equation of Angus *et al.*[3] are plotted for comparison.

TABLE 8. Summary of the data sets for the saturated liquid density of carbon dioxide

Source	Year	No. of data	Temp. range, T (K)	ΔT (mK)	$\Delta\rho'$ (%)	Group
Amagat[106]	1892	35	273–304			3
Behn[107]	1900	11	215–297			3
Lowry and Erickson[108]	1927	8	267–296		±0.1	3
Michels *et al.*[80]	1936	9	276–304	≤±10		3
Reamer *et al.*[83]	1951	2	279+294	±20	±0.2	3
Bierlein and Webster[84]	1953	9	274–304	±20	±0.5	3
Cook[85]	1953	11	293–303	±10	±0.5	3
Vukalovich *et al.*[92]	1968	4	301–304		±0.5	3
Straub[109]	1972	34	294–304			3
Gugoni *et al.*[96]	1974	3	241–269			3
Besserer and Robinson[97]	1975	1	274	±60		3
Baade[54]	1983	115	220–304	±3		3
Haynes[110]	1985	17	220–300	±30	±0.1	2
Esper[111,a]	1987	3	266–303		±0.2	2
Holste *et al.*[103,a]	1987	3	266–303	±10		2
Duschek *et al.*[58]	1990	50	217–304	±3	±0.015[b]	1
Abdulagatov *et al.*[59a]	1994	5	304			3

[a]The data sets of Esper[111] and Holste *et al.*[103] are different evaluations of the same measurements.
[b]At temperatures above 300 K, the uncertainty rises to ±0.2%.

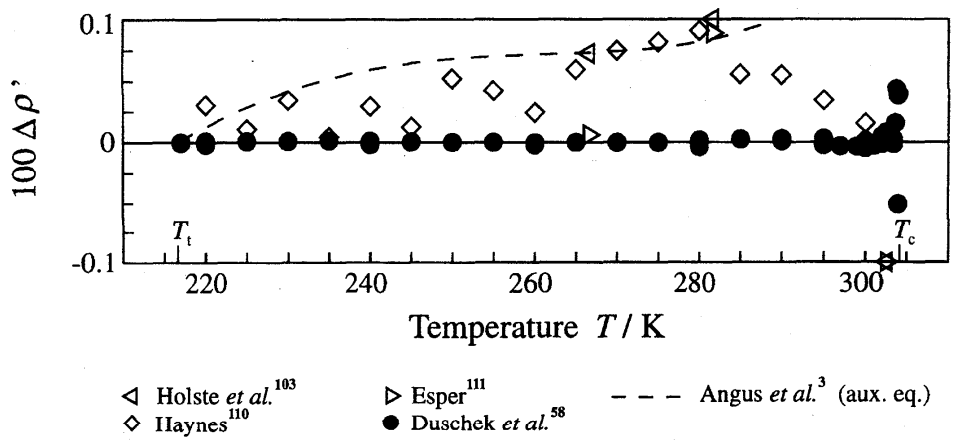

FIG. 4. Relative deviations $100\ \Delta\rho' = 100\ (\rho'_{exp} - \rho'_{calc})/\rho'_{exp}$ of selected experimental saturated liquid density data from values calculated from Eq. (3.14). Saturated liquid densities calculated from the corresponding equation of Angus *et al.*[3] are plotted for comparison.

zation procedure yields the same mathematical form used by Duschek *et al.*[58] to describe this data set in the IPTS-68 temperature scale; only the coefficients a_i have changed. The vapor pressure equation can be written as

$$\ln\left(\frac{p_s}{p_c}\right) = \frac{T_c}{T} \cdot \left[\sum_{i=1}^{4} a_i \left(1 - \frac{T}{T_c}\right)^{t_i}\right], \qquad (3.13)$$

with T_c=304.1282 K, p_c=7.3773 MPa, a_1=−7.060 2087, a_2=1.9391218, a_3=−1.6463597, a_4=−3.2995634, t_1=1.0, t_2=1.5, t_3=2.0, and t_4=4.0.

Figure 3 shows both the good agreement between the data sets marked as group 1 and group 2 data and the representation of the data measured by Duschek *et al.*[58] Considering the experimental uncertainty of these data, the uncertainty of Eq. (3.13) is estimated to be $\Delta p_s \leqslant \pm 0.012\%$ for the whole temperature range.

The dashed line in Fig. 3 corresponds to values calculated from the vapor pressure equation of Angus *et al.*[3] after conversion to ITS-90. The results of this correlation are remarkably good but, of course, the most accurate data available today are not represented to within their experimental uncertainty.

3.6 Saturated Liquid Density

Table 8 shows information on the 17 data sets of the saturated liquid density of carbon dioxide. Again, only the data

TABLE 9. Summary of the data sets for the saturated vapor density of carbon dioxide

Source	Year	No. of data	Temp. range, T (K)	ΔT (mK)	$\Delta\rho''$ (%)	Group
Amagat[106]	1892	35	273–304			3
Lowry and Erickson[108]	1927	8	267–296		±0.7	3
Michels *et al.*[80]	1936	9	276–304	⩽±10		3
Reamer *et al.*[83]	1951	2	279, 294	±20	±0.2	3
Bierlein and Webster[84]	1953	9	274–304	±20	±0.5	3
Cook[85]	1953	11	293–303	±10	±0.5	3
Vukalovich *et al.*[92]	1968	4	301–304		±0.8	3
Kholodov *et al.*[94]	1972	5	243–283			3
Straub[109]	1972	34	294–304			3
Besserer and Robinson[97]	1975	1	274	±60		3
Baade[54]	1983	145	220–304	±3		3
Esper[111.a]	1987	5	245–304		±0.5	3
Holste *et al.*[103a]	1987	5	245–304	±10		3
Duschek *et al.*[58]	1990	42	217–304	±3	±0.025[b]	1
Abdulagatov *et al.*[59a]	1994	2	304			3

[a]The data sets of Esper[111] and Holste *et al.*[103] are different evaluations of the same measurements.
[b]At temperatures above 295 K, the uncertainty rises to ±0.25%.

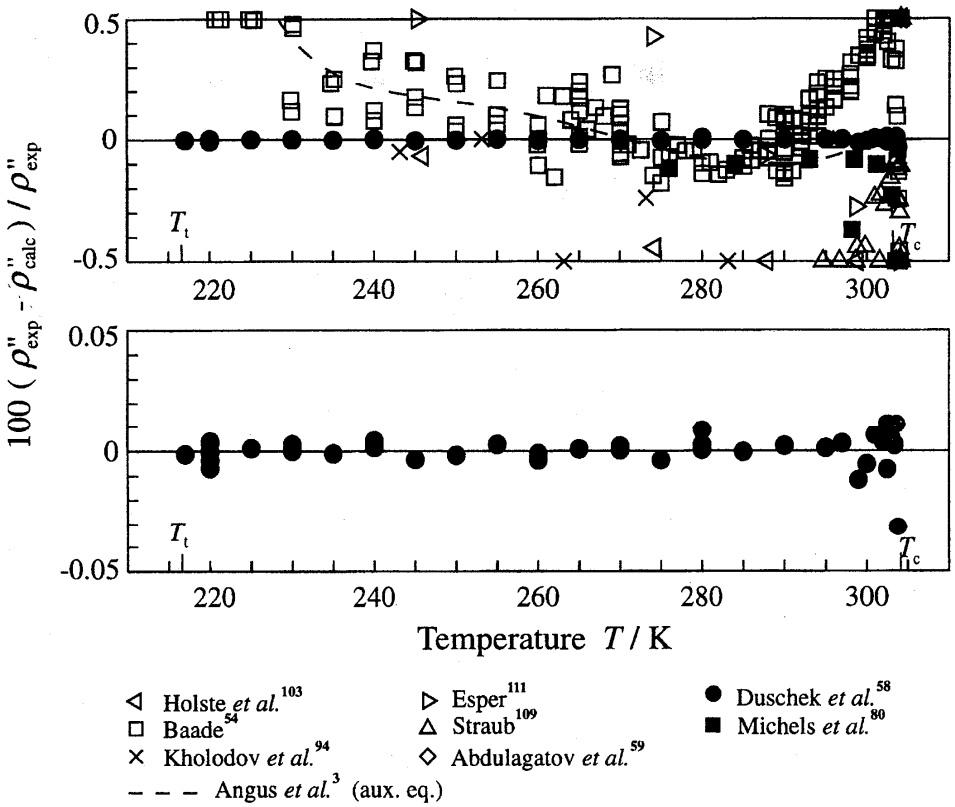

FIG. 5. Relative deviations of selected experimental saturated vapor density data from values calculated from Eq. (3.15). Saturated vapor densities calculated from the corresponding equation of Angus *et al.*[3] are plotted for comparison.

set of Duschek *et al.*[58] is used to develop a simple saturated liquid density equation. Group 2 is restricted to data sets which deliver uncertainties comparable with common uncertainties in the single phase region, that means $\Delta\rho' \leqslant \pm 0.2\%$ outside the critical region. Unfortunately, this criterion is only met by the data sets of Haynes,[110] Esper,[111] and Holste *et al.*;[103] all the other data proved to be less accurate.

For the whole temperature range, the simple correlation

$$\ln\left(\frac{\rho'}{\rho_c}\right) = \sum_{i=1}^{4} a_i \left(1 - \frac{T}{T_c}\right)^{t_i} \tag{3.14}$$

with $T_c = 304.1282$ K, $\rho_c = 467.6$ kg/m^3, $a_1 = 1.9245108$, $a_2 = -0.62385555$, $a_3 = -0.32731127$, $a_4 = 0.39245142$, $t_1 = 0.34$, $t_2 = \frac{1}{2}$, $t_3 = \frac{10}{6}$, and $t_4 = \frac{11}{6}$ describes the data of Duschek *et al.*[58] within their experimental uncertainty. For this equation, both the coefficients and the exponents differ from the formulation given by Duschek *et al.*,[58] which is valid for temperatures on IPTS-68. The changed functional form of the correlation resulted in slightly improved results in the critical region. According to the uncertainty of the selected data, the uncertainty of Eq. (3.14) is estimated to be $\Delta\rho' \leqslant \pm 0.015\%$ for $T_t \leqslant T \leqslant 295$ K, $\Delta\rho' \leqslant \pm 0.04\%$ for 295 K$<T\leqslant$303 K, and $\Delta\rho' \leqslant \pm 1\%$ for 303 K$<T\leqslant T_c$.

Figure 4 shows the poor situation regarding group 1 and group 2 data and the highly accurate representation of the group 1 data. The dashed line corresponds to values calculated from an auxiliary equation given by Angus *et al.*[3] for the saturated liquid density.

3.7 Saturated Vapor Density

Data on the saturated vapor density of carbon dioxide are given in 15 sources, which are listed in Table 9. If the same criterion as mentioned in Sec. 3.6 is used to distinguish between group 2 and group 3 data, only the data of Michels *et al.*[80] can be assigned to group 2. While numerous authors published accurate $p\rho T$ data for the homogeneous gas region, even recent data sets of the saturated vapor density scatter by up to $\pm 0.5\%$ in density.

The new correlation equation for the saturated vapor density,

$$\ln\left(\frac{\rho''}{\rho_c}\right) = \sum_{i=1}^{5} a_i \left(1 - \frac{T}{T_c}\right)^{t_i}, \tag{3.15}$$

with $T_c = 304.1282$ K, $\rho_c = 467.6$ kg/m^3, $a_1 = -1.7074879$, $a_2 = -0.82274670$, $a_3 = -4.6008549$, $a_4 = -10.111178$, $a_5 = -29.742252$, $t_1 = 0.340$, $t_2 = \frac{1}{2}$, $t_3 = 1$, $t_4 = \frac{7}{3}$, and $t_5 = \frac{14}{3}$,

TABLE 10. Summary of the data sets for caloric properties on the liquid–vapor phase boundary of carbon dioxide

Source	Year	Property	No. of data	Temp. range, T (K)	Uncertainty	Group
Eucken and Hauck[112]	1928	c_σ	8	223–293		3
Novikov and Trelin[113]	1960	w''	18	293–304		1
Amirkhanov *et al.*[114]	1972	c_v'[a]	11	304		3
Pecceu and Van Dael[115]	1972	w'	23	217–293	$\Delta w' = \pm 1\%$	1
Magee and Ely[116]	1986	c_σ	77	220–303		1
Abdulagatov *et al.*[59a]	1994	c_v'/c_v''[a]	8	304		3

[a]The specific isochoric heat capacity on the phase boundary cannot be measured directly; such data can only be determined by extrapolation from the homogeneous regions.

describes the group 1 data of Duschek *et al.*[58] within their experimental uncertainty. Compared with the corresponding equation of Duschek *et al.*,[58] both the coefficients and the exponents of the correlation have been revised in order to achieve a slightly improved representation of the data set which has been converted to the ITS-90 temperature scale. Again, the estimation of uncertainty can be guided by the experimental uncertainties. We expect the uncertainty of Eq. (3.15) to be $\Delta\rho'' \leqslant \pm 0.025\%$ for $T_t \leqslant T \leqslant 295$ K, $\Delta\rho'' \leqslant \pm 0.08\%$ for 295 K$<T\leqslant$303 K, and $\Delta\rho'' \leqslant \pm 1\%$ for 303 K$<T\leqslant T_c$.

Figure 5 shows the inexplicably poor data situation, although only measurements published since 1970 and the older data of Michels *et al.*[80] are plotted. The data set of Duschek *et al.*[58] is the only one which enabled the development of an accurate correlation for the saturated vapor density. The correlation equation of Angus *et al.*[3] yields reliable results at temperatures above 275 K, where it mainly depends on the data set of Michels *et al.*[80]

3.8 Caloric Data on the Liquid–Vapor Phase Boundary

Table 10 lists information on the data sets which contain measurements of different caloric properties on the liquid-vapor phase boundary of carbon dioxide. No auxiliary equations have been developed for the description of these data. Instead, group 1 data have been taken into account in the development of the new equation of state, namely in the linearized form during the optimization and in the direct form during the nonlinear fit. More detailed information on these data is given in Sec. 4.9 together with the selected data describing the Maxwell criterion.

The only data which have not been taken into account by direct nonlinear fitting are the data for the specific heat capacity c_σ along the saturated liquid line. Table 3 shows that the relation between the dimensionless Helmholtz energy and c_σ contains the first derivative of the vapor pressure. Therefore, the inclusion of this property into the nonlinear fit in a direct way would involve an interlocked relation to the Maxwell criterion according to Eq. (2.2). To avoid numerical problems, the specific heat capacity along the saturated liquid line has been transformed to the specific isobaric heat capacity at saturated liquid density according to the relation

$$c_p'(T) = c_\sigma(T) - \frac{T}{(\rho')^2} \frac{\left(\frac{\partial p}{\partial T}\right)_v \frac{\mathrm{d}p_s}{\mathrm{d}T}}{\left(\frac{\partial p}{\partial \rho}\right)_T}. \tag{3.16}$$

Up to temperatures of 295 K, the fraction in Eq. (3.16) remains smaller than 20% of c_σ and can be determined from a preliminary equation of state with an estimated uncertainty of less than 0.5%. Thus, the uncertainty caused by the transformation is less than 0.1% in c_p' and is therefore negligible compared with the experimental uncertainty of the c_σ data measured by Magee and Ely.[116] At temperatures above 295 K, the influence of the fractional term increases rapidly and likewise the uncertainty of the derivative $(\partial p/\partial \rho)_T$. Therefore, converted c_σ data at temperatures above 295 K were used only for comparison; see Fig. 20.

4. Experimental Basis of the New Equation of State

In this section, the data sets which describe the thermodynamic properties in the single-phase region of carbon dioxide are presented. For each property considered in this work, both general information on all available data sets and more detailed information on the selected data sets is given in corresponding tables. Again, the data sets are classified into three groups as explained in Sec. 3. Since the data situation in the homogeneous region is less unequivocal than the situation of the different properties on the phase boundaries, numerous data sets are associated with more than one group. Usually these data sets are selected in regions with a poor data situation, but they are used only for comparison in regions in which more reliable data exist.

The information given for the selected data sets comprises the uncertainties estimated by the authors, the uncertainties estimated by ourselves, and the mean square value of the weighting factor f_{wt}, defined by Eq. (2.7). Particularly for some data sets which are more than 20 years old, the uncertainties estimated by the authors and by ourselves differ considerably. The reason for this different assessment might be based on the difference between the scatter and the uncertainty of data, which was not considered by many of the

authors in the past. The uncertainties which we reviewed resulted from extensive comparisons and should be at least a reasonable estimation. These values were used in the weighting procedure.

Section 4.9 contains the corresponding information on all data used for the description of the liquid–vapor equilibrium.

4.1 Thermal Properties

Since 1903, the temperature and pressure dependence of the density of carbon dioxide has been investigated in 59 papers, covering the single-phase region with a total of 5508 data points. Table 11 presents information on the available data sets including their classification.

For temperatures of up to 360 K and pressures of up to 13 MPa, the description of the $p\rho T$ relation is based mainly on the data sets of Duschek *et al.*[154] and Gilgen *et al.*[159] These data sets are supported by the p_s, ρ', ρ'' data measured by Duschek *et al.*,[58] by $p\rho T$ data of the gas phase supplied by Guo *et al.*[157] and by $p\rho T$ data on the 313 K isotherm measured by Nowak *et al.*[160d] All these measurements were performed using the "two-sinker" buoyancy method,[161] which probably provides the most accurate $p\rho T$ data available today. The data from the different two-sinker apparatuses are consistent with each other far within their estimated uncertainties. Nevertheless, in the region of overlapping (mainly at pressures between 8 MPa and 9 MPa) the data sets of Duschek *et al.*[154] and Gilgen *et al.*[159] show small systematic deviations of up to about ±0.01% in density.

On seven isotherms between 233 K and 523 K the two-sinker measurements are supplemented by recent measurements[160,160b] with a new "single-sinker" apparatus[160,160e] which allows measurements up to pressures of 30 MPa. On principle, for densities above 100 kg/m^3, the accuracy of this apparatus is comparable with the accuracy of the two-sinker apparatus, but since the measurements for carbon dioxide were partly made in the test phase of the new apparatus, slightly enlarged uncertainties had to be assumed.

At pressures above 13 MPa, the adjusted data sets of Lau,[149] Kirillin *et al.*[93,137,140] and Michels *et al.*[123] (see Sec. 4.9.2) yield a smooth continuation of the course given by the data of Gilgen *et al.*[159] Up to 30 MPa the adjusted data are generally consistent with the new single-sinker data within ±0.05% in density, but the adjusted data reach up to significantly higher pressures. Due to their high quality, these adjusted data sets are used with substantially increased weighting factors; details are given in Table 12. For temperatures between 523 K and 698 K and pressures up to 34 MPa, the recent data of Fenghour *et al.*[160a] improve the data situ-

TABLE 11. Summary of the data sets available for the $p\rho T$ relation of carbon dioxide

Source	Year	No. of data	Temp. range, T (K)	Pressure range, p (MPa)	Group
Keesom[77]	1903	151	298–333	6.0–14.2	3
Jenkin[117]	1920	82	236–303	1.4–9.7	3
Maas and Mennie[118]	1926	16	203–373	0–0.1	3
Cooper and Maas[119]	1930	30	273–297	0–0.1	3
Cooper and Maas[120]	1931	47	242–350	0–0.1	3
Cawood and Patterson[121]	1933	8	273	0–0.4	3
Michels and Michels[122]	1935	190	273–423	1.6–25.3	1–2
Michels *et al.*[123]	1935	140	298–423	7.5–315.8	1–2
Michels *et al.*[80]	1936	179	276–413	3.6–9.9	2
Reamer *et al.*[124]	1944	147	344–510	0–70.0	3
Bottomley *et al.*[125]	1950	1	295	0.1	3
Batuecas and Losa[126]	1954	32	280–282	0–0.1	3
Kennedy[127,a]	1954		273–1273	2.5–140.0	3
Wentorf[88,b]	1956	106	304	7.4	1–2
Vukalovich and Altunin[128]	1959	120	348–773	2.7–32.7	1–2
Vukalovich and Altunin[129]	1962	205	473–1023	1.1–60.0	1–2
Vukalovich *et al.*[130]	1963	22	923–1076	2.1–15.0	1
Vukalovich *et al.*[131]	1963	124	313–423	2.1–60.0	1–2
Juza *et al.*[132,c]	1965	82	323–748	70.0–400.0	1
Ku and Dodge[133]	1967	13	373	0.6–25.1	3
Sass *et al.*[134]	1967	47	348–398	0.8–25.3	3
Vukalovich *et al.*[135]	1968	168	273–308	0.8–30.0	2
Golovskii and Tsymarnyi[136]	1969	129	217–303	13.0–60.0	1–2
Kirillin *et al.*[137]	1969	21	433–473	2.0–69.0	1–2
Kirillin *et al.*[93]	1969	39	283–308	1.6–49.2	1–2
Kirillin *et al.*[138,d]	1969	99	223–473	1.6–54.0	1–2
Tsiklis *et al.*[139]	1969	50	323–673	200.0–700.0	1
Kirillin *et al.*[140]	1970	24	223–273	2.0–56.0	1
Popov and Sayapov[141]	1970	117	223–303	0.7–30.0	1–2
Vukalovich *et al.*[142]	1970	95	238–268	0.7–19.0	1–2
Schönmann[143,e]	1971	85	373–573	0.4–5.9	3
Kholodov *et al.*[144]	1972	141	293–363	0.5–4.8	3

TABLE 11. Summary of the data sets available for the $p\rho T$ relation of carbon dioxide– Continued

Source	Year	No. of data	Temp. range, T (K)	Pressure range p (MPa)	Group
Kholodov *et al.*[94]	1972	85	243–283	0.5–4.4	3
Levelt Sengers and Chen[50]	1972	22	304–319	7.4–10.0	2
Straub[109]	1972	24	304	7.4	2
Besserer and Robinson[146]	1973	76	310–394	0.7–11.0	3
Rasskazov *et al.*[147]	1974	148	248–303	0.5–5.6	2
Shmonov and Shmulovich[148]	1974	64	681–980	50.0–800.0	1
Lau[149]	1986	69	240–350	1.6–70.0	1–2
Esper[111,f]	1987	73	246–320	0.1–47.7	1–2
Holste *et al.*[103,f]	1987	236	215–448	0.1–50.0	1–2
Jaeschke[150]	1987	245	260–360	0.2–28.5	1
Jaeschke[151]	1987	27	273–353	0.2–30.0	1
Magee and Ely[152]	1988	10	250–330	5.8–27.1	1–2
Ely *et al.*[17]	1989	61	250–330	2.2–35.4	1–2
Hoinkis[145]	1989	186	298–423	0.2–58.0	1–2
McElroy *et al.*[153]	1989	44	303–333	0.8–6.0	3
Duschek *et al.*[154]	1990	362	217–340	0.3–9.0	1
Duschek *et al.*[58,g]	1990	87	295–304	6.0–7.4	1
Jaeschke *et al.*[155]	1990	270	270–320	0.2–12.0	1
Nebendahl[156]	1990	21	337–413	1.9–4.4	3
Guo *et al.*[157]	1992	40	273–293	1.0–3.3	1
Weber[158]	1992	12	320	0.1–6.0	2
Gilgen *et al.*[159]	1993	264	220–360	0.3–13.0	1
Brachthäuser[160]	1993	29	233–523	0.8–30.1	1
Fenghour *et al.*[160a]	1995	120	330–698	3.0–34.2	1
Klimeck *et al.*[160b]	1995	60	300–430	0.5–30.1	1
Gokmenoglu *et al.*[160c]	1996	142	297–425	6.1–66.6	3
Nowak *et al.*[160d]	1997	21	313	8.4–12.1	1

[a]Property tables derived from measurements.
[b]Data partly within the two-phase region.
[c]We used the smoothed data originally published; the unsmoothed data published by Angus *et al.*[3] cannot be used because of very large scatterings.
[d]This paper also contains all data given in Refs. 137, 91 and 140.
[e]The data of Schönmann[143] were reevaluated by Hoinkis;[145] the reevaluated data were considered in this work.
[f]The data published by Esper[111] are reevaluations of the measurements published by Holste *et al.*[103] as experiment III.
[g]Duschek *et al.*[58] published $p\rho T$ data in the vicinity of the phase boundary which were used to determine saturated liquid- and vapor-densities in the near critical region.

ation significantly. The data set of Straub[109] was not included in the data set used for the development of the final equation, but it was used as a sensitive test for the description of the critical region.

4.2 Specific Isobaric Heat Capacity

As regards the specific isobaric heat capacity, the description of the data situation has to be split up into data sets which describe the caloric behavior of the ideal gas and data sets which in addition contain the residual behavior. While the data situation for the caloric properties of the ideal gas is dominated by theoretical approaches, the description of the real gas behavior, where both the ideal and the residual part of the heat capacity are considered, is virtually restricted to experimental investigations. In order to account for these different situations, this section is divided into two subsections.

4.2.1 Experimental Results for the Specific Isobaric Heat Capacity

Today, calorimetric measurements performed with flow apparatuses provide accurate data of the specific isobaric heat capacity over wide ranges of temperature and pressure. In the low density region, these results are usually more accurate than isochoric heat capacity measurements.

Since state-of-the-art data on the speed of sound for carbon dioxide are available only within a very limited temperature range and only up to pressures of 0.9 MPa, the data sets given in Table 13 and especially the selected data sets shown in Table 14 represent the most important source of information on the caloric behavior of carbon dioxide. While the data set of Bender *et al.*[177] provides an accurate description of the low density region, the data of Ernst and Hochberg[178] and Ernst *et al.*[179] allow a precise description of caloric properties up to 90 MPa. At least for subcritical pressures, the accuracy of these data sets is improved by suitable corrections; see Sec. 4.9.3.

TABLE 12. Summary of selected $p\rho T$ data for carbon dioxide; detailed information is given on the uncertainty values estimated by the authors and those estimated by ourselves and used in the weighting procedure

Source	No. of data Mean f^2_{wt}	Uncertainty estimated by the authors Uncertainty estimated by ourselves	Source	No. of data Mean f^2_{wt}	Uncertainty estimated by the authors Uncertainty estimated by ourselves
Michels	9	N.R.E.[a]			
and Michels[122]	4.00	Δp=1000 Pa, $\Delta\rho$=0.2%	Lau[149,c]	42	$\Delta\rho$=0.1%
Michels *et al.*[123,c]	75	$\Delta\rho^b$=0.05%		3.71	ΔT=10 mK, Δp=0.02%, $\Delta\rho$=0.1%
	1.00	Δp=0.02%, $\Delta\rho$=0.1%	Esper[111]	45	$\Delta\rho$=0.03–0.11%
Wentorf[88,c]	87	ΔT=1 mK, Δp=132 Pa, $\Delta\rho$=0.02%		1.00	ΔT=10 mK, Δp=0.015%, $\Delta\rho$=0.05%
	0.09	ΔT=2 mK, Δp=500 Pa, $\Delta\rho$=0.09%	Holste *et al.*[103]	80	ΔT=10 mK, Δp=0.015%,
Vukalovich	44	$\Delta\rho$=0.15–0.35%		0.80	ΔT=10 mK, Δp=0.015%, $\Delta\rho$=0.05%
and Altunin[128]	1.07	$\Delta\rho$=0.4%	Jaeschke[150]	245	N.R.E.
Vukalovich	134	N.R.E.		0.69	ΔT=5 mK, Δp=0.1%, $\Delta\rho$=0.1%
and Altunin[129]	1.00	$\Delta\rho$=0.2%	Jaeschke[151]	27	N.R.E.
Vukalovich *et al.*[130]	22	N.R.E.		1.14	ΔT=5 mK, Δp=0.05%, $\Delta\rho$=0.05%
	1.00	$\Delta\rho$=0.2%	Magee	9	ΔT=30 mK, Δp=0.01%, $\Delta\rho$=0.1%
Vukalovich *et al.*[131]	36	N.R.E.	and Ely[152]	0.16	ΔT=30 mK, Δp=0.01%, $\Delta\rho$=0.1%
	0.64	$\Delta\rho$=0.1%	Ely *et al.*[17]	52	ΔT=30 mK, Δp=0.01%, $\Delta\rho$=0.1–0.15%
Juza *et al.*[132]	82	Δp=2 MPa, $\Delta\rho$=0.3%		1.00	ΔT=30 mK, Δp=0.01%, $\Delta\rho$=0.1–0.15%
	1.00	ΔT=0.2 K, Δp=2 MPa, $\Delta\rho$=0.4%	Hoinkis[145]	72	ΔT=10 mK, Δp=0.01%, $\Delta\rho$=0.16%
Golovskii	108	ΔT=80 mK, Δp=0.08%, $\Delta\rho$=0.15%		1.83	ΔT=10 mK, Δp=0.01%, $\Delta\rho$=0.16%
and Tsymarnyi[136]	2.25	ΔT=80 mK, Δp=0.08%, $\Delta\rho$=0.15%	Duschek *et al.*[154]	362	ΔT=3 mK, Δp=0.006%, $\Delta\rho$=0.015%
Kirillin *et al.*[137,c]	17	$\Delta\rho^b$=0.1%		1.88	ΔT=3 mK, Δp=0.006%, $\Delta\rho$=0.015%
	9.65	Δp=0.05%, $\Delta\rho$=0.2%	Duschek *et al.*[58]	87	$\Delta\rho$=0.03–0.25%[d]
Kirillin *et al.*[93,c]	29	N.R.E.		2.25	$\Delta\rho$=0.03–0.25%
	4.00	Δp=0.05%, $\Delta\rho$=0.2%	Jaeschke *et al.*[155]	268	N.R.E.
				0.75	ΔT=5 mK, Δp=0.05–0.1%,
Kirillin *et al.*[138]	66	$\Delta\rho$=0.15–0.2%	Guo *et al.*[157]	40	$\Delta\rho$=0.05–0.01%
	1.00	Δp=0.05%, $\Delta\rho$=0.2%		2.25	ΔT=3 mK, Δp=0.005%, $\Delta\rho$=0.01%
Tsiklis *et al.*[139]	49	$\Delta\rho$=0.3%	Gilgen *et al.*[159]	264	ΔT=3 mK, Δp=0.005%, $\Delta\rho$=0.01%
	1.00	ΔT=0.5 K, Δp=1 MPa, $\Delta\rho$=1.0%		2.18	ΔT=1.5 mK, Δp=0.006%, $\Delta\rho$=0.015%
Kirillin *et al.*[140,c]	24	$\Delta\rho$=0.1%	Brachthäuser[160]	29	ΔT=1.5 mK, Δp=0.006%, $\Delta\rho$=0.015%
	4.00	Δp=0.05%, $\Delta\rho$=0.1%		1.00	$\Delta\rho$=0.016–0.051%
Popov	73	N.R.E.	Fenghour *et al.*[160a]	120	$\Delta\rho$=0.016–0.051%
and Sayapov[141]	1.00	ΔT=30 mK, Δp=0.05%, $\Delta\rho$=0.15%		1.00	$\Delta\rho$=0.05–0.10%
Vukalovich *et al.*[142]	86	$\Delta\rho$=0.08–0.15%	Klimeck *et al.*[160b]	60	$\Delta\rho$=0.10%
	1.00	ΔT=15 mK, Δp=0.005%,		1.00	ΔT=6 mK, Δp=0.006%, $\Delta\rho$=0.02–0.04%
		$\Delta\rho$=0.08–0.15%			ΔT=6 mK, Δp=0.006%, $\Delta\rho$=0.02–0.04%
Shmonov	60	$\Delta\rho$=0.25–0.5%	Nowak *et al.*[160d]	21	ΔT=1.5 mK, Δp=0.006%, $\Delta\rho$=0.015%
and Shmulovich[148]	1.44	ΔT=0.4 K, Δp=0.2%, $\Delta\rho$=1.0%		1.00	ΔT=1.5 mK, Δp=0.006%, $\Delta\rho$=0.015%

[a]N.R.E.: No reasonable estimation given by the authors.
[b]Consistency is given instead of uncertainty.
[c]Adjusted values were used in the final data sets, see Sec. 4.10.
[d]Uncertainties given for the corresponding saturated liquid and saturated vapor densities.

The data sets of Rivkin and Gukov[171,174] describe the supercritical region of carbon dioxide. Since empirical equations of state may produce misleading results regarding caloric properties within this region, these data sets were considered to be of great interest for the development of the new fundamental equation. Unfortunately, the data proved to be inconsistent with each other and with state-of-the-art $p\rho T$ data. Since the data given in Ref. 174 were deduced from measurements of a mixture with high carbon dioxide content, this data set was classified in group 3. The data set given in Ref. 171 was used only with a reduced weighting factor.

4.2.2 Results for the Specific Isobaric Heat Capacity in the Ideal-Gas State

According to Eq. (2.4), knowledge of the specific isobaric heat capacity in the ideal-gas state forms the basis for the

TABLE 13. Summary of the data sets available for the specific isobaric heat capacity of carbon dioxide

Source	Year	No. of data	Temp. range, T (K)	Pressure range, p (MPa)	Group
Keyes and Collins[162]	1932	1	300	0.2	3
Kistiakowsky and Rice[163,a]	1939	3	300–367	0.1	1
de Groot and Michels[164,a,b]	1948	92	298–423	0.1–206.5	3
Masi and Petkof[165,a]	1952	12	243–363	0.05–0.15	1
Schrock[166]	1952	26	311–783	0.1–7.0	2–3
Koppel and Smith[167]	1960	102	291–322	7.2–8.3	3
Vukalovich *et al.*[168]	1964	23	295–355	0.4–8.2	2–3
Vukalovich and Gureev[169]	1964	8	313–333	0.8–8.0	2–3
Vukalovich *et al.*[170]	1965	86	293–493	1.0–22.2	2–3
Rivkin and Gukov[171]	1968	221	283–403	8.8–24.5	1
Altunin and Kuznetsov[172]	1969	36	293–333	1.0–5.0	2–3
Altunin and Kuznetsov[173]	1970	54	283–373	1.0–6.0	2–3
Rivkin and Gukov[174,c]	1971	46	306–332	8.8–11.8	3
Altunin and Kuznetsov[175]	1972	30	253–323	0.9–6.0	2–3
Saegusa *et al.*[176]	1980	35	245–346	0.3–3.7	3
Bender *et al.*[177,a]	1981	60	233–473	0.1–1.5	1
Ernst and Hochberg[178,a]	1989	9	303	0.3–52.2	1
Ernst *et al.*[179,a]	1989	55	333–393	0.2–90.0	1
Dordain *et al.*[179a]	1994	40	327–416	5.1–25.1	3

[a]The paper also contains extrapolated values for the specific isobaric heat capacity of carbon dioxide in the ideal gas state.
[b]Data calculated from measurements of the $pρT$ relation.
[c]Measurements of a mixture with high carbon dioxide content; the results considered here were extrapolated from the mixture experiments to pure carbon dioxide.

description of the ideal-gas part of the Helmholtz energy, $A^0(\rho,T)$. Results for c_p^0 obtained by the extrapolation of c_p measurements to zero pressure (cf. Table 13) are neither accurate enough for this application nor do they cover a sufficiently wide range of temperature. Therefore, theoretical approaches which describe the caloric behavior of carbon dioxide in the ideal-gas state were reviewed.

Information on the fundamental frequencies of the carbon dioxide molecule can be found in various compilations, but only a few papers contain reliable data on c_p^0, where corrections to the simple rigid rotator, harmonic-oscillator model were taken into account in order to achieve high accuracy. Table 15 summarizes these data sets, of which the data set of Chao[184] is the most recent one. Chao considers first order corrections to the rigid rotator, harmonic-oscillator model, which were developed by Pennington and Kobe;[185] he estimates that the uncertainty of his results is less than ±0.02%.

TABLE 14. Summary of selected data for the specific isobaric heat capacity of carbon dioxide; detailed information is given on the uncertainty values estimated by the authors and those estimated by ourselves and used in the weighting procedure

Source	No. of data Mean f_{wt}^2	Uncertainty estimated by the authors Uncertainty estimated by ourselves
Kistiakowsky	3	$\Delta c_p=0.3\%$
and Rice[163]	1.00	$\Delta T=30$ mK, $\Delta c_p=0.3\%$
Masi	12	$\Delta T=30$ mK, $\Delta c_p=0.1\%$
and Petkof[165]	1.00	$\Delta T=30$ mK, $\Delta c_p=0.1\%$
Rivkin	220	$\Delta T=10$ mK,[a] $\Delta p=0.05\%$, $\Delta c_p=2\%$
and Gukov[171]	0.17	$\Delta T=25$ mK, $\Delta p=0.05\%$, $\Delta c_p=2\%$
Bender *et al.*[177,b]	60	$\Delta c_p=0.1\%$–0.15%
	1.00	$\Delta T=10$ mK, $\Delta p=0.01\%$, $\Delta c_p=0.12\%$
Ernst	9	$\Delta c_p=0.2\%$–0.9%
and Hochberg[178,b]	2.25	$\Delta T=20$ mK, $\Delta p=0.1\%$, $\Delta c_p=0.2$–0.9%
Ernst *et al.*[179,b]	55	$\Delta c_p=0.2\%$–0.9%
	1.92	$\Delta T=20$ mK, $\Delta p=0.1\%$, $\Delta c_p=0.2$–0.9%

[a]The consistency is given instead of the uncertainty.
[b]Corrected values were used in the final data set, see Sec. 4.10.

4.3 Specific Isochoric Heat Capacity

Seven data sets are available for the isochoric heat capacity of carbon dioxide. The information on these data sets is summarized in Table 16. More detailed information on the

TABLE 15. Data sets for the isobaric heat capacity in the ideal-gas state of carbon dioxide calculated by theoretical approaches

Source	Year	Temp. range, T (K)
Wooley[180]	1954	50–5 000
Baehr *et al.*[181]	1968	10–6 000
Gurvich[182]	1979	10–10 000
Chao[183]	1983	50–5 000
Chao[184]	1986	10–1 500

TABLE 16. Summary of the data sets available for the specific isochoric heat capacity of carbon dioxide

Source	Year	No. of data	Temp. range, T (K)	Density range, ρ (kg/m^3)	Group
Eucken and Hauck[112]	1928	8	223–293		3
Michels and Strijland[186,a]	1952	50	297–313	274–839	3
Amirkhanov *et al.*[187]	1970	214[b]	280–393	500–831	2
Amirkhanov and Polikhronidi[188]	1971	733[b]	276–403	512–903	1–2
Edwards[55]	1984	221[c]	301–312	434–467	1
Magee and Ely[116]	1986	113	223–330	88–1140	1–2
Abdulagatov *et al.*[59]	1991	331	304–357	460–510	1–2
Abdulagatov *et al.*[59,a]	1994	88[d]	304–357	460–510	1
Abdulagatov *et al.*[59,b]	1994	230[e]	280–357	460–519	1–2

[a]Evaluation of the data is hindered by unclear temperature assignment.
[b]Some of the data are in the two-phase region.
[c]Preselected numerical values provided by Sengers;[189] 97 measurements describe states within the two-phase region.
[d]These data are selected from the data given in Abdulagatov *et al.*[59]
[e]132 data are in the two-phase region; 88 of the 98 data in the single-phase region are already known from Abdulagatov *et al.*[59,59a]

selected data is given in Table 17. For carbon dioxide, measurements of the isochoric heat capacity are of great importance in the two regions discussed below.

The data set of Magee and Ely[116] yields the only comprehensive description of caloric properties within the high density region. At liquid densities, this data set is limited to pressures above the critical pressure, leaving a gap between the available caloric data in the homogeneous region and on the saturated liquid curve (see Sec. 7.2.2). At densities below 600 kg/m^3, these data can only be represented with systematic deviations clearly outside the uncertainty estimated by the authors. On the other hand, in this region several accurate equations of state[3,15–17] agree with each other and with the new equation of state within about 2% for the isochoric heat capacity, and data of the isobaric heat capacity are met within less than 0.5% by the new equation of state. Based on these facts, we concluded that deviations up to 8% in the isochoric heat capacity were probably due to shortcomings in the data set. Thus, the weighting factors were strongly reduced for the low density measurements.

Within the extended critical region, the data sets of Edwards[55] and of Abdulagatov *et al.*[59,59a,59b] had great influence on the development of the new equation of state. (Edwards's thesis[55] only contains graphical illustrations of the results. The data used here were provided by Sengers.[189]) The reduced weighting factors given in Table 17 were chosen because of the large number of data points within a small and very sensitive region. The use of these data sets with $f_{wt}=1$ would have resulted in an overemphasis of the critical region; details are given in Sec. 5.

The recent data of Abdulagatov *et al.*[59] were first presented in the *Proceedings of the 11th Symposium on Thermophysical Properties* in Boulder in 1991. When the corresponding paper[59a] was published three years later, it contained only 88 data points selected from the 331 data points given in the proceedings. In the same year, another paper[59b] was published which contains the 88 points published before, 10 additional points on one isochore in the homogeneous phase, and 132 additional points in the two

TABLE 17. Summary of selected data for the specific isochoric heat capacity of carbon dioxide; detailed information is given on the uncertainty values estimated by the authors and those estimated by ourselves and used in the weighting procedure

Source	No. of data Mean f_{wt}^2	Uncertainty estimated by the authors Uncertainty estimated by ourselves
Amirkhanov	18	$\Delta T=5$ mK, $\Delta c_v=2$–4%
and Polikhronidi[188]	1.00	$\Delta T=50$ mK, $\Delta\rho=0.05\%$, $\Delta c_v=2.5\%$
Edwards[55,a]	124	$\Delta c_v=0.75\%$[b]
	0.16	$\Delta T=1$ mK, $\Delta\rho=0.05\%$, $\Delta c_v=2\%$
Magee and Ely[116]	80	$\Delta T=10$ mK, $\Delta\rho=0.1\%$, $\Delta c_v=0.5$–2%
	0.37	$\Delta T=10$ mK, $\Delta\rho=0.1\%$, $\Delta c_v=0.5$–2%
Abdulagatov *et al.*[59]	233	$\Delta\rho=0.023\%$, $\Delta c_v=2$–3.5%
	0.25	$\Delta T=10$ mK, $\Delta\rho=0.05\%$, $\Delta c_v=5\%$
Abdulagatov *et al.*[59a]	88	$\Delta\rho=0.023\%$, $\Delta c_v=2$–3.5%
	0.25	$\Delta T=10$ mK, $\Delta\rho=0.05\%$, $\Delta c_v=5\%$
Abdulagatov *et al.*[59b]	10	$\Delta\rho=0.023\%$, $\Delta c_v=2$–3.5%
	0.25	$\Delta T=10$ mK, $\Delta\rho=0.05\%$, $\Delta c_v=5\%$

[a]Adjusted values were used in the final data set; see Sec. 4.10.
[b]The precision is given instead of the uncertainty.

TABLE 18. Summary of the data sets available for the speed of sound of carbon dioxide

Source	Year	No. of data	Temp. range, T (K)	Pressure range, p (MPa)	Group
Herget[191]	1940	195	301–311	7.0–10.3	2
Novikov and Trelin[192]	1962	236	288–373	3.0–10.0	1
Pitaevskaya and Bilevich[193,a]	1973	176	298–473	50.0–450.0	1–2
Lemming[194]	1989	50	240–360	0.4–0.9	1

[a]Smoothed data.

TABLE 19. Summary of selected data for the speeds of sound of carbon dioxide; detailed information is given on the uncertainty values estimated by the authors and those estimated by ourselves and used in the weighting procedure

Source	No. of data Mean f^2_{wt}	Uncertainty estimated by the authors Uncertainty estimated by ourselves
Novikov	234	N.R.E.[a]
and Trelin[192]	0.77	ΔT=0.1 K, Δp=0.1%, Δw=0.5%
Pitaevskaya	144	N.R.E.[a]
and Bilevich[193]	2.25	ΔT=0.1 K, Δp=0.2%, Δw=2%
Lemming[194]	44	ΔT=8 mK, Δp=4.2 mbar, Δw=0.015%
	0.06	ΔT=8 mK, Δp=4.2 mbar, Δw=0.015%

[a]N.R.E.: No reasonable estimation given by the author.

phase region. The uncertainty of the data of Abdulagatov *et al.* was estimated to be at least as big as the scatter visible in the original data set.[59]

The papers of Lipa *et al.*,[190,52] which are often cited in literature on carbon dioxide, do not contain numerical results. Since the data of Edwards[55] cover the same region, were measured with the same equipment, and are less influenced by impurities,[55] the data of Lipa *et al.* were not considered in this work.

4.4 Speed of Sound

Three of the four data sets available for the speed of sound of carbon dioxide were used for the development of the new equation of state. Table 18 contains the available data sets and Table 19 gives additional information on the selected data. The data sets of Novikov and Trelin[192] and of Pitaevskaya and Bilevich[193] provide important information on the extended critical region and the high pressure region, respectively. Though the quality of the data published by Lemming[194] is superior to the other data sets, these data were used only with reduced weighting factors. In the gas region, the residual part of the speed of sound is less than 2% of the total speed of sound at pressures below 1 MPa. Since the uncertainty of measurements is related to the total value of the speed of sound and not only to the residual part, the contribution of these data for the development of an empirical correlation describing the residual fluid behavior is very limited.

TABLE 20. Summary of the data sets available for enthalpy differences of carbon dioxide

Source	Year	No. of data	Temp. range, T (K)	Pressure range, p (MPa)	Group
Maas and Barnes[200]	1926	4	212–298	0.1	3
Koppel and Smith[167]	1960	102	291–322	7.2–8.3	3
Vukalovich and Masalov[201]	1964	54	423–523	2.5–9.8	2
Vukalovich and Masalov[202]	1964	68	573–773	2.5–9.8	2
Möller *et al.*[203]	1993	10	233–358	15.5	1

TABLE 21. Summary of the data sets for differences of the internal energy of carbon dioxide

Source	Year	No. of data	Temp. range, T (K)	Density range, ρ (kg/m^3)	Group
Krüger[204]	1964	454[a]	274–325	190–870	1–2
Baehr[205]	1968	47	291–316	466	3

[a]Some of the measured temperature intervals partly reach into the two-phase region.

Besides the data presented in Table 18, five papers[195–199] are available which deal with the speed of sound in the immediate vicinity of the critical point. None of these papers, which were published between 1951 and 1970, contains numerical results. We did not try to evaluate the graphical representations given in these papers since the special problems connected with experimental work in the critical region were not adequately considered at that time.

4.5 Enthalpy

The literature sources which deal with enthalpy measurements are summarized in Table 20. The data of Vukalovich and Masalov[201,202] and of Möller *et al.*[203] were considered in this work, but only the data of Möller *et al.* were used with the uncertainties given by the authors (10 data selected, mean value of f^2_{wt}=2.78, Δh=0.7% or Δh=0.6 kJ/kg, whichever is greater). These data provide important information at high densities where the data situation for caloric properties is poor. The data of Vukalovich and Masalov[201,202] were used to test the quality of the new equation with regard to caloric properties at high temperatures.

4.6 Internal Energy

Table 21 lists the general information on the two data sets which are available for differences of internal energy. The data measured on the critical isochore by Baehr[205] were not used since the temperature displacement of the $(\partial u/\partial T)_v$ maximum observed by Baehr could not be explained. The 150 selected data of Krüger,[204] which do not reach into the two-phase region, were used with estimated uncertainties of ΔT=40 mK, $\Delta\rho$=0.2%, Δu=2%–4%, and a mean weighting factor of f^2_{wt}=0.88. The uncertainties given by the author (ΔT=10 mK, $\Delta\rho$=0.03%, Δu=1.4%–3%) are too small to explain the scatter of the data.

4.7 Joule–Thomson Coefficient

Since data of the Joule–Thomson coefficient can only be used in the nonlinear fitting procedure and not in the linear algorithms of the optimization procedure, their influence on the development of an empirical fundamental equation is fairly small. The data of Bender *et al.*[177] are the only ones which were included in the data set used for the nonlinear fit

TABLE 22. Summary of the data sets available for the Joule–Thomson coefficient of carbon dioxide

Source	Year	No. of data	Temp. range, T (K)	Pressure range, p (MPa)	Group
Burnett[207]	1923	127	273–393	2.0–7.7	3
Roebuck *et al.*[81]	1942	151	198–573	0.1–20.7	3
de Groot and Michels[164,a]	1948	92	298–423	0.1–206.5	3
Vukalovich *et al.*[206,b]	1970	131	253–343	0.6–5.9	2
Altunin and Gureev[208]	1972	92	293–500	1.5–22.0	2–3
Bender *et al.*[177]	1981	35	233–473	0.1–1.5	1
Cusco *et al.*[208a,b]	1995	33	350–500	1.0–4.6	3

[a]Joule–Thomson coefficients calculated from measured $p\rho T$ data.
[b]Isothermal Joule–Thomson coefficients, $\delta_T = c_p\mu$.

(34 data were selected with ΔT=10 mK, Δp=0.01%, $\Delta\mu$=0.4%, and f^2_{wt}=0.36). The data of Vukalovich *et al.*[206] proved to be a sensitive test for the consistent description of the gas region. Table 22 gives a survey of the data sets dealing with the Joule–Thomson coefficient.

4.8 Virial Coefficients

The literature on carbon dioxide contains many papers in which information on the second and third virial coefficient is given. Table 23 summarizes the corresponding sources.

TABLE 23. Summary of the data sets available for the second and third virial coefficient of carbon dioxide. For reasons explained in the text, no data were assigned to Group 1

Source	Year	No. of data B/C	Temp. range, T (K)	Group
Michels and Michels[122]	1935	13/13	273–423	3/3
Schäfer[209]	1937	16/···	203–273	3/···
MacCormack and Schneider[210]	1950	9/9	273–873	3/3
Cottrel and Hamilton[211]	1955	7/···	303–333	3/···
Pfefferle *et al.*[212]	1955	2/2	303	3/3
Cottrell *et al.*[213]	1956	3/···	303–363	3/···
Cook[214]	1957	6/···	213–303	3/···
Masia and Pena[215]	1958	6/···	298–423	3/···
Butcher and Dadson[216]	1963	13/13	263–473	3/3
Huff and Reed[217]	1963	10/···	298–510	3/···
Vukalovich and Masalov[218]	1966	18/18	423–773	2/3
Dadson *et al.*[219]	1967	9/···	263–398	3/···
Ku and Dodge[133]	1967	1/1	373	3/3
Sass *et al.*[134,a]	1967	3/···	348–398	3/···
Timoshenko *et al.*[220]	1970	9/···	224–313	3/···
Vukalovich *et al.*[142]	1970	10/10	253–343	3/3
Vukalovich *et al.*[206]	1970	14/···	238–308	3/···
Waxman *et al.*[221]	1973	6/···	273–423	2/···
Bender *et al.*[177]	1981	4/···	233–263	3/···
Ohgaki *et al.*[222]	1984	2/···	423–473	3/···
Holste *et al.*[103]	1987	18/16	217–448	2/2
Mallu *et al.*[223]	1987	3/···	323–423	3/···
Hoinkis[145]	1989	4/4	298–423	2/2
Mallu *et al.*[224,b]	1989	···/3	323–423	···/3
Mc Elroy *et al.*[153]	1989	4/4	303–333	3/3
Duschek *et al.*[154]	1990	7/4	220–340	2/2

[a]Virial expansion developed in pressure.
[b]This paper additionally includes the values already published[223] in 1987.

Recently, Span[225] pointed out that it was not very useful to include experimental second and third virial coefficients into the data set used for the development of a wide-range equation. Most of the data sets descend from $p\rho T$ measurements which have been evaluated in order to determine virial coefficients. Thus, the use of the original measurements yields much better access to the desired experimental information. Furthermore, fitting an equation of state to virial coefficients is only useful if the terms of the equation corresponding to the virial coefficients are independent of each other, as is the case in a simple virial expansion. However, if an equation of state contains exponential functions, this condition is no longer met. Thus, in this article, the available values for virial coefficients were only used for comparison; none of the data sets was assigned to group 1.

At temperatures below 220 K, however, the whole contribution of the third virial coefficient $[p/(\rho RT) = \ldots + C\rho^2 + \ldots]$ is smaller than the uncertainty of the most recent $p\rho T$ data[154] throughout the gas region. Therefore, at low temperatures a physically unreasonable representation of the third virial coefficient calculated from an equation of state may occur if the equation was fitted only to $p\rho T$ data. Since reliable values of the third virial coefficient cannot be established by an evaluation of experimental $p\rho T$ data in this temperature range, 13 values of the third virial coefficient were calculated from a simple polynomial equation which describes *all* the selected data of the different thermodynamic properties in the gas region within their experimental uncertainty and yields a reasonable plot of the third virial coefficient at low temperatures. These "artificial" data of the third virial coefficient were then used during the development of the new equation of state.

4.9 Liquid–Vapor Equilibrium

During the procedure of optimizing the structure of the new equation of state, the liquid–vapor equilibrium was used in a linearized way.[32,30] The data set used for this purpose consists of values of $p_s(T)$, $\rho'(T)$, and $\rho''(T)$ at 205 temperatures which were calculated from Eqs. (3.13) to (3.15). These data cover the whole liquid–vapor phase boundary with temperature intervals which decrease when approaching the

TABLE 24. Summary of selected data describing the liquid–vapor phase equilibrium of carbon dioxide; detailed information is given on the uncertainty values estimated by the authors and those estimated by ourselves and used in the weighting procedure

Source	Property	No. of data Mean f^2_{wt}	Uncertainty estimated by the authors Uncertainty estimated by ourselves
Novikov and Trelin[113,b]	w''	18	N.R.E.[a]
		1.00	$\Delta T = 10\,\mathrm{mK}, \Delta w'' = 0.5\%$
Pecceu and Van Dael[115]	w'	23	$\Delta w' = 1\%$
		1.23	$\Delta T = 0.1\,\mathrm{K}, \Delta w' = 0.5\%$
Magee and Ely[116]	c_σ	73[c]	N.R.E.[a]
		2.04	$\Delta T = 10\,\mathrm{mK}, \Delta c_\sigma = 1\%$
Duschek *et al.*[58]	p_s	109	$\Delta T = 3\,\mathrm{mK}, \Delta p_s = 0.005\%$
		1.00	$\Delta T = 3\,\mathrm{mK}, \Delta p_s = 0.005\%$
Duschek *et al.*[58]	ρ'	50	$\Delta T = 3\,\mathrm{mK}, \Delta \rho' = 0.015\%$
		1.00	$\Delta T = 3\,\mathrm{mK}, \Delta \rho' = 0.015\%$
Duschek *et al.*[58]	ρ''	42	$\Delta T = 3\,\mathrm{mK}, \Delta \rho'' = 0.025\%$
		1.00	$\Delta T = 3\,\mathrm{mK}, \Delta \rho'' = 0.025\%$

[a]N.R.E.: No reasonable estimation given by the authors.
[b]In the final data set adjusted values were used; see Sec. 4.10.
[c]Only data at $T<295$ K were considered; see Sec. 3.8.

critical temperature. Additionally, the group 1 caloric data already presented in Table 10 were used to fit the new equation of state.

The final equation was nonlinearly fitted directly to the phase equilibrium data of Duschek *et al.*[58] and to the caloric data. Table 24 gives detailed information on the experimental caloric and thermal data used for the description of the liquid–vapor equilibrium.

4.10 Adjustment of Data

In order to achieve a final data set which is as consistent as possible, some of the selected data had to be adjusted. As a result, three groups of data can be distinguished which were corrected for different reasons. These three groups are explained in the following subsections.

4.10.1 Adjustment of Data Sets Describing the Critical Region

For the description of the thermodynamic surface in the immediate vicinity of the critical point, the difference between the measured temperature and the critical temperature is more important than the absolute temperature, and this temperature difference is probably also less influenced by systematic deviations or by impurities of the sample. If the corresponding critical temperature is given, the absolute temperature can be corrected by the difference between this value and the value used in this work [cf. Eq. (3.5)]. This technique was used for two important sets of caloric data:

Edwards[55]: $$T_{68} = T_{\mathrm{Ed.}} + 29.8\ \mathrm{mK}, \tag{4.1}$$

Novikov and Trelin[113]: $$T_{48} = T_{\mathrm{No.}} - 44\ \mathrm{mK}. \tag{4.2}$$

Wentorf[88] did not give any information on the critical temperature corresponding to his $p\rho T$ data, but a similar correction can be established based on the pressure on the critical isochore. In reasonable accordance with earlier suggestions,[154,24,17,50] we used

Wentorf[88]: $$T_{48} = T_{\mathrm{We.}} - 27\ \mathrm{mK}. \tag{4.3}$$

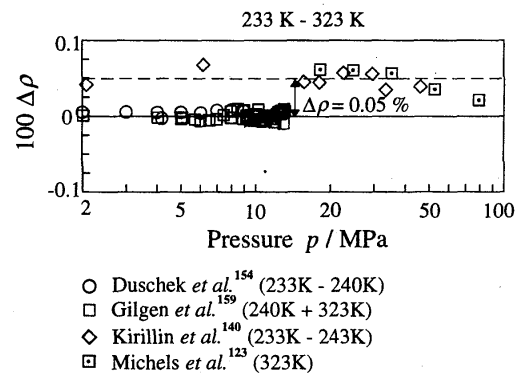

FIG. 6. Relative deviations $100\ \Delta\rho = 100\ (\rho_{\mathrm{exp}} - \rho_{\mathrm{calc}})/\rho_{\mathrm{exp}}$ of experimental $p\rho T$ data from values calculated from Eq. (6.1). This figure illustrates the reason for adjusting the data of Kirillin *et al.*[140] and Michels *et al.*[123] (see Sec. 4.10.2).

4.10.2 Adjustment of $p\rho T$ Data

Reasonable adjustments can be applied to $p\rho T$ measurements if systematic deviations occur in a region where a data set and a set of reference data overlap. In this way, accurate information on the $p\rho T$ relation can be obtained up to pressures of approximately 100 MPa, whereas the two-sinker data of Duschek *et al.*[154] and Gilgen *et al.*[159] are limited to 9 MPa and 13 MPa, respectively and the single-sinker data of Brachthäuser[164] and Klimeck *et al.*[160b] are limited to 30 MPa.

Such simple corrections were used for the data sets of the following:

Kirillin *et al.*[137,93,140]: $$\rho - \rho_{\mathrm{Ki.}} \cdot 0.999\,5, \tag{4.4}$$

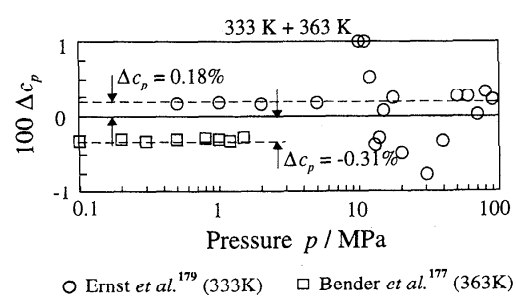

FIG. 7. Relative deviations $100\ \Delta c_p = 100\ (c_{p,\mathrm{exp}} - c_{p,\mathrm{calc}})/c_{p,\mathrm{exp}}$ of experimental c_p data from specific isobaric heat capacities calculated from Eq. (6.1). This figure illustrates the reason for correcting the data of Ernst *et al.*[179] and Bender *et al.*[177] (see Sec. 4.10.3).

TABLE 25. Temperature dependent corrections of isobaric heat capacity data

Temperature, T(K)	$\frac{c_{p,\text{cor.}}-c_{p,\text{exp.}}}{c_{p,\text{exp.}}}$
Bender *et al.*[177]	
233	+0.40%
243	+0.25%
273	+0.13%
323	+0.05%
363	+0.31%
393	+0.14%
423	+0.10%
473	−0.17%
Ernst and Hochberg[178]	
303	+0.36%
Ernst *et al.*[179]	
333	−0.18%
363	±0.00%
393	−0.37%

Michels *et al.*[123]: $\rho=\rho_{\text{Mi.}}\cdot 0.999\,5,$ (4.5)

Lau[149]: $\rho=\rho_{\text{La.}}\cdot 0.999\,3.$ (4.6)

Figure 6 shows an example for the justification of these adjustments by combining two very different isotherms in a single deviation plot. The 99 measurements published by Kirillin *et al.* only in Ref. 138 cannot be adjusted according to Eq. (4.4). The corrected data of Michels *et al.*[123] were used only at pressures above 18 MPa. In regions where the temperature and pressure dependence of the density is strong, the data adjusted according to Eq. (4.5) also yield unsatisfactory results.

During the last 20 years, different authors[50,21,24,27] have suggested corrections for the temperature scale used by Michels *et al.*[80,123] and Michels and Michels.[122] Possible corrections were tested in this work, but no reasonable temperature shift between the ITS-27 temperature scale and the temperature scale used at the Van der Waals laboratory at that time could be established. If the systematic deviation of these data is due to errors in the temperature scale, different scales have to be assumed for the measurements published in different papers of Michels. Since the data situation in the gas and extended critical region has improved significantly, it was decided not to use Michels' data within these regions.

4.10.3 Correction of Isobaric Heat Capacities

Since the low pressure limit of the isobaric heat capacity, c_p°, is known very well for carbon dioxide (see Sec. 6.1), temperature dependent errors of measured isobaric heat capacities can be determined easily. Figure 7 shows systematic deviations of data measured by Bender *et al.*[177] and by Ernst *et al.*[179] Again, two different isotherms are combined in a single deviation plot. A systematic error of the new equation for the residual part of the Helmholtz energy, Eq. (6.5), would result in deviations which increase with pressure since the residual contribution to the isobaric heat capacity increases.

To compensate for these temperature-dependent deviations, the data sets of Bender *et al.*,[177] Ernst and Hochberg,[178] and Ernst *et al.*[179] were corrected according to the values given in Table 25.

5. Description of Thermodynamic Properties in the Critical Region

It is well known[56,226] that thermodynamic properties can be described by so called "power laws" along certain paths throughout the critical region of a pure fluid. This kind of description, which was originally introduced in 1896 by Verschaffelt[227] as an empirical attempt, has been supported by recent theoretical results. In particular, the renormalization group approach introduced by Wilson[228] extended knowledge on the behavior of pure fluids in the critical region and resulted in "universal" values for the critical exponents. These values are defined as power-law exponents in the limit of vanishing distance to the critical point. Table 26 shows some of the most important power laws and gives different values for the corresponding critical exponents, which were established by evaluation of the renormalization group theory,[56] by expansion of a classical equation with a so-called three-point contact at the critical point, and by expansion of a classical equation with a so-called five-point contact at the critical point. None of the classical equations is able to reproduce the values predicted by the renormalization group theory.

TABLE 26. Examples for power laws describing thermodynamic properties along certain paths throughout the critical region

Property	Power law	Described path	Critical exponent	Values determined by evaluation of		
				RG theory[a]	3-point eq.[b]	5-point eq.[c]
Densities at saturation	$(\rho'-\rho'')\sim(T_c-T)^{\beta}$	phase boundary	β	0.326±0.002	0.5	0.25
Isothermal compressibility	$K_T\sim\lvert T-T_c\rvert^{-\gamma}$	crit. isochore	γ	1.239±0.002	1	1
Pressure	$\lvert p-p_c\rvert\sim\lvert\rho-\rho_c\rvert^{\delta}$	crit. isotherm	δ	4.80±0.02	3	5
Isochoric heat capacity	$c_v\sim\lvert T-T_c\rvert^{-\alpha}$	crit. isochore	α	0.110±0.003	0	0

[a]According to Sengers and Levelt Sengers.[56]
[b]Such an equation of state is constrained at the critical point by the conditions $(\partial p/\partial\rho)_T=0$ and $(\partial^2 p/\partial\rho^2)_T=0$, where $(\partial^3 p/\partial\rho^3)_T>0$.
[c]In addition to the conditions given in footnote b this equation yields $(\partial^3 p/\partial\rho^3)_T=0$ and $(\partial^4 p/\partial\rho^4)_T=0$, where $(\partial^5 p/\partial\rho^5)_T>0$.

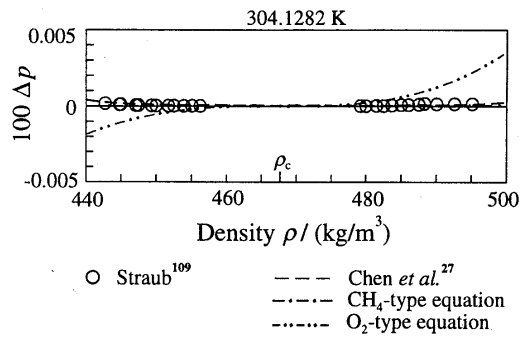

FIG. 8. Relative deviations $100\ \Delta p = 100\ (p_{exp} - p_{calc})/p_{exp}$ of experimental $p\rho T$ data on the critical isotherm from values calculated from Eq. (6.1). Values calculated from the crossover equation of Chen *et al.*[27] and from refitted equations using the CH_4- and O_2-form (see Sec. 5.1) are plotted for comparison.

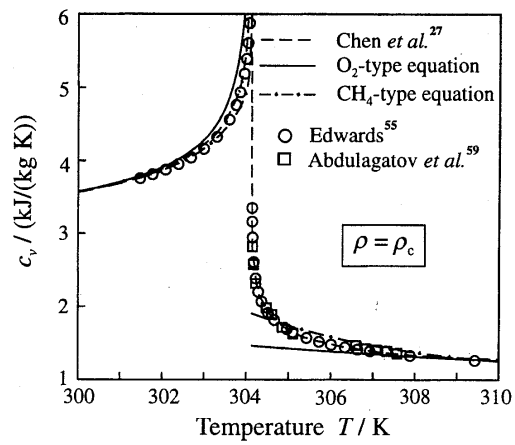

FIG. 9. Representation of representative isochoric heat capacity data in the critical region. The plotted curves correspond to values calculated from the crossover equation of Chen *et al.*[27] and from refitted equations using the CH_4- and O_2-form (see Sec. 5.1).

5.1 Limitations of Analytical Equations of State

Usually it is concluded that analytic equations of state cannot represent the properties of pure fluids within the critical region because they do not yield correct critical exponents. For most of the properties considered in this article, this conclusion is incorrect if state-of-the-art equations are considered.

In this section, the results obtained within the critical region from two wide-range equations are compared with experimental results and with values which were calculated from a nonanalytic equation especially designed for the description of the extended critical region. For this purpose, we chose the crossover equation of Chen *et al.*[27] The critical parameters of the crossover equation were changed to the values used in this work because otherwise the comparison of equations with different critical parameters would produce misleading results in the immediate vicinity of the critical point. To give an example, which is typical for a modern wide-range equation, we fitted the equation published by Schmidt and Wagner[4] for oxygen to the data set used in this work; this equation is referred to as O_2-type equation. The equations of Ely[14] and Ely *et al.*[15] use the same functional form but these equations are constrained to different critical parameters. To illustrate the limits of an analytic equation of state, we refitted the formulation published by Setzmann and Wagner[30] for methane which is referred to as a CH_4-type equation. As far as the description of the critical region is concerned, this equation is probably the most efficient analytic equation available today.

Figure 8 shows the relative deviation between pressures calculated from the new equation of state for carbon dioxide [Eq. (6.1)], from the refitted CH_4- and O_2-type equations, and from the crossover equation of Chen *et al.*,[27] compared with the very consistent data measured by Straub,[109] directly on the critical isotherm of carbon dioxide. (None of the wide-range equations was fitted to the data of Straub; these data only served as a consistency check for the critical region; cf. Sec. 4.1.) In the resolution chosen in Fig. 8, only the O_2-type equation shows the too steep course of the critical isotherm which is to be expected from an analytic equation of state. The analytic CH_4-type equation and the new equation of state yield almost identical results and represent the data as accurately as the crossover equation, even though they do not result in the limit for the corresponding critical exponent δ which is predicted by the renormalization group theory.

Along the critical isotherm, $p\rho T$ data can be very accurately described with a wide-range equation because the corresponding power law describes pressure differences which vanish when approaching the critical point (cf. Table 26). Thus, different values for the critical exponent δ, which is defined as limit $|\rho - \rho_c| \rightarrow 0$, hardly effect the representation of the $p\rho T$ surface. Most of the properties considered in this article show a similar behavior when approaching the critical point.

However, there are two properties which behave in a completely different way: the specific isochoric heat capacity, c_v, and the speed of sound, w. The evaluation of analytic equations yields a critical exponent $\alpha = 0$, which results in a finite value of c_v at the critical point, whereas the renormalization group theory predicts $\alpha = 0.110$, resulting in a slow divergence of the specific isochoric heat capacity at the critical point.

Figure 9 shows measured specific isochoric heat capacities on the critical isochore of carbon dioxide and the corresponding values calculated from the O_2-type equation, the CH_4-type equation, and the crossover equation. When approaching the critical temperature, only the crossover equation is able to follow the steep course of the data. The CH_4-type equation fails within an interval of approximately ± 0.5 K around the critical temperature and the O_2-type equation fails within an interval of approximately ± 2 K.

Similar results can be obtained for the speed of sound since it is related to the reciprocal value of the isochoric heat

capacity. From a theoretical point of view, the speed of sound is expected to vanish at the critical point, whereas analytic equations yield only a finite minimum. Again, the temperature interval, where the analytic equations fail, extends over approximately ± 0.5 K and ± 2 K, respectively, around the critical temperature.

5.2 Use of Nonanalytic Terms as an Integral Component in an Empirical Wide-Range Equation of State

The performance of a sophisticated analytic equation of state, such as the CH_4-type equation, is completely sufficient for any technical application within the critical region. However, because of the scientific importance of the critical region of carbon dioxide, an improved description of caloric properties was regarded as desirable at least as long as the numerical expense for the evaluation of the resulting correlation remains justifiable. Therefore, we rejected models which employ an iterative procedure for the relation between the physical variables T and ρ and the mathematical variables used, like switching[3,229] and transformation[26] approaches.

In the context where the fundamental equation presented in this article is clearly empirical, an asymptotic behavior corresponding to the predictions of the renormalization group theory was considered to be of minor importance; mixing up theoretical and empirical approaches may even produce misleading results. Therefore, the attempt was made to extend the qualitatively correct behavior of an empirical wide-range equation to the immediate vicinity of the critical point by introducing special nonanalytic terms.

The development of such formulations started with an examination of the relations between the reduced Helmholtz energy and caloric properties. The specific isobaric heat capacity can be expressed as

$$\frac{c_p}{R}=\underbrace{-\tau^2(\phi^{\mathrm{o}}_{\tau\tau}+\phi^{\mathrm{r}}_{\tau\tau})}_{\frac{c_v}{R}}+\frac{\overbrace{(1+\delta\phi^{\mathrm{r}}_{\delta}-\delta\tau\phi^{\mathrm{r}}_{\delta\tau})^2}^{\sim\left(\frac{\partial p}{\partial T}\right)_\rho^2}}{\underbrace{1+2\delta\phi^{\mathrm{r}}_{\delta}+\delta^2\phi^{\mathrm{r}}_{\delta\delta}}_{\sim\left(\frac{\partial p}{\partial \rho}\right)_T}}. \tag{5.1}$$

where R corresponds to the specific gas constant, ϕ to the ideal (superscript o) and residual (superscript r) part of the reduced Helmholtz energy, τ to the inverse reduced temperature, and δ to the reduced density. The quantities τ and δ used as subscripts indicate the corresponding derivative of ϕ; see the footnote of Table 3. Since $(\partial p/\partial\rho)_T^{-1}$ grows much faster when approaching the critical point than c_v, in Eq. (5.1) the specific isobaric heat capacity is dominated by the fraction, which is closely related to the representation of $p\rho T$ data. Thus, an equation which yields an accurate description of the $p\rho T$ surface within the critical region should also yield reliable values of the specific isobaric heat capacity.

The situation is different for the isochoric specific heat capacity which is given by

$$\frac{c_v}{R}=-\tau^2(\phi^{\mathrm{o}}_{\tau\tau}+\phi^{\mathrm{r}}_{\tau\tau}). \tag{5.2}$$

If the second derivative of the residual part of the Helmholtz energy with respect to τ is finite at the critical point, the value of the specific isochoric heat capacity is also finite. Only an equation with a nonanalytic behavior in $\phi^{\mathrm{r}}_{\tau\tau}$ can reproduce the expected divergence in c_v. At the same time, such a formulation would result in vanishing values of the speed of sound since w corresponds to

$$\frac{w^2}{RT}=\underbrace{1+2\delta\phi^{\mathrm{r}}_{\delta}+\delta^2\phi^{\mathrm{r}}_{\delta\delta}}_{\sim\left(\frac{\partial p}{\partial \rho}\right)_T}-\frac{\overbrace{(1+\delta\phi^{\mathrm{r}}_{\delta}-\delta\tau\phi^{\mathrm{r}}_{\delta\tau})^2}^{\sim\left(\frac{\partial p}{\partial T}\right)_\rho^2}}{\underbrace{\tau^2(\phi^{\mathrm{o}}_{\tau\tau}+\phi^{\mathrm{r}}_{\tau\tau})}_{-\frac{c_v}{R}}}. \tag{5.3}$$

At the critical point, the expression $(\partial p/\partial\rho)_T$ becomes zero and $(\partial p/\partial T)_\rho$ is a finite value. Thus, if c_v becomes infinite, the speed of sound becomes zero.

Consequently, a formulation has been developed which can be included into an empirical wide-range equation of state as a regular contribution to the usual sum of terms and which yields the intended nonanalytic behavior of $\phi^{\mathrm{r}}_{\tau\tau}$. Such a formulation has to fulfill three additional conditions:

- The values resulting for $\phi^{\mathrm{r}}_{\tau\tau}$ have to be finite everywhere except at the critical point.
- Singular behavior of the other second derivatives and all derivatives with respect to δ has to be avoided everywhere. However, there are no further restrictions for the behavior of these derivatives—the *complete* equation of state has to be designed to behave in a special way and not only a single term in the equation.
- Within the δ,τ surface of the critical region, the maximum of $\phi^{\mathrm{r}}_{\tau\tau}$ has to follow the course of the saturated vapor and saturated liquid line in order to avoid unreasonable c_v maxima in the single-phase region.

These conditions can be fulfilled if a formulation of the following mathematical form is introduced as the ith term in an equation for the residual part of the Helmholtz energy, namely

$$\phi^{\mathrm{r}}_i=n_i\Delta^{b_i}\delta\exp[-C_i(\delta-1)^2-D_i(\tau-1)^2] \tag{5.4}$$

with

$$\Delta=\{(1-\tau)+A_i[(\delta-1)^2]^{1/(2\beta_i)}\}^2+B_i[(\delta-1)^2]^{a_i}.$$

The exponential function damps the influence of this expression outside the critical region. The distance function Δ^{b_i} introduces the nonanalytic behavior and ensures that the

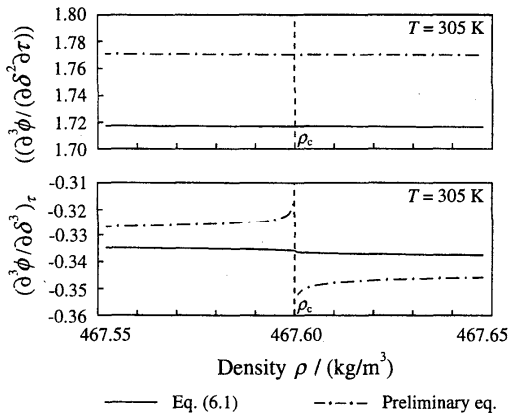

FIG. 10. While preliminary equations of state showed a discontinuous plot of the third density derivative of the reduced Helmholtz energy, the new equation of state, Eq. (6.1), yields continuous plots for the third derivatives.

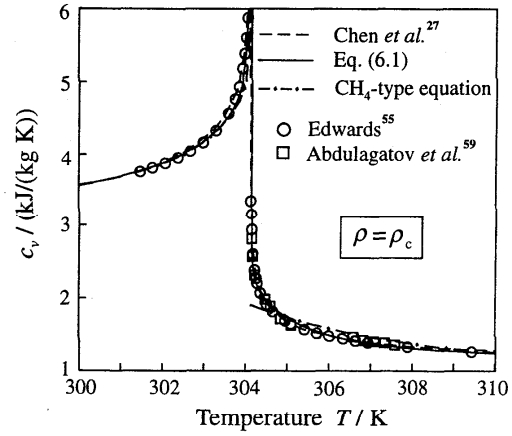

FIG. 11. Representation of representative isochoric heat capacity data in the critical region. The plotted curves correspond to values calculated from Eq. (6.1), the crossover equation of Chen *et al.*,[27] and a refitted equation using the CH_4-form (see Sec. 5.1).

maximum in c_v follows the phase boundary. Finally, the reduced density in the product of ϕ_i^r guarantees a physically correct behavior in the low-density limit.

Besides the coefficients n_i, Eq. (5.4) introduces seven "internal" parameters (A_i, B_i, C_i, D_i, a_i, b_i, β_i) for each of the terms i; in principle, these parameters can be included into a nonlinear fit of the entire equation. However, because of the highly correlated influence of these parameters, a simultaneous nonlinear fit turned out to be very difficult. Therefore, we decided to determine reasonable starting values for B_i, C_i, a_i, and b_i with our optimization strategy. The subsequent nonlinear fit of b_i, C_i, and D_i resulted only in minor improvements of the equation. B_i and a_i were not refitted in the current project. On principle, A_i and β_i correspond to the proportionality factor and to the critical exponent of the power law describing the densities of saturated liquid and saturated vapor (see Table 26) and can be independently determined. In the final bank of terms (see Table 30) a value for β_i was used which is slightly smaller than the value expected for the corresponding critical exponent in order to fulfill the conditions

$$b_i > 0.5 + \beta_i \tag{5.5}$$

and

$$\beta_i < \frac{1}{2a_i(1-b_i)+2}. \tag{5.6}$$

Equations (5.5) and (5.6) result from the condition that singular behavior has to be avoided everywhere except for derivatives of at least second degree with respect to temperature at the critical point. Unpublished preliminary equations did not fulfill these conditions and resulted in a discontinuous plot of the third density derivative of the reduced Helmholtz energy, $(\partial^3\phi/\partial\delta^3)_\tau$, at the critical isochore. Figure 10 shows an example for this possible misbehavior and shows that the final equation, Eq. (6.1), results in a continuous plot of the crucial third derivatives.

The smallest exponent b_i occurring in the equation of state is related to the critical exponent α, which describes the divergence of the specific isochoric heat capacity, by the expression

$$b_i = 1 - \frac{\alpha}{2}. \tag{5.7}$$

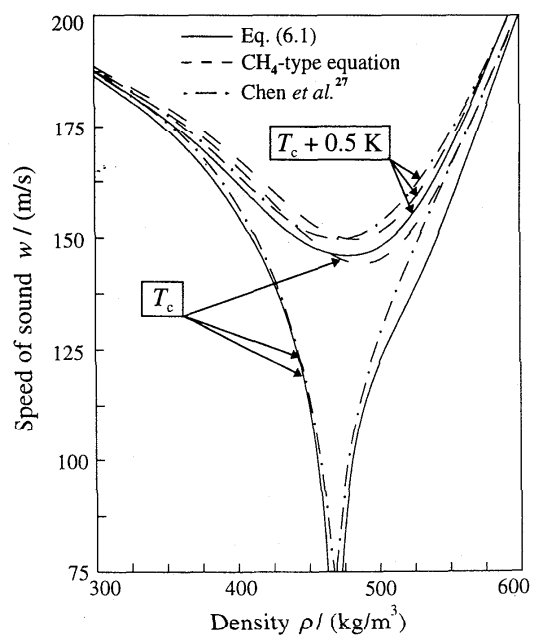

FIG. 12. Representation of the speed of sound on isotherms in the critical region. The plotted curves correspond to values calculated from Eq. (6.1), the crossover equation of Chen *et al.*,[27] and a refitted equation using CH_4-form (see Sec. 5.1).

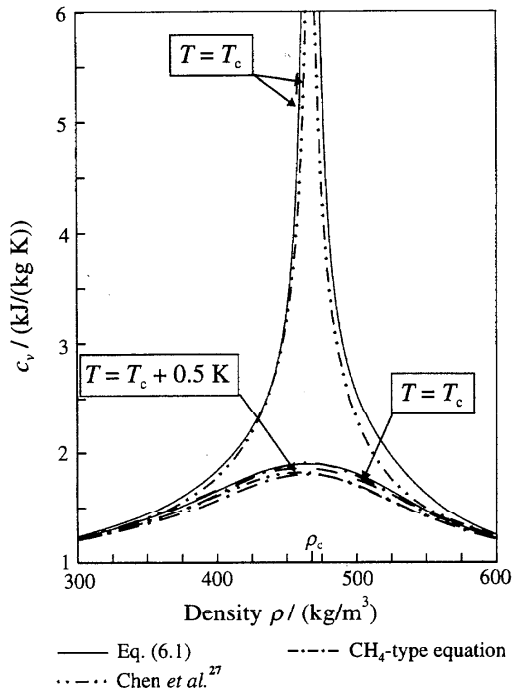

FIG. 13. Representation of the isochoric heat capacity on isotherms in the critical region. The plotted curves correspond to values calculated from Eq. (6.1), the crossover equation of Chen *et al.*,[27] and a refitted equation using the CH_4-form (see Sec. 5.1).

However, in combination with the sum of all terms of the entire equation of state, the asymptotically expected leading value of b_l=0.945 yielded unsatisfactory results. This discrepancy is discussed later in this section.

The final equation of state for carbon dioxide, which is presented in detail in Sec. 6, has been developed by the use of nonanalytic terms corresponding to Eq. (5.4). The procedure optimizing the structure of the equation of state was restricted to a maximum of four nonanalytic terms within a total number of 42 terms. Preliminary correlations with more than four nonanalytic terms tended to have an unreasonable behavior concerning the dependence of c_v and w on density in the critical region; moreover, when using more than four of such complex terms, the numerical expense would have been increased without a significant improvement in the quality of the equation. Anticipating Sec. 6 with regard to the critical region, Eq. (6.1) will be discussed in this section to avoid repeating a discussion of the representation of caloric properties in the critical region later in this paper.

Figure 11 shows the plot of c_v on the critical isochore; for analytic equations of state this plot was already shown in Fig. 9. In this figure, however, the solid line corresponds to Eq. (6.1). In contrast to the analytic CH_4-type equation, the new formulation is able to follow the strong curvature of the c_v plot in the immediate vicinity of the critical temperature and yields an infinite value for the specific isochoric heat capacity at the critical point. Accordingly, the evaluation of

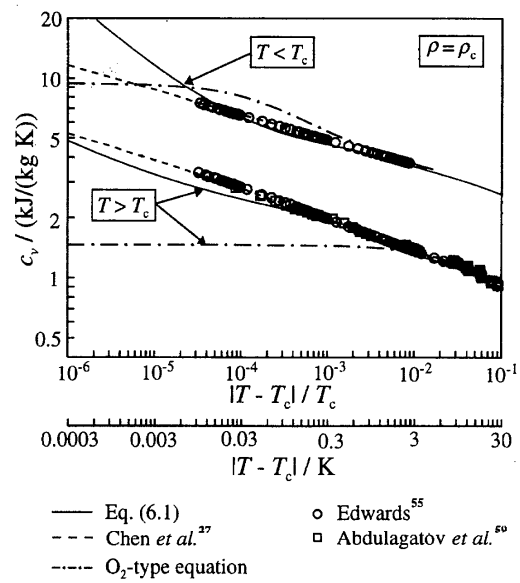

FIG. 14. Representation of experimental isochoric heat capacity data in the single phase ($T>T_c$) and two phase ($T<T_c$) region in a double logarithmic diagram. The plotted curves correspond to data on the critical isochore calculated from Eq. (6.1), the crossover equation of Chen *et al.*,[27] and a refitted equation using the O_2-form (see Sec. 5.1).

Eq. (6.1) yields a vanishing speed of sound at the critical point. Figure 12 shows the curve of the speed of sound, plotted on two isotherms as function of density. At the isotherm T_c+0.5 K, the analytic CH_4-type equation, the crossover equation of Chen *et al.*,[27] and Eq. (6.1) result in very

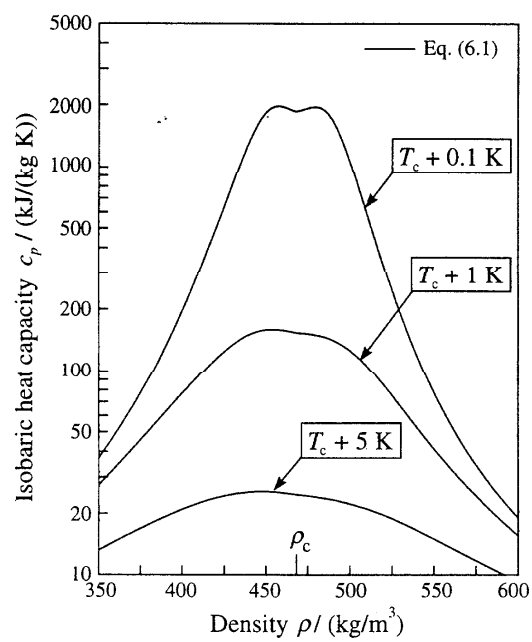

FIG. 15. For temperatures between T_c and T_c+1 K Eq. (6.1) results in an oscillating plot for the isobaric heat capacity around the critical density.

TABLE 27. Coefficients of the correlation equations, Eq. (6.2) and Eq. (6.3), for c_p^o and ϕ^o, respectively

i	a_i^o	θ_i^o	i	a_i^o	θ_i^o
1	8.373 044 56		5	0.621 052 48	6.111 90
2	−3.704 543 04		6	0.411 952 93	6.777 08
3	2.500 000 00		7	1.040 289 22	11.323 84
4	1.994 270 42	3.151 63	8	0.083 276 78	27.087 92

similar values for the speed of sound. However, on approaching the critical temperature, both the crossover equation and the nonanalytic wide-range equation, Eq. (6.1), develop a sharp minimum in the speed of sound, whereas the speed of sound calculated from the analytic equation does not change significantly when approaching the critical temperature. Within the same density range, Fig. 13 shows the corresponding plots of the specific isochoric heat capacity calculated from the same set of equations.

Thus, Eq. (6.1) is the first wide-range equation which yields a nonanalytic behavior of the isochoric heat capacity and the speed of sound in the immediate vicinity of the critical point and which is still explicit in the physical variables T and ρ. In Sec. 7 it will be shown that this nonanalytic behavior does not affect the quality of the equation with respect to the representation of other properties anywhere outside the critical region.

Nevertheless, empirical equations of state containing nonanalytic terms have certain limits if an exact fulfillment of the asymptotic power laws is required. The nonanalytic terms in Eq. (6.1) do not replace the contribution of the analytic terms in the surrounding of the critical point but they fill the increasing gap between the analytic and nonanalytic behavior. Therefore, efficient values of the exponent b_i are smaller than theoretically expected and result in a critical exponent α which is too large from an asymptotic point of view [see Eq. (5.5)].

Figure 14 shows that Eq. (6.1) represents the measured and theoretically predicted values of c_v without significant deviations for temperatures in the region $|T-T_c|>0.2$ K and within about $\pm 10\%$ for $0.2\ \mathrm{K} \geq (T-T_c) \geq 0.3$ mK in the homogeneous phase and for $-0.2\ \mathrm{K} \leq (T-T_c) \leq -10$ mK in the two-phase region. The plotted c_v courses correspond to the critical isochore in the one- ($T>T_c$) and two-phase ($T<T_c$)

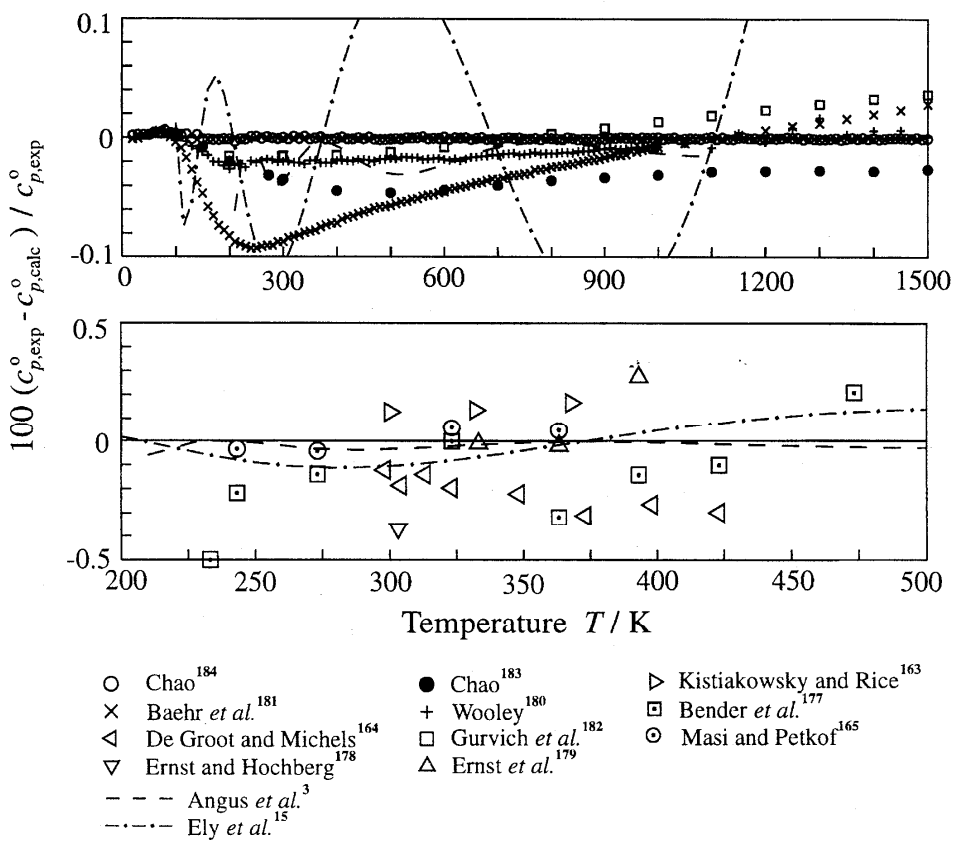

FIG. 16. Relative deviations of c_p^0 data from values calculated from Eq. (6.2). The upper diagram shows data calculated from statistical thermodynamics (see Table 15) and the lower diagram shows data extrapolated from experimental results (see Table 13). Values of c_p^0 calculated from the corresponding equations of Angus *et al.*[3] and Ely *et al.*[15] are plotted for comparison.

TABLE 28. The ideal-gas part of the dimensionless Helmholtz function ϕ^o and its derivatives[a]

ϕ^o	=	$\ln\delta$	+	a_1^o	+	$a_2^o\tau$	+	$a_3^o\ln(\tau)$	+	$\sum_{i=4}^{8} a_i^o \ln(1-e^{-\theta_i^o\tau})$
ϕ_δ^o	=	$1/\delta$	+	0	+	0	+	0	+	0
$\phi_{\delta\delta}^o$	=	$-1/\delta^2$	+	0	+	0	+	0	+	0
$\phi_{\delta\tau}^o$	=	0	+	0	+	0	+	0	+	0
ϕ_τ^o	=	0	+	0	+	a_2^o	+	a_3^o/τ	+	$\sum_{i=4}^{8} a_i^o\theta_i^o[(1-e^{-\theta_i^o\tau})^{-1}-1]$
$\phi_{\tau\tau}^o$	=	0	+	0	+	0	−	a_3^o/τ^2	−	$\sum_{i=4}^{8} a_i^o(\theta_i^o)^2 e^{-\theta_i^o\tau}(1-e^{-\theta_i^o\tau})^{-2}$

[a] $\phi_\delta^o=[\partial\phi^o/\partial\delta]_\tau$, $\phi_{\delta\delta}^o=[\partial^2\phi^o/\partial\delta^2]_\tau$, $\phi_\tau^o=[\partial\phi^o/\partial\tau]_\delta$, $\phi_{\tau\tau}^o=[\partial^2\phi^o/\partial\tau^2]_\delta$, and $\phi_{\delta\tau}^o=[\partial^2\phi^o/\partial\delta\partial\tau]$.

region. However, within a region of about +0.1 mK (outside the temperature range shown in Fig. 14) and −10 mK around the critical temperature, Eq. (6.1) yields specific isochoric heat capacities which are significantly larger than the values predicted by the crossover equation of state.

Figure 15 shows a problem which is related to a small oscillation in the derivative $(\partial p/\partial\rho)_T$ close to the critical point. Since the numerical value of this derivative is small close to the critical point, even a very small oscillation in this derivative results in a significant oscillation of properties related to its reciprocal value like the isobaric heat capacity [see Eq. (5.1)] or the isothermal compressibility. Derivatives of these properties [e.g., $(\partial c_p/\partial\rho)_T$] should not be used in the range 440 kg/m$^3\leq\rho\leq$500 kg/m^3 and $(T-T_c)\leq$2 K. Oscillations are also observed in the derivative $(\partial c_v/\partial T)_\rho$ for approximately 420 kg/m$^3\leq\rho\leq$550 kg/m^3 and $(T-T_c)\leq$15 K.

The quality of Eq. (6.1) should be sufficient for any application which requires numerical values of thermodynamic properties in the critical region. Equation (6.1), however, is not suitable to investigate the asymptotic behavior[c] of thermodynamic properties and the derivatives mentioned above should not be used in the regions indicated.

6. The New Equation of State

As discussed in Sec. 2.1 the new equation of state for carbon dioxide is a fundamental equation expressed in form of the Helmholtz energy as

$$A(\rho,T)/(RT)=\phi(\delta,\tau)=\phi^o(\delta,\tau)+\phi^r(\delta,\tau), \quad (6.1)$$

where $\delta=\rho/\rho_c$ and $\tau=T_c/T$ with $\rho_c=467.6$ kg/m^3 and $T_c=304.1282$ K.

The formulations which describe the ideal-gas part of the Helmholtz energy, Eq. (6.3), and the residual part of the Helmholtz energy, Eq. (6.5), are introduced in this section.

6.1 Ideal-Gas Part of the Helmholtz Energy

According to Eq. (2.4), the ideal-gas part of the Helmholtz energy can be easily obtained if the function $c_p^o(T)$ is known. A correlation equation for $c_p^o(T)$ has been established by means of a nonlinear fitting routine using the 150 c_p^o data of Chao[184] as input values (cf. Sec. 4.2.2). With the coefficients given in Table 27, the obtained equation

TABLE 29. Summary of selected data used for the linear optimization procedure and for the nonlinear fit

Property	Details of the data set are given in	Number of data: Linear optimization	Number of data: Nonlinear fit
$p(T,\rho)$	Table 12	2824	2824
$c_v(T,\rho)$	Table 14	553	553
$c_p(T,p)$	Table 17	359[a]	359
$c_p'(T)$	Table 24	73[a]	73
$w(T,p)$	Table 19	422[a]	422
$w'(T)$	Table 24	23[a]	23
$w''(T)$	Table 24	18[a]	18
$\Delta h(T,p)$	Sec. 4.5	10[a]	10
$\Delta u(T,\rho)$	Sec. 4.6	150	150
$\mu(T,p)$	Sec. 4.7		34
$p(T,\rho')$		205[b]	
$p(T,\rho'')$		205[b]	
Maxw.-crit.		205[b]	
$p_s(T)$	Table 7		109
$\rho'(T)$	Table 8		50
$\rho''(T)$	Table 9		42
Total number of data points		5047	4667

[a] Linearized data used in the optimization procedure; see Setzmann and Wagner.[30]

[b] Linearized solution of the Maxwell criterion when using data calculated from the auxiliary Eqs. (3.13) to (3.15); see Wagner.[32]

[c] The recent experimental results of Wagner *et al.*[230] for the "thermal" critical exponents β, γ, and δ, derived from $p\rho T$ measurements in the immediate vicinity of the critical point show clear differences from the corresponding values predicted by the renormalization group theory. These suprising results might be caused by an extended validity range of the so-called explicit influence of gravity (the implicit influence of gravity, e.g., the averaging errors based on density stratifications, was taken into account when evaluating the experimental $p\rho T$ data). Thus, we think that the "true" asymtotic behavior at the gas-liquid critical point of a pure fluid is not yet finally clarified.

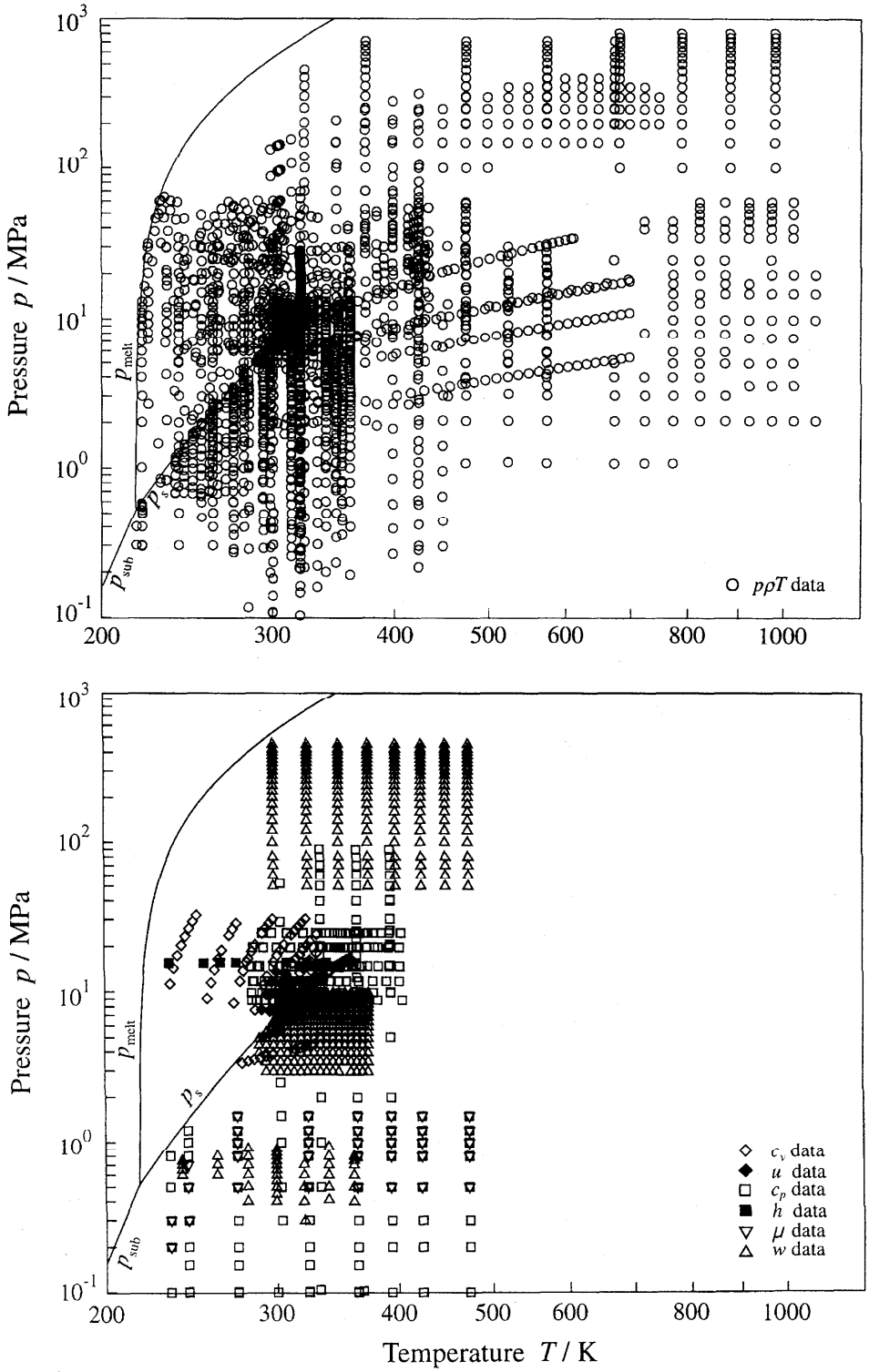

FIG. 17. Distribution of the experimental data used for the establishment of the residual part of the new fundamental equation, Eq. (6.5), in a pT diagram.

$$\frac{c_p^{\circ}(T)}{R}=1+a_3^{\circ}+\sum_{i=4}^{8} a_i^{\circ}(\theta_i^{\circ}\tau)^2 \frac{\exp(\theta_i^{\circ}\tau)}{[\exp(\theta_i^{\circ}\tau)-1]^2} \tag{6.2}$$

represents Chao's data with deviations less than $\pm 0.005\%$ for 10 K$\leqslant T<$210 K and less than $\pm 0.002\%$ for 210 K$\leqslant T\leqslant$1500 K. This means that the uncertainty of Eq. (6.2) is almost equal to the uncertainty of the data which was estimated by Chao to be less than $\pm 0.02\%$. Extrapolation of Eq. (6.2) yields results which are reliable to $\pm 1\%$ for $T\leqslant$4000 K and to $\pm 2\%$ for 4000 K$<T\leqslant$5000 K. Figure 16 shows deviations between values calculated from the c_p° correlations given by Angus *et al.*[3] and by Ely *et al.*,[15] data obtained by theoretical approaches and by extrapolation of experimental results, and values calculated from Eq. (6.2), which correspond to the zero line.

The expression for $\phi^{\circ}(\delta,\tau)$, which has been derived from Eq. (6.2) by integration, is

$$\phi^{\circ}(\delta,\tau)=\ln(\delta)+a_1^{\circ}+a_2^{\circ}\tau+a_3^{\circ}\ln(\tau)+\sum_{i=4}^{8} a_i^{\circ}\ln[1-\exp(-\tau\theta_i^{\circ})]. \tag{6.3}$$

The coefficients a_i° and θ_i° are given in Table 27. The coefficients a_1° and a_2° were adjusted to give zero for the ideal gas enthalpy at T_0 = 298.15 K and the ideal gas entropy at T_0=298.15 K and p_0 = 0.101 325 MPa. In Table 28, all derivatives of the ideal-gas part ϕ° required for the calculation of thermodynamic properties are explicitly given.

6.2 Residual Part of the Helmholtz Energy

The formulation for the residual part of the Helmholtz energy has been developed with the help of the procedure discussed in Sec. 2.3. The selected data which form the experimental basis of the new equation of state for carbon dioxide have been presented in Sec. 4. Table 29 gives a brief summary of the data used and refers to the corresponding tables, where detailed information is given. Figure 17 shows the distribution of the experimental data used. In addition, data have been calculated from auxiliary equations and from preliminary equations of state in order to guarantee reasonable behavior in regions where the existing measurements yield insufficient information. In detail, these are

- 13 values of the third virial coefficient, which have been calculated from an auxiliary equation (see Sec. 4.8),
- 23 values of the specific isochoric heat capacity, which have been calculated from the crossover equation of Chen *et al.*[27] in order to guarantee a reasonable dependence of c_v on density in the critical region,
- 27 $T\rho$ points describing the course of the Joule curve, which have been determined by graphical extrapolation (see Sec. 7.3.2),
- and 70 $p\rho T$ data, which have been calculated from a preliminary equation of state with an exceptionally good extrapolation behavior in order to preserve this progress (see Sec. 7.3.1).

All these "artificial" data are neither considered in Table 29 nor in Fig. 17. The consequences of the absence of caloric data within the liquid region and at temperatures above 500 K are discussed in Sec. 7.2.2.

The bank of terms which was used in the optimization of the final equation of state (see Sec. 2.3.2) contained a total of 860 terms. As far as parameter ranges are predetermined by this general form, these ranges have been established in extensive tests. This bank of terms can be written as

$$\begin{aligned}\phi^{r}=&\sum_{i=1}^{4}\sum_{j=0}^{20} n_{i,j}\,\delta^{i}\tau^{j/4}+\sum_{i=1}^{6}\sum_{j=0}^{10} n_{i,j}\,\delta^{i}\tau^{j/2}e^{-\delta}+\sum_{i=1}^{8}\sum_{j=0}^{8} n_{i,j}\,\delta^{i}\tau^{j}e^{-\delta^2}+\sum_{i=1}^{8}\sum_{j=0}^{16} n_{i,j}\,\delta^{i}\tau^{j}e^{-\delta^3}+\sum_{i=1}^{10}\sum_{j=0}^{12} n_{i,j}\,\delta^{i}\tau^{2j}e^{-\delta^4}\\&+\sum_{i=1}^{10}\sum_{j=5}^{16} n_{i,j}\,\delta^{i}\tau^{2j}e^{-\delta^5}+\sum_{i=8}^{15}\sum_{j=5}^{16} n_{i,j}\,\delta^{i}\tau^{2j}e^{-\delta^6}+\sum_{i=1}^{48} n_i\,\delta^{d_i}\tau^{t_i}e^{-\alpha_i(\delta-\epsilon_i)^2-\beta_i(\tau-\gamma_i)^2}\\&+\sum_{i=1}^{3}\sum_{j=1}^{2}\sum_{k=1}^{2}\sum_{l=1}^{3}\sum_{m=1}^{3} n_{i,j,k,l}\,\Delta^{b_j}\,\delta\,e^{-C_l(\delta-1)^2-D_m(\tau-1)^2}\end{aligned} \tag{6.4}$$

with $\Delta=\{(1-\tau)+A[(\delta-1)^2]^{1/(2\beta)}\}^2+B_k[(\delta-1)^2]^{a_i}$.

TABLE 30. Parameters of the nonanalytic terms in the bank of terms

i,j,k,l,m	a_i	b_j	B_k	C_l	D_m	A^{a}	β^{a}
1	3.00	0.875	0.30	10.00	225.0	0.700	0.300
2	3.50	0.925	1.00	12.50	250.0		
3	4.00			15.00	275.0		

[a]Predetermined from a simultaneous fit to saturated liquid and vapor densities in the critical region.

The parameters of the modified Gaussian terms originally introduced by Setzmann and Wagner[30] have been slightly changed for carbon dioxide; 48 of these expressions were used in the bank of terms covering the following parameter ranges: $1\leqslant d_i\leqslant 3$, $0\leqslant t_i\leqslant 3$, $15\leqslant\alpha_i\leqslant 25$, $275\leqslant\beta_i\leqslant 325$, and $1.16\leqslant\gamma_i\leqslant 1.25$ with ϵ_i = 1. The values which have been used for the parameters of the 108 nonanalytic terms in Eq. (6.1) are given in Table 30. The values used for b_j, C_l, and D_m resulted from a nonlinear fit of a preliminary formulation.

Proceeding from the bank of terms defined by Eq. (6.4),

TABLE 31. Coefficients and exponents of Eq. (6.5)[a]

i	n_i	d_i	t_i	c_i	α_i	β_i	γ_i	ϵ_i	a_i	b_i	A_i	B_i	C_i	D_i
1	$0.388\,568\,232\,031\,61\times10^{0}$	1	0.00											
2	$0.293\,854\,759\,427\,40\times10^{1}$	1	0.75											
3	$-0.558\,671\,885\,349\,34\times10^{1}$	1	1.00											
4	$-0.767\,531\,995\,924\,77\times10^{0}$	1	2.00											
5	$0.317\,290\,055\,804\,16\times10^{0}$	2	0.75											
6	$0.548\,033\,158\,977\,67\times10^{0}$	2	2.00											
7	$0.122\,794\,112\,203\,35\times10^{0}$	3	0.75											
8	$0.216\,589\,615\,432\,20\times10^{1}$	1	1.50	1										
9	$0.158\,417\,351\,097\,24\times10^{1}$	2	1.50	1										
10	$-0.231\,327\,054\,055\,03\times10^{0}$	4	2.50	1										
11	$0.581\,169\,164\,314\,36\times10^{-1}$	5	0.00	1										
12	$-0.553\,691\,372\,053\,82\times10^{0}$	5	1.50	1										
13	$0.489\,466\,159\,094\,22\times10^{0}$	5	2.00	1										
14	$-0.242\,757\,398\,435\,01\times10^{-1}$	6	0.00	1										
15	$0.624\,947\,905\,016\,78\times10^{-1}$	6	1.00	1										
16	$-0.121\,758\,602\,252\,46\times10^{0}$	6	2.00	1										
17	$-0.370\,556\,852\,700\,86\times10^{0}$	1	3.00	2										
18	$-0.167\,758\,797\,004\,26\times10^{-1}$	1	6.00	2										
19	$-0.119\,607\,366\,379\,87\times10^{0}$	4	3.00	2										
20	$-0.456\,193\,625\,087\,78\times10^{-1}$	4	6.00	2										
21	$0.356\,127\,892\,703\,46\times10^{-1}$	4	8.00	2										
22	$-0.744\,277\,271\,320\,52\times10^{-2}$	7	6.00	2										
23	$-0.173\,957\,049\,024\,32\times10^{-2}$	8	0.00	2										
24	$-0.218\,101\,212\,895\,27\times10^{-1}$	2	7.00	3										
25	$0.243\,321\,665\,592\,36\times10^{-1}$	3	12.00	3										
26	$-0.374\,401\,334\,234\,63\times10^{-1}$	3	16.00	3										
27	$0.143\,387\,157\,568\,78\times10^{0}$	5	22.00	4										
28	$-0.134\,919\,690\,832\,86\times10^{0}$	5	24.00	4										
29	$-0.231\,512\,250\,534\,80\times10^{-1}$	6	16.00	4										
30	$0.123\,631\,254\,929\,01\times10^{-1}$	7	24.00	4										
31	$0.210\,583\,219\,729\,40\times10^{-2}$	8	8.00	4										
32	$-0.339\,585\,190\,263\,68\times10^{-3}$	10	2.00	4										
33	$0.559\,936\,517\,715\,92\times10^{-2}$	4	28.00	5										
34	$-0.303\,351\,180\,556\,46\times10^{-3}$	8	14.00	6										
35	$-0.213\,654\,886\,883\,20\times10^{3}$	2	1.00		25	325	1.16	1.00						
36	$0.266\,415\,691\,492\,72\times10^{5}$	2	0.00		25	300	1.19	1.00						
37	$-0.240\,272\,122\,045\,57\times10^{5}$	2	1.00		25	300	1.19	1.00						
38	$-0.283\,416\,034\,239\,99\times10^{3}$	3	3.00		15	275	1.25	1.00						
39	$0.212\,472\,844\,001\,79\times10^{3}$	3	3.00		20	275	1.22	1.00						
40	$-0.666\,422\,765\,407\,51\times10^{0}$								3.500	0.875	0.700	0.3	10.0	275
41	$0.726\,086\,323\,498\,97\times10^{0}$								3.500	0.925	0.700	0.3	10.0	275
42	$0.550\,686\,686\,128\,42\times10^{-1}$								3.000	0.875	0.700	1.0	12.5	275

[a] $R = 0.188\,924\,1$ kJ/(kg K); $T_c = 304.128\,2$ K; $\rho_c = 467.6$ kg/m^3.

the modified optimization method (see Sec. 2.3.2) was used to determine the combination of terms which yields the best representation of the linearized data set. The resulting formulation for the residual part of the Helmholtz energy is

$$\phi^r = \sum_{i=1}^{7} n_i \delta^{d_i} \tau^{t_i} + \sum_{i=8}^{34} n_i \delta^{d_i} \tau^{t_i} e^{-\delta^{c_i}} + \sum_{i=35}^{39} n_i \delta^{d_i} \tau^{t_i} e^{-\alpha_i(\delta-\epsilon_i)^2-\beta_i(\tau-\gamma_i)^2} + \sum_{i=40}^{42} n_i \Delta^{b_i} \delta\, e^{-C_i(\delta-1)^2-D_i(\tau-1)^2} \tag{6.5}$$

with $\Delta = \{(1-\tau)+A_i[(\delta-1)^2]^{1/(2\beta_i)}\}^2 + B_i[(\delta-1)^2]^{a_i}$.

After this linear optimization process, the final values of the coefficients n_i of Eq. (6.5) have been determined by a direct nonlinear fit to the linear and nonlinear data. These values are given in Table 31 together with the parameters resulting from the optimization process. No further improve-

TABLE 32. The residual part of the dimensionless Helmholtz energy ϕ^{r} and its derivatives[a]

$$\phi^{\mathrm{r}}=\sum_{i=1}^{7} n_i\delta^{d_i}\tau^{t_i}+\sum_{i=8}^{34} n_i\delta^{d_i}\tau^{t_i}e^{-\delta^{c_i}}+\sum_{i=35}^{39} n_i\delta^{d_i}\tau^{t_i}e^{-\alpha_i(\delta-\epsilon_i)^2-\beta_i(\tau-\gamma_i)^2}+\sum_{i=40}^{42} n_i\Delta^{b_i}\delta\Psi \quad \text{with} \quad \Delta=\theta^2+B_i[(\delta-1)^2]^{a_i}$$

$$\theta=(1-\tau)+A_i[(\delta-1)^2]^{1/(2\beta_i)}$$

$$\Psi=e^{-C_i(\delta-1)^2-D_i(\tau-1)^2}$$

$$\phi^{\mathrm{r}}_{\delta}=\sum_{i=1}^{7} n_i d_i\delta^{d_i-1}\tau^{t_i}+\sum_{i=8}^{34} n_i e^{-\delta^{c_i}}[\delta^{d_i-1}\tau^{t_i}(d_i-c_i\delta^{c_i})]+\sum_{i=35}^{39} n_i\delta^{d_i}\tau^{t_i}e^{-\alpha_i(\delta-\epsilon_i)^2-\beta_i(\tau-\gamma_i)^2}\left[\frac{d_i}{\delta}-2\alpha_i(\delta-\epsilon_i)\right]+\sum_{i=40}^{42} n_i\left[\Delta^{b_i}\left(\Psi+\delta\frac{\partial\Psi}{\partial\delta}\right)+\frac{\partial\Delta^{b_i}}{\partial\delta}\delta\Psi\right]$$

$$\phi^{\mathrm{r}}_{\delta\delta}=\sum_{i=1}^{7} n_i d_i(d_i-1)\delta^{d_i-2}\tau^{t_i}+\sum_{i=8}^{34} n_i e^{-\delta^{c_i}}[\delta^{d_i-2}\tau^{t_i}((d_i-c_i\delta^{c_i})(d_i-1-c_i\delta^{c_i})-c_i^2\delta^{c_i})]+\sum_{i=35}^{39} n_i\tau^{t_i}e^{-\alpha_i(\delta-\epsilon_i)^2-\beta_i(\tau-\gamma_i)^2}$$

$$\cdot[-2\alpha_i\delta^{d_i}+4\alpha_i^2\delta^{d_i}(\delta-\epsilon_i)^2-4d_i\alpha_i\delta^{d_i-1}(\delta-\epsilon_i)+d_i(d_i-1)\delta^{d_i-2}]+\sum_{i=40}^{42} n_i\left[\Delta^{b_i}\left(2\frac{\partial\Psi}{\partial\delta}+\delta\frac{\partial^2\Psi}{\partial\delta^2}\right)+2\frac{\partial\Delta^{b_i}}{\partial\delta}\left(\Psi+\delta\frac{\partial\Psi}{\partial\delta}\right)+\frac{\partial^2\Delta^{b_i}}{\partial\delta^2}\delta\Psi\right]$$

$$\phi^{\mathrm{r}}_{\tau}=\sum_{i=1}^{7} n_i t_i\delta^{d_i}\tau^{t_i-1}+\sum_{i=8}^{34} n_i t_i\delta^{d_i}\tau^{t_i-1}e^{-\delta^{c_i}}+\sum_{i=35}^{39} n_i\delta^{d_i}\tau^{t_i}e^{-\alpha_i(\delta-\epsilon_i)^2-\beta_i(\tau-\gamma_i)^2}\left[\frac{t_i}{\tau}-2\beta_i(\tau-\gamma_i)\right]+\sum_{i=40}^{42} n_i\delta\left[\frac{\partial\Delta^{b_i}}{\partial\tau}\Psi+\Delta^{b_i}\frac{\partial\Psi}{\partial\tau}\right]$$

$$\phi^{\mathrm{r}}_{\tau\tau}=\sum_{i=1}^{7} n_i t_i(t_i-1)\delta^{d_i}\tau^{t_i-2}+\sum_{i=8}^{34} n_i t_i(t_i-1)\delta^{d_i}\tau^{t_i-2}e^{-\delta^{c_i}}+\sum_{i=35}^{39} n_i\delta^{d_i}\tau^{t_i}e^{-\alpha_i(\delta-\epsilon_i)^2-\beta_i(\tau-\gamma_i)^2}\left[\left(\frac{t_i}{\tau}-2\beta_i(\tau-\gamma_i)\right)^2-\frac{t_i}{\tau^2}-2\beta_i\right]$$

$$+\sum_{i=40}^{42} n_i\delta\left[\frac{\partial^2\Delta^{b_i}}{\partial\tau^2}\Psi+2\frac{\partial\Delta^{b_i}}{\partial\tau}\frac{\partial\Psi}{\partial\tau}+\Delta^{b_i}\frac{\partial^2\Psi}{\partial\tau^2}\right]$$

$$\phi^{\mathrm{r}}_{\delta\tau}=\sum_{i=1}^{7} n_i d_i t_i\delta^{d_i-1}\tau^{t_i-1}+\sum_{i=8}^{34} n_i e^{-\delta^{c_i}}\delta^{d_i-1}t_i\tau^{t_i-1}(d_i-c_i\delta^{c_i})+\sum_{i=35}^{39} n_i\delta^{d_i}\tau^{t_i}e^{-\alpha_i(\delta-\epsilon_i)^2-\beta_i(\tau-\gamma_i)^2}\left[\frac{d_i}{\delta}-2\alpha_i(\delta-\epsilon_i)\right]\left[\frac{t_i}{\tau}-2\beta_i(\tau-\gamma_i)\right]$$

$$+\sum_{i=40}^{42} n_i\left[\Delta^{b_i}\left(\frac{\partial\Psi}{\partial\tau}+\delta\frac{\partial^2\Psi}{\partial\delta\partial\tau}\right)+\delta\frac{\partial\Delta^{b_i}}{\partial\delta}\frac{\partial\Psi}{\partial\tau}+\frac{\partial\Delta^{b_i}}{\partial\tau}\left(\Psi+\delta\frac{\partial\Psi}{\partial\delta}\right)+\frac{\partial^2\Delta^{b_i}}{\partial\delta\partial\tau}\delta\Psi\right]$$

Derivatives of the distance function Δ^{b_i}:

$$\frac{\partial\Delta^{b_i}}{\partial\delta}=b_i\Delta^{b_i-1}\frac{\partial\Delta}{\partial\delta}$$

$$\frac{\partial^2\Delta^{b_i}}{\partial\delta^2}=b_i\left[\Delta^{b_i-1}\frac{\partial^2\Delta}{\partial\delta^2}+(b_i-1)\Delta^{b_i-2}\left(\frac{\partial\Delta}{\partial\delta}\right)^2\right]$$

$$\frac{\partial\Delta^{b_i}}{\partial\tau}=-2\theta b_i\Delta^{b_i-1}$$

$$\frac{\partial^2\Delta^{b_i}}{\partial\tau^2}=2b_i\Delta^{b_i-1}+4\theta^2b_i(b_i-1)\Delta^{b_i-2}$$

$$\frac{\partial^2\Delta^{b_i}}{\partial\delta\partial\tau}=-A_ib_i\frac{2}{\beta_i}\Delta^{b_i-1}(\delta-1)[(\delta-1)^2]^{1/(2\beta_i)-1}-2\theta b_i(b_i-1)\Delta^{b_i-2}\frac{\partial\Delta}{\partial\delta}$$

$$\frac{\partial\Delta}{\partial\delta}=(\delta-1)\left\{A_i\theta\frac{2}{\beta_i}[(\delta-1)^2]^{1/(2\beta_i)-1}+2B_ia_i[(\delta-1)^2]^{a_i-1}\right\}$$

$$\frac{\partial^2\Delta}{\partial\delta^2}=\frac{1}{(\delta-1)}\frac{\partial\Delta}{\partial\delta}+(\delta-1)^2\left\{4B_ia_i(a_i-1)[(\delta-1)^2]^{a_i-2}+2A_i^2\left(\frac{1}{\beta_i}\right)^2\{[(\delta-1)^2]^{1/(2\beta_i)-1}\}^2+A_i\theta\frac{4}{\beta_i}\left(\frac{1}{2\beta_i}-1\right)[(\delta-1)^2]^{1/(2\beta_i)-2}\right\}$$

Derivatives of the exponential function Ψ:

$$\frac{\partial\Psi}{\partial\delta}=-2C_i(\delta-1)\Psi$$

$$\frac{\partial^2\Psi}{\partial\delta^2}=[2C_i(\delta-1)^2-1]2C_i\Psi$$

$$\frac{\partial\Psi}{\partial\tau}=-2D_i(\tau-1)\Psi$$

$$\frac{\partial^2\Psi}{\partial\tau^2}=[2D_i(\tau-1)^2-1]2D_i\Psi$$

$$\frac{\partial^2\Psi}{\partial\delta\partial\tau}=4C_iD_i(\delta-1)(\tau-1)\Psi$$

[a] $\phi^{\mathrm{r}}_{\delta}=\left(\frac{\partial\phi^{\mathrm{r}}}{\partial\delta}\right)_{\tau}$, $\phi^{\mathrm{r}}_{\delta\delta}=\left(\frac{\partial^2\phi^{\mathrm{r}}}{\partial\delta^2}\right)_{\tau}$, $\phi^{\mathrm{r}}_{\tau}=\left(\frac{\partial\phi^{\mathrm{r}}}{\partial\tau}\right)_{\delta}$, $\phi^{\mathrm{r}}_{\tau\tau}=\left(\frac{\partial^2\phi^{\mathrm{r}}}{\partial\tau^2}\right)_{\delta}$, and $\phi^{\mathrm{r}}_{\delta\tau}=\left(\frac{\partial^2\phi^{\mathrm{r}}}{\partial\delta\partial\tau}\right)$.

ment was achieved by refitting the b_i, C_i, and D_i of the nonanalytic terms.

The new fundamental equation for carbon dioxide, Eq. (6.1), in combination with the formulations according to Eqs. (6.3) and (6.5), is constrained to the critical parameters given in Sec. 3.2. It is valid for the entire fluid region covered by reliable data, namely for

$$216\ \mathrm{K}\leq T\leq 1100\ \mathrm{K} \quad \text{and} \quad 0\ \mathrm{MPa}\leq p\leq 800\ \mathrm{MPa}.$$

Estimations for the uncertainty of Eq. (6.1) are given in Sec. 8; the quality of the new equation of state is discussed in Sec. 7. The necessary derivatives of Eq. (6.5) are given in Table 32.

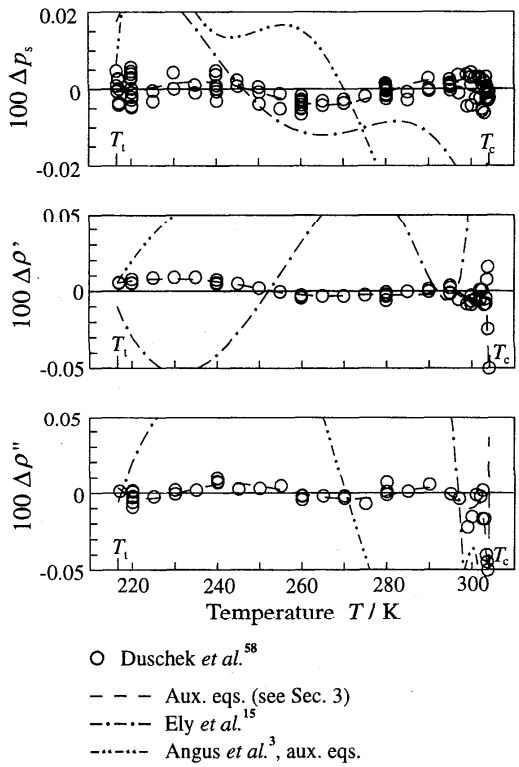

FIG. 18. Relative deviations $100\Delta y = 100\ (y_{exp} - y_{calc})/y_{exp}(y = p_s, \rho', \rho'')$ of the experimental saturation data of Duschek *et al.*[58] from values calculated from Eq. (6.1). Values calculated from auxiliary equations presented in Sec. 3, the equation of state of Ely *et al.*[15] and the auxiliary equations of Angus *et al.*[3] are plotted for comparison.

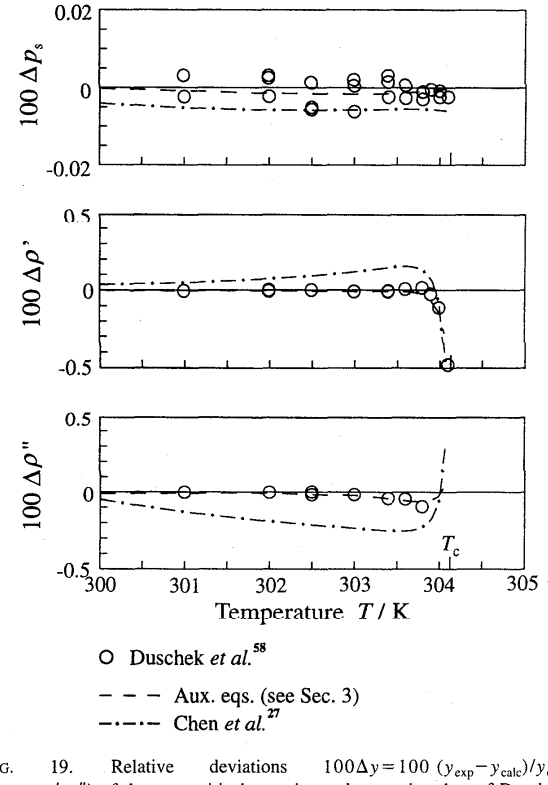

FIG. 19. Relative deviations $100\Delta y = 100\ (y_{exp} - y_{calc})/y_{exp}$ $(y = p_s, \rho', \rho'')$ of the near critical experimental saturation data of Duschek *et al.*[58] from values calculated from Eq. (6.1). Values calculated from the auxiliary equations presented in Sec. 3 and from the crossover of Chen *et al.*[27] are plotted for comparison.

7. Comparisons of the New Equation of State with Experimental Data and Other Equations of State

In this section, the quality of the new equation of state is discussed based on comparisons with selected experimental data. In addition, most figures also show values calculated from the equation of state published by Angus *et al.*,[3] which is commonly accepted as an international standard for carbon dioxide, and by Ely *et al.*,[15] which proved to be the best of the available equations of state for carbon dioxide.

For the extended critical region, comparisons should be performed with the complete IUPAC equation (Angus *et al.*[3]) which consists of an analytic wide-range equation, a switching function, and a scaled equation for the description of the critical region (see Sec. 1.2). Since the evaluation of the combined equation causes numerical problems,[d] we decided to use the equation of Pitzer and Schreiber[16] for comparisons in the extended critical region. This formulation yields very similar results to the IUPAC equation but at clearly less numerical expense. All the figures presenting data in this region also contain values calculated from the crossover equation of Chen *et al.*[27] which is the most sophisticated scaled equation of state published for carbon dioxide. The representation of the specific isochoric heat capacity and the speed of sound in the critical region was discussed in detail in Sec. 5.

None of the existing equations of state for carbon dioxide is valid on the ITS-90 temperature scale. Therefore, temperatures were reconverted to the IPTS-68 scale by using the procedure of Preston-Thomas *et al.*,[37] before values were calculated from these equations.

7.1 Liquid–Vapor Boundary

7.1.1 Thermal Properties on the Coexistence Curve

As shown in Sec. 3, the discussion of thermal properties on the liquid–vapor boundary can be restricted to the representation of the data of Duschek *et al.*[58] The deviations between these data and values calculated from Eq. (6.1) by using the phase equilibrium condition [see Eq. (2.2)] is shown in Fig. 18. The additional lines in this deviation plot correspond to values calculated from the auxiliary equations

[d]The data published in the IUPAC tables use temperatures according to the IPTS-68 temperature scale, but regarding the equations there seems to be some inconsistency in the temperature scales used. In the critical region, the published isochoric heat capacity data are partly determined graphically, since the evaluation of the combined equation yields unreasonable results.

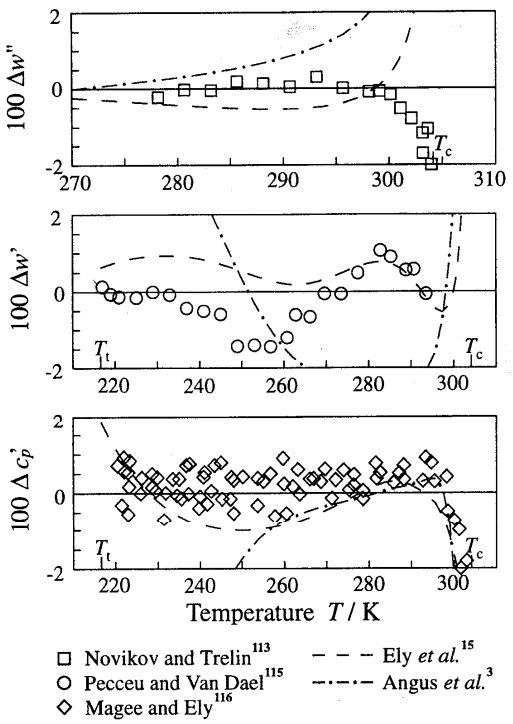

FIG. 20. Relative deviations $100\Delta y = 100\ (y_{\mathrm{exp}} - y_{\mathrm{calc}})/y_{\mathrm{exp}}\ (y = w'', w', c_p')$ of experimental caloric data at saturation from values calculated from Eq. (6.1). Data calculated from the wide-range equations of Ely *et al.*[15] and Angus *et al.*[3] are plotted for comparison.

presented in this work (see Sec.3), to values calculated from the equation of state of Ely *et al.*[15] by using the phase equilibrium condition and to values calculated from auxiliary equations for the saturation properties established by Angus *et al.*[3] Angus *et al.* recommend the use of their auxiliary equations for phase equilibrium calculations since they yield better results than the IUPAC equation of state.

Figure 18 shows that Eq. (6.1) represents the very accurate vapor pressure data of Duschek *et al.*[58] to within ±0.006% in pressure. Saturated liquid and vapor densities are represented to within ±0.01% in density up to 303.6 K and 297.0 K, respectively. Approaching the critical point the deviations in density increase, but these deviations are still within the experimental uncertainty of the data; thus, all the data are represented to within their experimental uncertainty. None of the equations hitherto known is able to reproduce the data at least roughly within their uncertainty (the uncertainty values are given in Tables 7–9).

Figure 19 shows the representation of the saturation properties in the critical region where a larger deviation scale is used. The very good representation of the vapor pressure data is practically not affected when approaching the critical temperature and the density deviations increase only slightly, except for the last point measured for the saturated liquid density. Duschek *et al.*[58] do not give any estimation for the uncertainty of this point, but only 36 mK below the critical temperature a deviation of 0.48% in the saturated liquid density can be considered to be within the experimental uncertainty.

The crossover equation of Chen *et al.*[27] is able to reproduce the vapor pressure data within their experimental uncertainty but it cannot represent the saturated vapor and liquid densities within the uncertainty of these state-of-the-art measurements. The auxiliary equations presented in Sec.3 reproduce the experimental data slightly better than Eq. (6.1) does. If one is interested in thermodynamically consistent values for all properties on the phase boundary, the evaluation of Eq. (6.1) in combination with Eq. (2.2) should be used and not the simpler auxiliary equations given in Sec. 3.

7.1.2 Caloric Properties on the Coexistence Curve

Figure 20 shows the representation of group 1 data providing information on the caloric behavior on the phase boundary. The speed of sound data of the saturated vapor state measured by Novikov and Trelin[113] are reproduced within ±0.5% for $T<301$ K and to ±3% for $T>301$ K. Only the last point 30 mK below the critical temperature exceeds this limit, but since the temperature scale of Novikov and Trelin is uncertain by more than 30 mK (see Sec. 4.10), we did not rely on this data point. The analytic equations of state of Angus *et al.*[3] and Ely *et al.*[15] are not able to follow the decreasing speed of sound when approaching the critical point.

Equation (6.1) represents both the speed of sound and the specific isobaric heat capacity in the saturated liquid state to within ±1%; the greater deviations of the w' data of Pecceu and Van Dael[115] at temperatures between 249 K and 261 K are due to a systematic offset in the data set. The equation of Ely *et al.*[15] yields results which are at least similar to those calculated from Eq. (6.1), but the formulation of Angus *et al.*[3] fails in describing caloric properties in the saturated liquid state (see also the representation of c_v in the homogeneous liquid region, Sec. 7.2.2 and Fig. 31).

The new equation of state was fitted to the c_p' data of Magee and Ely[116] up to temperatures of 295 K since the conversion of c_σ to c_p' seems to be uncertain for higher temperatures (see Sec. 3.8). Above 295 K the deviations between the converted data and the new fundamental equation remain within about ±2%; keeping in mind that c_p' is strongly diverging when approaching the critical point, this result underlines the consistent description of the critical region by Eq.(6.1).

7.2 Single-Phase Region

7.2.1 Thermal Properties in the Single-Phase Region

For carbon dioxide, the region where $p\rho T$ data in reference quality are available extends up to pressures of 13 MPa at temperatures up to 360 K. Within this region, the data sets of Duschek *et al.*,[58,154] Gilgen *et al.*,[159] Nowak *et al.*,[160d] and Guo *et al.*[157] describe the $p\rho T$ surface with an uncertainty of approximately ±0.02% in density and in the extended criti-

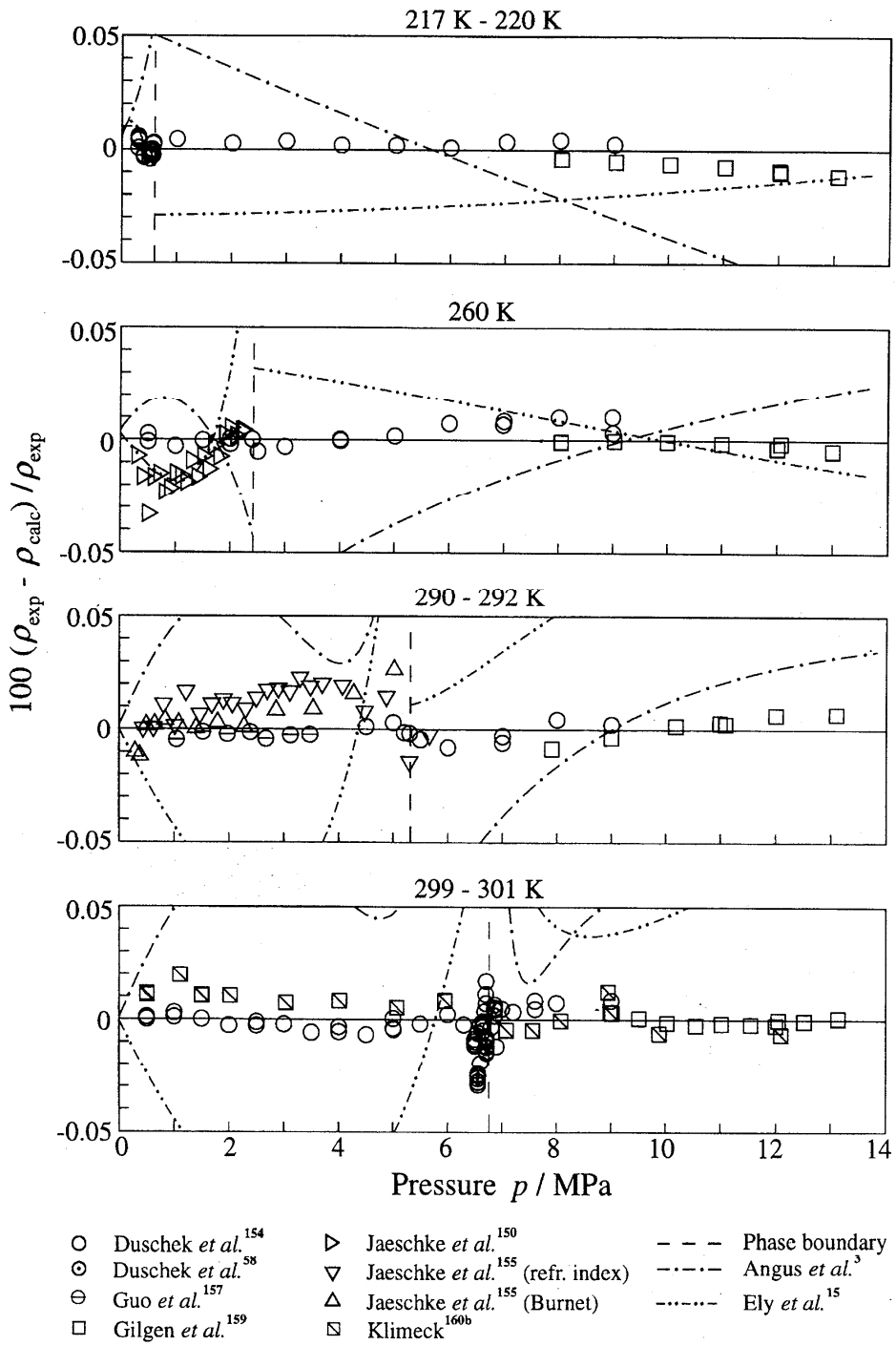

FIG. 21. Relative density deviations of very accurate $p\rho T$ data at subcritical temperatures from values calculated from Eq. (6.1). Values calculated from the wide-range equations of Ely *et al.*[15] and Angus *et al.*[3] are plotted for comparison.

cal region of ±0.02% in pressure. In an extended region reaching up to pressures of 30 MPa and temperatures of 523 K, the data of Brachthäuser[160] and Klimeck *et al.*[160b] describe the $p\rho T$ surface with an uncertainty of ±0.02% to ±0.05% in density. None of the existing equations of state had access to these data sets because the data have been published since 1990. Equation (6.1) is able to reproduce these data within their experimental uncertainty (for the nu-

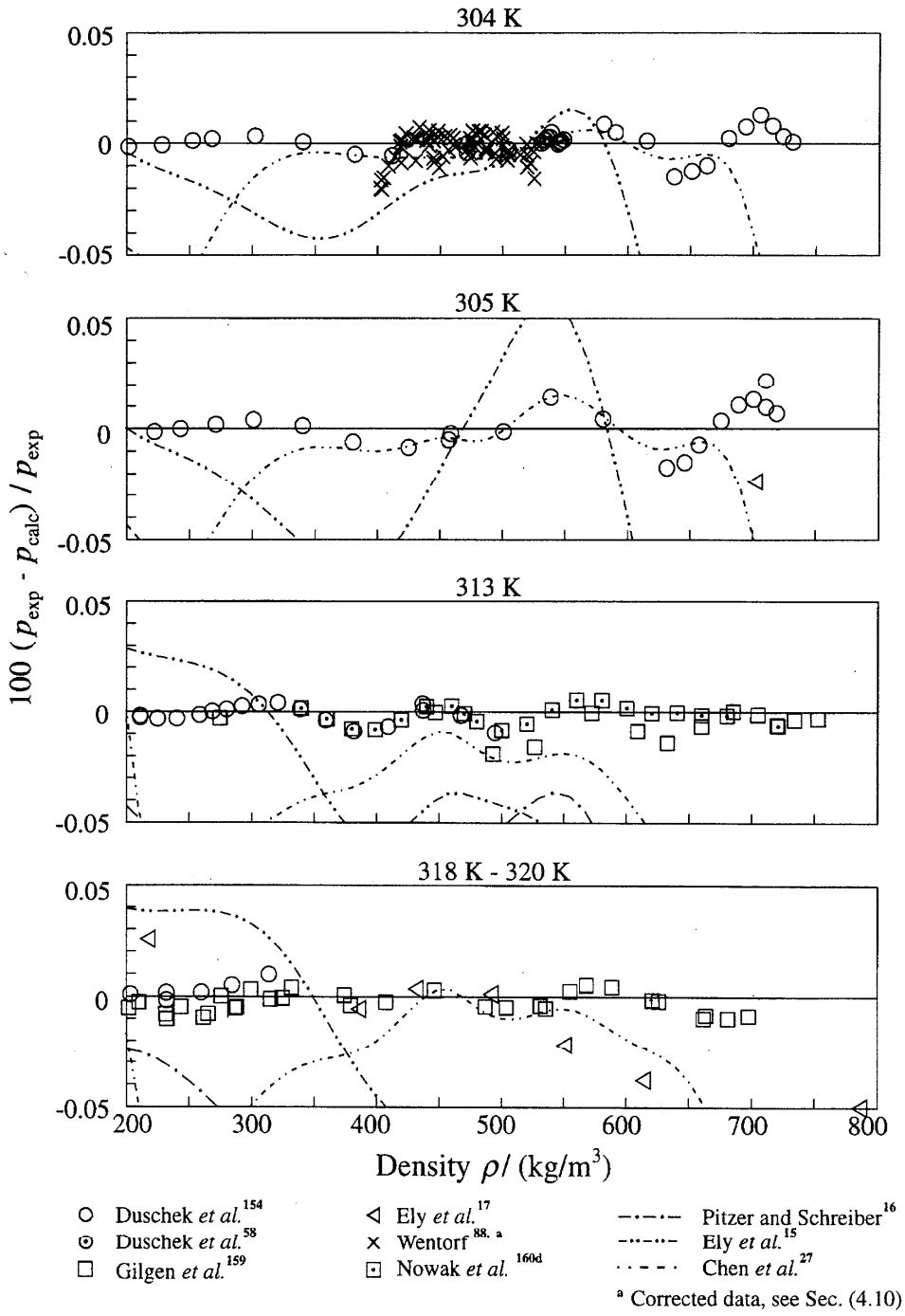

FIG. 22. Relative pressure deviations of very accurate $p\rho T$ data in the extended critical region from values calculated from Eq. (6.1). Values calculated from the wide-range equations of Ely *et al.*[15] and Pitzer and Schreiber[16] and from the crossover equation of Chen *et al.*[27] are plotted for comparison.

merical values of the uncertainty see Table 12). Figures 21 to 23 show the representation of some reference data on typical isotherms in order to illustrate this statement.

Figure 21 additionally contains data of Jaeschke[150,155] which also give a high-quality description of the $p\rho T$ surface in the gas and supercritical region. The equation of Ely *et al.*[15] yields a suitable description of the gas region at low temperatures but it has problems for temperatures above about 250 K. The equation of Angus *et al.*[3] is not able to reproduce the state-of-the-art data in the gas region. In the

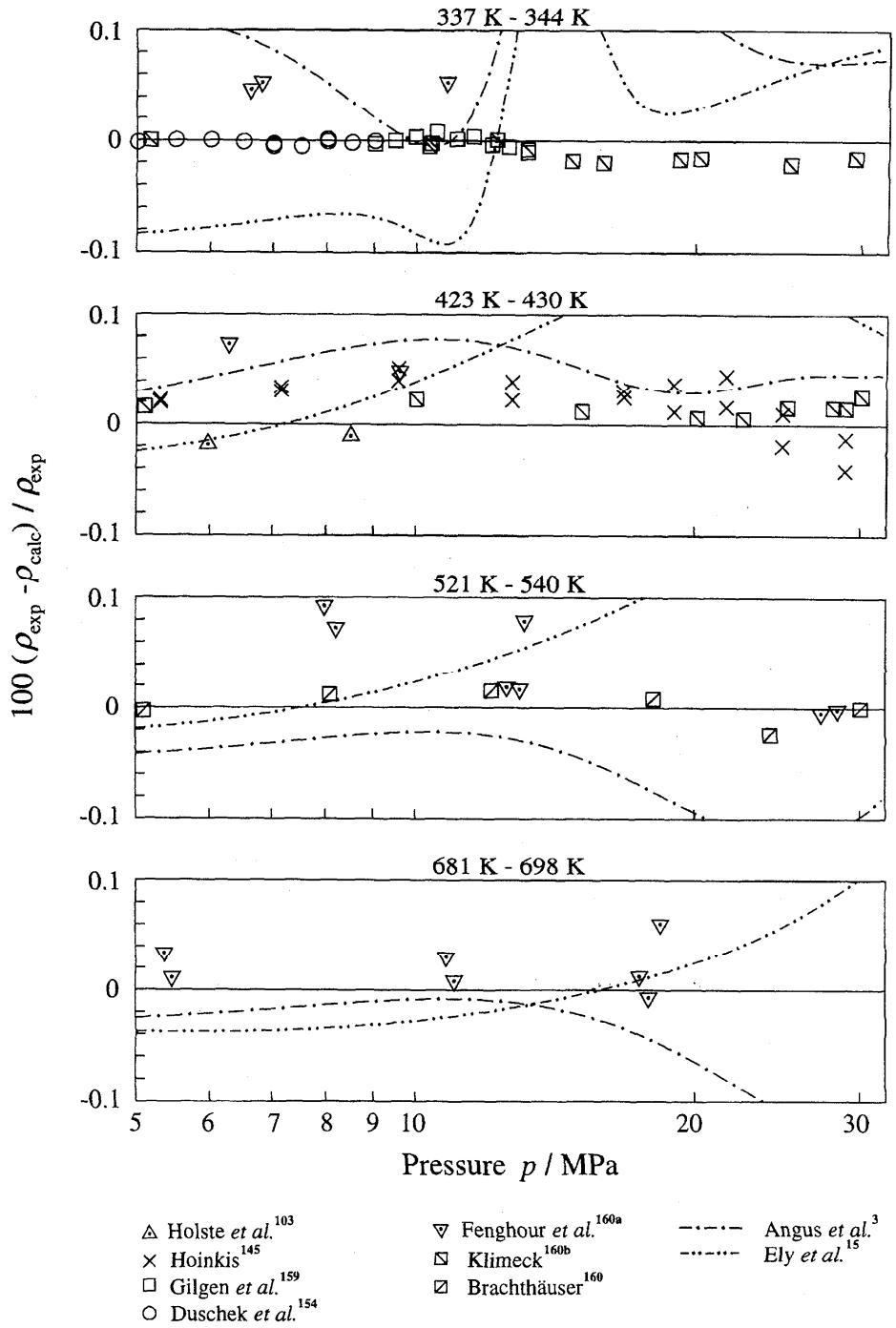

FIG. 23. Relative density deviations of very accurate $p\rho T$ data at supercritical temperatures from values calculated from Eq. (6.1). Values calculated from the wide-range equations of Ely *et al.*[15] and Angus *et al.*[3] are plotted for comparison.

liquid region, none of the existing equations of state is able to represent the reference data of Duschek *et al.*[154] and Gilgen *et al.*[159] at least roughly to within their experimental uncertainty.

High-quality $p\rho T$ data in the extended critical region are shown in Fig. 22. The data of Duschek *et al.*[58,154] and Gilgen *et al.*[159] are supplemented by the selected data of Wentorf[88] and by the data of Ely *et al.*[17] which are consistent with the

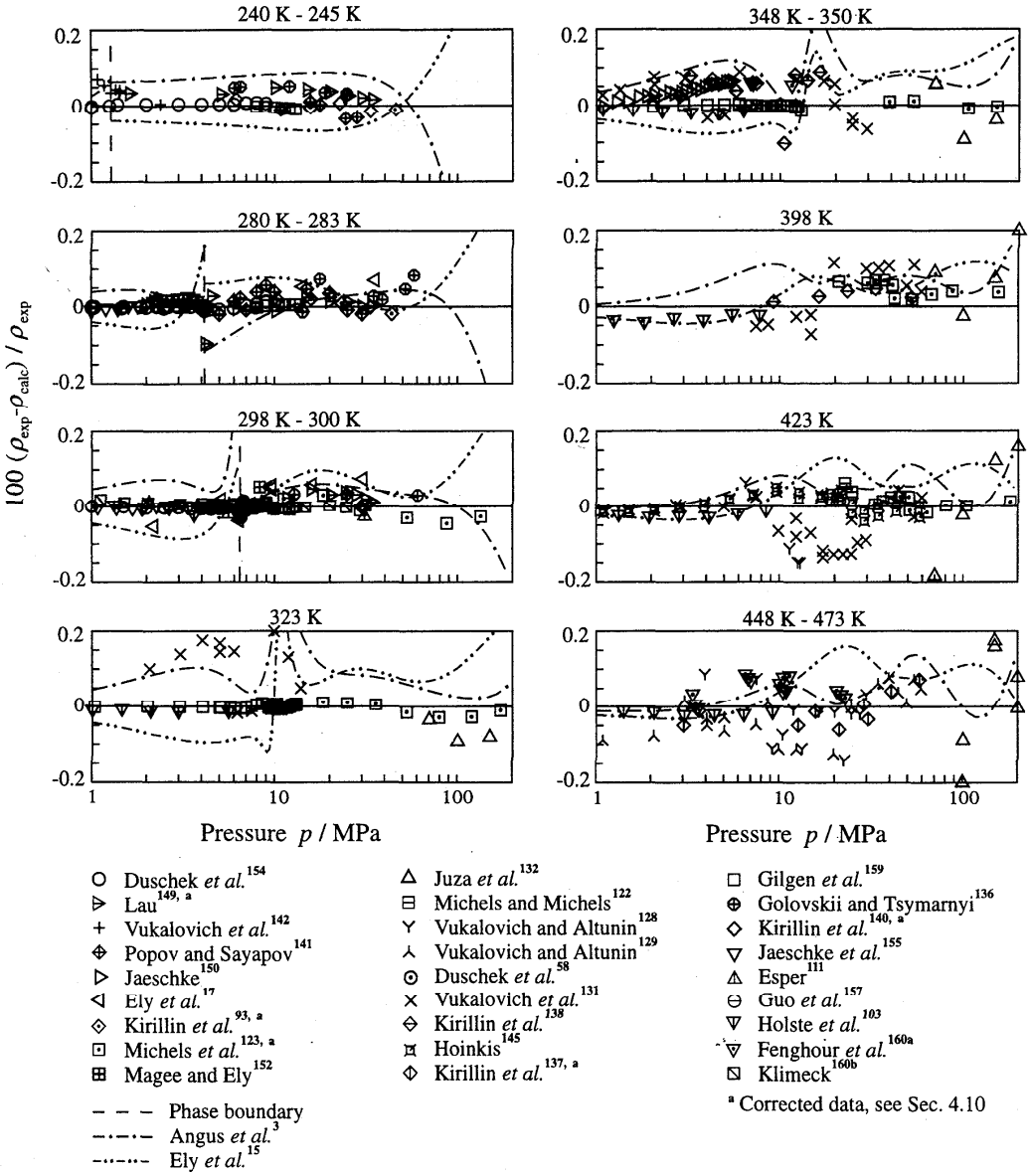

FIG. 24. Relative density deviations of selected $p\rho T$ data from values calculated from Eq. (6.1). Values calculated from the wide-range equations of Ely *et al.*[15] and Angus *et al.*[3] are plotted for comparison.

reference data by approximately ±0.03% in pressure. Even in this region, Eq. (6.1) represents the reference data to within their experimental uncertainty. The deviations between the data and values calculated from the equation of Ely *et al.*[15] increase up to 0.1% in pressure, which corresponds to five times the uncertainty of the data, while the equation of Pitzer and Schreiber[16] deviates by up to 0.2%. The equation of Chen *et al.*,[27] which is especially designed for the description of this region, yields a very suitable representation of the $p\rho T$ data in the surrounding of the critical isochore. However, at lower and higher densities, but clearly within the range of its validity, the crossover equation does not reproduce the reference data within their experimental uncertainty.

Figure 23 shows the representation of high-quality data at higher temperatures and pressures. Up to 523 K and 30 MPa, the $p\rho T$ surface is defined by the data of Brachthäuser[160] and Klimeck *et al.*[160b] with an uncertainty of less than ±0.05%

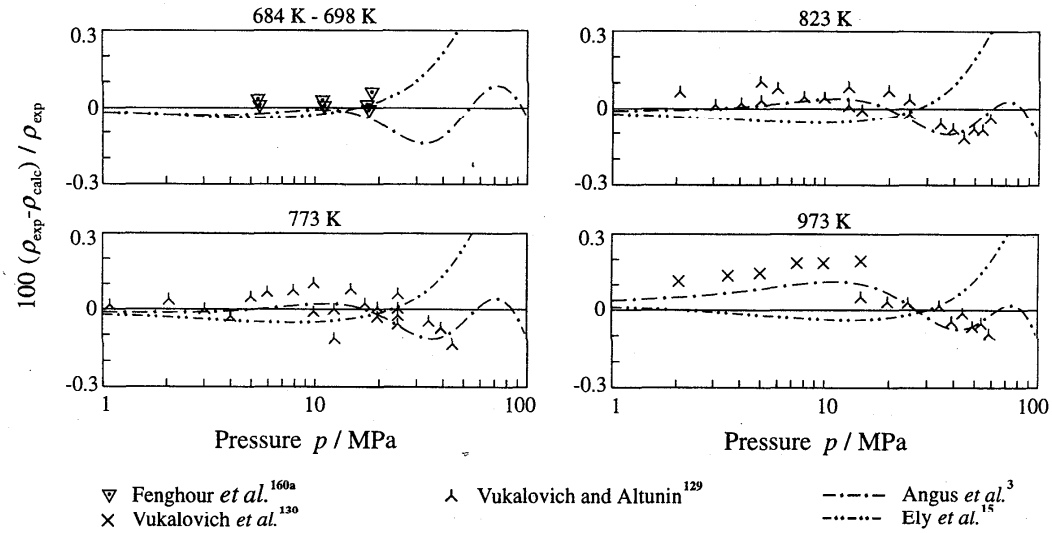

FIG. 25. Relative density deviations of selected $p\rho T$ data at high temperatures from values calculated from Eq. (6.1). Values calculated from the wide-range equations of Ely *et al.*[15] and Angus *et al.*[3] are plotted for comparison.

in density. For temperatures up to 698 K, the recent data of Fenghour *et al.*[160a] improve the uncertainty of the $p\rho$T surface to less than $\pm 0.1\%$ in density.

A representative view on the complete group 1 set of the $p\rho$T data up to temperatures of 473 K and pressures of 200 MPa is given in Fig. 24. Generally, the new equation of state describes the reliable data better than the older equations. The comparison with the data sets of Duschek *et al.*[154] and Gilgen *et al.*[159] shows that the use of adjusted data (see Sec. 4.10) was reasonable.

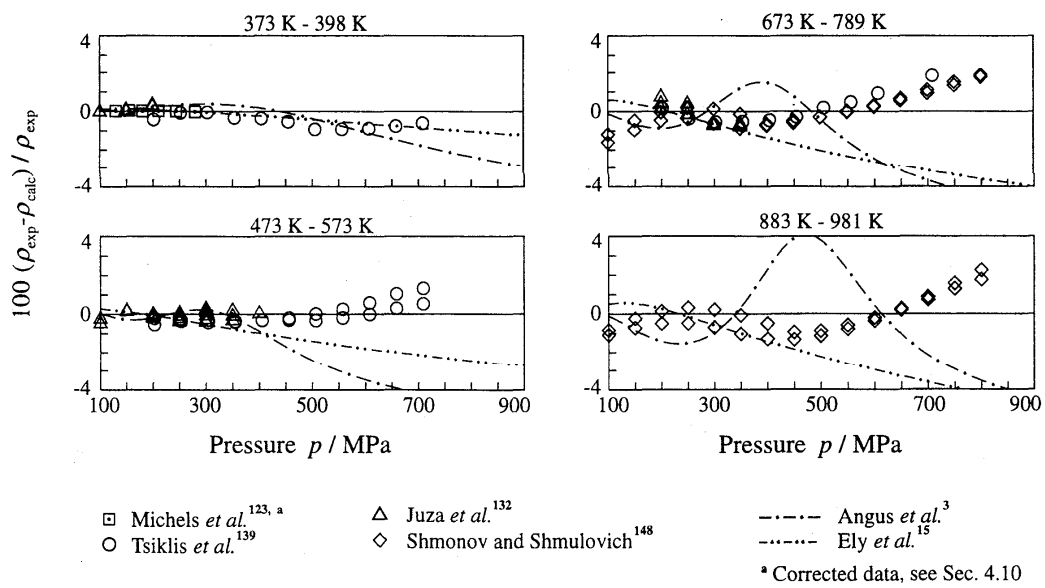

FIG. 26. Relative density deviations of selected $p\rho T$ data at high pressures from values calculated from Eq. (6.1). Values calculated from the wide-range equations of Ely *et al.*[15] and Angus *et al.*[3] are plotted for comparison; in this pressure range, these two equations of state are at least partly extrapolated (see Table 1).

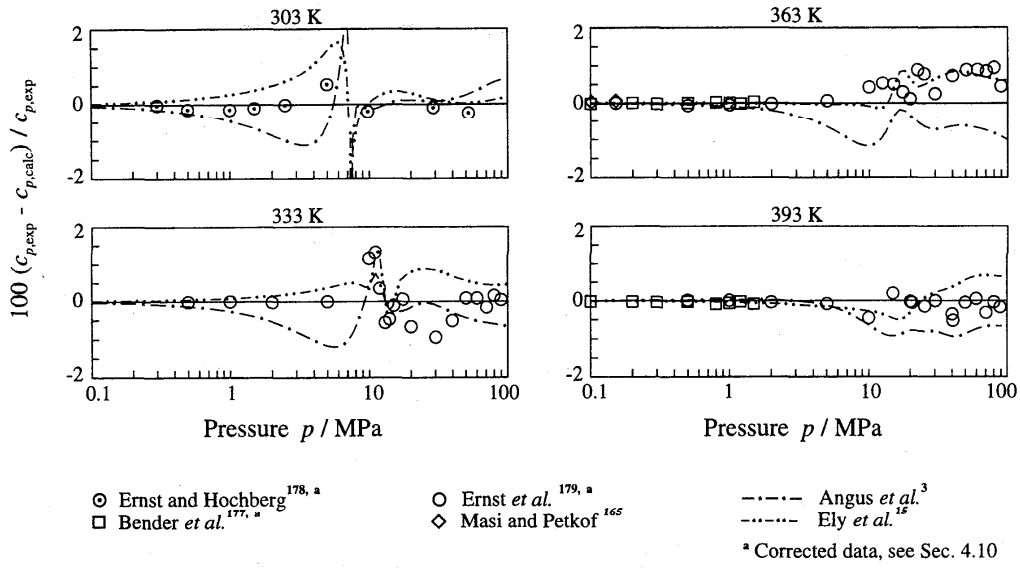

FIG. 27. Relative deviations of selected isobaric heat capacity data from values calculated from Eq. (6.1). Values calculated from the wide-range equations of Ely *et al.*[15] and Angus *et al.*[3] are plotted for comparison.

At temperatures above 698 K, Eq. (6.1) is essentially based on the same data sets as the equations of Ely *et al.*[15] and Angus *et al.*[3] Nevertheless, the three equations show significantly different courses for pressures above 15 MPa. Figure 25 shows that the equation of Angus *et al.*[3] yields the best representation of the data of Vukalovich and Altunin.[128,129] However, in order to achieve a consistent description of the caloric and thermal properties in other regions, we had to assume that this data set exhibits a systematic error. The data of Fenghour *et al.*[160a] support our interpretation of the $p\rho T$ surface for temperatures up to 698 K.

Figure 26 shows how the $p\rho T$ data at very high pressures are represented. Since the range of validity is limited to 100 MPa for the equation of Angus *et al.*[3] and to 300 MPa for the equation of Ely *et al.*,[15] these equations are already extrapolated when plotting values calculated from these equations in Fig. 26. With an estimated uncertainty ranging from 1% to 2% in density, the data of Tsiklis *et al.*[139] and Shmonov and Shmulovich[148] represent the transition to the extrapolation range of Eq. (6.1) which is discussed in Sec. 7.3. Equation (6.1) yields a suitable representation of these data.

7.2.2 Caloric Properties in the Single-Phase Region

In the gas and the supercritical region, the caloric behavior of an equation of state for carbon dioxide can be discussed most advantageously by the example of the specific isobaric heat capacity. Figure 27 shows the deviation between values calculated from Eq. (6.1) and reliable measurements of c_p. The data of Bender *et al.*,[177] Ernst and Hochberg,[178] and of Ernst *et al.*[179] were corrected according to the descriptions in Sec. 4.10. The excellent representation of the data within the gas region, where the well-known contribution of c_p° is predominant, justifies this correction. In the region of the supercritical maximum of c_p, the deviations increase to about $\pm 1\%$ ($+1.3\%$ for a single data point) but the authors estimate that the uncertainty of their data also increases to $\pm 0.9\%$ in this region.

In Fig. 28, absolute values of the specific isobaric heat capacity in the low temperature gas region are plotted. When approaching the sublimation curve, Eq. (6.1) yields a reason-

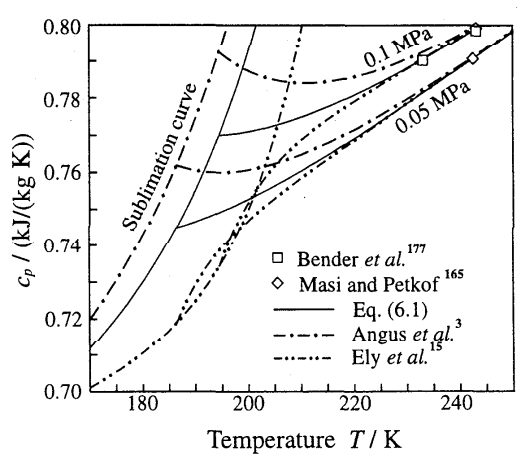

FIG. 28. Representation of the isobaric heat capacity on isobars in the gas region and in states on the sublimation curve (saturated vapor). Values calculated from the wide-range equations of Ely *et al.*[15] and Angus *et al.*[3] are plotted for comparison.

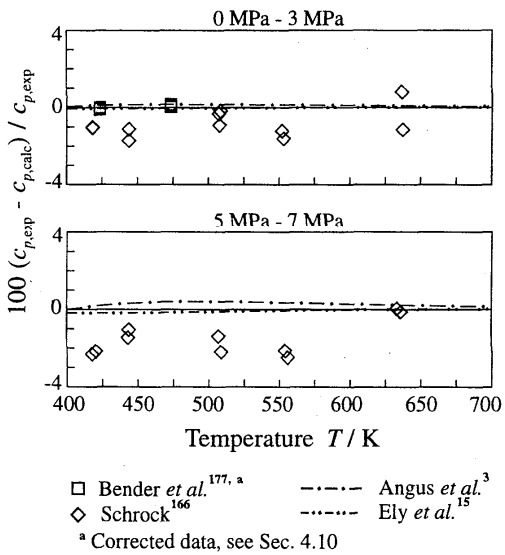

FIG. 29. Relative deviations of isobaric heat capacity data at high temperatures from values calculated from Eq. (6.1). Values calculated from the wide-range equations of Ely *et al.*[15] and Angus *et al.*[3] are plotted for comparison.

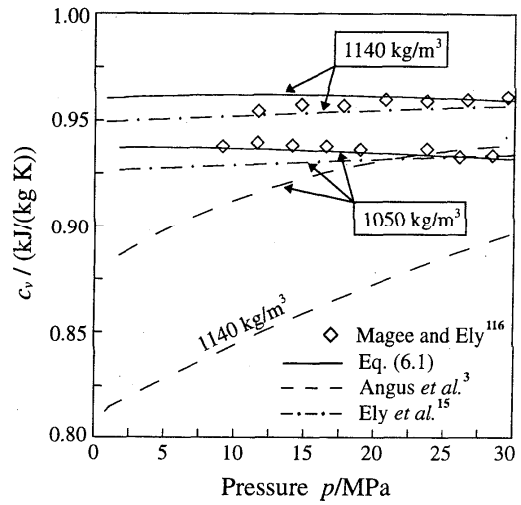

FIG. 31. Representation of the isochoric heat capacity on high-density isochores. For each of the isochores the plotted pressure range starts at the corresponding vapor pressure. Values calculated from the wide-range equations of Ely *et al.*[15] and Angus *et al.*[3] are plotted for comparison.

able extrapolation of the plotted isobars. The equation of Angus *et al.*[3] also shows a reasonable extrapolation behavior, but comparisons with recent data[177] at a temperature of 233 K indicate that the resulting values are too high. In contrast to this, the isobars calculated from the equation of Ely *et al.*[15] intersect with each other and with the specific isobaric heat capacity on the sublimation line at temperatures below T_t. Due to the high triple-point pressure of CO_2 (p_t = 0.51795 MPa) and the widespread use of dry ice, an unreasonable behavior in this region is less acceptable for carbon dioxide than for other substances.

At temperatures above 400 K, the values calculated from the different equations of state agree much better with each other than with the data of Schrock[166] which are plotted in

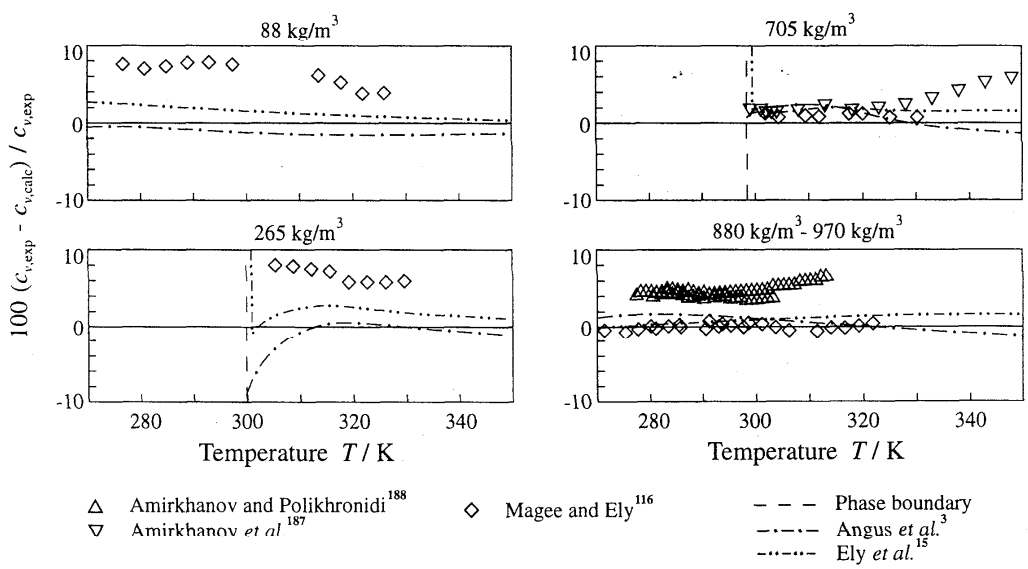

FIG. 30. Relative deviations of selected isochoric heat capacity data from values calculated from Eq. (6.1). Values calculated from the wide-range equations of Ely *et al.*[15] and Angus *et al.*[3] are plotted for comparison.

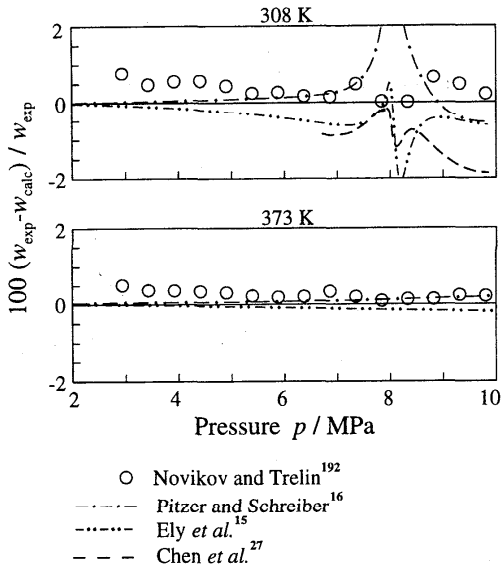

FIG. 32. Relative deviations of speed of sound data at supercritical temperatures from values calculated from Eq. (6.1). Values calculated from the wide-range equations of Ely *et al.*[15] and of Pitzer and Schreiber,[16] and, in the range of validity, from the crossover equation of Chen *et al.*[27] are plotted for comparison.

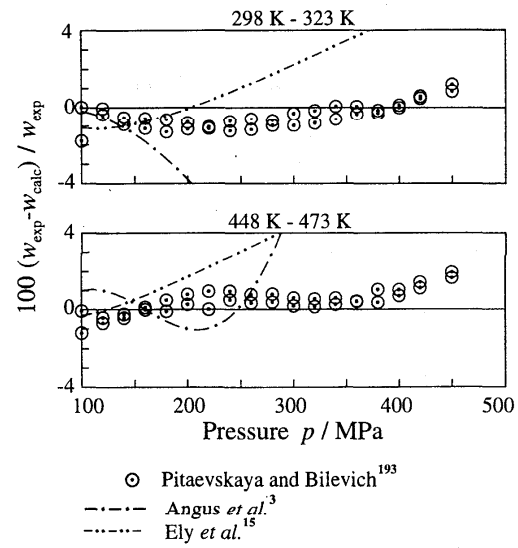

FIG. 33. Relative deviations of speed of sound data at high pressures from values calculated from Eq. (6.1). Values calculated from the wide-range equations of Ely *et al.*[15] and Angus *et al.*[3] are plotted for comparison; in this pressure range, these two equations of state are at least partly extrapolated (see Table 1).

Fig. 29. Up to 473 K, the data of Bender *et al.* support the results of the equations of state. At higher temperatures and moderate pressures, the influence of the residual part of c_p decreases. Since the uncertainty of $c_p^o(T)$ is very small (see Sec. 6.1) and at least some information on the residual part of the equations of state is available from $p\rho T$ data, the equations seem to be more reliable than the available c_p data in this region.

Deviations with regard to the specific isochoric heat capacity at gas and liquid densities are presented in Fig. 30. In the gas region, the behavior of the new fundamental equation concerning caloric properties is based on the precise data of c_p and w; the deviations between the c_v data of Magee and Ely[116] and values calculated from Eq. (6.1) and from the other equations of state, respectively, probably reflect the uncertainty in the data. This fact has resulted in the low average weighting factor listed in Table 17. At high densities, however, the c_v experiments of Magee and Ely[116] yielded reliable results which form the most important source of information on the caloric properties at liquid densities.

Unfortunately, these c_v data only describe states at supercritical pressures (see Fig. 17), so that there is a wide gap between caloric data in the single-phase region and in the saturated liquid state. Figure 31 shows absolute values of the specific isochoric heat capacity on two liquid isochors, plotted versus pressure. Equation (6.1) follows the measurements on the 880 kg/m^3, 970 kg/m^3, and 1050 kg/m^3 isochors and yields with decreasing pressure slightly increasing deviations from the c_v values at the 1140 kg/m^3 isochore. In contrast to this behavior, the equation of Ely *et al.* follows the course of the 1140 kg/m^3 isochore, but it yields slightly too low specific isochoric heat capacities at lower densities. In spite of these different tendencies, the deviations between c_v values calculated from these equations do not exceed 1.5% throughout the extrapolation down to the vapor pressure. Since the uncertainty in the specific heat capacity calculated from Eq. (6.1) is estimated to be $\leqslant \pm 1.5\%$ in the whole high-density region for pressures up to 40 MPa (see Sec. 8), we believe that the uncertainty at subcritical pressures does not increase due to the gap in the data set. New data which describe the caloric behavior of liquid carbon dioxide more accurately would be desirable in order to prove whether this assessment is correct.

The equation of Angus *et al.*[3] fails completely in the description of the specific isochoric heat capacity at high densities. In the liquid region, the deviation between Eq. (6.1) and this formulation grows to 16%.

For carbon dioxide, the representation of speed of sound measurements is a sensitive test for the quality of an equation of state in the following two regions. The data of Novikov and Trelin[192] describe the caloric behavior within the gas and supercritical region. Figure 32 illustrates the representation of w values on two representative isotherms of this data set. While all the considered formulations represent the data within their uncertainty at 373 K, only Eq. (6.1) is able to reproduce the measurements at 308 K; in the extended critical region, the deviations do not exceed $\pm 0.7\%$. On the 308 K isotherm the crossover equation of Chen *et al.*[27] yields deviations up to 2%.

At temperatures between 298 K and 473 K, Pitaevskaya and Bilevich[193] measured speed of sound data at pressures to

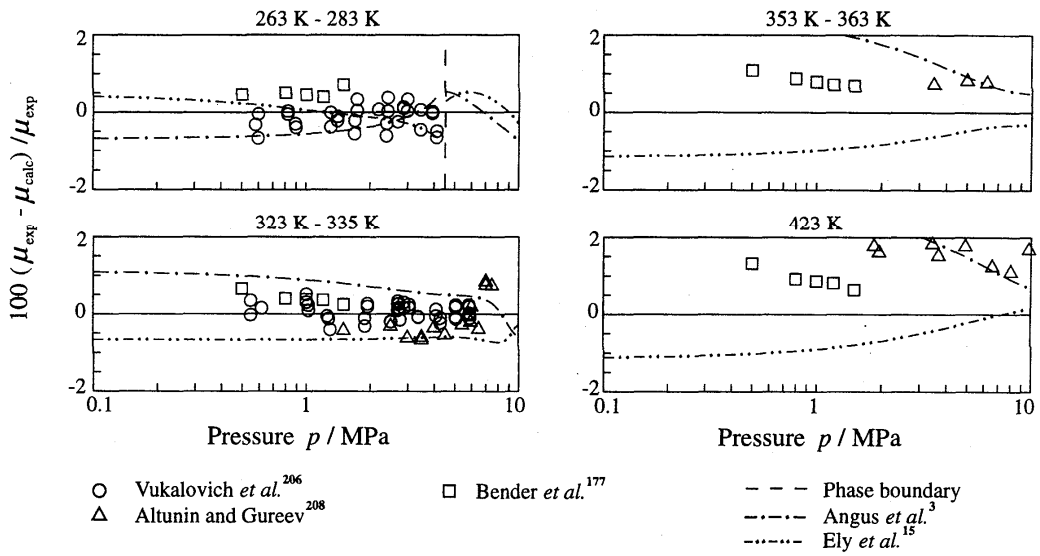

FIG. 34. Relative deviations of experimentally determined Joule–Thomson coefficients from values calculated from Eq. (6.1). Values calculated from the wide-range equations of Ely *et al.*[15] and Angus *et al.*[3] are plotted for comparison. The data of Vukalovich *et al.*[206] were not used when establishing Eq. (6.1).

450 MPa. These data are represented by Eq. (6.1) to within their expected uncertainty of approximately ±2%. Figure 33 shows representative deviation plots covering the lowest and highest temperatures of this data set. None of the previous equations of state is able to yield a reasonable representation of these data. The equation of Angus *et al.*[3] is only valid up to 100 MPa, and extrapolated values of the speed of sound are expected to be uncertain. But the equation of Ely *et al.*[15] should yield reliable results at least within the range of its validity, namely up to 300 MPa.

At pressures up to 1.5 MPa, the Joule–Thomson measurements of Bender *et al.*[177] were used in the nonlinear fit but these data could not be represented without systematic, slightly temperature dependent deviations. After work on the new equation of state had been completed, the isothermal Joule–Thomson coefficients measured by Vukalovich *et al.*[206] were converted into differential Joule–Thomson coefficients by the use of the specific isobaric heat capacity calculated from Eq. (6.1). The new equation represents the converted data of Vukalovich *et al.* without systematic deviations (see Fig. 34); the very accurate $p\rho T$ data set in the gas region prevented the representation of the measurements of Bender *et al.* which deviate from the correlation by approximately 0.5% to 1%.

7.3 Extrapolation Behavior of the New Fundamental Equation

Inspired by the discussion at the Fifth International Workshop on Equations of State, which took place in Bochum in 1990, the extrapolation behavior of empirical equations of state was examined in some detail during the work on carbon dioxide. Since these results cover features of different substances and general approaches, they will be discussed elsewhere.[35] Here, the considerations are restricted to the new fundamental equation for carbon dioxide; the following subsections will give only a brief survey on the extrapolation behavior of Eq. (6.1).

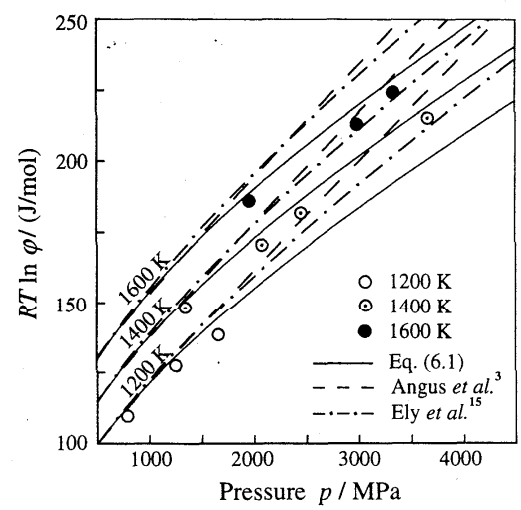

FIG. 35. Representation of experimentally determined fugacities on isotherms at very high temperatures and pressures. Values calculated from the wide-range equations of Ely *et al.*[15] and Angus *et al.*[3] are plotted for comparison.

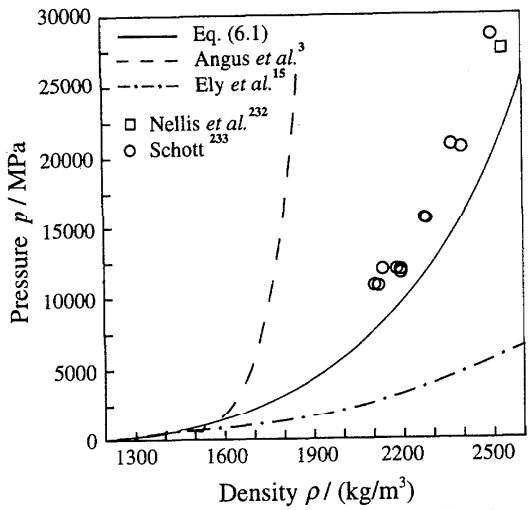

FIG. 36. Representation of experimental data describing the Hugoniot curve of carbon dioxide. Hugoniot curves calculated from the wide-range equations of Ely *et al.*[15] and Angus *et al.*[3] are plotted for comparison.

7.3.1 Extrapolation Beyond the Range of Primary Data

The range of validity of Eq. (6.1) is based on the range where reliable data of thermodynamical properties exist. However, two kinds of data exceed this range.

Figure 35 shows the representation of fugacities reaching up to approximately 3600 MPa at temperatures between 1200 K and 1600 K. The data of Haselton *et al.*[231] were not used when developing Eq. (6.1) since it is difficult to estimate the uncertainty of data originating from measurements of chemical equilibria and since the logarithmic structure of the dependency between the fugacity φ and the reduced Helmholtz energy (see Table 3) prevents an inclusion into the linear optimization procedure. Nevertheless, Eq. (6.1) follows the course of the measurements, whereas both the equation of Angus *et al.*[3] and the equation of Ely *et al.*[15] yield fugacities which are significantly too large. At least at low pressures, the remaining systematic deviations cannot be explained by a misbehavior of the equation of state. All equations of state which have been investigated result in very similar fugacities at pressures below 1000 MPa. In this region, the experimental results are inconsistent with $p\rho T$ data at lower temperatures.

At even higher pressures, shock wave measurements result in data for the Hugoniot relation

TABLE 33. The definition of the zeroth- and first-order ideal curves of the compression factor

Name of the ideal curve	Definition
Classical ideal curve	$Z=pv/RT=1$
Boyle curve	$(\partial Z/\partial p)_T=0$
Joule–Thomson inversion curve	$(\partial Z/\partial T)_p=0$
Joule inversion curve	$(\partial Z/\partial p)_p=0$

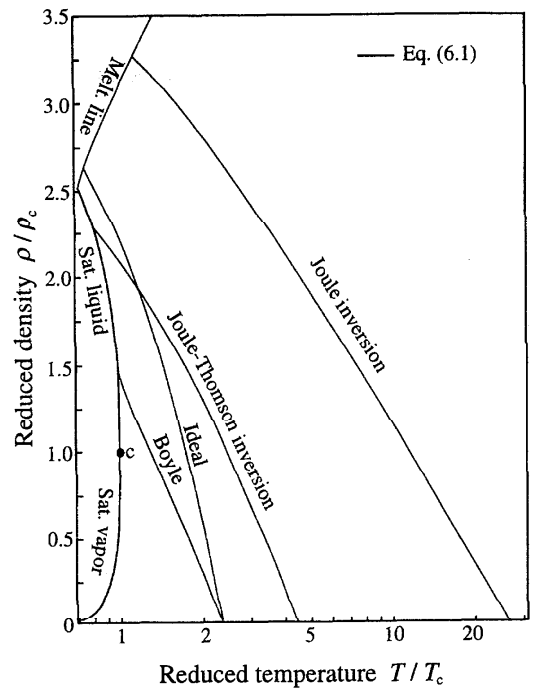

FIG. 37. The so-called ideal curves calculated from Eq. (6.1) and plotted in a ρ/ρ_c, $\log(T/T_c)$ diagram. The Joule–Thomson inversion curve and the Joule inversion curve exceed the temperature range in which Eq. (6.1) is fitted to experimental data.

$$h-h_{0H}=0.5(p-p_{0H})\cdot(1/\rho_{0H}+1/\rho), \qquad (7.1)$$

where h is the enthalpy, p the pressure, and ρ the density after releasing the shock wave and h_{0H}, p_{0H}, and ρ_{0H} are the initial values. Even though it is not yet clear whether these measurements describe equilibrium states at all, comparisons with these data are the only source of experimental information on the extrapolation behavior of an equation of state at very high pressures. Figure 36 shows Hugoniot plots calculated from Eq. (6.1) and from the other two equations of state considered here, compared with the data of Nellis *et al.*[232] and Schott.[233] At approximately 34 000 MPa, Nellis *et al.* observed a kink in the course of the Hugoniot curve which is interpreted as an indication of a spontaneous disintegration reaction. So it can be seen that Eq. (6.1) yields a reasonable description of the Hugoniot curve of carbon dioxide up to the limits of chemical stability. A $T\rho$ plot, which is not given here, shows that the Hugoniot curves calculated from the equations of Ely *et al.*[15] and Angus *et al.*[3] run into low temperature solutions corresponding to solid states above densities of about 1400 kg/m^3.

7.3.2 Representation of "Ideal Curves"

Various authors (see Refs. 234 to 238) have discussed plots of so-called ideal curves[e] as a universal behavior of

[e]"Ideal curves" are curves which connect all states where a special property of a fluid is equal to the corresponding property of the hypothetic ideal gas in the same state.

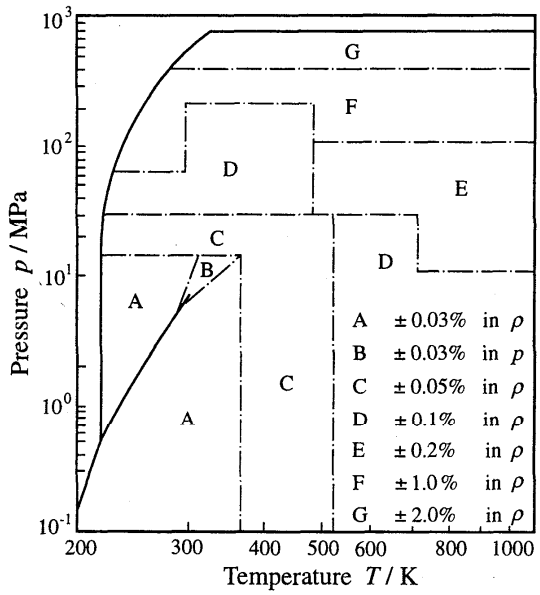

FIG. 38. Tolerance diagram for densities calculated from Eq. (6.1). In region B the uncertainty in pressure is given.

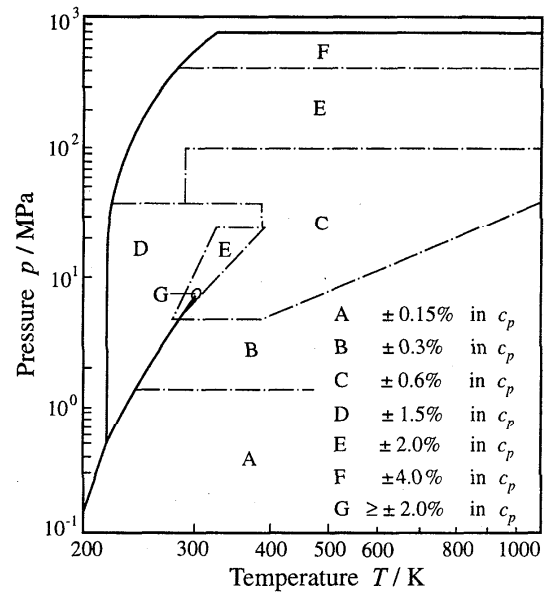

FIG. 40. Tolerance diagram for isobaric heat capacities calculated from Eq. (6.1). In the immediate vicinity of the critical point (region G) it is difficult to estimate an uncertainty in c_p because of the growing influence of uncertainties in temperature and pressure measurement.

pure substances. In 1991, de Reuck[239] gave a brief survey on this topic.

The most common ideal curves are the zeroth and first order curves of the compression factor which are defined by the relations given in Table 33. Figure 37 shows the plot of these curves calculated from Eq. (6.1). The new fundamental equation was fitted to data up to reduced pressures of $p/p_c \approx 108$ and up to reduced temperatures of $T/T_c \approx 3.5$. Thus, the course of the ideal curves does not significantly exceed the pressure range covered by data, but both the Joule–Thomson inversion curve and the Joule inversion curve reach up to temperatures which clearly exceed the range of the data used to fit Eq. (6.1).

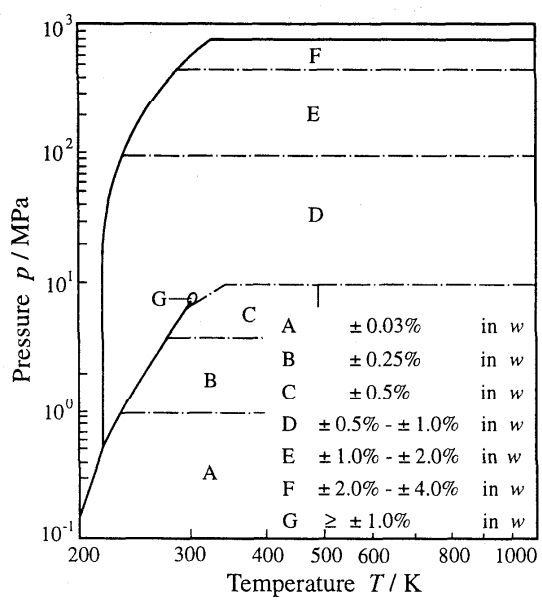

FIG. 39. Tolerance diagram for speed of sound data calculated from Eq. (6.1). In the immediate vicinity of the critical point (region G) it is difficult to estimate an uncertainty in w because of the growing influence of uncertainties in temperature and pressure measurement.

Preliminary equations showed an unreasonable plot of the Joule inversion curve at very high temperatures. In order to force the equation to form a maximum in the course of the second virial coefficient and to ensure that the equation of state yields an intersection of the Joule inversion curve with the zero pressure line at that temperature, 27 $T\rho$ data were determined by graphical extrapolation of the Joule inversion curve in a ρT plot (see Ref. 35). At these values of the state variables, the condition of the Joule inversion curve, $\phi^{r}_{\delta\tau} = 0$. was introduced into the data set used during the adjustment of Eq. (6.1). Since it is difficult to estimate the uncertainty of the inversion condition, the weight of these data was determined by using estimations for the uncertainty of the independent variables T and ρ in combination with the Gaussian error propagation formula [see Eq. (2.6)].

Equation (6.1) shows reasonable plots of the ideal curves in the high temperature region, see Fig. 37. The temperature at which the Joule inversion curve intersects the zero pressure line and at which the second virial coefficient passes through a maximum corresponds to about $T/T_c = 26.9$. Thus, the reasonable behavior of Eq. (6.1) reaches even up to tem-

peratures beyond the limits of the chemical stability of carbon dioxide.

8. Uncertainty of the New Equation of State

Estimates for the uncertainty of an empirical equation of state have to be guided by comparisons with experimental data. In regions where no data are available, comparisons with existing equations of state can be used as a substitute. A conservative estimation of the uncertainty of $p\rho T$, w, and c_p values calculated from Eq. (6.1) is illustrated in the tolerance diagrams Figs. 38 to 40. Uncertainties in c_v correspond to the uncertainties given for c_p in the liquid and gas region. In the extended critical region, the uncertainty in c_v may exceed the uncertainty in c_p. The uncertainty of Δh or Δu values calculated from Eq. (6.1) is less than or equal to the uncertainty in c_p or c_v, respectively.

Outside the range of its validity, Eq. (6.1) should yield reasonable results for the basic thermodynamic properties like pressure, enthalpy, and fugacity within the whole chemically stable region of carbon dioxide. Of course, the extrapolation results have an increased uncertainty which cannot be estimated. The calculation of derived properties such as the speed of sound or specific heat capacities is not recommended beyond the limits of validity. If such data are needed, the results should be checked carefully.

9. Conclusions

Based on a comprehensive study on the experimental data for the thermodynamic properties of carbon dioxide, a new fundamental equation in the form of the Helmholtz energy has been developed. This empirical formulation is valid in the fluid region up to temperatures of 1100 K and at pressures up to 800 MPa. The equation is able to represent almost all the reliable data in the homogeneous region and on the liquid-vapor phase boundary within their experimental uncertainty. The consideration of state-of-the-art data has resulted in a previously unequalled accuracy for the regions of major technical interest. Intensive work on the consistency of the data set used has led to reasonable results in regions with a poor data situation.

Special interest has been focused on the behavior of caloric properties in the critical region and on the extrapolation behavior of empirical equations of state. The introduction of nonanalytic terms enables the new wide-range equation of state to represent the isochoric heat capacity and the speed of sound even in the immediate vicinity of the critical point; up to now, this attribute has only been a domain of scaled equations of state which introduce iterative dependencies between different sets of variables and a limited range of validity. An examination of the extrapolation behavior of empirical equations of state has resulted in new approaches which have been used for the new formulation. For the basic properties of carbon dioxide such as pressure, enthalpy, and fugacity, the new fundamental equation should yield reasonable results within the whole region of chemical stability.

10. Appendix: Thermodynamic Properties of Carbon Dioxide

In order to preserve thermodynamic consistency all values presented in Tables 34 and 35 were calculated only from the new equation of state, Eq. (6.1). Ideally, each entry in the table should be given to one more significant figure than the input data warrant, but a strict adherence to this principle is difficult, and a possible conflict has always been avoided by including more figures than are strictly necessary. Especially in the extended critical region, interpolation between values given may result in uncertainties which are significantly larger then the uncertainties of Eq. (6.1). For sophisticated applications, values should be calculated directly from Eq. (6.1); a computer-code suitable for such applications can be obtained from the authors.

TABLE 34. Thermodynamic properties of saturated carbon dioxide

Temperature (K)	Pressure (MPa)	Density (kg/m^3)	Enthalpy (kJ/kg)	Entropy [kJ/(kg K)]	c_v [kJ/(kg K)]	c_p [kJ/(kg K)]	Speed of sound (m/s)
216.592[a]	0.51796	1178.46	−426.74	−2.2177	0.97466	1.9532	975.85
		13.761	−76.364	−0.59999	0.62921	0.90872	222.78
218	0.55042	1173.40	−423.98	−2.2051	0.97264	1.9566	965.66
		14.584	−75.847	−0.60815	0.63318	0.91743	222.94
220	0.59913	1166.14	−420.05	−2.1873	0.96983	1.9618	951.21
		15.817	−75.142	−0.61957	0.63894	0.93032	223.15
222	0.65102	1158.81	−416.11	−2.1697	0.96707	1.9676	936.79
		17.131	−74.473	−0.63080	0.64485	0.94386	223.31
224	0.70621	1151.40	−412.16	−2.1522	0.96437	1.9739	922.37
		18.530	−73.840	−0.64185	0.65091	0.95807	223.44
226	0.76484	1143.92	−408.19	−2.1348	0.96174	1.9810	907.95
		20.016	−73.246	−0.65274	0.65712	0.97302	223.52
228	0.82703	1136.34	−404.21	−2.1175	0.95917	1.9886	893.53
		21.595	−72.692	−0.66347	0.66350	0.98875	223.57
230	0.89291	1128.68	−400.21	−2.1003	0.95667	1.9970	879.09
		23.271	−72.178	−0.67406	0.67004	1.0053	223.57
232	0.96262	1120.93	−396.19	−2.0832	0.95425	2.0061	864.63
		25.050	−71.708	−0.68452	0.67675	1.0228	223.54
234	1.0363	1113.08	−392.16	−2.0661	0.95190	2.0160	850.14
		26.936	−71.283	−0.69487	0.68363	1.0412	223.46
236	1.1141	1105.12	−388.11	−2.0492	0.94963	2.0267	835.61
		28.935	−70.903	−0.70511	0.69068	1.0608	223.33
238	1.1961	1097.05	−384.04	−2.0323	0.94745	2.0384	821.02
		31.052	−70.573	−0.71526	0.69792	1.0814	223.17
240	1.2825	1088.87	−379.94	−2.0155	0.94535	2.0510	806.38
		33.295	−70.293	−0.72532	0.70534	1.1033	222.96
242	1.3734	1080.56	−375.82	−1.9988	0.94335	2.0647	791.67
		35.670	−70.066	−0.73533	0.71297	1.1265	222.70
244	1.4690	1072.13	−371.68	−1.9821	0.94145	2.0795	776.87
		38.184	−69.894	−0.74527	0.72081	1.1513	222.40
246	1.5693	1063.56	−367.51	−1.9654	0.93965	2.0956	761.97
		40.845	−69.780	−0.75518	0.72889	1.1778	222.06
248	1.6746	1054.84	−363.30	−1.9488	0.93797	2.1131	746.95
		43.662	−69.726	−0.76506	0.73725	1.2061	221.66
250	1.7850	1045.97	−359.07	−1.9323	0.93643	2.1320	731.78
		46.644	−69.736	−0.77492	0.74591	1.2366	221.22
252	1.9007	1036.93	−354.80	−1.9157	0.93506	2.1527	716.44
		49.801	−69.813	−0.78479	0.75489	1.2693	220.72
254	2.0217	1027.72	−350.50	−1.8991	0.93390	2.1751	700.88
		53.144	−69.960	−0.79467	0.76421	1.3047	220.17
256	2.1483	1018.32	−346.15	−1.8826	0.93300	2.1995	685.08
		56.685	−70.181	−0.80458	0.77388	1.3429	219.56
258	2.2806	1008.71	−341.77	−1.8660	0.93244	2.2262	668.99
		60.438	−70.480	−0.81453	0.78390	1.3844	218.90
260	2.4188	998.89	−337.34	−1.8495	0.93227	2.2554	652.58
		64.417	−70.862	−0.82456	0.79426	1.4295	218.19
262	2.5630	988.83	−332.86	−1.8329	0.93258	2.2874	635.84
		68.640	−71.332	−0.83467	0.80498	1.4787	217.41
264	2.7134	978.51	−328.33	−1.8162	0.93344	2.3226	618.75
		73.124	−71.896	−0.84488	0.81604	1.5326	216.59
266	2.8701	967.92	−323.74	−1.7995	0.93488	2.3617	601.31
		77.891	−72.561	−0.85523	0.82749	1.5919	215.70
268	3.0334	957.04	−319.09	−1.7827	0.93693	2.4050	583.54
		82.965	−73.334	−0.86573	0.83935	1.6575	214.76
270	3.2033	945.83	−314.37	−1.7658	0.93959	2.4534	565.46
		88.374	−74.223	−0.87641	0.85168	1.7307	213.75
272	3.3802	934.26	−309.57	−1.7488	0.94283	2.5079	547.11
		94.148	75.240	0.88732	0.86454	1.8128	212.68
274	3.5642	922.30	−304.70	−1.7317	0.94659	2.5694	528.51
		100.32	−76.395	−0.89849	0.87801	1.9057	211.55
276	3.7555	909.90	−299.73	−1.7144	0.95082	2.6396	509.71
		106.95	−77.702	−0.90995	0.89218	2.0117	210.35

TABLE 34. Thermodynamic properties of saturated carbon dioxide—Continued

Temperature (K)	Pressure (MPa)	Density (kg/m^3)	Enthalpy (kJ/kg)	Entropy [kJ/(kg K)]	c_v [kJ/(kg K)]	c_p [kJ/(kg K)]	Speed of sound (m/s)
278	3.9542	897.02	−294.66	−1.6969	0.95545	2.7203	490.72
		114.07	−79.177	−0.92178	0.90719	2.1341	209.07
280	4.1607	883.58	−289.48	−1.6792	0.96046	2.8141	471.54
		121.74	−80.840	−0.93401	0.92316	2.2769	207.72
282	4.3752	869.52	−284.17	−1.6611	0.96584	2.9246	452.19
		130.05	−82.713	−0.94674	0.94029	2.4458	206.28
284	4.5978	854.74	−278.71	−1.6428	0.97166	3.0569	432.63
		139.09	−84.825	−0.96006	0.95878	2.6490	204.74
286	4.8289	839.12	−273.08	−1.6239	0.97806	3.2181	412.81
		148.98	−87.214	−0.97407	0.97895	2.8979	203.10
288	5.0688	822.50	−267.24	−1.6046	0.98528	3.4189	392.63
		159.87	−89.926	−0.98894	1.0012	3.2104	201.34
290	5.3177	804.67	−261.15	−1.5846	0.99373	3.6756	371.95
		171.96	−93.025	−1.0049	1.0260	3.6142	199.45
292	5.5761	785.33	−254.76	−1.5637	1.0041	4.0145	350.49
		185.55	−96.599	−1.0221	1.0543	4.1558	197.38
294	5.8443	764.09	−247.97	−1.5418	1.0177	4.4834	327.85
		201.06	100.77	1.0411	1.0872	4.9196	195.09
296	6.1227	740.28	−240.68	−1.5183	1.0371	5.1813	303.44
		219.14	−105.74	−1.0624	1.1269	6.0741	192.49
298	6.4121	712.77	−232.64	−1.4926	1.0675	6.3473	276.42
		240.90	−111.83	−1.0872	1.1774	8.0128	189.38
300	6.7131	679.24	−223.40	−1.4631	1.1199	8.6979	245.67
		268.58	−119.70	−1.1175	1.2476	11.921	185.33
301	6.8683	658.69	−218.03	−1.4460	1.1631	11.053	228.18
		286.15	−124.73	−1.1361	1.2972	15.859	182.61
302	7.0268	633.69	−211.76	−1.4261	1.2316	15.786	208.08
		308.15	−131.05	−1.1588	1.3676	23.800	178.91
303	7.1890	599.86	−203.73	−1.4004	1.3702	30.233	182.14
		339.00	−139.91	−1.1897	1.4925	47.599	172.71
304	7.3555	530.30	−188.42	−1.3509	2.0531	386.88	134.14
		406.42	−158.84	−1.2536	2.0679	555.58	147.62
304.1282[b]	7.3773	467.60	−174.53	−1.3054			

[a]Triple point.
[b]Critical point.

TABLE 35. Thermodynamic properties of carbon dioxide

Temperature (K)	Density (kg/m^3)	Internal energy (kJ/kg)	Enthalpy (kJ/kg)	Entropy [kJ/(kg K)]	c_v [kJ/(kg K)]	c_p [kJ/(kg K)]	Speed of sound (m/s)
			0.05 MPa Isobar				
186.436[a]	1.4370	−123.74	−88.944	−0.23757	0.54404	0.74495	216.947
190	1.4089	−121.78	−86.286	−0.22345	0.54661	0.74660	218.90
200	1.3359	−116.22	−78.792	−0.18501	0.55478	0.75266	224.26
210	1.2704	−110.59	−71.228	−0.14811	0.56398	0.76029	229.41
220	1.2112	−104.86	−63.582	−0.11254	0.57386	0.76897	234.38
230	1.1575	−99.044	−55.846	−0.07816	0.58417	0.77834	239.20
240	1.1084	−93.125	−48.014	−0.04483	0.59473	0.78815	243.88
250	1.0634	−87.104	−40.082	−0.01245	0.60542	0.79823	248.44
260	1.0219	−80.978	−32.049	0.01906	0.61612	0.80845	252.88
270	0.98360	−74.747	−23.913	0.04976	0.62679	0.81871	257.23
280	0.94810	−68.412	−15.675	0.07972	0.63737	0.82895	261.49
290	0.91510	−61.973	−7.3344	0.10899	0.64782	0.83912	265.67
300	0.88434	−55.432	1.1072	0.13761	0.65812	0.84917	269.77
325	0.81585	−38.641	22.645	0.20655	0.68307	0.87366	279.71
350	0.75726	−21.246	44.781	0.27216	0.70681	0.89707	289.27
375	0.70656	−3.2771	67.489	0.33481	0.72932	0.91933	298.50
400	0.66224	15.237	90.738	0.39483	0.75063	0.94046	307.42
425	0.62317	34.268	114.50	0.45245	0.77081	0.96051	316.08
450	0.58847	53.788	138.76	0.50789	0.78995	0.97953	324.50
475	0.55743	73.774	163.47	0.56134	0.80811	0.99760	332.69
500	0.52951	94.201	188.63	0.61295	0.82537	1.0148	340.67
525	0.50426	115.05	214.20	0.66286	0.84179	1.0312	348.46
550	0.48130	136.29	240.18	0.71120	0.85744	1.0468	356.08
575	0.46035	157.92	266.54	0.75806	0.87236	1.0616	363.53
600	0.44115	179.92	293.26	0.80354	0.88660	1.0758	370.83
700	0.37809	271.21	403.45	0.97331	0.93747	1.1266	398.65
800	0.33081	367.15	518.30	1.1266	0.97994	1.1690	424.64
900	0.29404	466.98	637.03	1.2664	1.0155	1.2045	449.13
1000	0.26463	570.06	759.01	1.3949	1.0452	1.2342	472.37
1100	0.24057	675.87	883.71	1.5137	1.0702	1.2592	494.54
			0.10 MPa Isobar				
194.525[a]	2.7796	−120.24	−84.267	−0.34184	0.56013	0.76998	219.98
200	2.6980	−117.11	−80.049	−0.32046	0.56339	0.77091	223.00
210	2.5617	−111.36	−72.323	−0.28276	0.57062	0.77476	228.33
220	2.4394	−105.54	−64.547	−0.24659	0.57907	0.78067	233.45
230	2.3288	−99.645	−56.705	−0.21173	0.58833	0.78795	238.38
240	2.2282	−93.664	−48.785	−0.17803	0.59811	0.79618	243.15
250	2.1363	−87.589	−40.780	−0.14535	0.60818	0.80501	247.79
260	2.0519	−81.419	−32.684	−0.11360	0.61843	0.81424	252.31
270	1.9741	−75.151	−24.494	−0.08269	0.62872	0.82371	256.72
280	1.9021	−68.784	−16.209	−0.05256	0.63900	0.83330	261.03
290	1.8352	−62.317	−7.8279	−0.02315	0.64922	0.84293	265.25
300	1.7730	−55.751	0.64941	0.00559	0.65932	0.85253	269.39
325	1.6348	−38.911	22.260	0.07477	0.68392	0.87619	279.42
350	1.5167	−21.479	44.452	0.14054	0.70743	0.89903	289.04
375	1.4147	−3.4815	67.203	0.20332	0.72978	0.92090	298.31
400	1.3257	15.056	90.488	0.26342	0.75099	0.94173	307.28
425	1.2472	34.105	114.28	0.32111	0.77109	0.96156	315.97
450	1.1776	53.640	138.56	0.37661	0.79017	0.98041	324.41
475	1.1154	73.639	163.29	0.43011	0.80829	0.99835	332.62
500	1.0594	94.076	188.47	0.48175	0.82552	1.0154	340.62

TABLE 35. Thermodynamic properties of carbon dioxide—Continued

Temperature (K)	Density (kg/m^3)	Internal energy (kJ/kg)	Enthalpy (kJ/kg)	Entropy [kJ/(kg K)]	c_v [kJ/(kg K)]	c_p [kJ/(kg K)]	Speed of sound (m/s)
			0.10 MPa Isobar				
525	1.0088	114.93	214.06	0.53169	0.84192	1.0317	348.43
550	0.96283	136.19	240.05	0.58005	0.85755	1.0473	356.06
575	0.92087	157.82	266.42	0.62693	0.87245	1.0621	363.52
600	0.88242	179.82	293.15	0.67243	0.88668	1.0762	370.83
700	0.75619	271.13	403.38	0.84226	0.93752	1.1269	398.68
800	0.66158	367.09	518.24	0.99558	0.97997	1.1692	424.68
900	0.58803	466.93	636.99	1.1354	1.0155	1.2046	449.19
1000	0.52921	570.02	758.98	1.2639	1.0452	1.2343	472.43
1100	0.48109	675.83	883.69	1.3827	1.0702	1.2593	494.61
			0.101325 MPa Isobar				
194.685[a]	2.8147	−120.18	−84.180	−0.34383	0.56049	0.77056	220.03
200	2.7345	−117.14	−80.083	−0.32307	0.56362	0.77141	222.97
210	2.5963	−111.38	−72.352	−0.28535	0.57080	0.77516	228.30
220	2.4722	−105.56	−64.573	−0.24916	0.57921	0.78098	233.42
230	2.3601	−99.661	−56.728	−0.21429	0.58845	0.78821	238.36
240	2.2581	−93.678	−48.806	−0.18057	0.59820	0.79639	243.14
250	2.1649	−87.602	−40.798	−0.14789	0.60826	0.80519	247.78
260	2.0793	−81.431	−32.701	−0.11613	0.61849	0.81440	252.30
270	2.0004	−75.162	−24.509	−0.08522	0.62878	0.82384	256.71
280	1.9274	−68.793	−16.223	−0.05508	0.63905	0.83341	261.02
290	1.8597	−62.326	−7.8410	−0.02567	0.64925	0.84303	265.24
300	1.7966	−55.760	0.63726	0.00307	0.65935	0.85262	269.38
325	1.6565	−38.918	22.250	0.07226	0.68394	0.87625	279.41
350	1.5369	−21.486	44.443	0.13803	0.70745	0.89908	289.03
375	1.4335	−3.4869	67.196	0.20082	0.72980	0.92094	298.31
400	1.3433	15.051	90.482	0.26092	0.75100	0.94177	307.28
425	1.2638	34.100	114.28	0.31862	0.77110	0.96159	315.97
450	1.1932	53.637	138.55	0.37412	0.79018	0.98044	324.41
475	1.1302	73.635	163.29	0.42761	0.80829	0.99837	332.62
500	1.0735	94.073	188.46	0.47926	0.82552	1.0155	340.62
525	1.0222	114.93	214.06	0.52920	0.84192	1.0317	348.43
550	0.97559	136.18	240.04	0.57756	0.85755	1.0473	356.06
575	0.93308	157.82	266.41	0.62444	0.87246	1.0621	363.52
600	0.89412	179.82	293.14	0.66994	0.88668	1.0762	370.83
700	0.76621	271.13	403.38	0.83977	0.93752	1.1269	398.68
800	0.67035	367.09	518.24	0.99309	0.97997	1.1692	424.69
900	0.59582	466.93	636.99	1.1329	1.0155	1.2046	449.19
1000	0.53622	570.02	758.98	1.2614	1.0452	1.2343	472.44
1100	0.48746	675.83	883.69	1.3803	1.0702	1.2593	494.61

TABLE 35. Thermodynamic properties of carbon dioxide—Continued

Temperature (K)	Density (kg/m^3)	Internal energy (kJ/kg)	Enthalpy (kJ/kg)	Entropy [kJ/(kg K)]	c_v [kJ/(kg K)]	c_p [kJ/(kg K)]	Speed of sound (m/s)
			0.20 MPa Isobar				
203.314[a]	5.4054	−116.97	−79.973	−0.44750	0.58210	0.80842	222.32
210	5.2116	−112.95	−74.577	−0.42138	0.58456	0.80597	226.10
220	4.9495	−106.93	−66.522	−0.38391	0.58993	0.80556	231.52
230	4.7152	−100.87	−58.456	−0.34806	0.59692	0.80819	236.70
240	4.5039	−94.758	−50.352	−0.31357	0.60502	0.81291	241.68
250	4.3120	−88.575	−42.193	−0.28026	0.61383	0.81906	246.49
260	4.1369	−82.313	−33.967	−0.24800	0.62310	0.82618	251.16
270	3.9761	−75.967	−25.667	−0.21668	0.63264	0.83396	255.69
280	3.8280	−69.534	−17.286	−0.18620	0.64231	0.84219	260.10
290	3.6909	−63.010	−8.8222	−0.15650	0.65203	0.85070	264.42
300	3.5636	−56.394	−0.27188	−0.12751	0.66174	0.85938	268.64
325	3.2819	−39.454	21.487	−0.05786	0.68562	0.88131	278.83
350	3.0423	−21.947	43.792	0.00825	0.70867	0.90300	288.58
375	2.8360	−3.8914	66.631	0.07127	0.73072	0.92405	297.95
400	2.6562	14.692	89.987	0.13156	0.75170	0.94429	306.99
425	2.4981	33.778	113.84	0.18939	0.77166	0.96367	315.74
450	2.3580	53.344	138.16	0.24500	0.79062	0.98219	324.23
475	2.2328	73.368	162.94	0.29858	0.80865	0.99986	332.49
500	2.1204	93.827	188.15	0.35030	0.82582	1.0167	340.53
525	2.0188	114.70	213.77	0.40030	0.84217	1.0329	348.37
550	1.9265	135.97	239.79	0.44871	0.85776	1.0482	356.02
575	1.8424	157.62	266.18	0.49563	0.87263	1.0630	363.51
600	1.7653	179.63	292.93	0.54117	0.88684	1.0770	370.83
700	1.5124	270.99	403.22	0.71109	0.93761	1.1274	398.74
800	1.3230	366.97	518.13	0.86447	0.98003	1.1696	424.78
900	1.1759	466.82	636.91	1.0043	1.0155	1.2049	449.30
1000	1.0582	569.93	758.93	1.1329	1.0452	1.2345	472.56
1100	0.96197	675.75	883.66	1.2517	1.0702	1.2594	494.75
			0.30 MPa Isobar				
208.797[a]	8.0141	−115.37	−77.936	−0.51088	0.59903	0.84154	223.07
210	7.9594	−114.62	−76.925	−0.50605	0.59918	0.84031	223.78
220	7.5367	−108.37	−68.563	−0.46715	0.60144	0.83277	229.53
230	7.1633	−102.13	−60.253	−0.43021	0.60593	0.82996	234.98
240	6.8298	−95.878	−51.953	−0.39488	0.61219	0.83067	240.18
250	6.5292	−89.579	−43.632	−0.36091	0.61964	0.83382	245.17
260	6.2564	−83.222	−35.271	−0.32812	0.62788	0.83863	249.98
270	6.0072	−76.795	−26.855	−0.29636	0.63662	0.84459	254.64
280	5.7785	−70.293	−18.376	−0.26553	0.64567	0.85136	259.17
290	5.5675	−63.710	−9.8262	−0.23553	0.65488	0.85869	263.58
300	5.3723	−57.043	−1.2010	−0.20629	0.66418	0.86640	267.88
325	4.9416	−40.000	20.709	−0.13615	0.68733	0.88653	278.24
350	4.5770	−22.417	43.128	−0.06970	0.70992	0.90702	288.11
375	4.2638	−4.3028	66.057	−0.00643	0.73165	0.92723	297.58
400	3.9916	14.326	89.485	0.05404	0.75242	0.94687	306.70

TABLE 35. Thermodynamic properties of carbon dioxide—Continued

Temperature (K)	Density (kg/m^3)	Internal energy (kJ/kg)	Enthalpy (kJ/kg)	Entropy [kJ/(kg K)]	c_v [kJ/(kg K)]	c_p [kJ/(kg K)]	Speed of sound (m/s)
			0.30 MPa Isobar				
425	3.7526	33.450	113.40	0.11202	0.77222	0.96580	315.52
450	3.5410	53.048	137.77	0.16774	0.79107	0.98397	324.06
475	3.3523	73.097	162.59	0.22141	0.80902	1.0014	332.36
500	3.1829	93.578	187.83	0.27320	0.82612	1.0180	340.43
525	3.0299	114.47	213.48	0.32326	0.84242	1.0340	348.30
550	2.8911	135.76	239.53	0.37172	0.85797	1.0492	355.98
575	2.7646	157.42	265.94	0.41868	0.87282	1.0638	363.49
600	2.6487	179.45	292.71	0.46426	0.88699	1.0778	370.84
700	2.2687	270.84	403.07	0.63428	0.93770	1.1279	398.80
800	1.9844	366.84	518.02	0.78771	0.98009	1.1699	424.87
900	1.7635	466.72	636.83	0.92761	1.0156	1.2052	449.41
1000	1.5870	569.84	758.87	1.0562	1.0453	1.2347	472.69
1100	1.4426	675.67	883.63	1.1750	1.0703	1.2596	494.88
			0.50 MPa Isobar				
216.075[a]	13.282	−114.05	76.405	−0.59404	0.62692	0.90323	222.86
220	12.974	−111.42	−72.876	−0.57785	0.62625	0.89522	225.33
230	12.265	−104.78	−64.010	−0.53843	0.62547	0.87913	231.38
240	11.646	−98.202	−55.270	−0.50124	0.62750	0.86991	237.06
250	11.097	−91.650	−46.594	−0.46582	0.63186	0.86583	242.44
260	10.606	−85.086	−37.941	−0.43188	0.63782	0.86526	247.58
270	10.161	−78.487	−29.281	−0.39920	0.64484	0.86710	252.51
280	9.7568	−71.840	−20.594	−0.36761	0.65255	0.87063	257.27
290	9.3864	−65.133	−11.865	−0.33697	0.66071	0.87537	261.87
300	9.0456	−58.359	−3.0836	−0.30721	0.66916	0.88096	266.35
325	8.2996	−41.105	19.139	−0.23606	0.69081	0.89726	277.05
350	7.6736	−23.365	41.793	−0.16892	0.71244	0.91523	287.18
375	7.1393	−5.1305	64.905	−0.10514	0.73353	0.93370	296.85
400	6.6770	13.593	88.478	−0.04430	0.75386	0.95209	306.13
425	6.2725	32.793	112.51	0.01397	0.77335	0.97010	315.07
450	5.9154	52.453	136.98	0.06991	0.79197	0.98757	323.72
475	5.5975	72.554	161.88	0.12376	0.80975	1.0044	332.10
500	5.3126	93.079	187.19	0.17570	0.82672	1.0207	340.25
525	5.0558	114.01	212.91	0.22588	0.84292	1.0363	348.18
550	4.8229	135.33	239.00	0.27443	0.85840	1.0512	355.91
575	4.6108	157.02	265.46	0.32148	0.87318	1.0656	363.47
600	4.4168	179.07	292.28	0.36713	0.88731	1.0794	370.85
700	3.7814	270.54	402.76	0.53734	0.93789	1.1289	398.92
800	3.3067	366.60	517.81	0.69090	0.98022	1.1707	425.06
900	2.9383	466.51	636.68	0.83087	1.0157	1.2057	449.64
1000	2.6439	569.65	758.77	0.95947	1.0453	1.2352	472.94
1100	2.4033	675.51	883.56	1.0784	1.0703	1.2600	495.15

TABLE 35. Thermodynamic properties of carbon dioxide—Continued

Temperature (K)	Density (kg/m^3)	Internal energy (kJ/kg)	Enthalpy (kJ/kg)	Entropy [kJ/(kg K)]	c_v [kJ/(kg K)]	c_p [kJ/(kg K)]	Speed of sound (m/s)
			0.75 MPa Isobar				
216.642[b]	1178.77	−427.22	−426.58	−2.2178	0.97489	1.9518	976.77
220	1166.48	−420.66	−420.01	−2.1878	0.97002	1.9607	952.10
225	1147.71	−410.82	−410.17	−2.1435	0.96306	1.9772	915.26
225.505[c]	1145.78	−409.83	−409.17	−2.1391	0.96238	1.9792	911.52
225.505[c]	19.640	−111.58	−73.389	−0.65006	0.65557	0.96925	223.51
230	19.095	−108.34	−69.068	−0.63108	0.65297	0.95402	226.53
235	18.535	−104.80	−64.335	−0.61073	0.65047	0.93952	229.79
240	18.018	−101.29	−59.668	−0.59107	0.64888	0.92783	232.92
245	17.536	−97.821	−55.052	−0.57204	0.64826	0.91866	235.94
250	17.087	−94.371	−50.477	−0.55356	0.64852	0.91161	238.87
255	16.665	−90.937	−45.933	−0.53556	0.64951	0.90630	241.70
260	16.269	−87.513	−41.412	−0.51800	0.65110	0.90241	244.46
265	15.894	−84.094	−36.907	−0.50084	0.65318	0.89969	247.14
270	15.540	−80.676	−32.414	−0.48404	0.65565	0.89792	249.76
275	15.204	−77.256	−27.927	−0.46757	0.65844	0.89696	252.32
280	14.884	−73.831	−23.443	−0.45141	0.66150	0.89665	254.83
285	14.580	−70.399	−18.959	−0.43554	0.66478	0.89691	257.29
290	14.290	−66.957	−14.473	−0.41994	0.66824	0.89764	259.70
295	14.013	−63.505	−9.9821	−0.40458	0.67184	0.89878	262.07
300	13.747	−60.041	−5.4847	−0.38947	0.67556	0.90026	264.41
305	13.493	−56.564	−0.97908	−0.37457	0.67937	0.90202	266.70
310	13.249	−53.072	3.5360	−0.35989	0.68326	0.90404	268.96
315	13.015	−49.566	8.0617	−0.34540	0.68720	0.90627	271.19
320	12.789	−46.044	12.599	−0.33111	0.69120	0.90868	273.39
325	12.572	−42.507	17.149	−0.31701	0.69523	0.91126	275.56
330	12.363	−38.952	21.712	−0.30307	0.69928	0.91397	277.70
335	12.162	−35.381	26.289	−0.28931	0.70336	0.91680	279.82
340	11.967	−31.793	30.880	−0.27570	0.70744	0.91973	281.91
345	11.779	−28.187	35.486	−0.26225	0.71154	0.92274	283.98
350	11.597	−24.563	40.107	−0.24896	0.71562	0.92583	286.02
360	11.251	−17.262	49.397	−0.22279	0.72378	0.93217	290.05
370	10.927	−9.8882	58.751	−0.19716	0.73188	0.93869	294.00
380	10.621	−2.4415	68.171	−0.17204	0.73991	0.94532	297.88
390	10.333	5.0782	77.658	−0.14739	0.74784	0.95202	301.68
400	10.062	12.671	87.212	−0.12321	0.75568	0.95875	305.42
410	9.8042	20.336	96.833	−0.09945	0.76340	0.96549	309.11
420	9.5603	28.072	106.52	−0.07610	0.77101	0.97221	312.73
430	9.3287	35.880	116.28	−0.05315	0.77850	0.97890	316.31
440	9.1085	43.758	126.10	−0.03057	0.78586	0.98554	319.83
450	8.8987	51.706	135.99	−0.00835	0.79310	0.99212	323.30
460	8.6988	59.723	145.94	0.01353	0.80022	0.99864	326.73
470	8.5079	67.807	155.96	0.03508	0.80722	1.0051	330.12
480	8.3254	75.957	166.04	0.05631	0.81409	1.0115	333.46
490	8.1508	84.174	176.19	0.07723	0.82084	1.0178	336.76
500	7.9835	92.455	186.40	0.09785	0.82748	1.0240	340.03

TABLE 35. Thermodynamic properties of carbon dioxide—Continued

Temperature (K)	Density (kg/m^3)	Internal energy (kJ/kg)	Enthalpy (kJ/kg)	Entropy [kJ/(kg K)]	c_v [kJ/(kg K)]	c_p [kJ/(kg K)]	Speed of sound (m/s)
			0.75 MPa Isobar				
525	7.5946	113.43	212.19	0.14818	0.84355	1.0391	348.03
550	7.2425	134.79	238.35	0.19686	0.85893	1.0537	355.83
575	6.9222	156.52	264.87	0.24401	0.87363	1.0678	363.44
600	6.6294	178.60	291.74	0.28974	0.88769	1.0813	370.87
625	6.3608	201.02	318.93	0.33415	0.90115	1.0943	378.14
650	6.1133	223.76	346.45	0.37732	0.91402	1.1068	385.26
675	5.8846	246.82	374.27	0.41931	0.92634	1.1188	392.23
700	5.6725	270.16	402.38	0.46021	0.93812	1.1302	399.08
800	4.9589	366.29	517.53	0.61391	0.98037	1.1716	425.30
900	4.4056	466.25	636.49	0.75398	1.0158	1.2064	449.93
1000	3.9639	569.43	758.63	0.88265	1.0454	1.2357	473.27
1100	3.6030	675.32	883.47	1.0016	1.0704	1.2604	495.50
			1.00 MPa Isobar				
216.695[b]	1179.10	−427.26	−426.41	−2.2180	0.97514	1.9503	977.76
220	1167.03	−420.80	−419.95	−2.1884	0.97034	1.9589	953.55
225	1148.32	−410.99	−410.11	−2.1442	0.96337	1.9751	916.83
230	1128.97	−401.08	−400.19	−2.1006	0.95680	1.9959	879.82
233.028[c]	1116.90	−395.02	−394.12	−2.0744	0.95303	2.0111	857.18
233.028[c]	26.006	−109.94	−71.484	−0.68986	0.68026	1.0322	223.50
235	25.665	−108.42	−69.459	−0.68120	0.67819	1.0220	224.93
240	24.857	−104.64	−64.408	−0.65993	0.67332	0.99915	228.46
245	24.117	−100.92	−59.460	−0.63953	0.66959	0.98058	231.84
250	23.435	−97.266	−54.595	−0.61987	0.66716	0.96579	235.08
255	22.803	−93.650	−49.797	−0.60087	0.66588	0.95411	238.19
260	22.215	−90.065	−45.050	−0.58243	0.66557	0.94495	241.19
265	21.664	−86.503	−40.344	−0.56450	0.66605	0.93783	244.10
270	21.147	−82.957	−35.669	−0.54703	0.66718	0.93235	246.91
275	20.660	−79.422	−31.018	−0.52996	0.66884	0.92821	249.66
280	20.199	−75.892	−26.385	−0.51326	0.67092	0.92518	252.33
285	19.763	−72.364	−21.765	−0.49691	0.67335	0.92307	254.93
290	19.349	−68.836	−17.153	−0.48087	0.67607	0.92172	257.49
295	18.955	−65.303	−12.547	−0.46512	0.67902	0.92103	259.98
300	18.579	−61.765	−7.9420	−0.44964	0.68217	0.92089	262.43
305	18.221	−58.220	−3.3370	−0.43442	0.68547	0.92121	264.83
310	17.878	−54.665	1.2707	−0.41943	0.68890	0.92192	267.20
315	17.549	−51.100	5.8828	−0.40467	0.69243	0.92298	269.52
320	17.234	−47.523	10.501	−0.39013	0.69605	0.92433	271.80
325	16.932	−43.934	15.126	−0.37578	0.69974	0.92594	274.06
330	16.641	−40.331	19.761	−0.36163	0.70349	0.92777	276.28
335	16.361	−36.715	24.405	−0.34767	0.70729	0.92981	278.46
340	16.092	−33.084	29.059	−0.33387	0.71112	0.93200	280.62
345	15.832	−29.438	33.725	−0.32025	0.71498	0.93435	282.76
350	15.581	−25.777	38.403	−0.30679	0.71885	0.93681	284.86

TABLE 35. Thermodynamic properties of carbon dioxide—Continued

Temperature (K)	Density (kg/m^3)	Internal energy (kJ/kg)	Enthalpy (kJ/kg)	Entropy [kJ/(kg K)]	c_v [kJ/(kg K)]	c_p [kJ/(kg K)]	Speed of sound (m/s)
			1.00 MPa Isobar				
360	15.105	−18.406	47.797	−0.28033	0.72664	0.94206	289.00
370	14.659	−10.970	57.245	−0.25444	0.73442	0.94763	293.05
380	14.241	−3.4677	66.750	−0.22909	0.74217	0.95345	297.02
390	13.848	4.1027	76.315	−0.20425	0.74988	0.95944	300.91
400	13.477	11.741	85.939	−0.17988	0.75751	0.96555	304.72
410	13.127	19.449	95.626	−0.15596	0.76505	0.97174	308.47
420	12.796	27.224	105.37	−0.13247	0.77251	0.97798	312.16
430	12.482	35.068	115.19	−0.10939	0.77986	0.98423	315.79
440	12.183	42.979	125.06	−0.08669	0.78710	0.99049	319.37
450	11.899	50.957	135.00	−0.06436	0.79424	0.99673	322.89
460	11.629	59.001	144.99	−0.04238	0.80126	1.0029	326.37
470	11.371	67.112	155.05	−0.02075	0.80817	1.0091	329.79
480	11.125	75.287	165.18	0.00056	0.81497	1.0152	333.18
490	10.889	83.526	175.36	0.02156	0.82166	1.0213	336.52
500	10.664	91.829	185.60	0.04225	0.82823	1.0273	339.81
525	10.141	112.86	211.47	0.09273	0.84418	1.0420	347.90
550	9.6675	134.26	237.70	0.14154	0.85946	1.0563	355.76
575	9.2375	156.02	264.28	0.18879	0.87408	1.0700	363.42
600	8.8449	178.14	291.19	0.23462	0.88808	1.0833	370.90
625	8.4849	200.58	318.44	0.27910	0.90149	1.0961	378.20
650	8.1535	223.35	345.99	0.32233	0.91432	1.1084	385.36
675	7.8474	246.42	373.85	0.36438	0.92660	1.1202	392.37
700	7.5638	269.79	402.00	0.40533	0.93835	1.1315	399.24
800	6.6102	365.98	517.26	0.55918	0.98053	1.1725	425.54
900	5.8718	465.99	636.29	0.69934	1.0159	1.2071	450.22
1000	5.2826	569.20	758.50	0.82807	1.0455	1.2362	473.59
1100	4.8014	675.12	883.39	0.94708	1.0704	1.2608	495.84
			2.00 MPa Isobar				
216.908[b]	1180.41	−427.40	−425.70	−2.2187	0.97612	1.9443	981.71
220	1169.23	−421.39	−419.68	−2.1911	0.97160	1.9517	959.33
225	1150.73	−411.63	−409.89	−2.1471	0.96458	1.9667	923.07
230	1131.64	−401.78	−400.01	−2.1037	0.95796	1.9858	886.59
235	1111.85	−391.82	−390.02	−2.0607	0.95178	2.0100	849.70
240	1091.24	−381.73	−379.90	−2.0181	0.94610	2.0404	812.17
245	1069.65	−371.47	−369.60	−1.9756	0.94098	2.0786	773.73
250	1046.88	−361.01	−359.10	−1.9332	0.93660	2.1271	733.93
253.647[c]	1029.36	−353.20	−351.26	−1.9021	0.93409	2.1710	703.64
253.647[c]	52.540	−107.99	−69.929	−0.79292	0.76254	1.2983	220.27
255	51.941	−106.69	−68.187	−0.78607	0.75793	1.2773	221.55
260	49.914	−102.04	−61.969	−0.76192	0.74331	1.2130	226.07
265	48.129	−97.586	−56.031	−0.73930	0.73233	1.1646	230.27
270	46.533	−93.285	−50.304	−0.71789	0.72439	1.1276	234.21
275	45.090	−89.098	−44.742	−0.69748	0.71881	1.0987	237.93

TABLE 35. Thermodynamic properties of carbon dioxide—Continued

Temperature (K)	Density (kg/m^3)	Internal energy (kJ/kg)	Enthalpy (kJ/kg)	Entropy [kJ/(kg K)]	c_v [kJ/(kg K)]	c_p [kJ/(kg K)]	Speed of sound (m/s)
			2.00 MPa Isobar				
280	43.772	−84.999	−39.308	−0.67789	0.71503	1.0758	241.45
285	42.560	−80.969	−33.977	−0.65902	0.71265	1.0574	244.82
290	41.438	−76.992	−28.728	−0.64076	0.71135	1.0425	248.05
295	40.395	−73.058	−23.547	−0.62305	0.71092	1.0305	251.15
300	39.420	−69.155	−18.420	−0.60581	0.71116	1.0206	254.15
305	38.506	−65.278	−13.338	−0.58901	0.71195	1.0125	257.06
310	37.645	−61.420	−8.2920	−0.57260	0.71317	1.0059	259.89
315	36.832	−57.577	−3.2763	−0.55655	0.71475	1.0005	262.63
320	36.063	−53.744	1.7152	−0.54083	0.71664	0.99621	265.31
325	35.333	−49.917	6.6872	−0.52541	0.71879	0.99276	267.93
330	34.639	−46.095	11.644	−0.51028	0.72117	0.99008	270.49
335	33.977	−42.273	16.589	−0.49541	0.72373	0.98805	272.99
340	33.346	−38.451	21.526	−0.48078	0.72645	0.98659	275.45
345	32.743	−34.627	26.456	−0.46638	0.72929	0.98561	277.85
350	32.165	−30.798	31.382	−0.45221	0.73225	0.98506	280.22
360	31.078	−23.121	41.232	−0.42446	0.73841	0.98503	284.83
370	30.075	−15.414	51.087	−0.39746	0.74484	0.98616	289.30
380	29.143	−7.6685	60.958	−0.37113	0.75144	0.98819	293.64
390	28.276	0.12033	70.853	−0.34543	0.75815	0.99093	297.87
400	27.464	7.9565	80.778	−0.32030	0.76494	0.99423	301.99
410	26.704	15.843	90.739	−0.29571	0.77175	0.99798	306.02
420	25.989	23.782	100.74	−0.27161	0.77856	1.0021	309.96
430	25.314	31.775	110.78	−0.24798	0.78535	1.0064	313.83
440	24.678	39.824	120.87	−0.22479	0.79211	1.0110	317.61
450	24.075	47.929	131.00	−0.20202	0.79881	1.0158	321.33
460	23.504	56.091	141.18	−0.17964	0.80545	1.0207	324.99
470	22.961	64.310	151.42	−0.15763	0.81202	1.0256	328.58
480	22.444	72.587	161.70	−0.13599	0.81852	1.0307	332.12
490	21.952	80.920	172.03	−0.11468	0.82493	1.0358	335.60
500	21.482	89.311	182.41	−0.09371	0.83126	1.0409	339.03
525	20.396	110.54	208.59	−0.04261	0.84670	1.0537	347.41
550	19.419	132.11	235.10	0.00670	0.86158	1.0664	355.52
575	18.536	154.02	261.91	0.05438	0.87589	1.0790	363.39
600	17.733	176.26	289.04	0.10056	0.88964	1.0912	371.05
625	16.999	198.82	316.47	0.14535	0.90284	1.1031	378.52
650	16.325	221.69	344.20	0.18884	0.91550	1.1147	385.81
675	15.705	244.85	372.20	0.23112	0.92764	1.1259	392.94
700	15.130	268.30	400.49	0.27227	0.93928	1.1367	399.92
800	13.207	364.75	516.19	0.42670	0.98114	1.1762	426.52
900	11.724	464.95	635.54	0.56724	1.0163	1.2099	451.40
1000	10.544	568.30	757.99	0.69622	1.0459	1.2384	474.89
1100	9.5815	674.33	883.06	0.81542	1.0707	1.2625	497.22

TABLE 35. Thermodynamic properties of carbon dioxide—Continued

Temperature (K)	Density (kg/m^3)	Internal energy (kJ/kg)	Enthalpy (kJ/kg)	Entropy [kJ/(kg K)]	c_v [kJ/(kg K)]	c_p [kJ/(kg K)]	Speed of sound (m/s)
			3.00 MPa Isobar				
217.121[b]	1181.71	−427.54	−425.00	−2.2193	0.97705	1.9386	985.63
220	1171.40	−421.97	−419.41	−2.1938	0.97282	1.9449	965.03
225	1153.10	−412.25	−409.65	−2.1499	0.96576	1.9587	929.22
230	1134.25	−402.46	−399.82	−2.1067	0.95909	1.9763	893.25
235	1114.74	−392.57	−389.88	−2.0639	0.95286	1.9986	856.93
240	1094.46	−382.56	−379.82	−2.0216	0.94711	2.0265	820.08
245	1073.29	−372.40	−369.61	−1.9795	0.94190	2.0613	782.45
250	1051.02	−362.05	−359.19	−1.9374	0.93737	2.1051	743.69
255	1027.42	−351.46	−348.54	−1.8952	0.93383	2.1608	703.23
260	1002.13	−340.55	−337.56	−1.8526	0.93209	2.2331	660.22
265	974.65	−329.24	−326.16	−1.8091	0.93362	2.3306	613.45
267.598[c]	959.25	−323.15	−320.03	−1.7861	0.93647	2.3959	587.14
267.598[c]	81.919	−109.79	−73.169	−0.86360	0.83693	1.6438	214.95
270	79.807	−106.92	−69.327	−0.84931	0.82029	1.5582	217.92
275	76.011	−101.35	−61.879	−0.82197	0.79485	1.4301	223.53
280	72.805	−96.166	−54.960	−0.79703	0.77747	1.3423	228.55
285	70.025	−91.258	−48.416	−0.77387	0.76520	1.2784	233.14
290	67.568	−86.550	−42.151	−0.75207	0.75645	1.2300	237.39
295	65.368	−81.993	−36.099	−0.73138	0.75024	1.1923	241.37
300	63.376	−77.552	−30.215	−0.71160	0.74589	1.1623	245.13
305	61.556	−73.203	−24.466	−0.69260	0.74293	1.1380	248.70
310	59.881	−68.927	−18.827	−0.67426	0.74101	1.1181	252.12
315	58.332	−64.710	−13.280	−0.65650	0.73994	1.1016	255.40
320	56.890	−60.540	−7.8071	−0.63927	0.73955	1.0878	258.56
325	55.544	−56.409	−2.3975	−0.62249	0.73974	1.0763	261.61
330	54.281	−52.309	2.9594	−0.60614	0.74041	1.0667	264.56
335	53.092	−48.233	8.2721	−0.59016	0.74148	1.0586	267.43
340	51.970	−44.178	13.548	−0.57453	0.74287	1.0518	270.21
345	50.908	−40.137	18.792	−0.55921	0.74453	1.0462	272.93
350	49.901	−36.108	24.011	−0.54419	0.74643	1.0414	275.58
360	48.031	−28.073	34.387	−0.51496	0.75077	1.0343	280.71
370	46.327	−20.052	44.705	−0.48669	0.75568	1.0296	285.63
380	44.765	−12.030	54.986	−0.45928	0.76102	1.0269	290.37
390	43.326	−3.9958	65.247	−0.43262	0.76667	1.0256	294.95
400	41.992	4.0597	75.502	−0.40666	0.77255	1.0255	299.39
410	40.752	12.143	85.760	−0.38133	0.77858	1.0263	303.70
420	39.594	20.261	96.030	−0.35658	0.78472	1.0279	307.90
430	38.509	28.416	106.32	−0.33237	0.79093	1.0301	312.00
440	37.491	36.613	116.63	−0.30866	0.79717	1.0327	316.00
450	36.531	44.854	126.98	−0.28542	0.80343	1.0358	319.91
460	35.625	53.141	137.35	−0.26261	0.80967	1.0392	323.74
470	34.768	61.475	147.76	−0.24023	0.81589	1.0428	327.50
480	33.956	69.858	158.21	−0.21823	0.82207	1.0467	331.19
490	33.185	78.291	168.69	−0.19661	0.82821	1.0507	334.81
500	32.451	86.774	179.22	−0.17534	0.83429	1.0549	338.37

TABLE 35. Thermodynamic properties of carbon dioxide—Continued

Temperature (K)	Density (kg/m^3)	Internal energy (kJ/kg)	Enthalpy (kJ/kg)	Entropy [kJ/(kg K)]	c_v [kJ/(kg K)]	c_p [kJ/(kg K)]	Speed of sound (m/s)
			3.00 MPa Isobar				
525	30.761	108.20	205.73	−0.12361	0.84921	1.0656	347.04
550	29.252	129.95	232.51	−0.07378	0.86369	1.0768	355.39
575	27.893	152.01	259.57	−0.02567	0.87769	1.0880	363.46
600	26.661	174.38	286.91	0.02087	0.89118	1.0992	371.30
625	25.540	197.06	314.53	0.06597	0.90418	1.1102	378.92
650	24.513	220.03	342.42	0.10972	0.91667	1.1211	386.34
675	23.569	243.29	370.58	0.15223	0.92868	1.1316	393.58
700	22.697	266.82	399.00	0.19357	0.94020	1.1419	400.65
800	19.789	363.53	515.13	0.34859	0.98175	1.1799	427.55
900	17.556	463.91	634.79	0.48950	1.0168	1.2126	452.61
1000	15.783	567.41	757.48	0.61874	1.0462	1.2405	476.21
1100	14.340	673.54	882.75	0.73811	1.0710	1.2642	498.61
			4.00 MPa Isobar				
217.334[b]	1182.98	−427.67	−424.29	−2.2200	0.97796	1.9330	989.53
220	1173.53	−422.54	−419.13	−2.1964	0.97402	1.9384	970.66
225	1155.43	−412.87	−409.41	−2.1527	0.96691	1.9510	935.29
230	1136.80	−403.13	−399.62	−2.1096	0.96020	1.9673	899.79
235	1117.56	−393.31	−389.73	−2.0671	0.95391	1.9878	864.02
240	1097.60	−383.37	−379.73	−2.0250	0.94810	2.0134	827.80
245	1076.81	−373.30	−369.59	−1.9832	0.94281	2.0452	790.92
250	1055.01	−363.06	−359.26	−1.9415	0.93814	2.0849	753.10
255	1032.00	−352.60	−348.72	−1.8997	0.93435	2.1348	713.89
260	1007.49	−341.86	−337.89	−1.8577	0.93199	2.1986	672.67
265	981.06	−330.78	−326.70	−1.8150	0.93201	2.2823	628.62
270	952.10	−319.22	−315.02	−1.7714	0.93573	2.3972	580.72
275	919.56	−306.99	−302.64	−1.7259	0.94504	2.5660	527.52
278.450[c]	894.05	−297.98	−293.51	−1.6929	0.95655	2.7401	486.42
278.450[c]	115.74	−114.09	−79.534	−0.92449	0.91069	2.1642	208.78
280	113.08	−111.66	−76.288	−0.91286	0.89131	2.0294	211.36
285	106.02	−104.65	−66.920	−0.87969	0.84827	1.7461	218.60
290	100.47	−98.453	−58.641	−0.85089	0.82129	1.5780	224.72
295	95.884	−92.766	−51.048	−0.82493	0.80299	1.4657	230.14
300	91.965	−87.427	−43.932	−0.80101	0.79011	1.3850	235.04
305	88.543	−82.340	−37.165	−0.77864	0.78082	1.3244	239.56
310	85.508	−77.445	−30.665	−0.75750	0.77402	1.2773	243.77
315	82.781	−72.697	−24.376	−0.73737	0.76906	1.2397	247.73
320	80.306	−68.066	−18.256	−0.71809	0.76551	1.2092	251.49
325	78.043	−63.529	−12.275	−0.69955	0.76308	1.1842	255.07
330	75.958	−59.068	−6.4078	−0.68163	0.76156	1.1633	258.49
335	74.028	−54.670	−0.63601	−0.66427	0.76076	1.1459	261.78
340	72.231	−50.322	5.0556	−0.64741	0.76054	1.1312	264.95
345	70.552	−46.017	10.679	−0.63099	0.76080	1.1187	268.01
350	68.976	−41.746	16.245	−0.61497	0.76145	1.1080	270.98

TABLE 35. Thermodynamic properties of carbon dioxide—Continued

Temperature (K)	Density (kg/m^3)	Internal energy (kJ/kg)	Enthalpy (kJ/kg)	Entropy [kJ/(kg K)]	c_v [kJ/(kg K)]	c_p [kJ/(kg K)]	Speed of sound (m/s)
			4.00 MPa Isobar				
360	66.092	−33.284	27.237	−0.58400	0.76371	1.0912	276.67
370	63.509	−24.899	38.084	−0.55428	0.76695	1.0789	282.06
380	61.173	−16.562	48.826	−0.52564	0.77091	1.0700	287.22
390	59.045	−8.2521	59.493	−0.49793	0.77542	1.0637	292.17
400	57.094	0.04711	70.107	−0.47105	0.78032	1.0595	296.93
410	55.294	8.3478	80.688	−0.44493	0.78553	1.0569	301.53
420	53.627	16.660	91.249	−0.41948	0.79097	1.0555	305.99
430	52.076	24.990	101.80	−0.39465	0.79657	1.0552	310.31
440	50.628	33.346	112.35	−0.37039	0.80228	1.0556	314.52
450	49.270	41.732	122.92	−0.34665	0.80808	1.0568	318.63
460	47.995	50.151	133.49	−0.32341	0.81391	1.0585	322.64
470	46.794	58.607	144.09	−0.30062	0.81978	1.0607	326.55
480	45.659	67.102	154.71	−0.27826	0.82564	1.0633	330.39
490	44.585	75.638	165.35	−0.25631	0.83150	1.0661	334.15
500	43.566	84.217	176.03	−0.23474	0.83733	1.0692	337.84
525	41.233	105.86	202.87	−0.18237	0.85173	1.0779	346.77
550	39.160	127.79	229.93	−0.13201	0.86580	1.0873	355.36
575	37.302	150.00	257.24	−0.08346	0.87948	1.0971	363.63
600	35.625	172.51	284.79	−0.03655	0.89272	1.1072	371.63
625	34.103	195.30	312.60	0.00885	0.90551	1.1174	379.39
650	32.712	218.38	340.66	0.05287	0.91784	1.1274	386.93
675	31.437	241.73	368.97	0.09561	0.92971	1.1374	394.28
700	30.262	265.35	397.52	0.13715	0.94111	1.1471	401.45
800	26.355	362.32	514.09	0.29274	0.98236	1.1835	428.62
900	23.367	462.88	634.07	0.43402	1.0172	1.2153	453.84
1000	21.001	566.52	756.99	0.56351	1.0465	1.2425	477.55
1100	19.077	672.77	882.44	0.68306	1.0712	1.2658	500.01
			5.00 MPa Isobar				
217.546[b]	1184.25	−427.80	−423.58	−2.2206	0.97883	1.9275	993.41
220	1175.62	−423.10	−418.85	−2.1990	0.97518	1.9321	976.23
225	1157.72	−413.48	−409.16	−2.1554	0.96803	1.9436	941.27
230	1139.31	−403.79	−399.41	−2.1125	0.96127	1.9586	906.23
235	1120.32	−394.03	−389.57	−2.0702	0.95493	1.9775	870.97
240	1100.66	−384.17	−379.62	−2.0283	0.94906	2.0011	835.35
245	1080.22	−374.18	−369.55	−1.9868	0.94369	2.0302	799.17
250	1058.86	−364.03	−359.31	−1.9454	0.93891	2.0663	762.21
255	1036.39	−353.69	−348.87	−1.9041	0.93492	2.1112	724.10
260	1012.57	−343.12	−338.18	−1.8626	0.93209	2.1678	684.39
265	987.07	−332.23	−327.16	−1.8206	0.93107	2.2407	642.50
270	959.39	−320.94	−315.73	−1.7779	0.93262	2.3377	597.75
275	928.78	−309.11	−303.72	−1.7338	0.93765	2.4735	549.26
280	893.90	−296.47	−290.88	−1.6875	0.94778	2.6797	495.52
285	852.04	−282.54	−276.67	−1.6373	0.96716	3.0437	433.50

TABLE 35. Thermodynamic properties of carbon dioxide—Continued

Temperature (K)	Density (kg/m^3)	Internal energy (kJ/kg)	Enthalpy (kJ/kg)	Entropy [kJ/(kg K)]	c_v [kJ/(kg K)]	c_p [kJ/(kg K)]	Speed of sound (m/s)
			5.00 MPa Isobar				
287.434[c]	827.32	−274.96	−268.91	−1.6101	0.98314	3.3572	398.39
287.434[c]	156.67	−121.04	−89.122	−0.98464	0.99465	3.1142	201.86
290	148.41	−115.58	−81.892	−0.95959	0.94334	2.5783	207.56
295	136.85	−106.98	−70.445	−0.92044	0.88615	2.0671	216.24
300	128.40	−99.772	−60.830	−0.88811	0.85258	1.8025	223.25
305	121.69	−93.344	−52.258	−0.85977	0.83051	1.6378	229.28
310	116.13	−87.423	−44.367	−0.83411	0.81508	1.5246	234.66
315	111.37	−81.856	−36.961	−0.81041	0.80388	1.4418	239.55
320	107.22	−76.552	−29.917	−0.78822	0.79562	1.3786	244.08
325	103.53	−71.448	−23.153	−0.76724	0.78951	1.3289	248.32
330	100.22	−66.502	−16.612	−0.74727	0.78505	1.2890	252.30
335	97.221	−61.681	−10.251	−0.72814	0.78185	1.2564	256.08
340	94.478	−56.961	−4.0388	−0.70973	0.77963	1.2294	259.68
345	91.955	−52.325	2.0498	−0.69195	0.77820	1.2067	263.13
350	89.619	−47.757	8.0342	−0.67473	0.77739	1.1875	266.45
360	85.418	−38.785	19.750	−0.64172	0.77727	1.1573	272.74
370	81.726	−29.974	31.205	−0.61034	0.77863	1.1349	278.64
380	78.440	−21.276	42.467	−0.58030	0.78109	1.1182	284.23
390	75.484	−12.655	53.584	−0.55142	0.78436	1.1058	289.55
400	72.804	−4.0846	64.593	−0.52355	0.78824	1.0965	294.63
410	70.355	4.4545	75.523	−0.49656	0.79259	1.0898	299.52
420	68.104	12.978	86.396	−0.47036	0.79729	1.0850	304.24
430	66.024	21.498	97.228	−0.44487	0.80226	1.0818	308.79
440	64.094	30.024	108.03	−0.42003	0.80743	1.0798	313.21
450	62.295	38.564	118.83	−0.39578	0.81274	1.0788	317.50
460	60.613	47.123	129.61	−0.37207	0.81817	1.0787	321.68
470	59.035	55.707	140.40	−0.34886	0.82367	1.0792	325.75
480	57.550	64.320	151.20	−0.32613	0.82921	1.0804	329.73
490	56.150	72.964	162.01	−0.30384	0.83478	1.0820	333.62
500	54.826	81.644	172.84	−0.28196	0.84035	1.0840	337.43
525	51.807	103.51	200.02	−0.22893	0.85423	1.0903	346.63
550	49.140	125.62	227.37	−0.17803	0.86790	1.0979	355.43
575	46.761	147.99	254.92	−0.12904	0.88126	1.1064	363.88
600	44.621	170.64	282.69	−0.08177	0.89425	1.1153	372.04
625	42.685	193.55	310.69	−0.03605	0.90684	1.1245	379.93
650	40.921	216.73	338.92	0.00823	0.91900	1.1338	387.59
675	39.307	240.17	367.38	0.05120	0.93073	1.1431	395.04
700	37.823	263.87	396.07	0.09293	0.94202	1.1523	402.30
800	32.904	361.11	513.07	0.24911	0.98296	1.1871	429.72
900	29.156	461.86	633.35	0.39075	1.0176	1.2179	455.10
1000	26.196	565.64	756.51	0.52048	1.0469	1.2446	478.91
1100	23.793	671.99	882.14	0.64021	1.0715	1.2674	501.43

TABLE 35. Thermodynamic properties of carbon dioxide—Continued

Temperature (K)	Density (kg/m^3)	Internal energy (kJ/kg)	Enthalpy (kJ/kg)	Entropy [kJ/(kg K)]	c_v [kJ/(kg K)]	c_p [kJ/(kg K)]	Speed of sound (m/s)
			6.00 MPa Isobar				
217.758[b]	1185.49	−427.93	−422.87	−2.2212	0.97967	1.9222	997.26
220	1177.69	−423.65	−418.56	−2.2015	0.97632	1.9260	981.74
225	1159.97	−414.07	−408.90	−2.1581	0.96912	1.9366	947.17
230	1141.77	−404.44	−399.19	−2.1154	0.96232	1.9504	912.57
235	1123.02	−394.73	−389.39	−2.0733	0.95593	1.9678	877.80
240	1103.65	−384.94	−379.50	−2.0316	0.95000	1.9894	842.74
245	1083.55	−375.03	−369.49	−1.9903	0.94456	2.0162	807.22
250	1062.59	−364.98	−359.33	−1.9493	0.93968	2.0491	771.04
255	1040.62	−354.75	−348.99	−1.9083	0.93551	2.0897	733.92
260	1017.43	−344.31	−338.42	−1.8673	0.93233	2.1402	695.50
265	992.74	−333.60	−327.56	−1.8259	0.93057	2.2042	655.38
270	966.16	−322.55	−316.34	−1.7840	0.93070	2.2873	613.08
275	937.12	−311.04	−304.64	−1.7410	0.93321	2.3994	568.01
280	904.68	−298.90	−292.27	−1.6965	0.93889	2.5598	519.20
285	867.13	−285.81	−278.89	−1.6491	0.94979	2.8131	464.94
290	820.77	−271.08	−263.77	−1.5965	0.97135	3.2947	401.70
295	753.39	−252.51	−244.55	−1.5308	1.0250	4.7540	317.23
295.128[c]	751.03	−251.92	−243.93	−1.5288	1.0277	4.8386	314.35
295.128[c]	210.88	−131.91	−103.46	−1.0528	1.1086	5.5056	193.67
300	182.31	−117.53	−84.623	−0.98943	0.96413	2.9858	207.78
305	166.26	−107.73	−71.643	−0.94650	0.90457	2.3038	217.07
310	154.99	−99.750	−61.037	−0.91200	0.87020	1.9705	224.44
315	146.25	−92.751	−51.726	−0.88220	0.84761	1.7687	230.73
320	139.11	−86.373	−43.243	−0.85548	0.83170	1.6322	236.30
325	133.08	−80.425	−35.341	−0.83098	0.82010	1.5335	241.37
330	127.87	−74.792	−27.869	−0.80816	0.81151	1.4588	246.04
335	123.27	−69.398	−20.726	−0.78668	0.80512	1.4004	250.39
340	119.18	−64.191	−13.846	−0.76629	0.80035	1.3536	254.48
345	115.48	−59.133	−7.1762	−0.74682	0.79684	1.3154	258.36
350	112.12	−54.197	−0.68096	−0.72812	0.79430	1.2837	262.05
360	106.19	−44.606	11.897	−0.69269	0.79142	1.2346	268.98
370	101.10	−35.295	24.054	−0.65937	0.79070	1.1988	275.41
380	96.643	−26.182	35.903	−0.62778	0.79152	1.1722	281.43
390	92.694	−17.210	47.519	−0.59760	0.79347	1.1521	287.12
400	89.155	−8.3384	58.960	−0.56863	0.79627	1.1368	292.53
410	85.954	0.46261	70.268	−0.54071	0.79971	1.1252	297.71
420	83.036	9.2162	81.474	−0.51371	0.80365	1.1164	302.67
430	80.360	17.940	92.604	−0.48752	0.80797	1.1099	307.45
440	77.892	26.648	103.68	−0.46206	0.81258	1.1051	312.07
450	75.605	35.351	114.71	−0.43726	0.81742	1.1018	316.54
460	73.477	44.059	125.72	−0.41307	0.82242	1.0996	320.88
470	71.488	52.778	136.71	−0.38944	0.82755	1.0984	325.10
480	69.625	61.513	147.69	−0.36632	0.83277	1.0980	329.21
490	67.874	70.271	158.67	−0.34367	0.83805	1.0983	333.23
500	66.223	79.054	169.66	−0.32148	0.84337	1.0991	337.15

TABLE 35. Thermodynamic properties of carbon dioxide—Continued

Temperature (K)	Density (kg/m^3)	Internal energy (kJ/kg)	Enthalpy (kJ/kg)	Entropy [kJ/(kg K)]	c_v [kJ/(kg K)]	c_p [kJ/(kg K)]	Speed of sound (m/s)
			6.00 MPa Isobar				
525	62.477	101.14	197.18	−0.26777	0.85672	1.1030	346.60
550	59.186	123.45	224.82	−0.21633	0.86998	1.1087	355.60
575	56.264	145.98	252.62	−0.16690	0.88302	1.1157	364.23
600	53.645	168.76	280.61	−0.11925	0.89577	1.1234	372.54
625	51.282	191.80	308.80	−0.07323	0.90815	1.1317	380.56
650	49.136	215.09	337.20	−0.02868	0.92015	1.1402	388.32
675	47.176	238.62	365.81	0.01451	0.93174	1.1488	395.86
700	45.377	262.41	394.64	0.05645	0.94292	1.1574	403.20
800	39.435	359.91	512.06	0.21320	0.98356	1.1906	430.87
900	34.924	460.85	632.65	0.35520	1.0181	1.2206	456.39
1000	31.368	564.76	756.04	0.48518	1.0472	1.2466	480.28
1100	28.486	671.23	881.85	0.60507	1.0718	1.2691	502.86
			7.00 MPa Isobar				
217.969[b]	1186.73	−428.06	−422.16	−2.2218	0.98048	1.9170	1001.1
220	1179.72	−424.19	−418.26	−2.2040	0.97743	1.9202	987.18
225	1162.17	−414.66	−408.64	−2.1607	0.97018	1.9298	952.99
230	1144.18	−405.07	−398.96	−2.1182	0.96334	1.9425	918.81
235	1125.67	−395.42	−389.21	−2.0763	0.95691	1.9585	884.52
240	1106.56	−385.69	−379.36	−2.0348	0.95092	1.9785	849.99
245	1086.78	−375.85	−369.41	−1.9938	0.94542	2.0030	815.07
250	1066.20	−365.89	−359.33	−1.9530	0.94045	2.0330	779.62
255	1044.69	−355.77	−349.07	−1.9124	0.93613	2.0699	743.39
260	1022.07	−345.46	−338.61	−1.8718	0.93267	2.1152	706.11
265	998.11	−334.91	−327.90	−1.8310	0.93037	2.1718	667.47
270	972.50	−324.07	−316.87	−1.7898	0.92952	2.2439	627.14
275	944.77	−312.83	−305.42	−1.7478	0.93042	2.3383	584.70
280	914.25	−301.09	−293.43	−1.7045	0.93353	2.4674	539.49
285	879.80	−288.61	−280.65	−1.6593	0.94003	2.6565	490.42
290	839.25	−275.01	−266.66	−1.6107	0.95290	2.9683	435.61
295	787.63	−259.35	−250.47	−1.5553	0.97893	3.5994	371.18
300	706.06	−238.25	−228.34	−1.4810	1.0529	5.9775	281.10
301.833[c]	638.31	−223.87	−212.90	−1.4297	1.2173	14.685	211.72
301.833[c]	304.03	−152.89	−129.87	−1.1546	1.3535	21.953	179.63
305	243.08	−131.34	−102.55	−1.0644	1.0602	5.0681	199.60
310	210.63	−116.70	−83.469	−1.0024	0.95569	3.0512	212.29
315	191.97	−106.54	−70.071	−0.95947	0.90676	2.3936	221.05
320	178.74	−98.192	−59.029	−0.92468	0.87690	2.0539	228.16
325	168.48	−90.870	−49.322	−0.89458	0.85650	1.8433	234.30
330	160.11	−84.207	−40.487	−0.86760	0.84183	1.6992	239.80
335	153.05	−78.004	−32.266	−0.84287	0.83102	1.5942	244.81
340	146.95	−72.139	−24.503	−0.81987	0.82293	1.5144	249.45
345	141.59	−66.532	−17.094	−0.79823	0.81682	1.4517	253.79
350	136.82	−61.129	−9.9662	−0.77772	0.81220	1.4012	257.89

TABLE 35. Thermodynamic properties of carbon dioxide—Continued

Temperature (K)	Density (kg/m^3)	Internal energy (kJ/kg)	Enthalpy (kJ/kg)	Entropy [kJ/(kg K)]	c_v [kJ/(kg K)]	c_p [kJ/(kg K)]	Speed of sound (m/s)
			7.00 MPa Isobar				
360	128.61	−50.782	3.6440	−0.73937	0.80615	1.3254	265.47
370	121.75	−40.880	16.616	−0.70383	0.80311	1.2718	272.42
380	115.86	−31.289	29.127	−0.67046	0.80216	1.2325	278.88
390	110.73	−21.922	41.298	−0.63885	0.80271	1.2030	284.94
400	106.18	−12.716	53.210	−0.60869	0.80437	1.1805	290.66
410	102.11	−3.6281	64.925	−0.57976	0.80688	1.1632	296.11
420	98.436	5.3748	76.487	−0.55189	0.81003	1.1499	301.31
430	95.090	14.318	87.932	−0.52496	0.81369	1.1396	306.30
440	92.024	23.220	99.287	−0.49886	0.81773	1.1317	311.11
450	89.200	32.097	110.57	−0.47350	0.82208	1.1258	315.75
460	86.584	40.960	121.81	−0.44880	0.82666	1.1214	320.24
470	84.151	49.820	133.00	0.42472	0.83141	1.1183	324.61
480	81.880	58.684	144.18	−0.40120	0.83631	1.1162	328.85
490	79.752	67.559	155.33	−0.37820	0.84130	1.1150	332.98
500	77.753	76.450	166.48	−0.35568	0.84636	1.1145	337.01
525	73.239	98.773	194.35	−0.30129	0.85919	1.1158	346.69
550	69.294	121.27	222.29	−0.24930	0.87205	1.1196	355.89
575	65.807	143.97	250.34	−0.19942	0.88478	1.1250	364.68
600	62.694	166.90	278.55	−0.15140	0.89727	1.1316	373.12
625	59.892	190.05	306.93	−0.10506	0.90945	1.1388	381.25
650	57.354	213.45	335.50	−0.06025	0.92129	1.1465	389.12
675	55.041	237.08	364.26	−0.01683	0.93275	1.1545	396.75
700	52.922	260.95	393.22	0.02530	0.94382	1.1625	404.16
800	45.945	358.71	511.07	0.18262	0.98415	1.1942	432.04
900	40.668	459.84	631.96	0.32498	1.0185	1.2232	457.70
1000	36.517	563.89	755.58	0.45520	1.0475	1.2486	481.67
1100	33.158	670.46	881.58	0.57527	1.0720	1.2707	504.30
			7.50 MPa Isobar				
218.074[b]	1187.34	−428.12	−421.80	−2.2221	0.98087	1.9145	1003.0
220	1180.72	−424.46	−418.11	−2.2052	0.97797	1.9173	989.88
225	1163.26	−414.95	−408.50	−2.1621	0.97071	1.9265	955.88
230	1145.37	−405.39	−398.84	−2.1196	0.96384	1.9387	921.90
235	1126.97	−395.76	−389.11	−2.0777	0.95738	1.9541	887.83
240	1107.99	−386.06	−379.29	−2.0364	0.95138	1.9732	853.55
245	1088.36	−376.26	−369.37	−1.9955	0.94584	1.9967	818.94
250	1067.96	−366.34	−359.32	−1.9549	0.94083	2.0254	783.82
255	1046.67	−356.27	−349.10	−1.9144	0.93644	2.0605	748.00
260	1024.32	−346.02	−338.70	−1.8740	0.93286	2.1036	711.24
265	1000.70	−335.55	−328.05	−1.8334	0.93034	2.1570	673.27
270	975.52	−324.79	−317.10	−1.7925	0.92912	2.2243	633.79
275	948.38	−313.68	−305.78	−1.7510	0.92943	2.3115	592.46
280	918.68	−302.10	−293.94	−1.7083	0.93163	2.4284	548.71
285	885.48	−289.88	−281.41	−1.6640	0.93668	2.5947	501.67

TABLE 35. Thermodynamic properties of carbon dioxide—Continued

Temperature (K)	Density (kg/m^3)	Internal energy (kJ/kg)	Enthalpy (kJ/kg)	Entropy [kJ/(kg K)]	c_v [kJ/(kg K)]	c_p [kJ/(kg K)]	Speed of sound (m/s)
			7.50 MPa Isobar				
290	847.07	−276.69	−267.84	−1.6168	0.94689	2.8557	449.91
295	799.88	−261.88	−252.50	−1.5643	0.96694	3.3335	390.87
300	733.90	−243.62	−233.40	−1.5001	1.0115	4.5507	317.38
305	389.85	−171.22	−151.98	−1.2323	1.5317	67.567	168.55
310	253.36	−129.11	−99.510	−1.0611	1.0261	4.5173	204.64
315	222.11	−115.30	−81.528	−1.0035	0.94620	2.9805	215.79
320	203.04	−105.22	−68.283	−0.96181	0.90445	2.3876	223.97
325	189.27	−96.845	−57.220	−0.92750	0.87759	2.0648	230.79
330	178.52	−89.456	−47.442	−0.89764	0.85879	1.8598	236.76
335	169.70	−82.714	−38.518	−0.87080	0.84513	1.7176	242.13
340	162.24	−76.430	−30.204	−0.84616	0.83499	1.6131	247.06
345	155.80	−70.486	−22.346	−0.82322	0.82734	1.5331	251.64
350	150.13	−64.802	−14.845	−0.80163	0.82151	1.4699	255.93
360	140.52	−54.014	−0.64140	−0.76161	0.81370	1.3768	263.84
370	132.60	−43.777	12.785	−0.72482	0.80942	1.3121	271.05
380	125.88	−33.921	25.660	−0.69048	0.80754	1.2652	277.72
390	120.06	−24.337	38.129	−0.65809	0.80736	1.2302	283.95
400	114.95	−14.951	50.293	−0.62729	0.80844	1.2036	289.83
410	110.40	−5.7101	62.222	−0.59783	0.81047	1.1832	295.40
420	106.31	3.4250	73.971	−0.56952	0.81323	1.1673	300.72
430	102.60	12.483	85.580	−0.54220	0.81654	1.1550	305.81
440	99.215	21.487	97.080	−0.51576	0.82030	1.1454	310.71
450	96.102	30.454	108.50	−0.49011	0.82440	1.1381	315.43
460	93.227	39.399	119.85	−0.46516	0.82877	1.1325	319.99
470	90.558	48.331	131.15	−0.44085	0.83334	1.1284	324.42
480	88.072	57.262	142.42	−0.41713	0.83807	1.1254	328.72
490	85.747	66.197	153.66	−0.39394	0.84291	1.1235	332.91
500	83.566	75.143	164.89	−0.37126	0.84785	1.1224	336.99
525	78.652	97.585	192.94	−0.31651	0.86041	1.1223	346.78
550	74.369	120.18	221.03	−0.26425	0.87307	1.1251	356.07
575	70.592	142.97	249.21	−0.21414	0.88565	1.1297	364.93
600	67.225	165.96	277.53	−0.16594	0.89802	1.1357	373.44
625	64.201	189.18	306.00	−0.11944	0.91010	1.1424	381.63
650	61.464	212.63	334.65	−0.07450	0.92186	1.1497	389.54
675	58.972	236.31	363.49	−0.03096	0.93325	1.1573	397.21
700	56.691	260.22	392.52	0.01126	0.94426	1.1651	404.66
800	49.193	358.12	510.58	0.16887	0.98445	1.1959	432.65
900	43.532	459.34	631.63	0.31141	1.0187	1.2245	458.36
1000	39.083	563.46	755.36	0.44175	1.0477	1.2496	482.37
1100	35.485	670.08	881.44	0.56190	1.0722	1.2714	505.03
			8.00 MPa Isobar				
218.180[b]	1187.95	−428.17	−421.44	−2.2224	0.98126	1.9120	1004.9
220	1181.72	−424.73	−417.96	−2.2065	0.97851	1.9145	992.56
225	1164.35	−415.23	−408.36	−2.1634	0.97122	1.9233	958.75
230	1146.54	−405.70	−398.72	−2.1210	0.96433	1.9349	924.97
235	1128.26	−396.10	−389.01	−2.0792	0.95786	1.9497	891.12

TABLE 35. Thermodynamic properties of carbon dioxide—Continued

Temperature (K)	Density (kg/m^3)	Internal energy (kJ/kg)	Enthalpy (kJ/kg)	Entropy [kJ/(kg K)]	c_v [kJ/(kg K)]	c_p [kJ/(kg K)]	Speed of sound (m/s)
			8.00 MPa Isobar				
240	1109.41	−386.43	−379.22	−2.0380	0.95182	1.9681	857.09
245	1089.93	−376.66	−369.32	−1.9972	0.94626	1.9906	822.75
250	1069.70	−366.78	−359.30	−1.9567	0.94120	2.0181	787.97
255	1048.62	−356.76	−349.13	−1.9164	0.93676	2.0516	752.55
260	1026.53	−346.57	−338.77	−1.8762	0.93307	2.0925	716.27
265	1003.23	−336.16	−328.19	−1.8359	0.93036	2.1429	678.91
270	978.46	−325.50	−317.32	−1.7952	0.92882	2.2060	640.22
275	951.86	−314.51	−306.10	−1.7541	0.92864	2.2867	599.89
280	922.92	−303.08	−294.41	−1.7119	0.93010	2.3931	557.45
285	890.82	−291.08	−282.10	−1.6684	0.93400	2.5408	512.17
290	854.20	−278.25	−268.88	−1.6224	0.94218	2.7633	462.96
295	810.40	−264.09	−254.22	−1.5722	0.95803	3.1417	408.04
300	753.17	−247.44	−236.82	−1.5138	0.98934	3.9320	343.66
305	656.77	−223.65	−211.47	−1.4301	1.0822	7.3125	255.09
310	327.71	−149.25	−124.84	−1.1485	1.1499	9.5864	194.28
315	261.29	−126.27	−95.650	−1.0550	0.99624	4.0300	210.19
320	231.91	−113.35	−78.854	−1.0021	0.93636	2.8750	219.80
325	212.90	−103.49	−65.909	−0.96190	0.90103	2.3574	227.35
330	198.87	−95.152	−54.926	−0.92836	0.87714	2.0594	233.83
335	187.79	−87.747	−45.146	−0.89894	0.86009	1.8648	239.57
340	178.65	−80.965	−36.184	−0.87239	0.84758	1.7274	244.79
345	170.89	−74.629	−27.814	−0.84795	0.83820	1.6253	249.61
350	164.16	−68.627	−19.893	−0.82515	0.83106	1.5463	254.10
360	152.93	−57.348	−5.0372	−0.78329	0.82137	1.4326	262.32
370	143.82	−46.747	8.8792	−0.74516	0.81579	1.3552	269.78
380	136.18	−36.607	22.140	−0.70979	0.81295	1.2998	276.65
390	129.63	−26.793	34.923	−0.67659	0.81202	1.2588	283.05
400	123.90	−17.218	47.348	−0.64513	0.81251	1.2277	289.07
410	118.84	−7.8163	59.501	−0.61512	0.81406	1.2038	294.76
420	114.31	1.4561	71.442	−0.58634	0.81641	1.1852	300.19
430	110.21	10.634	83.219	−0.55863	0.81939	1.1708	305.37
440	106.49	19.742	94.868	−0.53185	0.82286	1.1594	310.36
450	103.07	28.802	106.42	−0.50589	0.82671	1.1506	315.15
460	99.928	37.829	117.89	−0.48068	0.83087	1.1438	319.79
470	97.016	46.837	129.30	−0.45614	0.83525	1.1386	324.28
480	94.307	55.834	140.66	−0.43221	0.83982	1.1348	328.64
490	91.778	64.831	152.00	−0.40884	0.84452	1.1321	332.88
500	89.410	73.833	163.31	−0.38599	0.84933	1.1302	337.00
525	84.085	96.397	191.54	−0.33090	0.86163	1.1288	346.90
550	79.458	119.09	219.78	−0.27835	0.87409	1.1306	356.28
575	75.385	141.96	248.08	−0.22802	0.88651	1.1345	365.22
600	71.762	165.03	276.51	−0.17963	0.89876	1.1398	373.78
625	68.511	188.31	305.08	−0.13298	0.91075	1.1460	382.03
650	65.573	211.81	333.82	−0.08790	0.92242	1.1529	389.98
675	62.901	235.54	362.73	−0.04425	0.93375	1.1601	397.69

TABLE 35. Thermodynamic properties of carbon dioxide—Continued

Temperature (K)	Density (kg/m^3)	Internal energy (kJ/kg)	Enthalpy (kJ/kg)	Entropy [kJ/(kg K)]	c_v [kJ/(kg K)]	c_p [kJ/(kg K)]	Speed of sound (m/s)
			8.00 MPa Isobar				
700	60.457	259.50	391.82	−0.00193	0.94470	1.1676	405.18
800	52.435	357.53	510.10	0.15596	0.98474	1.1977	433.26
900	46.389	458.84	631.29	0.29867	1.0189	1.2257	459.03
1000	41.644	563.03	755.14	0.42913	1.0478	1.2506	483.08
1100	37.807	669.71	881.31	0.54937	1.0723	1.2722	505.75
			10.00 MPa Isobar				
218.600[b]	1190.34	−428.40	−420.00	−2.2235	0.98274	1.9023	1012.5
220	1185.63	−425.77	−417.34	−2.2113	0.98061	1.9039	1003.1
225	1168.59	−416.36	−407.80	−2.1685	0.97323	1.9111	970.04
230	1151.15	−406.91	−398.22	−2.1264	0.96625	1.9208	937.02
235	1133.28	−397.41	−388.59	−2.0849	0.95969	1.9333	904.01
240	1114.92	−387.85	−378.88	−2.0441	0.95356	1.9488	870.91
245	1095.99	−378.22	−369.09	−2.0037	0.94788	1.9679	837.63
250	1076.42	−368.49	−359.20	−1.9637	0.94269	1.9910	804.05
255	1056.11	−358.64	−349.18	−1.9240	0.93803	2.0189	770.05
260	1034.95	−348.66	−339.00	−1.8845	0.93400	2.0524	735.50
265	1012.80	−338.51	−328.64	−1.8450	0.93072	2.0930	700.25
270	989.46	−328.16	−318.06	−1.8055	0.92828	2.1425	664.15
275	964.71	−317.56	−307.20	−1.7656	0.92676	2.2034	627.04
280	938.22	−306.65	−296.00	−1.7253	0.92632	2.2798	588.67
285	909.56	−295.36	−284.36	−1.6841	0.92734	2.3782	548.68
290	878.06	−283.55	−272.16	−1.6416	0.93072	2.5108	506.63
295	842.67	−271.03	−259.16	−1.5972	0.93777	2.7009	461.99
300	801.62	−257.46	−244.98	−1.5496	0.94964	2.9906	414.28
305	751.67	−242.25	−228.94	−1.4965	0.96817	3.4711	363.01
310	685.77	−224.06	−209.48	−1.4333	0.99962	4.4460	307.04
315	586.02	−199.41	−182.35	−1.3465	1.0487	6.6962	249.42
320	448.28	−166.19	−143.88	−1.2253	1.0577	7.6175	219.14
325	358.04	−140.73	−112.80	−1.1289	1.0095	4.9438	219.84
330	310.25	−124.28	−92.049	−1.0655	0.96291	3.5312	225.91
335	280.11	−112.06	−76.359	−1.0183	0.92780	2.8165	232.23
340	258.62	−102.06	−63.396	−0.97991	0.90255	2.4017	238.14
345	242.11	−93.404	−52.100	−0.94692	0.88431	2.1341	243.58
350	228.80	−85.626	−41.921	−0.91762	0.87083	1.9480	248.62
360	208.25	−71.776	−23.756	−0.86644	0.85262	1.7065	257.77
370	192.74	−59.374	−7.4896	−0.82186	0.84146	1.5574	265.97
380	180.38	−47.885	7.5523	−0.78174	0.83458	1.4570	273.47
390	170.18	−37.015	21.746	−0.74486	0.83060	1.3856	280.40
400	161.53	−26.584	35.325	−0.71048	0.82867	1.3327	286.88
410	154.05	−16.473	48.443	−0.67809	0.82827	1.2927	292.99
420	147.48	−6.5998	61.208	−0.64733	0.82901	1.2616	298.77
430	141.63	3.0936	73.698	−0.61794	0.83064	1.2373	304.28
440	136.39	12.651	85.972	−0.58972	0.83297	1.2181	309.55
450	131.63	22.106	98.073	−0.56252	0.83584	1.2028	314.60
460	127.30	31.483	110.04	−0.53623	0.83915	1.1906	319.48
470	123.32	40.803	121.89	−0.51073	0.84280	1.1809	324.18

TABLE 35. Thermodynamic properties of carbon dioxide—Continued

Temperature (K)	Density (kg/m^3)	Internal energy (kJ/kg)	Enthalpy (kJ/kg)	Entropy [kJ/(kg K)]	c_v [kJ/(kg K)]	c_p [kJ/(kg K)]	Speed of sound (m/s)
			10.00 MPa Isobar				
480	119.65	50.083	133.66	−0.48595	0.84672	1.1732	328.74
490	116.24	59.335	145.36	−0.46183	0.85085	1.1671	333.16
500	113.07	68.569	157.01	−0.43830	0.85516	1.1624	337.45
525	106.01	91.633	185.97	−0.38178	0.86644	1.1552	347.71
550	99.930	114.74	214.81	−0.32811	0.87812	1.1527	357.39
575	94.626	137.95	243.63	−0.27686	0.88993	1.1533	366.58
600	89.941	161.31	272.49	−0.22773	0.90169	1.1561	375.37
625	85.761	184.84	301.45	−0.18045	0.91329	1.1603	383.79
650	81.999	208.57	330.52	−0.13485	0.92464	1.1655	391.91
675	78.592	232.49	359.73	−0.09075	0.93571	1.1714	399.76
700	75.486	256.61	389.09	−0.04804	0.94645	1.1777	407.36
800	65.349	355.17	508.20	0.11097	0.98591	1.2046	435.79
900	57.759	456.85	629.99	0.25438	1.0198	1.2308	461.77
1000	51.825	561.32	754.28	0.38532	1.0485	1.2545	485.94
1100	47.040	668.21	880.79	0.50588	1.0728	1.2753	508.69
			15.00 MPa Isobar				
219.644[b]	1196.11	−428.91	−416.37	−2.2260	0.98604	1.8799	1030.9
220	1194.96	−428.25	−415.70	−2.2230	0.98548	1.8801	1028.7
225	1178.64	−419.02	−406.29	−2.1807	0.97789	1.8841	997.14
230	1162.02	−409.76	−396.86	−2.1392	0.97070	1.8900	965.81
235	1145.06	−400.49	−387.39	−2.0985	0.96394	1.8980	934.61
240	1127.73	−391.17	−377.87	−2.0584	0.95760	1.9081	903.50
245	1109.98	−381.82	−368.30	−2.0190	0.95169	1.9206	872.40
250	1091.77	−372.40	−358.66	−1.9800	0.94623	1.9358	841.27
255	1073.03	−362.92	−348.94	−1.9415	0.94121	1.9539	810.04
260	1053.71	−353.35	−339.12	−1.9034	0.93667	1.9752	778.68
265	1033.73	−343.69	−329.18	−1.8655	0.93264	2.0002	747.13
270	1013.01	−333.92	−319.11	−1.8279	0.92914	2.0294	715.36
275	991.45	−324.01	−308.88	−1.7903	0.92619	2.0635	683.32
280	968.93	−313.95	−298.47	−1.7528	0.92381	2.1034	650.96
285	945.30	−303.70	−287.83	−1.7152	0.92211	2.1501	618.23
290	920.40	−293.25	−276.95	−1.6773	0.92132	2.2055	585.07
295	894.00	−282.54	−265.76	−1.6390	0.92183	2.2727	551.45
300	865.82	−271.52	−254.20	−1.6002	0.92380	2.3557	517.40
305	835.48	−260.12	−242.17	−1.5604	0.92683	2.4583	483.07
310	802.54	−248.27	−229.58	−1.5195	0.93036	2.5830	448.77
315	766.51	−235.86	−216.30	−1.4770	0.93449	2.7343	414.97
320	726.83	−222.81	−202.18	−1.4325	0.93978	2.9188	382.22
325	683.09	−209.02	−187.06	−1.3857	0.94662	3.1280	351.34
330	635.51	−194.51	−170.91	−1.3363	0.95475	3.3309	323.89
335	585.40	−179.47	−153.85	−1.2850	0.96004	3.4748	301.72
340	535.55	−164.42	−136.41	−1.2333	0.95711	3.4738	286.11
345	489.42	−150.03	−119.38	−1.1836	0.94688	3.3164	276.63
350	449.20	−136.79	−103.39	−1.1376	0.93439	3.0688	271.76
360	387.08	−114.04	−75.292	−1.0584	0.91214	2.5672	270.06
370	343.43	−95.274	−51.596	−0.99347	0.89468	2.1949	273.34

TABLE 35. Thermodynamic properties of carbon dioxide—Continued

Temperature (K)	Density (kg/m^3)	Internal energy (kJ/kg)	Enthalpy (kJ/kg)	Entropy [kJ/(kg K)]	c_v [kJ/(kg K)]	c_p [kJ/(kg K)]	Speed of sound (m/s)
			15.00 MPa Isobar				
380	311.48	−79.159	−31.001	−0.93853	0.88143	1.9402	278.46
390	286.97	−64.804	−12.533	−0.89055	0.87178	1.7638	284.22
400	267.42	−51.652	4.4406	−0.84757	0.86502	1.6376	290.12
410	251.33	−39.353	20.329	−0.80833	0.86053	1.5445	295.97
420	237.78	−27.678	35.405	−0.77200	0.85782	1.4739	301.68
430	226.14	−16.471	49.860	−0.73798	0.85650	1.4192	307.22
440	215.98	−5.6217	63.828	−0.70587	0.85630	1.3761	312.59
450	207.01	4.9509	77.410	−0.67534	0.85698	1.3416	317.79
460	199.00	15.307	90.682	−0.64617	0.85839	1.3138	322.83
470	191.79	25.492	103.70	−0.61817	0.86037	1.2911	327.70
480	185.24	35.541	116.52	−0.59119	0.86283	1.2725	332.43
490	179.26	45.484	129.16	−0.56511	0.86568	1.2572	337.03
500	173.76	55.342	141.67	−0.53985	0.86884	1.2445	341.50
525	161.74	79.733	172.48	−0.47972	0.87776	1.2218	352.18
550	151.63	103.91	202.83	−0.42323	0.88763	1.2080	362.24
575	142.97	128.01	232.93	−0.36972	0.89803	1.2002	371.77
600	135.43	152.12	262.88	−0.31873	0.90867	1.1963	380.86
625	128.78	176.29	292.77	−0.26992	0.91936	1.1953	389.55
650	122.86	200.57	322.66	−0.22303	0.92998	1.1963	397.91
675	117.54	224.98	352.59	−0.17784	0.94044	1.1987	405.96
700	112.72	249.53	382.60	−0.13418	0.95067	1.2022	413.74
800	97.199	349.41	503.73	0.02753	0.98876	1.2213	442.71
900	85.740	452.00	626.95	0.17264	1.0218	1.2430	469.01
1000	76.856	557.14	752.31	0.30470	1.0501	1.2639	493.37
1100	69.730	664.55	879.66	0.42606	1.0741	1.2828	516.21
			20.00 MPa Isobar				
220.677[b]	1201.58	−429.34	−412.70	2.2283	0.98884	1.8600	1048.9
225	1188.00	−421.49	−404.66	−2.1922	0.98212	1.8614	1022.8
230	1172.07	−412.41	−395.34	−2.1513	0.97475	1.8644	992.92
235	1155.89	−403.31	−386.01	−2.1111	0.96780	1.8690	963.24
240	1139.41	−394.20	−376.65	−2.0717	0.96128	1.8753	933.74
245	1122.62	−385.07	−367.25	−2.0330	0.95519	1.8833	904.38
250	1105.47	−375.91	−357.81	−1.9948	0.94951	1.8932	875.14
255	1087.95	−366.70	−348.32	−1.9572	0.94426	1.9050	845.98
260	1070.01	−357.45	−338.76	−1.9201	0.93944	1.9188	816.88
265	1051.60	−348.15	−329.13	−1.8834	0.93504	1.9349	787.84
270	1032.69	−338.77	−319.41	−1.8471	0.93107	1.9533	758.85
275	1013.23	−329.33	−309.59	−1.8110	0.92753	1.9742	729.90
280	993.16	−319.80	−299.66	−1.7753	0.92441	1.9979	701.00
285	972.43	−310.17	−289.61	−1.7397	0.92176	2.0245	672.16
290	950.97	−300.44	−279.41	−1.7042	0.91964	2.0543	643.38
295	928.71	−290.59	−269.06	−1.6688	0.91824	2.0881	614.69
300	905.57	−280.61	−258.52	−1.6334	0.91763	2.1267	586.17
305	881.46	−270.47	−247.78	−1.5979	0.91763	2.1709	557.91
310	856.27	−260.16	−236.80	−1.5622	0.91780	2.2204	530.04
315	829.92	−249.67	−225.57	−1.5262	0.91794	2.2743	502.71

TABLE 35. Thermodynamic properties of carbon dioxide—Continued

Temperature (K)	Density (kg/m^3)	Internal energy (kJ/kg)	Enthalpy (kJ/kg)	Entropy [kJ/(kg K)]	c_v [kJ/(kg K)]	c_p [kJ/(kg K)]	Speed of sound (m/s)
			20.00 MPa Isobar				
320	802.33	−238.98	−214.05	−1.4900	0.91835	2.3324	476.13
325	773.46	−228.09	−202.24	−1.4533	0.91938	2.3952	450.59
330	743.30	−217.00	−190.10	−1.4163	0.92095	2.4610	426.44
335	711.96	−205.72	−177.63	−1.3788	0.92254	2.5246	404.10
340	679.68	−194.29	−164.87	−1.3410	0.92342	2.5778	384.01
345	646.90	−182.80	−151.88	−1.3030	0.92298	2.6122	366.45
350	614.18	−171.35	−138.79	−1.2654	0.92115	2.6207	351.52
360	551.54	−149.10	−112.84	−1.1923	0.91549	2.5511	329.54
370	496.14	−128.36	−88.048	−1.1243	0.90910	2.3976	316.94
380	449.68	−109.47	−64.990	−1.0628	0.90195	2.2129	311.16
390	411.63	−92.347	−43.760	−1.0077	0.89472	2.0369	309.69
400	380.50	−76.728	−24.165	−0.95804	0.88827	1.8868	310.75
410	354.77	−62.306	−5.9310	−0.91301	0.88304	1.7645	313.29
420	333.19	−48.819	11.205	−0.87171	0.87912	1.6664	316.66
430	314.83	−36.064	27.462	−0.83346	0.87643	1.5878	320.52
440	298.99	−23.881	43.011	−0.79771	0.87484	1.5244	324.64
450	285.14	−12.151	57.989	−0.76405	0.87419	1.4729	328.91
460	272.92	−0.78247	72.500	−0.73215	0.87434	1.4307	333.22
470	262.02	10.296	86.627	−0.70177	0.87517	1.3959	337.54
480	252.21	21.140	100.44	−0.67269	0.87657	1.3671	341.84
490	243.34	31.794	113.98	−0.64476	0.87845	1.3430	346.09
500	235.24	42.292	127.31	−0.61783	0.88074	1.3228	350.29
525	217.77	68.036	159.88	−0.55427	0.88779	1.2852	360.49
550	203.30	93.302	191.68	−0.49509	0.89618	1.2606	370.28
575	191.06	118.30	222.98	−0.43943	0.90540	1.2446	379.65
600	180.50	143.15	253.95	−0.38670	0.91508	1.2344	388.65
625	171.28	167.96	284.73	−0.33644	0.92499	1.2284	397.29
650	163.12	192.79	315.40	−0.28833	0.93496	1.2254	405.62
675	155.83	217.68	346.02	−0.24210	0.94487	1.2246	413.67
700	149.27	242.66	376.64	−0.19756	0.95465	1.2253	421.46
800	128.34	343.83	499.67	−0.03329	0.99149	1.2370	450.47
900	113.04	447.31	624.23	0.11340	1.0238	1.2545	476.80
1000	101.27	553.10	750.60	0.24652	1.0516	1.2727	501.16
1100	91.857	661.01	878.74	0.36864	1.0754	1.2898	523.98
			25.00 MPa Isobar				
221.701[b]	1206.79	−429.71	−409.00	−2.2303	0.99124	1.8421	1066.4
225	1196.78	−423.81	−402.92	−2.2031	0.98601	1.8419	1047.3
230	1181.45	−414.87	−393.71	−2.1626	0.97846	1.8427	1018.6
235	1165.92	−405.93	−384.49	−2.1230	0.97135	1.8448	990.21
240	1150.17	−396.99	−375.26	−2.0841	0.96468	1.8482	962.06
245	1134.16	−388.05	−366.00	−2.0460	0.95843	1.8530	934.14
250	1117.90	−379.09	−356.73	−2.0085	0.95259	1.8591	906.41
255	1101.35	−370.11	−347.41	−1.9716	0.94717	1.8666	878.88
260	1084.49	−361.11	−338.06	−1.9352	0.94215	1.8755	851.52
265	1067.29	−352.08	−328.65	−1.8994	0.93752	1.8859	824.34

TABLE 35. Thermodynamic properties of carbon dioxide—Continued

Temperature (K)	Density (kg/m^3)	Internal energy (kJ/kg)	Enthalpy (kJ/kg)	Entropy [kJ/(kg K)]	c_v [kJ/(kg K)]	c_p [kJ/(kg K)]	Speed of sound (m/s)
			25.00 MPa Isobar				
270	1049.74	−343.01	−319.20	−1.8641	0.93329	1.8978	797.36
275	1031.80	−333.90	−309.67	−1.8291	0.92943	1.9111	770.56
280	1013.45	−324.75	−300.08	−1.7946	0.92595	1.9259	743.98
285	994.67	−315.55	−290.41	−1.7603	0.92283	1.9422	717.64
290	975.42	−306.29	−280.66	−1.7264	0.92013	1.9600	691.56
295	955.68	−296.97	−270.81	−1.6927	0.91792	1.9794	665.77
300	935.42	−287.59	−260.86	−1.6593	0.91623	2.0008	640.35
305	914.62	−278.13	−250.80	−1.6260	0.91497	2.0242	615.36
310	893.25	−268.60	−240.61	−1.5929	0.91387	2.0495	590.90
315	871.29	−258.99	−230.30	−1.5599	0.91273	2.0760	567.03
320	848.72	−249.31	−219.85	−1.5270	0.91162	2.1032	543.81
325	825.55	−239.55	−209.27	−1.4942	0.91081	2.1309	521.34
330	801.80	−229.72	−198.54	−1.4614	0.91044	2.1592	499.77
335	777.50	−219.83	−187.68	−1.4287	0.91042	2.1876	479.28
340	752.73	−209.88	−176.67	−1.3961	0.91046	2.2143	460.05
345	727.58	−199.90	−165.54	−1.3636	0.91032	2.2369	442.23
350	702.22	−189.91	−154.31	−1.3313	0.90989	2.2525	425.97
360	651.72	−170.10	−131.74	−1.2677	0.90829	2.2554	398.41
370	603.10	−150.79	109.34	−1.2064	0.90620	2.2187	377.41
380	557.99	−132.28	−87.474	−1.1480	0.90373	2.1495	362.54
390	517.36	−114.74	−66.415	−1.0933	0.90075	2.0598	352.86
400	481.55	−98.223	−46.307	−1.0424	0.89744	1.9613	347.18
410	450.35	−82.696	−27.183	−0.99520	0.89418	1.8644	344.41
420	423.27	−68.058	−8.9932	−0.95136	0.89131	1.7753	343.67
430	399.72	−54.187	8.3578	−0.91053	0.88902	1.6967	344.32
440	379.13	−40.963	24.978	−0.87232	0.88742	1.6290	345.93
450	361.01	−28.279	40.971	−0.83637	0.88650	1.5713	348.19
460	344.95	−16.042	56.432	−0.80239	0.88624	1.5222	350.90
470	330.61	−4.1769	71.440	−0.77011	0.88657	1.4806	353.92
480	317.72	7.3809	86.066	−0.73932	0.88744	1.4453	357.14
490	306.07	18.683	100.36	−0.70983	0.88878	1.4153	360.51
500	295.46	29.772	114.39	−0.68150	0.89052	1.3897	363.96
525	272.64	56.782	148.48	−0.61496	0.89633	1.3407	372.76
550	253.87	83.077	181.55	−0.55341	0.90365	1.3073	381.59
575	238.08	108.92	213.93	−0.49583	0.91195	1.2845	390.28
600	224.54	134.50	245.84	−0.44152	0.92086	1.2689	398.77
625	212.77	159.92	277.42	−0.38994	0.93012	1.2586	407.04
650	202.40	185.28	308.80	−0.34072	0.93954	1.2520	415.08
675	193.18	210.63	340.05	−0.29354	0.94899	1.2483	422.90
700	184.90	236.02	371.23	−0.24818	0.95838	1.2465	430.51
800	158.65	338.44	496.02	−0.08156	0.99409	1.2516	459.06
900	139.62	442.77	621.83	0.06661	1.0258	1.2653	485.14
1000	125.04	549.19	749.14	0.20073	1.0532	1.2810	509.32
1100	113.42	657.58	878.01	0.32355	1.0766	1.2964	531.99

TABLE 35. Thermodynamic properties of carbon dioxide—Continued

Temperature (K)	Density (kg/m^3)	Internal energy (kJ/kg)	Enthalpy (kJ/kg)	Entropy [kJ/(kg K)]	c_v [kJ/(kg K)]	c_p [kJ/(kg K)]	Speed of sound (m/s)
			30.00 MPa Isobar				
222.715[b]	1211.77	−430.02	−405.26	−2.2321	0.99332	1.8259	1083.4
225	1205.06	−425.99	−401.09	−2.2135	0.98964	1.8251	1070.6
230	1190.25	−417.17	−391.97	−2.1734	0.98193	1.8241	1043.0
235	1175.29	−408.37	−382.85	−2.1342	0.97467	1.8242	1015.8
240	1160.15	−399.58	−373.72	−2.0958	0.96786	1.8254	988.76
245	1144.83	−390.80	−364.59	−2.0581	0.96147	1.8277	962.05
250	1129.30	−382.01	−355.45	−2.0211	0.95550	1.8311	935.59
255	1113.55	−373.22	−346.28	−1.9848	0.94994	1.8355	909.37
260	1097.57	−364.42	−337.09	−1.9491	0.94478	1.8410	883.41
265	1081.34	−355.61	−327.87	−1.9140	0.94000	1.8475	857.70
270	1064.86	−346.78	−318.61	−1.8794	0.93559	1.8550	832.25
275	1048.09	−337.94	−309.32	−1.8453	0.93153	1.8635	807.08
280	1031.04	−329.07	−299.97	−1.8116	0.92783	1.8729	782.21
285	1013.68	−320.18	−290.58	−1.7784	0.92446	1.8831	757.65
290	996.01	−311.26	−281.14	−1.7456	0.92145	1.8942	733.44
295	978.02	−302.32	−271.64	−1.7131	0.91882	1.9060	709.61
300	959.70	−293.34	−262.08	−1.6809	0.91659	1.9186	686.21
305	941.04	−284.33	−252.45	−1.6491	0.91471	1.9322	663.31
310	922.04	−275.29	−242.76	−1.6176	0.91301	1.9464	640.96
315	902.69	−266.22	−232.99	−1.5863	0.91135	1.9610	619.20
320	883.00	−257.12	−223.15	−1.5553	0.90973	1.9756	598.05
325	862.99	−248.00	−213.23	−1.5246	0.90830	1.9899	577.56
330	842.66	−238.85	−203.25	−1.4941	0.90721	2.0041	557.78
335	822.06	−229.69	−193.19	−1.4639	0.90648	2.0179	538.80
340	801.21	−220.51	−183.07	−1.4339	0.90599	2.0312	520.72
345	780.17	−211.34	−172.88	−1.4041	0.90560	2.0432	503.62
350	758.98	−202.17	−162.64	−1.3746	0.90520	2.0529	487.58
360	716.55	−183.92	−142.05	−1.3166	0.90427	2.0618	458.95
370	674.75	−165.93	−121.47	−1.2602	0.90323	2.0517	435.21
380	634.51	−148.37	−101.09	−1.2059	0.90215	2.0224	416.28
390	596.59	−131.36	−81.073	−1.1539	0.90099	1.9781	401.73
400	561.50	−114.99	−61.559	−1.1045	0.89970	1.9233	390.99
410	529.46	−99.289	−42.627	−1.0577	0.89833	1.8625	383.45
420	500.50	−84.257	−24.317	−1.0136	0.89698	1.7995	378.49
430	474.48	−69.860	−6.6324	−0.97200	0.89581	1.7378	375.55
440	451.16	−56.044	10.452	−0.93272	0.89494	1.6799	374.14
450	430.25	−42.746	26.982	−0.89557	0.89446	1.6270	373.89
460	411.46	−29.901	43.010	−0.86034	0.89440	1.5796	374.49
470	394.52	−17.449	58.593	−0.82682	0.89476	1.5378	375.74
480	379.18	−5.3349	73.783	−0.79484	0.89554	1.5011	377.47
490	365.24	6.4911	88.629	−0.76423	0.89671	1.4689	379.56
500	352.51	18.071	103.18	−0.73484	0.89824	1.4409	381.92
525	325.03	46.167	138.47	−0.66595	0.90339	1.3857	388.60
550	302.37	73.376	172.59	−0.60245	0.91002	1.3465	395.90
575	283.31	99.995	205.89	−0.54324	0.91767	1.3187	403.46

TABLE 35. Thermodynamic properties of carbon dioxide—Continued

Temperature (K)	Density (kg/m^3)	Internal energy (kJ/kg)	Enthalpy (kJ/kg)	Entropy [kJ/(kg K)]	c_v [kJ/(kg K)]	c_p [kJ/(kg K)]	Speed of sound (m/s)
			30.00 MPa Isobar				
600	266.99	126.23	238.59	−0.48756	0.92601	1.2990	411.10
625	252.82	152.22	270.88	−0.43483	0.93476	1.2852	418.70
650	240.36	178.08	302.89	−0.38462	0.94374	1.2757	426.21
675	229.30	203.86	334.70	−0.33660	0.95281	1.2695	433.60
700	219.39	229.64	366.38	−0.29051	0.96185	1.2657	440.86
800	188.05	333.24	492.77	−0.12174	0.99658	1.2650	468.48
900	165.44	438.40	619.73	0.02779	1.0277	1.2752	494.02
1000	148.15	545.42	747.91	0.16283	1.0547	1.2887	517.84
1100	134.40	654.27	877.48	0.28631	1.0778	1.3026	540.25
			40.00 MPa Isobar				
224.715[b]	1221.12	−430.49	−397.73	−2.2352	0.99675	1.7975	1116.0
225	1220.33	−429.99	−397.22	−2.2329	0.99628	1.7973	1114.5
230	1206.41	−421.40	−388.24	−2.1935	0.98829	1.7937	1088.7
235	1192.39	−412.82	−379.28	−2.1549	0.98078	1.7910	1063.3
240	1178.27	−404.28	−370.33	−2.1172	0.97373	1.7892	1038.2
245	1164.03	−395.75	−361.39	−2.0804	0.96713	1.7881	1013.4
250	1149.68	−387.24	−352.45	−2.0442	0.96096	1.7877	988.91
255	1135.19	−378.74	−343.51	−2.0088	0.95520	1.7881	964.76
260	1120.58	−370.26	−334.56	−1.9741	0.94983	1.7892	940.93
265	1105.83	−361.79	−325.61	−1.9400	0.94484	1.7908	917.41
270	1090.93	−353.32	−316.65	−1.9065	0.94022	1.7931	894.22
275	1075.88	−344.86	−307.68	−1.8736	0.93594	1.7959	871.38
280	1060.68	−336.41	−298.69	−1.8412	0.93198	1.7991	848.90
285	1045.33	−327.96	−289.69	−1.8093	0.92835	1.8027	826.79
290	1029.82	−319.51	−280.67	−1.7779	0.92502	1.8066	805.09
295	1014.16	−311.07	−271.62	−1.7470	0.92201	1.8108	783.81
300	998.35	−302.62	−262.56	−1.7166	0.91930	1.8152	762.99
305	982.39	−294.19	−253.47	−1.6865	0.91688	1.8198	742.65
310	966.29	−285.76	−244.36	−1.6569	0.91467	1.8245	722.85
315	950.05	−277.33	−235.23	−1.6277	0.91261	1.8291	703.59
320	933.68	−268.91	−226.07	−1.5988	0.91069	1.8334	684.89
325	917.21	−260.50	−216.89	−1.5704	0.90894	1.8375	666.75
330	900.63	−252.11	−207.70	−1.5423	0.90743	1.8412	649.20
335	883.97	−243.73	−198.48	−1.5146	0.90618	1.8444	632.25
340	867.25	−235.37	−189.25	−1.4872	0.90518	1.8473	615.94
345	850.50	−227.04	−180.01	−1.4602	0.90437	1.8497	600.32
350	833.72	−218.73	−170.76	−1.4336	0.90369	1.8514	585.39
360	800.23	−202.22	−152.23	−1.3814	0.90261	1.8525	557.71
370	767.03	−185.87	−133.72	−1.3307	0.90182	1.8492	533.02
380	734.39	−169.74	−115.27	−1.2815	0.90130	1.8400	511.44
390	702.64	−153.87	−96.942	−1.2339	0.90102	1.8242	493.01
400	672.08	−138.32	−78.806	−1.1880	0.90094	1.8021	477.59
410	642.96	−123.13	−60.917	−1.1438	0.90101	1.7750	464.90
420	615.44	−108.31	−43.316	−1.1014	0.90123	1.7446	454.60
430	589.59	−93.874	−26.030	−1.0607	0.90157	1.7123	446.38

TABLE 35. Thermodynamic properties of carbon dioxide—Continued

Temperature (K)	Density (kg/m^3)	Internal energy (kJ/kg)	Enthalpy (kJ/kg)	Entropy [kJ/(kg K)]	c_v [kJ/(kg K)]	c_p [kJ/(kg K)]	Speed of sound (m/s)
			40.00 MPa Isobar				
440	565.45	−79.814	−9.0735	−1.0217	0.90206	1.6790	439.96
450	542.98	−66.118	7.5496	−0.98436	0.90270	1.6457	435.07
460	522.12	−52.769	23.842	−0.94855	0.90351	1.6129	431.49
470	502.79	39.744	39.812	0.91420	0.90452	1.5814	429.01
480	484.89	−27.017	55.476	−0.88122	0.90574	1.5516	427.45
490	468.31	−14.563	70.851	−0.84952	0.90717	1.5238	426.63
500	452.94	−2.3539	85.959	−0.81899	0.90882	1.4981	426.42
525	419.10	27.259	122.70	−0.74727	0.91383	1.4435	427.89
550	390.67	55.849	158.24	−0.68114	0.91996	1.4013	431.27
575	366.46	83.699	192.85	−0.61959	0.92697	1.3692	435.81
600	345.60	111.02	226.76	−0.56185	0.93462	1.3451	441.07
625	327.40	137.98	260.16	−0.50733	0.94271	1.3271	446.76
650	311.36	164.69	293.16	−0.45555	0.95107	1.3139	452.71
675	297.09	191.24	325.88	−0.40615	0.95957	1.3043	458.80
700	284.29	217.70	358.40	−0.35885	0.96810	1.2975	464.97
800	243.83	323.44	487.49	−0.18646	1.0012	1.2880	489.58
900	214.66	430.11	616.45	−0.03457	1.0313	1.2926	513.34
1000	192.37	538.25	746.18	0.10210	1.0575	1.3024	535.98
1100	174.67	647.97	876.98	0.22676	1.0802	1.3137	557.53
			50.00 MPa Isobar				
226.679[b]	1229.78	−430.78	−390.13	−2.2377	0.99951	1.7735	1146.9
230	1221.01	−425.19	−384.24	−2.2119	0.99412	1.7700	1130.8
235	1207.74	−416.81	−375.41	−2.1739	0.98640	1.7654	1106.8
240	1194.42	−408.45	−366.59	−2.1368	0.97918	1.7615	1083.2
245	1181.04	−400.13	−357.79	−2.1005	0.97242	1.7582	1059.9
250	1167.59	−391.83	−349.01	−2.0650	0.96609	1.7556	1037.0
255	1154.07	−383.56	−340.23	−2.0303	0.96020	1.7534	1014.4
260	1140.47	−375.31	−331.47	−1.9962	0.95470	1.7518	992.10
265	1126.80	−367.09	−322.71	−1.9629	0.94958	1.7507	970.17
270	1113.05	−358.88	−313.96	−1.9301	0.94483	1.7500	948.60
275	1099.22	−350.70	−305.21	−1.8980	0.94042	1.7496	927.39
280	1085.32	−342.53	−296.47	−1.8665	0.93634	1.7496	906.55
285	1071.33	−334.39	−287.72	−1.8355	0.93257	1.7498	886.10
290	1057.27	−326.26	−278.97	−1.8051	0.92910	1.7502	866.05
295	1043.14	−318.15	−270.21	−1.7752	0.92592	1.7507	846.42
300	1028.94	−310.05	261.46	1.7458	0.92303	1.7514	827.23
305	1014.67	−301.98	−252.70	−1.7168	0.92039	1.7521	808.50
310	1000.35	−293.92	−243.94	−1.6883	0.91799	1.7527	790.25
315	985.97	−285.88	−235.17	−1.6603	0.91578	1.7533	772.50
320	971.55	−277.87	−226.41	−1.6326	0.91376	1.7538	755.25
325	957.10	−269.88	−217.64	−1.6055	0.91193	1.7540	738.51
330	942.63	−261.91	−208.87	−1.5787	0.91030	1.7539	722.28
335	928.14	−253.97	−200.10	−1.5523	0.90890	1.7536	706.59
340	913.66	−246.06	−191.33	−1.5263	0.90769	1.7529	691.43
345	899.19	−238.17	−182.57	−1.5007	0.90668	1.7520	676.84

TABLE 35. Thermodynamic properties of carbon dioxide—Continued

Temperature (K)	Density (kg/m^3)	Internal energy (kJ/kg)	Enthalpy (kJ/kg)	Entropy [kJ/(kg K)]	c_v [kJ/(kg K)]	c_p [kJ/(kg K)]	Speed of sound (m/s)
			50.00 MPa Isobar				
350	884.76	−230.32	−173.81	−1.4755	0.90581	1.7507	662.81
360	856.03	−214.73	−156.32	−1.4263	0.90448	1.7469	636.48
370	827.61	−199.29	−138.88	−1.3785	0.90360	1.7414	612.45
380	799.62	−184.03	−121.50	−1.3321	0.90311	1.7340	590.70
390	772.18	−168.96	−104.21	−1.2872	0.90297	1.7243	571.22
400	745.45	−154.10	−87.024	−1.2437	0.90314	1.7120	554.02
410	719.54	−139.47	−69.977	−1.2016	0.90357	1.6970	539.02
420	694.59	−125.08	−53.092	−1.1609	0.90423	1.6796	526.11
430	670.67	−110.94	−36.392	−1.1216	0.90508	1.6602	515.13
440	647.87	−97.069	−19.893	−1.0837	0.90612	1.6394	505.87
450	626.20	−83.452	−3.6055	−1.0471	0.90732	1.6180	498.11
460	605.67	−70.087	12.466	1.0118	0.90868	1.5964	491.68
470	586.26	−56.964	28.322	−0.97766	0.91018	1.5749	486.40
480	567.95	−44.071	43.965	−0.94473	0.91184	1.5538	482.14
490	550.68	−31.396	59.400	−0.91290	0.91363	1.5333	478.77
500	534.42	−18.926	74.634	−0.88213	0.91557	1.5136	476.18
525	497.78	11.454	111.90	−0.80939	0.92101	1.4687	472.48
550	466.18	40.875	148.13	−0.74197	0.92723	1.4308	471.73
575	438.78	69.547	183.50	−0.67907	0.93410	1.3999	472.96
600	414.84	97.651	218.18	−0.62003	0.94148	1.3753	475.52
625	393.77	125.33	252.31	−0.56429	0.94924	1.3561	479.00
650	375.06	152.71	286.02	−0.51141	0.95724	1.3412	483.09
675	358.33	179.87	319.40	−0.46101	0.96537	1.3300	487.62
700	343.27	206.88	352.54	−0.41281	0.97355	1.3215	492.43
800	295.34	314.44	483.74	−0.23759	1.0055	1.3064	513.16
900	260.55	422.42	614.33	−0.08378	1.0347	1.3070	534.47
1000	233.89	531.57	745.34	0.05425	1.0603	1.3140	555.44
1100	212.66	642.08	877.19	0.17991	1.0825	1.3232	575.78
			75.00 MPa Isobar				
231.448[b]	1249.06	−430.98	−370.94	−2.2420	1.0049	1.7265	1217.6
235	1240.63	−425.27	−364.81	−2.2157	0.99929	1.7213	1202.5
240	1228.76	−417.26	−356.22	−2.1795	0.99178	1.7146	1181.5
245	1216.90	−409.30	−347.67	−2.1442	0.98477	1.7083	1160.9
250	1205.04	−401.38	−339.14	−2.1098	0.97824	1.7025	1140.6
255	1193.18	−393.50	−330.64	−2.0761	0.97215	1.6972	1120.6
260	1181.32	−385.66	−322.17	−2.0432	0.96649	1.6922	1101.0
265	1169.46	−377.85	−313.72	−2.0110	0.96122	1.6876	1081.7
270	1157.60	−370.08	−305.29	−1.9795	0.95633	1.6833	1062.7
275	1145.74	−362.34	−296.88	−1.9487	0.95179	1.6793	1044.1
280	1133.89	−354.64	−288.50	−1.9184	0.94758	1.6756	1025.9
285	1122.04	−346.97	−280.13	−1.8888	0.94369	1.6720	1008.0
290	1110.20	−339.33	−271.78	−1.8598	0.94010	1.6687	990.43
295	1098.37	−331.72	−263.44	−1.8313	0.93680	1.6654	973.27
300	1086.56	−324.15	−255.12	−1.8033	0.93376	1.6623	956.50

TABLE 35. Thermodynamic properties of carbon dioxide—Continued

Temperature (K)	Density (kg/m^3)	Internal energy (kJ/kg)	Enthalpy (kJ/kg)	Entropy [kJ/(kg K)]	c_v [kJ/(kg K)]	c_p [kJ/(kg K)]	Speed of sound (m/s)
			75.00 MPa Isobar				
305	1074.76	−316.60	−246.82	−1.7759	0.93097	1.6593	940.12
310	1062.97	−309.09	−238.53	−1.7489	0.92843	1.6563	924.14
315	1051.22	−301.60	−230.25	−1.7224	0.92610	1.6534	908.56
320	1039.49	−294.15	−222.00	−1.6964	0.92399	1.6504	893.38
325	1027.79	−286.72	−213.75	−1.6708	0.92208	1.6474	878.62
330	1016.13	279.33	−205.52	−1.6457	0.92037	1.6444	864.28
335	1004.51	−271.97	−197.31	−1.6210	0.91884	1.6413	850.35
340	992.95	−264.64	−189.11	−1.5967	0.91750	1.6381	836.84
345	981.43	−257.35	−180.93	−1.5728	0.91632	1.6348	823.75
350	969.98	−250.08	−172.76	−1.5493	0.91530	1.6314	811.08
360	947.28	−235.66	−156.48	−1.5035	0.91369	1.6244	787.00
370	924.90	−221.36	−140.27	−1.4591	0.91262	1.6170	764.58
380	902.87	−207.21	−124.14	−1.4160	0.91202	1.6091	743.77
390	881.23	−193.20	−108.09	−1.3744	0.91184	1.6009	724.52
400	860.03	−179.33	−92.126	−1.3339	0.91204	1.5924	706.78
410	839.31	−165.61	−76.246	−1.2947	0.91258	1.5836	690.47
420	819.07	−152.02	−60.456	−1.2567	0.91342	1.5745	675.53
430	799.37	−138.58	−44.757	−1.2197	0.91452	1.5652	661.90
440	780.21	−125.28	−29.152	−1.1838	0.91585	1.5557	649.53
450	761.62	−112.12	−13.643	−1.1490	0.91738	1.5460	638.34
460	743.60	−99.093	1.7669	−1.1151	0.91910	1.5360	628.29
470	726.18	−86.204	17.076	−1.0822	0.92098	1.5258	619.31
480	709.36	−73.446	32.283	−1.0502	0.92300	1.5155	611.32
490	693.14	−60.816	47.387	−1.0190	0.92515	1.5052	604.25
500	677.52	−48.311	62.387	−0.98873	0.92742	1.4949	598.02
525	641.03	−17.555	99.444	−0.91641	0.93352	1.4699	585.62
550	608.02	12.545	135.90	−0.84857	0.94012	1.4468	576.92
575	578.19	42.085	171.80	−0.78473	0.94711	1.4260	571.08
600	551.22	71.136	207.22	−0.72443	0.95439	1.4077	567.48
625	526.81	99.843	242.21	−0.66730	0.96187	1.3920	565.64
650	504.66	128.22	276.84	−0.61297	0.96949	1.3786	565.16
675	484.49	156.36	311.16	−0.56116	0.97717	1.3675	565.73
700	466.06	184.31	345.23	−0.51159	0.98486	1.3585	567.31
800	405.95	295.12	479.87	−0.33177	1.0149	1.3379	577.61
900	361.14	405.66	613.33	−0.17457	1.0424	1.3330	592.07
1000	326.23	516.83	746.72	−0.03403	1.0668	1.3356	608.08
1100	298.11	628.97	880.55	0.09352	1.0880	1.3414	624.65

TABLE 35. Thermodynamic properties of carbon dioxide—Continued

Temperature (K)	Density (kg/m^3)	Internal energy (kJ/kg)	Enthalpy (kJ/kg)	Entropy [kJ/(kg K)]	c_v [kJ/(kg K)]	c_p [kJ/(kg K)]	Speed of sound (m/s)
			100.00 MPa Isobar				
236.031[b]	1265.83	−430.62	−351.62	−2.2443	1.0097	1.6919	1280.4
240	1257.21	−424.46	−344.92	−2.2162	1.0037	1.6854	1265.1
245	1246.37	−416.74	−336.51	−2.1815	0.99659	1.6778	1246.2
250	1235.57	−409.07	−328.14	−2.1477	0.98997	1.6706	1227.6
255	1224.80	−401.45	−319.80	−2.1147	0.98383	1.6637	1209.4
260	1214.06	−393.87	−311.50	−2.0824	0.97812	1.6573	1191.4
265	1203.36	−386.33	−303.23	−2.0509	0.97282	1.6512	1173.7
270	1192.69	−378.83	−294.99	−2.0201	0.96790	1.6454	1156.4
275	1182.06	−371.37	−286.77	−1.9900	0.96335	1.6399	1139.3
280	1171.46	−363.95	−278.59	−1.9605	0.95913	1.6347	1122.6
285	1160.90	−356.57	−270.43	−1.9316	0.95524	1.6297	1106.2
290	1150.37	−349.22	−262.29	−1.9033	0.95164	1.6249	1090.2
295	1139.89	−341.90	−254.18	−1.8755	0.94833	1.6203	1074.5
300	1129.45	−334.63	−246.09	−1.8484	0.94528	1.6158	1059.1
305	1119.04	−327.38	−238.02	−1.8217	0.94249	1.6115	1044.0
310	1108.69	−320.17	−229.97	−1.7955	0.93993	1.6073	1029.3
315	1098.38	−312.99	−221.94	−1.7698	0.93760	1.6032	1015.0
320	1088.12	−305.84	−213.94	−1.7446	0.93548	1.5992	1001.0
325	1077.91	−298.72	−205.95	−1.7198	0.93356	1.5953	987.36
330	1067.76	−291.64	−197.99	−1.6955	0.93183	1.5914	974.07
335	1057.66	−284.59	−190.04	−1.6716	0.93028	1.5876	961.13
340	1047.62	−277.56	−182.11	−1.6481	0.92891	1.5838	948.54
345	1037.64	−270.57	−174.20	−1.6250	0.92769	1.5800	936.31
350	1027.73	−263.61	−166.31	−1.6023	0.92663	1.5762	924.42
360	1008.12	−249.78	−150.58	−1.5580	0.92495	1.5687	901.70
370	988.80	−236.07	−134.93	−1.5151	0.92378	1.5612	880.34
380	969.80	−222.47	−119.36	−1.4736	0.92309	1.5537	860.31
390	951.13	−209.00	−103.86	−1.4333	0.92283	1.5461	841.58
400	932.81	−195.64	−88.438	−1.3943	0.92295	1.5386	824.08
410	914.87	−182.39	−73.089	−1.3564	0.92341	1.5311	807.78
420	897.31	−169.26	−57.815	−1.3196	0.92418	1.5237	792.60
430	880.14	−156.23	−42.614	−1.2838	0.92522	1.5164	778.51
440	863.37	−143.31	−27.486	−1.2490	0.92650	1.5092	765.42
450	847.00	−130.49	−12.430	−1.2152	0.92801	1.5021	753.30
460	831.05	−117.77	2.5559	−1.1823	0.92970	1.4952	742.08
470	815.51	−105.15	17.473	−1.1502	0.93157	1.4884	731.73
480	800.39	−92.616	32.324	−1.1189	0.93359	1.4817	722.18
490	785.67	−80.171	47.108	−1.0884	0.93574	1.4752	713.39
500	771.37	−67.812	61.828	−1.0587	0.93801	1.4688	705.34
525	737.38	−37.261	98.354	−0.98741	0.94412	1.4534	688.12
550	705.86	−7.1663	134.50	0.92014	0.95070	1.4388	674.60
575	676.71	22.527	170.30	−0.85649	0.95763	1.4251	664.18
600	649.77	51.872	205.77	−0.79610	0.96480	1.4127	656.31
625	624.90	80.921	240.95	−0.73867	0.97211	1.4016	650.49
650	601.91	109.72	275.86	−0.68389	0.97951	1.3918	646.36

TABLE 35. Thermodynamic properties of carbon dioxide—Continued

Temperature (K)	Density (kg/m^3)	Internal energy (kJ/kg)	Enthalpy (kJ/kg)	Entropy [kJ/(kg K)]	c_v [kJ/(kg K)]	c_p [kJ/(kg K)]	Speed of sound (m/s)
			100.00 MPa Isobar				
675	580.64	138.32	310.55	−0.63153	0.98693	1.3833	643.59
700	560.93	166.76	345.04	−0.58135	0.99434	1.3760	641.95
800	494.96	279.54	481.58	−0.39900	1.0231	1.3573	643.10
900	444.32	391.83	616.89	−0.23962	1.0494	1.3505	651.25
1000	404.15	504.47	751.91	−0.09737	1.0728	1.3507	662.59
1100	371.36	617.86	887.14	0.03152	1.0931	1.3544	675.48
			200.00 MPa Isobar				
252.864[b]	1318.45	−426.12	−274.43	−2.2449	1.0320	1.6131	1476.5
255	1314.84	−423.09	−270.99	−2.2314	1.0295	1.6096	1470.1
260	1306.44	−416.05	−262.96	−2.2002	1.0240	1.6016	1455.4
265	1298.11	−409.04	−254.97	−2.1697	1.0188	1.5940	1440.8
270	1289.84	−402.08	−247.02	−2.1400	1.0141	1.5867	1426.6
275	1281.64	−395.15	−239.10	−2.1110	1.0097	1.5797	1412.5
280	1273.50	−388.27	−231.22	−2.0826	1.0057	1.5730	1398.7
285	1265.43	−381.42	−223.37	−2.0548	1.0020	1.5666	1385.1
290	1257.43	−374.61	−215.55	−2.0276	0.99855	1.5604	1371.8
295	1249.48	−367.83	−207.77	−2.0010	0.99539	1.5545	1358.7
300	1241.61	−361.09	−200.01	−1.9749	0.99248	1.5488	1345.9
305	1233.79	−354.38	−192.28	−1.9493	0.98981	1.5434	1333.3
310	1226.04	−347.70	−184.57	−1.9243	0.98736	1.5381	1321.0
315	1218.35	−341.05	−176.90	−1.8997	0.98512	1.5331	1308.9
320	1210.72	−334.43	−169.24	−1.8756	0.98307	1.5282	1297.1
325	1203.16	−327.84	−161.61	−1.8519	0.98121	1.5235	1285.5
330	1195.66	−321.28	−154.01	−1.8287	0.97952	1.5190	1274.2
335	1188.22	−314.74	−146.42	−1.8059	0.97799	1.5146	1263.1
340	1180.84	−308.23	−138.86	−1.7835	0.97662	1.5104	1252.2
345	1173.53	−301.75	−131.32	−1.7615	0.97539	1.5064	1241.6
350	1166.27	−295.28	−123.80	−1.7398	0.97430	1.5025	1231.2
360	1151.94	−282.43	−108.81	−1.6976	0.97249	1.4950	1211.2
370	1137.86	−269.67	−93.896	−1.6568	0.97114	1.4880	1192.1
380	1124.01	−256.98	−79.049	−1.6172	0.97020	1.4815	1173.9
390	1110.41	−244.38	−64.266	−1.5788	0.96963	1.4753	1156.5
400	1097.04	−231.85	−49.543	−1.5415	0.96940	1.4695	1140.0
410	1083.91	−219.39	−34.876	−1.5053	0.96947	1.4640	1124.3
420	1071.02	−207.00	−20.262	−1.4700	0.96981	1.4588	1109.4
430	1058.36	−194.67	−5.6992	−1.4358	0.97040	1.4539	1095.3
440	1045.94	−182.40	8.8159	−1.4024	0.97121	1.4492	1081.9
450	1033.74	−170.19	23.286	−1.3699	0.97222	1.4448	1069.2
460	1021.78	−158.02	37.713	−1.3382	0.97341	1.4406	1057.1
470	1010.04	−145.91	52.099	−1.3072	0.97477	1.4367	1045.7
480	998.53	−133.85	66.447	−1.2770	0.97627	1.4329	1034.8
490	987.24	−121.83	80.758	−1.2475	0.97791	1.4294	1024.6
500	976.16	−109.85	95.035	−1.2187	0.97967	1.4260	1014.9
525	949.42	−80.066	130.59	−1.1493	0.98451	1.4185	992.79
550	923.96	−50.491	165.97	−1.0835	0.98986	1.4120	973.51
575	899.74	−21.088	201.20	−1.0208	0.99559	1.4065	956.68
600	876.69	8.1703	236.30	−0.96106	1.0016	1.4019	942.00

TABLE 35. Thermodynamic properties of carbon dioxide—Continued

Temperature (K)	Density (kg/m^3)	Internal energy (kJ/kg)	Enthalpy (kJ/kg)	Entropy [kJ/(kg K)]	c_v [kJ/(kg K)]	c_p [kJ/(kg K)]	Speed of sound (m/s)
			200.00 MPa Isobar				
625	854.75	37.312	271.30	−0.90391	1.0078	1.3980	929.18
650	833.86	66.359	306.21	−0.84915	1.0140	1.3948	918.02
675	813.97	95.331	341.04	−0.79656	1.0204	1.3922	908.32
700	795.00	124.25	375.82	−0.74597	1.0267	1.3900	899.91
800	727.46	239.61	514.53	−0.56073	1.0513	1.3851	876.78
900	671.10	354.93	652.94	−0.39771	1.0740	1.3836	865.84
1000	623.57	470.58	791.32	−0.25192	1.0942	1.3841	862.60
1100	583.00	586.76	929.81	−0.11992	1.1119	1.3860	864.16
			400.00 MPa Isobar				
281.544[b]	1392.45	−410.72	−123.46	−2.2315	1.0894	1.5590	1732.5
285	1388.17	−406.23	−118.08	−2.2125	1.0870	1.5546	1724.6
290	1382.04	−399.75	−110.32	−2.1855	1.0838	1.5485	1713.3
295	1375.97	−393.30	−102.59	−2.1591	1.0808	1.5426	1702.1
300	1369.95	−386.88	−94.895	−2.1332	1.0780	1.5369	1691.2
305	1364.00	−380.48	−87.224	−2.1078	1.0754	1.5314	1680.4
310	1358.11	−374.11	−79.581	−2.0830	1.0729	1.5260	1669.9
315	1352.28	−367.76	−71.964	−2.0586	1.0707	1.5209	1659.5
320	1346.50	−361.44	−64.371	−2.0347	1.0686	1.5160	1649.3
325	1340.78	355.14	56.803	−2.0112	1.0667	1.5112	1639.3
330	1335.11	−348.86	−49.259	−1.9882	1.0650	1.5067	1629.5
335	1329.50	−342.60	−41.737	−1.9656	1.0633	1.5022	1619.8
340	1323.95	−336.36	−34.236	−1.9433	1.0618	1.4980	1610.3
345	1318.44	−330.14	−26.757	−1.9215	1.0605	1.4939	1601.1
350	1312.99	−323.94	−19.297	−1.9000	1.0592	1.4899	1591.9
360	1302.24	−311.60	−4.4362	−1.8582	1.0570	1.4824	1574.2
370	1291.69	−299.32	10.353	−1.8177	1.0552	1.4754	1557.2
380	1281.33	−287.10	25.074	−1.7784	1.0537	1.4690	1540.8
390	1271.16	−274.94	39.733	−1.7403	1.0525	1.4630	1525.0
400	1261.17	−262.83	54.335	−1.7033	1.0516	1.4574	1509.8
410	1251.35	−250.77	68.883	−1.6674	1.0510	1.4522	1495.3
420	1241.70	−238.76	83.381	−1.6325	1.0506	1.4475	1481.2
430	1232.22	−226.78	97.833	−1.5985	1.0504	1.4430	1467.7
440	1222.89	−214.85	112.24	−1.5654	1.0503	1.4389	1454.8
450	1213.72	−202.95	126.61	−1.5331	1.0505	1.4352	1442.3
460	1204.70	−191.08	140.95	−1.5016	1.0508	1.4317	1430.3
470	1195.83	−179.25	155.25	−1.4708	1.0513	1.4285	1418.8
480	1187.10	−167.44	169.52	−1.4408	1.0519	1.4255	1407.7
490	1178.51	−155.65	183.76	−1.4114	1.0526	1.4228	1397.1
500	1170.05	−143.89	197.97	−1.3827	1.0534	1.4203	1386.9
525	1149.47	−114.58	233.41	−1.3135	1.0559	1.4149	1363.0
550	1129.67	−85.361	268.72	−1.2478	1.0588	1.4106	1341.4
575	1110.59	−56.223	303.94	−1.1852	1.0622	1.4072	1321.8
600	1092.21	−27.143	339.09	−1.1253	1.0659	1.4045	1304.1
625	1074.47	1.8990	374.18	−1.0681	1.0698	1.4025	1288.1

TABLE 35. Thermodynamic properties of carbon dioxide—Continued

Temperature (K)	Density (kg/m^3)	Internal energy (kJ/kg)	Enthalpy (kJ/kg)	Entropy [kJ/(kg K)]	c_v [kJ/(kg K)]	c_p [kJ/(kg K)]	Speed of sound (m/s)
			400.00 MPa Isobar				
650	1057.35	30.916	409.22	−1.0131	1.0739	1.4011	1273.5
675	1040.82	59.921	444.23	−0.96022	1.0781	1.4001	1260.4
700	1024.84	88.926	479.23	−0.90931	1.0825	1.3995	1248.5
800	966.02	205.09	619.16	−0.72246	1.0999	1.3997	1211.0
900	914.22	321.71	759.24	−0.55747	1.1165	1.4023	1185.7
1000	868.27	438.97	899.65	−0.40954	1.1316	1.4060	1168.7
1100	827.20	556.88	1040.44	−0.27535	1.1451	1.4098	1157.6
			600.00 MPa Isobar				
305.996[b]	1448.66	−391.42	22.754	−2.2128	1.1462	1.5467	1910.7
310	1444.64	−386.39	28.939	−2.1927	1.1442	1.5427	1903.0
315	1439.67	−380.12	36.640	−2.1681	1.1419	1.5377	1893.5
320	1434.75	−373.88	44.317	−2.1439	1.1397	1.5329	1884.2
325	1429.88	−367.65	51.970	−2.1201	1.1376	1.5283	1875.1
330	1425.06	−361.44	59.600	−2.0969	1.1357	1.5238	1866.1
335	1420.28	−355.24	67.208	−2.0740	1.1338	1.5194	1857.3
340	1415.56	−349.07	74.794	−2.0515	1.1321	1.5152	1848.6
345	1410.88	−342.91	82.360	−2.0294	1.1305	1.5111	1840.1
350	1406.25	−336.76	89.905	−2.0077	1.1290	1.5071	1831.7
360	1397.12	−324.52	104.94	−1.9653	1.1263	1.4996	1815.4
370	1388.16	−312.33	119.90	−1.9243	1.1240	1.4925	1799.7
380	1379.38	−300.19	134.79	−1.8846	1.1219	1.4858	1784.5
390	1370.75	−288.10	149.62	−1.8461	1.1201	1.4796	1769.8
400	1362.28	276.05	164.38	1.8087	1.1186	1.4738	1755.6
410	1353.97	−264.05	179.09	−1.7724	1.1174	1.4683	1741.9
420	1345.79	−252.08	193.75	−1.7371	1.1163	1.4633	1728.7
430	1337.76	−240.15	208.36	−1.7027	1.1154	1.4585	1715.9
440	1329.87	−228.25	222.92	−1.6692	1.1147	1.4541	1703.6
450	1322.10	−216.38	237.44	−1.6366	1.1142	1.4500	1691.6
460	1314.46	−204.54	251.92	−1.6048	1.1139	1.4462	1680.1
470	1306.94	−192.72	266.37	−1.5737	1.1136	1.4427	1668.9
480	1299.54	−180.92	280.78	−1.5434	1.1135	1.4394	1658.1
490	1292.26	−169.15	295.16	−1.5137	1.1135	1.4363	1647.7
500	1285.08	−157.39	309.50	−1.4847	1.1137	1.4335	1637.5
525	1267.60	−128.07	345.26	−1.4149	1.1144	1.4275	1613.7
550	1250.74	−98.828	380.89	−1.3487	1.1157	1.4226	1591.6
575	1234.45	−69.645	416.40	−1.2855	1.1174	1.4187	1571.3
600	1218.69	−40.503	451.83	−1.2252	1.1195	1.4157	1552.5
625	1203.43	−11.386	487.19	−1.1675	1.1218	1.4134	1535.1
650	1188.63	17.720	522.50	−1.1121	1.1243	1.4117	1519.1
675	1174.27	46.825	557.78	−1.0588	1.1271	1.4106	1504.2
700	1160.32	75.938	593.04	−1.0075	1.1299	1.4099	1490.5
800	1108.23	192.61	734.02	−0.81926	1.1419	1.4103	1445.3
900	1061.27	309.84	875.20	−0.65298	1.1538	1.4134	1412.4
1000	1018.66	427.73	1016.74	−0.50386	1.1649	1.4175	1388.8
1100	979.76	546.30	1158.69	−0.36856	1.1749	1.4216	1371.9

TABLE 35. Thermodynamic properties of carbon dioxide—Continued

Temperature (K)	Density (kg/m^3)	Internal energy (kJ/kg)	Enthalpy (kJ/kg)	Entropy [kJ/(kg K)]	c_v [kJ/(kg K)]	c_p [kJ/(kg K)]	Speed of sound (m/s)
			800.00 MPa Isobar				
327.673[b]	1495.70	−369.91	164.96	−2.1926	1.1961	1.5477	2052.8
330	1493.71	−367.02	168.56	−2.1817	1.1951	1.5457	2048.9
335	1489.46	−360.83	176.28	−2.1585	1.1931	1.5415	2040.7
340	1485.25	−354.66	183.97	−2.1357	1.1912	1.5373	2032.6
345	1481.08	−348.50	191.65	−2.1132	1.1894	1.5333	2024.6
350	1476.96	−342.35	199.31	−2.0912	1.1877	1.5294	2016.8
360	1468.83	−330.09	214.56	−2.0482	1.1846	1.5218	2001.6
370	1460.85	−317.88	229.74	−2.0066	1.1817	1.5147	1986.8
380	1453.03	−305.72	244.86	−1.9663	1.1791	1.5080	1972.5
390	1445.35	−293.59	259.90	−1.9272	1.1769	1.5016	1958.7
400	1437.82	−281.51	274.89	−1.8893	1.1748	1.4956	1945.4
410	1430.42	−269.46	289.82	−1.8524	1.1730	1.4899	1932.4
420	1423.15	−257.45	304.69	−1.8166	1.1714	1.4845	1919.9
430	1416.00	−245.46	319.51	−1.7817	1.1699	1.4795	1907.8
440	1408.98	−233.51	334.28	−1.7478	1.1687	1.4748	1896.0
450	1402.08	221.58	349.01	1.7147	1.1676	1.4703	1884.6
460	1395.29	−209.67	363.69	−1.6824	1.1667	1.4661	1873.5
470	1388.60	−197.79	378.33	−1.6509	1.1659	1.4622	1862.8
480	1382.03	−185.93	392.93	−1.6202	1.1652	1.4586	1852.4
490	1375.55	−174.08	407.50	−1.5901	1.1647	1.4551	1842.3
500	1369.17	−162.26	422.04	−1.5608	1.1642	1.4519	1832.5
525	1353.64	−132.76	458.24	−1.4901	1.1636	1.4448	1809.1
550	1338.65	−103.33	494.29	−1.4230	1.1636	1.4389	1787.4
575	1324.16	−73.959	530.20	−1.3592	1.1640	1.4340	1767.1
600	1310.14	−44.627	566.00	−1.2982	1.1648	1.4301	1748.1
625	1296.54	−15.319	601.71	−1.2399	1.1659	1.4269	1730.4
650	1283.34	13.975	637.35	−1.1840	1.1673	1.4244	1713.8
675	1270.52	43.267	672.93	−1.1303	1.1688	1.4225	1698.2
700	1258.04	72.565	708.47	−1.0786	1.1706	1.4211	1683.6
800	1211.18	189.94	850.45	−0.88900	1.1785	1.4193	1633.6
900	1168.47	307.80	992.46	−0.72175	1.1868	1.4212	1594.8
1000	1129.16	426.25	1134.74	−0.57184	1.1948	1.4247	1564.9
1100	1092.77	545.32	1277.40	−0.43587	1.2020	1.4286	1542.2

[a]Sublimation temperature.
[b]Melting temperature.
[c]Saturation temperature.

11. Acknowledgments

The authors are grateful to the Deutsche Forschungsgemeinschaft for their financial support of this project.

12. References

[1] IUPAC Commission on Atomic Weights and Isotopic Abundances, J. Phys. Chem. Ref. Data **24**, 1561 (1995).
[2] E. R. Cohen and B. N. Taylor, *The 1986 Adjustment of the Fundamental Physical Constants*, CODATA Bull. No. 63 (Pergamon, Oxford, 1986).
[3] S. Angus, B. Armstrong, and K. M. de Reuck, *International Tables of the Fluid State—3: Carbon Dioxide* (Pergamon, Oxford, 1976).
[4] R. Schmidt and W. Wagner, Fluid Phase Equilibria **19**, 175 (1985).
[5] A. Saul and W. Wagner, J. Phys. Chem. Ref. Data **18**, 1537 (1989).
[6] U. Setzmann and W. Wagner, Int. J. Thermophys. **10**, 1103 (1989).
[7] E. Bender, "*Equations of State Exactly Representing the Phase Behavior of Pure Substances*," in *Proceedings of the Fifth Symposium on Thermophysics Properties*, C. F. Bonila, coordinating editor (ASME, New York, 1970).
[8] V. V. Altunin and O. G. Gadetskii, Teploenergetica **18**, 81 (1971).
[9] W. A. Stein, Chem. Eng. Sci. **27**, 1371 (1972).
[10] K. E. Starling, P. N. Batdorf, and Y. C. Kwok, Hydrogen Proc. **51**, 2, 86 (1972).
[11] R. Meyer-Pittroff, Dissertation, TU München (1973).
[12] F. H. Huang, M. H. Li, L. L. Lee, K. E. Starling, and F. T. H. Chung, J. Chem. Eng. Jpn. **18**, 490 (1985).
[13] J. Ewers and W. Wagner, *A Method for Optimizing the Structure of Equations of State and its Application to an Equation of State for Oxygen*, in Proc. 8th Symp. Thermophys. Prop. - Vol. 1, J. V. Sengers, coordinating editor (Am. Soc. Mech. Eng., New York, 1982).
[14] J. F. Ely, *An Equation of State Model for Pure CO_2 and CO_2 Rich Mixtures*, in Proc. 65th Annu. Convention Gas Proc. Assoc. (San Antonio, Texas, 1986).
[15] J. F. Ely, J. W. Magee, and W. M. Haynes, *CO2PAC*, Program available at the Natl. Bur. Stand. (Boulder, Colorado, 1987).
[16] K. S. Pitzer and D. R. Schreiber, Fluid Phase Equilibria **41**, 1 (1988).
[17] J. F. Ely, W. M. Haynes, and B. C. Bain, J. Chem. Thermodyn. **21**, 879 (1989).
[18] R. T. Jacobsen and R. B. Stewart, J. Phys. Chem. Ref. Data **2**, 757 (1972).
[18a] K. S. Pitzer and S. M. Sterner, J. Chem. Phys. **101**, 4, 3111 (1994).
[19] P. Schofield, Phys. Rev. Lett. **22**, 606 (1969).
[20] G. A. Chapela and J. S. Rowlinson, J. Chem. Soc., Faraday Trans. (I) **70**, 584 (1974).
[21] J. F. Ely, J. W. Magee, and W. M. Haynes, *Thermophysical Properties of*

[188] K. I. Amirkhanov and N. G. Polikhronidi, Teploenergetica **18**, 12, 59 (1971).
[189] J. V. Sengers (private communication) (1986).
[190] J. A. Lipa, C. Edwards, and M. J. Buckingham, Phys. Rev. Lett. **25**, 1086 (1970).
[191] C. M. Herget, J. Chem. Phys. **8**, 537 (1940).
[192] I. I. Novikov and Y. S. Trelin, Teploenergetica **9**, 2, 79 (1962).
[193] L. L. Pitaevskaya and A. V. Bilevich, Russ. J. Phys. Chem. **47**, 126 (1973).
[194] W. Lemming, VDI Fortschritt-Ber., Reihe 19, Nr. 32 (VDI-Verlag, Düsseldorf, 1989).
[195] J. Noury, *Etude de la vitesse des ultrasons dans les fluides au voisinage du point critique* (Academy of Sciences, 1951).
[196] Y. S. Trelin and E. P. Sheludiakov, J.E.T.P. Lett. **3**, 2, 63 (1966).
[197] R. W. Gammon, H. L. Swinney, and H. Z. Cummins, Phys. Rev. Lett. **19**, 1467 (1967).
[198] G. T. Feke, K. Fritsch, and E. F. Carome, Phys. Rev. Lett. **23**, 1282 (1969)
[199] K. Fritsch and E. F. Carome, *Behavior of Fluids in the Vicinity of the Critical Point*, NASA Research Report CR-1670 (1970).
[200] O. Maass and W. H. Barnes, Proc. R. Soc. A **111**, 224 (1926).
[201] M. P. Vukalovich and Y. F. Masalov, Teploenergetica **11**, 7, 78 (1964).
[202] M. P. Vukalovich and Y. F. Masalov, Teploenergetica **11**, 11, 75 (1964).
[203] D. Möller, B. E. Gammon, K. N. Marsh, K. R. Hall, and J. C. Holste, J. Chem. Thermodyn. **25**, 1273 (1993).
[204] K. Krüger, VDI Fortschritt-Ber., Reihe 6, Nr. 1 (VDI-Verlag, Düsseldorf, 1964).
[205] H. D. Baehr, "*Measurements of the Internal Energy and the Influence of Gravity Near the Critical Point of CO_2,*" in *Proceedings of the Fourth Symposium on Thermophysical Properties* (ASME, New York, 1968).
[206] M. P. Vukalovich, V. V. Altunin, K. Bulle, D. S. Rasskazov, and D. Ertel, Teploenergetica **17**, 5, 60 (1970).
[207] E. S. Burnett, Phys. Rev. **22**, 590 (1923).
[208] V. V. Altunin and A. N. Gureev, Teploenergetica **19**, 1, 59 (1972).
[208a] L. Cusco, S. E. McBain, and G. Saville, J. Chem. Thermodyn. **27**, 721 (1995).
[209] K. Schäfer, Z. Phys. Chem. B **36**, 85 (1937).
[210] K. E. MacCormack and W. G. Schneider, J. Chem. Phys. **18**, 1269 (1950).
[211] T. L. Cottrell and R. A. Hamilton, Trans. Faraday Soc. **51**, 156 (1955).
[212] W. C. Pfefferle, J. A. Goff, and J. G. Miller, J. Chem. Phys. **23**, 509 (1955).
[213] T. L. Cottrell, R. A. Hamilton, and R. P. Taubinger, Trans. Faraday Soc. **52**, 1310 (1956).
[214] D. Cook, Can. J. Chem. **35**, 268 (1957).
[215] A. P. Masia and M. D. Pena, An. Fis. Quim. B **54**, 661 (1958).
[216] E. G. Butcher and R. S. Dadson, Proc. R. Soc. **227**, 448 (1963).
[217] J. A. Huff and T. M. Reed, J. Chem. Eng. Data **8**, 306 (1963).
[218] M. P. Vukalovich and Y. F. Masalov, Teploenergetica **13**, 5, 58 (1966).
[219] R. S. Dadson, E. J. Evans, and J. H. King, Proc. Phys. Soc. **92**, 1115 (1967).
[220] N. I. Timoshenko, V. P. Kobelev, and E. P. Kholodov, Teploenergetica **17**, 9, 64 (1970).
[221] M. Waxman, H. Davis, and J. R. Hastings, "*A New Determination of the Second Virial Coefficient of Carbon Dioxide at Temperatures Between 0° and 150 °C, and an Evaluation of Its Reliability,*" in *Proceedings of the Sixth Symposium on Thermophysical Properties* (ASME, New York, 1973).
[222] K. Ohgaki, N. Sakai, Y. Kano, and T. Katayama, J. Chem. Eng. Jpn. **17**, 545 (1984).
[223] B. V. Mallu, G. Natarajan, and D. S. Viswanath, J. Chem. Thermodyn. **19**, 549 (1987).
[224] B. V. Mallu, G. Natarajan, and D. S. Viswanath, J. Chem. Thermodyn. **21**, 989 (1989).
[225] R. Span, VDI Fortschritt-Ber., Reihe 6, Nr. 285 (VDI-Verlag, Düsseldorf, 1993).
[226] J. M. H. Levelt Sengers, W. L. Greer, and J. V. Sengers, J. Phys. Chem. Ref. Data **5**, 1 (1976).
[227] J. E. Verschaffelt, Com. Phys. Lab. Leiden **28** (1896).
[228] K. G. Wilson, Phys. Rev. **4**, 3174 (1974).
[229] P. Hill, J. Phys. Chem. Ref. Data **19**, 1233 (1990).
[230] W. Wagner, N. Kurzeja, and B. Pieperbeck, Fluid Phase Equilibria **79**, 151 (1992).
[231] H. T. Haselton, W. E. Sharp, and R. C. Newton, Geophys. Res. Lett. **5**, 753 (1978).
[232] W. J. Nellis, A. C. Mitchell, F. H. Ree, N. C. Holmes, and R. J. Trainor, J. Chem. Phys. **95**, 5268 (1991).
[233] G. L. Schott, High Pres. Res. **6**, 187 (1991).
[234] E. H. Brown, Bul. Int. Inst. Refrig. **1**, 169 (1960).
[235] T. E. Morsy, Dissertation, TH Karlsruhe (1963).
[236] D. Straub, Dissertation, TH Karlsruhe (1964).
[237] A. Schaber, Dissertation, TH Karlsruhe (1965).
[238] D. G. Miller, Ind. Eng. Chem. Fund. **9**, 585 (1970).
[239] K. M. de Reuck (private communication) (1991).

[107] U. Behn, Ann. Phys. **3**, 733 (1900).
[108] H. H. Lowry and W. R. Erickson, J. Am. Chem. Soc. **49**, 2729 (1927).
[109] J. Straub, Wärme und Stoffübertragung **5**, 56 (1972).
[110] W. M. Haynes, *Orthobaric Liquid Densities and Dielectric Constants of Carbon Dioxide*, paper presented at the Cryog. Eng. Conf., Mass. Inst. of. Tech., Cambridge, 1985.
[111] G. J. Esper, Dissertation, Ruhr-Universität Bochum (1987).
[112] A. Eucken and F. Hauck, Z. Phys. Chem. **134**, 161 (1928).
[113] I. I. Novikov and Y. S. Trelin, Zur. Prik. Mech. Tech. Fiz. **2**, 112 (1960).
[114] K. I. Amirkhanov, N. G. Polikhronidi, B. G. Alibekov, and R. G. Batyrova, Teploenergetica **19**, 1, 61 (1972).
[115] W. Pecceu and W. Van Dael, Physica **63**, 154 (1972).
[116] J. W. Magee and J. F. Ely, Int. J. Thermophys. **7**, 1163 (1986).
[117] C. F. Jenkin, Proc. R. Soc. A **98**, 170 (1920).
[118] O. Maass and J. H. Mennie, Proc. R. Soc. A **110**, 198 (1926).
[119] D. LeB. Cooper and O. Maass, Can. J. Res. **2**, 388 (1930).
[120] D. LeB. Cooper and O. Maass, Can. J. Res. **4**, 283 (1931).
[121] W. Cawood and H. S. Patterson, J. Chem. Soc., 619 (1933).
[122] A. Michels and C. Michels, Proc. R. Soc. A **153**, 201 (1935).
[123] A. Michels, C. Michels, and H. Wouters, Proc. R. Soc. A **153**, 214 (1935).
[124] H. H. Reamer, R. H. Olds, B. H. Sage, and W. N. Lacey, Ind. Eng. Chem. **36**, 88 (1944).
[125] G. A. Bottomley, D. S. Massie, and R. Whitlaw-Gray, Proc. R. Soc. A **200**, 201 (1950).
[126] T. Batuecas and C. G. Losa, An. Fis. Quim. B **50**, 845 (1954).
[127] G. C. Kennedy. Am. J. Scie. **252**. 225 (1954).
[128] M. P. Vukalovich and V. V. Altunin, Teploenergetica **6**, 11, 58 (1959).
[129] M. P. Vukalovich and V. V. Altunin, Teploenergetica **9**, 5, 56 (1962).
[130] M. P. Vukalovich, V. V. Altunin, and N. I. Timoshenko, Teploenergetica **10**, 2, 92 (1963).
[131] M. P. Vukalovich, V. V. Altunin, and N. I. Timoshenko, Teploenergetica **10**, 1, 85 (1963).
[132] J. Juza, V. Kmonicek, and O. Sifner, Physica **31**, 1735 (1965).
[133] P. S. Ku and B. F. Dodge, J. Chem. Eng. Data **12**, 158 (1967).
[134] A. Sass, B. F. Dodge, and R. H. Bretton, J. Chem. Eng. Data **12**, 168 (1967).
[135] M. P. Vukalovich, V. P. Kobelev, and N. I. Timoshenko, Teploenergetica **15**, 4, 81 (1968).
[136] E. A. Golovskii and V. A. Tsymarnyi, Teploenergetica **16**, 1, 67 (1969).
[137] V. A. Kirillin, S. A. Ulybin, and E. P. Zherdev, Teploenergetica **16**, 2, 94 (1969).
[138] V. A. Kirillin, S. A. Ulybin, and E. P. Zherdev, "Experimental Investigation of Carbon Dioxide Density at Temperatures from −50 to +200 °C and Pressures up to 500 bar," in *Proceedings of the First International Conference on Calorimetry and Thermodynamics*, Warsaw, 1969.
[139] D. S. Tsiklis, L. R. Linshits, and S. S. Tsimmermann, "Measurement and Calculation of the Molar Volume and Thermodynamic Properties of Carbon Dioxide at High Pressures and Temperatures," in *Proceedings of the 1st International Conference on Calorimetry and Thermodynamics*, Warsaw, 1969.
[140] V. A. Kirillin, S. A. Ulybin, and E. P. Zherdev, Teploenergetica **17**, 5, 69 (1970).
[141] V. N. Popov and M. K. Sayapov, Teploenergetica **17**, 4, 76 (1970).
[142] M. P. Vukalovich, N. I. Timoshenko, and V. P. Kobelev, Teploenergetica **17**, 12, 59 (1970).
[143] W. Schönmann, Dissertation, TH Karlsruhe (1971).
[144] E. P. Kholodov, N. I. Timoshenko, and A. L. Yamnov, Teploenergetica **19**, 3, 84 (1972).
[145] J. Hoinkis, Dissertation, TH Karlsruhe (1989).
[146] G. J. Besserer and D. B. Robinson, J. Chem. Eng. Data **18**, 137 (1973).
[147] D. S. Rasskazov, E. K. Petrov, G. A. Spiridonov, and E. R. Ushmaikin, Teploenergetica **21**, 1, 80 (1974).
[148] V. M. Shmonov and K. I. Shmulovich, Akad. Wouk SSSR **217**, 935 (1974).
[149] W.-W. R. Lau, Ph.D. Thesis, Texas A&M University (1986).
[150] M. Jaeschke, pρT Data from Refractive Index Measurements (private communication) (1987).
[151] M. Jaeschke, pρT Data from Burnett Measurements (private communication) (1987).
[152] J. W. Magee and J. F. Ely, Int. J. Thermophys. **9**, 547 (1988).
[153] P. J. McElroy, R. Battino, and M. K. Dowd, J. Chem. Thermodyn. **21**, 1287 (1989).
[154] W. Duschek, R. Kleinrahm, and W. Wagner, J. Chem. Thermodyn. **22**, 827 (1990).
[155] M. Jaeschke, A. E. Humphreys, P. Van Caneghem, M. Fauveau, R. Janssen-Van Rosmalen, and Q. Pellei, *GERG Technical Monograph 4—The GERG Databank of High Accuracy Compressibility Factor Measurements*, edited by Group Europeen de Recherches Gazieres (VDI-Verlag, Düsseldorf, 1990).
[156] P. Nebendahl, VDI Fortschritt-Ber., Reihe 3, Nr. 212 (VDI-Verlag, Düsseldorf, 1990).
[157] X. Y. Guo, R. Kleinrahm, and W. Wagner, *Experimentelle Untersuchung der systematischen Meßfehler von Betriebsdichteaufnehmern für Erdgas-Meßtrecken - Teil 1: Meßergebnisse für Stickstoff, Kohlendioxid, Argon, Neon, Ethan und Ethen*, Report Lehrstuhl für Thermodynamik, Ruhr-Universität Bochum, Bochum, 1992.
[158] L. A. Weber, Int. J. Thermophys. **13**, 1011 (1992).
[159] R. Gilgen, R. Kleinrahm, and W. Wagner, J. Chem. Thermodyn. **24**, 1493 (1992).
[160] K. Brachthäuser, R. Kleinrahm, H.-W. Lösch, and W. Wagner, VDI Fortschritt-Ber., Reihe 8, Nr. 371 (VDI-Verlag Düsseldorf, 1993).
[160a] A. Fenghour, W. A. Wakeham, and J. T. R. Watson, J. Chem. Thermodyn. **27**, 219 (1995).
[160b] J. Klimeck, R. Kleinrahm, and W. Wagner (private communication) (1995).
[160c] Z. Gokmenoglu, Y. Xiong, and E. Kiran, J. Chem. Eng. Data **41**, 354 (1996).
[160d] P. Nowak, T. Tielkes, R. Kleinrahm, and W. Wagner (unpublished).
[160e] W. Wagner, K. Brachthäuser, R. Kleinrahm, and H.-W. Lösch, Int. J. Thermophys. **16**, 399 (1995).
[161] R. Kleinrahm and W. Wagner, VDI Fortschritt-Ber., Reihe 3, Nr. 92 (VDI-Verlag, Düsseldorf, 1986).
[162] F. G. Keyes and S. C. Collins, Proc. N. A. S. **18**, 328 (1932).
[163] G. B. Kistiakowsky and W. W. Rice, J. Chem. Phys. **7**, 5, 281 (1939).
[164] S. R. de Groot and A. Michels, Physica **14**, 218 (1948).
[165] J. F. Masi and B. Petkof, J. Res. Natl. Bur. Stand. **48**, 179 (1952).
[166] V. E. Schrock, *Calorimetric Determination of Constant-Pressure Specific Heats of Carbon Dioxide at Elevated Pressures and Temperatures*, National Advisory Committee for Aeronautics, Tech. Note 2838 (1952).
[167] L. B. Koppel and J. M. Smith, J. Chem. Eng. Data **5**, 437 (1960).
[168] M. P. Vukalovich, V. V. Altunin, and A. N. Gureev, Teploenergetica **11**, 9, 68 (1964).
[169] M. P. Vukalovich and A. N. Gureev, Teploenergetica **11**, 8, 80 (1964).
[170] M. P. Vukalovich, V. V. Altunin, and A. N. Gureev, Teploenergetica **12**, 7, 58 (1965).
[171] S. L. Rivkin and V. M. Gukov, Teploenergetica **15**, 10, 72 (1968).
[172] V. V. Altunin and D. O. Kuznetsov, Teploenergetica **16**, 8, 82 (1969).
[173] V. V. Altunin and D. O. Kuznetsov, Teploenergetica **17**, 11, 91 (1970).
[174] S. L. Rivkin and V. M. Gukov, Teploenergetica **18**, 10, 82 (1971).
[175] V. V. Altunin and D. O. Kuznetsov, Teploenergetica **19**, 6, 67 (1972).
[176] S. Saegusa, T. Kobayashi, Y. Takaishi, and K. Watanabe, Bull. JSME **23**, 2055 (1980).
[177] R. Bender, K. Bier, and G. Maurer, Ber. Bunsenges. Phys. Chem. **85**, 778 (1981).
[178] G. Ernst and U. E. Hochberg, J. Chem. Thermodyn. **21**, 407 (1989).
[179] G. Ernst, G. Maurer, and E. Wiederuh, J. Chem. Thermodyn. **21**, 53 (1989).
[179a] L. Dordain, J.-Y. Coxam, and J.-P. E. Golier, Rev. Sci. Instrum. **65**, 10, 3263 (1994).
[180] H. W. Wooley, J. Natl. Bur. Stand. **52**, 289 (1954).
[181] H. D. Baehr, H. Hartmann, H.-C. Pohl, and H. Schomäcker, *Thermodynamische Funktionen idealer Gase für Temperaturen bis 6000 °K*, edited by H. D. Baehr (Springer-Verlag, Berlin, 1968).
[182] L. V. Gurvich, *Thermodynamic Properties of Characteristic Substances* (Nauka, Moskwa, 1979), Vol. II, Part II.
[183] J. Chao, in *TRC Thermodynamic Tables Hydrocarbons*, K. W. Marsh, coordinating editor (Texas A&M University, Austin, 1983), Vol. VIII.
[184] J. Chao (private communication) (1986).
[185] R. E. Pennington and K. A. Kobe, J. Chem. Phys. **22**, 1442 (1954)
[186] A. Michels and J. Strijland, Physica **18**, 613 (1952).
[187] K. I. Amirkhanov, N. G. Polikhronidi, and R. G. Batyrova, Teploenergetica **17**, 3, 70 (1970).

[188] K. I. Amirkhanov and N. G. Polikhronidi, Teploenergetica **18**, 12, 59 (1971).
[189] J. V. Sengers (private communication) (1986).
[190] J. A. Lipa, C. Edwards, and M. J. Buckingham, Phys. Rev. Lett. **25**, 1086 (1970).
[191] C. M. Herget, J. Chem. Phys. **8**, 537 (1940).
[192] I. I. Novikov and Y. S. Trelin, Teploenergetica **9**, 2, 79 (1962).
[193] L. L. Pitaevskaya and A. V. Bilevich, Russ. J. Phys. Chem. **47**, 126 (1973).
[194] W. Lemming, VDI Fortschritt-Ber., Reihe 19, Nr. 32 (VDI-Verlag, Düsseldorf, 1989).
[195] J. Noury, *Etude de la vitesse des ultrasons dans les fluides au voisinage du point critique* (Academy of Sciences, 1951).
[196] Y. S. Trelin and E. P. Sheludiakov, J.E.T.P. Lett. **3**, 2, 63 (1966).
[197] R. W. Gammon, H. L. Swinney, and H. Z. Cummins, Phys. Rev. Lett. **19**, 1467 (1967).
[198] G. T. Feke, K. Fritsch, and E. F. Carome, Phys. Rev. Lett. **23**, 1282 (1969)
[199] K. Fritsch and E. F. Carome, *Behavior of Fluids in the Vicinity of the Critical Point*, NASA Research Report CR-1670 (1970).
[200] O. Maass and W. H. Barnes, Proc. R. Soc. A **111**, 224 (1926).
[201] M. P. Vukalovich and Y. F. Masalov, Teploenergetica **11**, 7, 78 (1964).
[202] M. P. Vukalovich and Y. F. Masalov, Teploenergetica **11**, 11, 75 (1964).
[203] D. Möller, B. E. Gammon, K. N. Marsh, K. R. Hall, and J. C. Holste, J. Chem. Thermodyn. **25**, 1273 (1993).
[204] K. Krüger, VDI Fortschritt-Ber., Reihe 6, Nr. 1 (VDI-Verlag, Düsseldorf, 1964).
[205] H. D. Baehr, "*Measurements of the Internal Energy and the Influence of Gravity Near the Critical Point of CO_2,*" in *Proceedings of the Fourth Symposium on Thermophysical Properties* (ASME, New York, 1968).
[206] M. P. Vukalovich, V. V. Altunin, K. Bulle, D. S. Rasskazov, and D. Ertel, Teploenergetica **17**, 5, 60 (1970).
[207] E. S. Burnett, Phys. Rev. **22**, 590 (1923).
[208] V. V. Altunin and A. N. Gureev, Teploenergetica **19**, 1, 59 (1972).
[208a] L. Cusco, S. E. McBain, and G. Saville, J. Chem. Thermodyn. **27**, 721 (1995).
[209] K. Schäfer, Z. Phys. Chem. B **36**, 85 (1937).
[210] K. E. MacCormack and W. G. Schneider, J. Chem. Phys. **18**, 1269 (1950).
[211] T. L. Cottrell and R. A. Hamilton, Trans. Faraday Soc. **51**, 156 (1955).
[212] W. C. Pfefferle, J. A. Goff, and J. G. Miller, J. Chem. Phys. **23**, 509 (1955).
[213] T. L. Cottrell, R. A. Hamilton, and R. P. Taubinger, Trans. Faraday Soc. **52**, 1310 (1956).
[214] D. Cook, Can. J. Chem. **35**, 268 (1957).
[215] A. P. Masia and M. D. Pena, An. Fis. Quim. B **54**, 661 (1958).
[216] E. G. Butcher and R. S. Dadson, Proc. R. Soc. **227**, 448 (1963).
[217] J. A. Huff and T. M. Reed, J. Chem. Eng. Data **8**, 306 (1963).
[218] M. P. Vukalovich and Y. F. Masalov, Teploenergetica **13**, 5, 58 (1966).
[219] R. S. Dadson, E. J. Evans, and J. H. King, Proc. Phys. Soc. **92**, 1115 (1967).
[220] N. I. Timoshenko, V. P. Kobelev, and E. P. Kholodov, Teploenergetica **17**, 9, 64 (1970).
[221] M. Waxman, H. Davis, and J. R. Hastings, "*A New Determination of the Second Virial Coefficient of Carbon Dioxide at Temperatures Between 0° and 150 °C, and an Evaluation of Its Reliability*," in *Proceedings of the Sixth Symposium on Thermophysical Properties* (ASME, New York, 1973).
[222] K. Ohgaki, N. Sakai, Y. Kano, and T. Katayama, J. Chem. Eng. Jpn. **17**, 545 (1984).
[223] B. V. Mallu, G. Natarajan, and D. S. Viswanath, J. Chem. Thermodyn. **19**, 549 (1987).
[224] B. V. Mallu, G. Natarajan, and D. S. Viswanath, J. Chem. Thermodyn. **21**, 989 (1989).
[225] R. Span, VDI Fortschritt-Ber., Reihe 6, Nr. 285 (VDI-Verlag, Düsseldorf, 1993).
[226] J. M. H. Levelt Sengers, W. L. Greer, and J. V. Sengers, J. Phys. Chem. Ref. Data **5**, 1 (1976).
[227] J. E. Verschaffelt, Com. Phys. Lab. Leiden **28** (1896).
[228] K. G. Wilson, Phys. Rev. **4**, 3174 (1974).
[229] P. Hill, J. Phys. Chem. Ref. Data **19**, 1233 (1990).
[230] W. Wagner, N. Kurzeja, and B. Pieperbeck, Fluid Phase Equilibria **79**, 151 (1992).
[231] H. T. Haselton, W. E. Sharp, and R. C. Newton, Geophys. Res. Lett. **5**, 753 (1978).
[232] W. J. Nellis, A. C. Mitchell, F. H. Ree, N. C. Holmes, and R. J. Trainor, J. Chem. Phys. **95**, 5268 (1991).
[233] G. L. Schott, High Pres. Res. **6**, 187 (1991).
[234] E. H. Brown, Bul. Int. Inst. Refrig. **1**, 169 (1960).
[235] T. E. Morsy, Dissertation, TH Karlsruhe (1963).
[236] D. Straub, Dissertation, TH Karlsruhe (1964).
[237] A. Schaber, Dissertation, TH Karlsruhe (1965).
[238] D. G. Miller, Ind. Eng. Chem. Fund. **9**, 585 (1970).
[239] K. M. de Reuck (private communication) (1991).